THE UNIVERSITY
of EDINBURGH

Ignition of suspensions of coal and biomass particles in air and oxy-fuel for Carbon Capture and Storage (CCS) and Climate Change mitigation

Ignacio Trabadela

Thesis submitted for the Degree of Doctor of Philosophy in Engineering to the University of Edinburgh

THE UNIVERSITY *of* EDINBURGH

School of Engineering
University of Edinburgh

March 2015

In memory of Susan Anne Kivlin

Dedicated to my parents Enrique and Pilar

"We are the first generation to feel the impact of climate change and the last generation that can do something about it".

Gov. Jay Inslee, State of Washington, quoted in the United Nations' Climate Summit by Barack Obama, President of the United States, New York, 23 September 2014.

"Ours is the first generation that can end poverty, and the last that can take steps to avoid the worst impacts of climate change. In this 70th anniversary year in which we renew our commitment to the goals and principles of the UN charter, the international community must rise to the moment".

BAN Ki-moon, Secretary-General of the United Nations, January 2015.

Declaration of originality

The work included in this Ph.D. thesis, except when referenced, is the result of the effort of years that has been done by the author alone under the guidance of his supervisors Prof. Jon Gibbins and Dr. Hannah Chalmers. The author acknowledges essential contributions by others in the acknowledgment section of this thesis and in further sections of the work where required. This Ph.D. thesis has not been submitted for any other degree or professional qualification in the UK or elsewhere. The author recommends referencing this thesis as follows:

Trabadela I. (2015), Ignition of suspensions of coal and biomass particles in air and oxy-fuel for Carbon Capture and Storage (CCS) and Climate Change mitigation, Ph.D. Thesis, School of Engineering, University of Edinburgh, United Kingdom of Great Britain and Northern Ireland (UK).

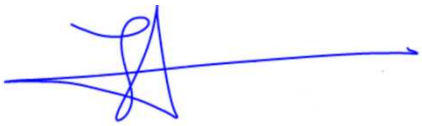

IGNACIO TRABADELA ROBLES

Edinburgh, March 2015

Abstract

Carbon Capture and Storage (CCS) is a legitimate technology option that should be part of a balanced portfolio of mitigation technologies available Post-Kyoto Protocol framework after Paris 2015 and beyond the 2020s or the cost achieving 2 degrees Celsius stabilisation scenario will significantly increase. Oxy-fuel combustion as a CCS technology option increases fuel flexibility. Additionally, oxy-biomass as a bio-energy with CCS (BECCS) technology can achieve negative carbon dioxide (CO_2) emissions in sustainable biomass systems. Also, oxygen (O_2) production in an air separation unit (ASU) gives potential for extra operational flexibility and energy storage. In this work, new designs of 20 litre spherical (R-20) and 30 litre non-spherical (R-30) ignition chambers have been built at the University of Edinburgh to carry-out dust ignition experiments with different ignition energies for evaluating pulverised fuel ignitability as a function of primary recycle (PR) O_2 content for oxy-fuel PF milling safety. A set of coals and biomasses being used (at the time of submitting this work) in the utility pulverised fuel boilers in the UK have been employed. Coal and biomass dusts were ignited in air and oxy-fuel mixtures up to 30 % v/v O_2 balance mixture CO_2 where peak pressures (P_{max}) from ignition were recorded. Pressure ratios ($P_{max}/P_{initial}$) were determined the key parameter for positive ignition identification with a value above 2.5 to be considered positive. Particle size effects in coal and biomass ignition were evaluated. Results on biomass were more variable than with coals, requiring a stronger ignition source (5,000 J) mainly due to larger particle sizes. Finer biomass particles behaved similarly to air ignition in 25 % v/v O_2 in CO_2. Larger particles of biomass did not ignite at all for most cases even reaching 30 % v/v O_2 in CO_2. A reference coal used, El Cerrejon, behaved as expected with 30 % v/v O_2 balance CO_2 matching air case; particles between 75-53 microns had lower ignitability than finer below 53 microns but were critical in devolatilisation. Most fuels did not ignite in 21 % v/v in CO_2 below 200 g/m^3 concentrations. The use of adequate ignition energy strength is needed for the PF mill safety case, with 5,000 J energy required for the biomasses tested. An indication of potential ignition chamber volume and geometry effect has also been observed when comparing results from R-20 and R-30 ignition chambers. Important implications include that oxy-biomass PR with 21 % v/v O_2 content would give improved pulverised fuel (PF) milling safety when compared to air firing but reduced ignitability and a 25 % v/v O_2 balance CO_2 atmosphere would approach to oxy-biomass ignition behaviour in air in mills.

Table of Contents

List of Figures

List of Tables

Nomenclature

0.25G	Biomass particle size grounded with 0.25 mm sieve ring.
0.5G	Biomass particle size grounded with 0.5 mm sieve ring.
°C	Degrees Celsius, Temperature unit.
21 Oxy	21 volume % oxygen in 79 volume % carbon dioxide.
25 Oxy	25 volume % oxygen in 75 volume % carbon dioxide.
30 Oxy	30 volume % oxygen in 70 volume % carbon dioxide.
AISI 304	American Iron and Steel Institute Grade of stainless steel for 304 type with low carbon content useful in corrosive environments.
bar (a)	(Absolute) Pressure unit.
CO_2	Carbon dioxide.
daf	Dry ash free, fuel content expressed in weight (wt.) %.
E	Energy, in the context of ignition energy, units J.
EJ	Exajoules, 10^{18} J.
Gt	Gigatonne, 10^{12} Kg.
$GtCO_2eq$	Gigatonne of CO_2 equivalent
g/m^3	Grams per cubic metre.
J	Joule, SI unit for energy.
Kg	Kilogram, SI unit for mass.
kPa (a)	Kilo Pascal, 10^3 Pascal (Absolute pressure unit in kPa).
K_{st}	Maximum rate of pressure rise of dust ignition assuming “cubic law”, St for “Staub” (dust in German), units in bar m/s or kPa m/s.
L	Litre, volume unit.
m	Mass of gas.
mm	Millimetre, 10^{-3} metre.
m^3	Cubic metre, SI unit for volume.
M	Molecular weight.
M48	Standard external Metric thread and fastener/bolt size.
Mt	Megaton, 10^9 Kg.
Mtoe	Million tonnes oil equivalent.
MW	Megawatt, 10^6 watts.
MW_e	Megawatt electric.

MW_{th}	Megawatt thermal.
N_2	Nitrogen.
O_2	Oxygen.
O_2/CO_2	Oxygen and carbon dioxide mixtures used in oxy-fuel.
p	System absolute pressure.
P_0	Pressure at start of ignition (or P initial) for pressure ratio calculation.
Pa	Pascal, SI unit for pressure.
PF	Pulverised fuel.
P_{max}	Maximum absolute pressure during dust ignition or peak pressure, bar or kPa.
psi	Pound per square inch, pressure unit.
PR	Primary recycle in oxy-fuel combustion.
P/R	Pressure ratio (dimensionless).
PTFE	Polytetrafluoroethylene, commercially Teflon.
r	Radius.
R	Universal gas constant.
R-20	20 litre spherical ignition chamber designed and built at the University of Edinburgh.
R-30	30 litre non-spherical ignition chamber designed and built at the University of Edinburgh.
rpm	Revolutions per minute, rotational speed unit.
S_b	Flame speed defined as the density ratio at constant pressure of unburned to burned gases ρ_u/ρ_b
T	System absolute temperature.
T_0	Absolute temperature at the start of the experiment.
T_b	Absolute temperature of the burnt gas.
TWh	Terawatt-hour, 10^{12} watts per hour, electricity generation or electrical energy unit.
µm	Micrometre, 10^{-6} metre.
V_o	System volume.
% v/v	Volume per volume percentage concentration.
vol.%	Volume percentage concentration.
VM	Volatile matter.
W	Watt, SI unit for power.

Abbreviations and acronyms

2DS	2 degrees -Celsius- scenario.
ADP	Ad Hoc Working Group on the Durban Platform for Enhanced Action.
AFT	Adiabatic Flame Temperature.
AH	Air Heater.
AIT	Autoignition Temperature.
ASC	Advance Supercritical Coal.
ASU	Air Separation Unit.
BAT	Best Available Techniques.
BCURA	British Coal Utilisation Research Association.
BECCS	Bio-energy with CCS.
CAPEX	Capital Expenditure.
CBDR	Common But Differentiated Responsibilities.
CCC	Committee on Climate Change.
CCGT	Combined Cycle Gas Turbine.
CCS	Carbon Capture and Storage.
CCSA	Carbon Capture and Storage Association.
CCR	Carbon Capture Ready.
CCT	Carbon Capture Technology.
CCUS	Carbon Capture Utilisation and Storage.
CDR	Carbon Dioxide Removal.
CFB	Circulating Fluidised Bed.
CFD	Computational Fluid Dynamics.
CfD	Contract for Difference.
CMP	Meeting of the Parties to the Kyoto Protocol.
COP	Conference of the Parties to the UNFCCC.
CPU	Compression and Purification Unit.
CTF	Combustion Test Facility.
DACS	Direct Air Capture and Sequestration.
DCC	Direct Contact Cooler.
DECC	Department of Energy and Climate Change.
DTF	Drop Tube Furnace.

EA	Environment Agency.
EC	European Commission.
EMR	Electricity Market Reform.
EOR	Enhanced Oil Recovery.
EPS	Emissions Performance Standards.
EPSRC	Engineering and Physical Science Research Council.
ESP	Electrostatic Precipitator.
ETI	Energy Technology Institute.
ETP	Energy Technology Perspectives.
EU	European Union.
EU ETS	European Union's Emissions Trading Scheme.
FEED	Front End Engineering Design.
FGD	Flue Gas Desulphurisation.
FGFWH	Flue Gas Feed Water Heater
FNPT	Female National Pipe Thread Taper.
FOAK	First of a Kind.
FT	Fischer-Tropsch.
GCCSI	Global CCS Institute.
GCF	Green Climate Fund.
GDP	Gross Domestic Product.
GHG	Greenhouse Gases.
ID	Inside Diameter.
IEA	International Energy Agency.
IED	Industrial Emissions Directive.
IEAGHG	International Energy Greenhouse Gas Control Programme.
IGCC	Integrated Gasification Combined Cycle.
IM-A(B)	Igniter Mounting design A or B.
INDCs	Intended Nationally Determined Contributions.
IPCC	Intergovernmental Panel on Climate Change.
IRENA	International Renewable Energy Agency.
KP	Kyoto Protocol, 1997.
LCPD	Large Combustion Plant Directive.
LCE	Low Carbon Economy.

LCOE	Levelised Cost of Electricity.
LES	Large Eddy Simulation.
LFL	Lean Flammable Limit.
MEC	Minimum Explosible Concentration.
MNPT	Male National Pipe Thread Taper.
NIOSH	National Institute for Occupational Safety and Health.
NPT	National Pipe Thread Taper.
OD	Outside Diameter.
OECD	Organisation for Economic Co-operation and Development.
OPEX	Operational Expenditure.
OxyCAP UK	Oxy-fuel Combustion Academic Programme for the UK.
PA	Primary Air.
PACT	Pilot-scale Advanced Capture Technology.
PC	Post-Combustion Capture.
PF	Pulverised Fuel.
PFD	Process Flow Diagram.
PPC	Pittsburgh Pulverised Coal.
PR	Primary Recycle.
PRL	Pittsburgh Research Laboratory.
RAN	Reynolds-averaged modelling.
RC	Respective Capabilities.
RCP	Representative Concentration Pathway.
RFG	Recycled Flue Gas.
SCR	Selective Catalytic Reduction.
SR	Secondary Recycle.
TGA	Thermogravimetric Analysis.
UK	United Kingdom of Great Britain and Northern Ireland.
UKCCSRC	UK CCS Research Centre.
UN	United Nations.
UNFCCC	United Nations Framework Convention on Climate Change.
US/USA	United States of America.
USBM	United States Bureau of Mines.
WEO	World Energy Outlook.

ZEP	Zero Emissions Platform.

Acknowledgements

This thesis is the result of work done after the generous opportunity given by my mentors and supervisors Prof. Jon Gibbins (University of Edinburgh) and Dr. Hannah Chalmers (University of Edinburgh). Thanks to both for their essential support to get this Ph.D. work completed and for keeping me interested in the subject and in the "broader picture" of CCS with the potential for impacting on Energy and Climate Change Policies. Dr. Mathieu Lucquiaud (University of Edinburgh) is also gratefully acknowledged for his mentoring contribution. Their mark has proven important in the recent months and surely will be in the years to come.

Many thanks to Mr. Greg Green and Dr. Chi Man from the National Institute for Occupational Safety and Health (NIOSH) in the USA, for their extremely valuable input and training on coal dust ignition science in the Fall of 2011. Thanks to all staff members at NIOSH in Pittsburgh and the US Government for welcoming me as a visiting researcher to their facilities in DOE Complex in Pittsburgh, Pennsylvania. Although I did not have the privilege to meet him before passing away, I want to acknowledge Mr. Ken Cashdollar (NIOSH, formerly US Bureau of Mines) for his extensive publications on coal ignition in PRL-20 chamber that allowed me to learn about the subject.

Special thanks to Mrs. Susan Kivlin (Electronics), Mr. George Cairns (Mechanical), Mr. Gordon Paterson (Mechanical), Mr. Douglas Carmichael (LabVIEW™) and Mr. Kevin Anderson (Mechanical) from the School of Engineering for their crucial help on making the ignition chamber(s) at the University of Edinburgh a set of reliable pressure vessels for carrying out dust ignition experiments. Mr. Bob Gusthart, Mr. Steve Gourlay, Mrs. Fiona Alderson, Mr. Paul Aitken, Mr. Graeme Lynch, Mr. Scott Dalgleish, Mr. Rab Louden, Mr. Kevin Tierney, Mr. Bill Lesley, Mr. Ewan McLean, Mr. Derek Jardine and Mr. Bryan Mitchell are also gratefully acknowledged. A Ph.D. research project based on experimental work gave me the opportunity to meet wonderful people while understanding how important members of technical staff are.

Thanks to my fellow Ph.D. students, Ms. Olivia Errey, Mr. Bill Buschle, Ms. Maria Sanchez, Ms. Laura Herraiz, Mr. Alasdair Bruce, Mr. Paul Tait and Ms. Abigail Gonzalez for their support and unforgettable time spent together. Ms. Robin Cathcart, Dr. Roger Watson and Dr. Eva Sanchez are also gratefully thanked.

Thanks to NIOSH, the British Coal Utilisation Research Association (BCURA), E.ON and Cranfield University for supplying part of the coal and biomass used in this research.

Dr. Blanca Antizar, Dr. Andrea Semiao and Mr. Ioannis Stamou (School of Engineering, University of Edinburgh) are thanked for granting access to Retsch grinder. Thanks to Mrs. Ann Mennim (School of Geosciences, University of Edinburgh) for providing dusts particle size analysis. Thanks to Prof. Konstantin Kamenev's group (School of Engineering, University of Edinburgh) for carrying-out ANSYS stress analysis for ignition chamber.

Thanks to my flatmate, Dr. Cristian Maluk for his support while sharing the adventure of getting a Ph.D in the School of Engineering, University of Edinburgh. Thanks to staff members in the School of Engineering that helped me and made my life in the School enjoyable the last four years, including but not all (sorry for missing people): Agnes, Vincent, Anne, Alan, Dot, Sue, Gillian, Karen, Helen, Lorraine, Kathy, Liz, Neil, June and Pauline.

Thanks to project partners of the Oxy-fuel Combustion Academic Programme for the UK (OxyCAP UK). The biannual meetings we had were critical in the learning process and research output. Thanks to the Carbon Capture Group in the School of Engineering, Scottish Carbon Capture and Storage (SCCS) and the UK Carbon Capture and Storage Research Centre (UKCCSRC). Engineering and Physical Sciences Research Council (EPSRC) and E.ON are gratefully acknowledged as sponsors of my Ph.D. project. The views are my own.

Thanks to the Climate Change Support Team and staff members at the Executive Office of the Secretary-General of the United Nations.

Sincere thanks to everyone mentioned above for their friendship.

Finally, thanks to my family.

1. Introduction, CCS and Climate Change, oxy-fuel and BECCS

The work presented in this Ph.D. thesis is motivated towards contributing to safely develop oxy-fuel combustion as one the technological options available for Carbon Capture and Storage (CCS). Biomass ignitability as pulverised fuel under oxy-fuel atmospheres is tested and compared with data for coals to support the implementation of Bio-energy with CCS (BECCS) for achieving potential negative carbon dioxide (CO_2) emissions in the power generation sector [IPCC, (2014c)]. Climate change is happening according to wide scientific evidence [e.g. IPCC, (2013)]; tackling the problem will be less costly than the cost of inaction, with overall costs of Climate Change ranging from 5 % to 20 % of global GDP per year while the cost of action would be equivalent to 1 % of global GDP annually [Stern, (2007)].

CCS is a technology needed for effectively tackling Climate Change. CCS technology is available and a new industry is being born. The historic launch in 2014 of Boundary Dam Carbon Capture Project in Canada, with 110 MWe (net) coal retrofit capturing 1 Million tonnes of CO_2 per year, is the first large scale power plant with a full chain CCS in operation [Saskpower, (2014); IEA Press release, (2014)]. However, there is a need to scale-up CCS and having proven reserves of CO_2 at Gigatonne (Gt) levels is the key [Herzog, (2011)]. CO_2 storage is not covered in this thesis. Nevertheless, safe and reliable long-term CO_2 storage, although technically feasible, remains as one the key elements in the full CCS business chain that demands clear regulatory and economic frameworks for a successful deployment of the technology. Sound energy and climate policies should aim to fill the gaps in this area. This thesis does not attempt to fill any gap on energy and climate policies. CO_2 utilisation, despite small scale versus potential total CO_2 emissions captured, is considered quite important for successfully progressing CCS in the short-term, with techno-economic analysis, modelling work, demonstration projects and perception work carried-out for local markets of CCS with enhanced oil recovery (EOR) [e.g. Roussanaly and Grimstad, (2014); Kemp and Kasim, (2013); Zhang et al, (2015); Liang et al., (2011)]. EOR which is the real driver for CO_2 utilisation in what has been lately known as Carbon Capture Utilisation and Storage (CCUS) [Gale, (2013)]. Direct Air Capture [e.g. Lackner, (2013)] and Sequestration (DACS) as a form carbon dioxide removal (CDR) strategy is seen a "*low risk*" option that in the future could be part of a system portfolio that complement CCS and other strategies for mitigating climate change and ocean acidification [NAS, (2015)]. In principle, a quick

response and dynamic system where "buffering" CO_2 concentration in the atmosphere could be possible in a cost effective way, having a direct impact on a limited carbon budget.

In this first chapter, the bigger picture behind this experimental research is explained. Attention is paid to the role of CCS in mitigating Climate Change, critical process stages for oxy-fuel technology roll-out and the potential impact of the research in this thesis. In Chapter 2 of this work, a literature review on the dust ignition science with examples for coal and biomass ignition in air and oxy-fuel is developed. Chapter 3 and Chapter 4 constitute the core of the tools used for the experimental programme, where ignition chambers of 20 litre (R-20) and 30 litre (R-30) designed and built in Edinburgh are described. The manufacturing process with the first design options considered is explained in Chapter 3. In Chapter 4 the experimental methodology is defined, with attention to dusts particle size preparation in coal and biomass in this experimental work. Chapters 5 and 6 are the results and discussion arising from this programme for coal and biomass respectively. Chapter 7 describes the main implications from this work with suggestions for future work and for enhancing the impact of this research if interest from industry is gained after its publication. Chapter 8 summarises the main conclusions from this Ph.D. thesis and the Appendix section attached includes additional information and technical drawings that have not been included in the text of the thesis.

1.1. Background to Carbon Capture and Storage (CCS)

CCS is a Climate Change mitigation technology that has been developed at small scale and which requires more political and societal support to successfully move from a demonstration to commercialisation phase beyond 2020. In this section, the role of CCS for tackling Climate Change, CCS in the low carbon economy context, CCS as a cohesion technology in that economy and the impact of the potential new climate agreement in 2015 are discussed, paying attention to the most recent science from the Intergovernmental Panel on Climate Change (IPCC) under the United Nations (UN) and to the negotiations in the United Nations Framework Convention on Climate Change (UNFCCC).

1.1.1. CCS and Climate Change

Atmospheric concentrations of carbon dioxide (CO_2), methane (CH_4), nitrous oxide (N_2O) and other greenhouse gases (GHG) have increased as a result of human activity [IPCC, (2014c)]. From 1750 to 2011, cumulative anthropogenic CO_2 emissions were 2,040 ± 310 Gigatonne of CO_2 ($GtCO_2$), with 40 % of the emissions accounted for in the last 40 years [IPCC AR5, (2014)]. Fossil fuels used in energy and industry were responsible for about 78 % of the GHG emissions rise since 1970 [IPCC, (2014c)].

CCS is a low carbon economy technology primarily for Climate Change mitigation but with other potential impacts on Climate Change adaptation and resilience. According to Figure 1.1, CO_2 emissions remain the major contributor to GHG emitted not just from fossil fuels use and industrial processes but due to deforestation and land use. Limiting the increase in global average temperature to 2 degrees Celsius from pre-industrial levels, known as the 2 degrees scenario (2DS) according to the International Energy Agency (IEA), has become the major objective in climate policy. The IEA in their latest Energy Technology Perspective report, on 2DS shows that economic growth can be decoupled from energy demand including oil [IEA ETP, (2014)]. In order to limit average global temperature increase, CCS can be deployed beyond the 2020s. Mitigating Climate Change is compatible with economic growth and CCS, from a climate mitigation perspective, could be highly valuable [The Global Commission on the Economy and Climate, (2014)]. In fact, technology-driven solutions are the solid basis for sustainable economic growth in the transition of economic regimes from primary to tertiary sectors that want to safeguard their industrial base structure in a Low Carbon Economy (LCE) context.

In Figure 1.1, CO_2 fossil fuel and industrial processes account for 65 % of the total anthropogenic emissions by gases in the 1970-2010 period. An additional 11 % is due to CO_2 emissions from deforestation and land use (GHG emissions in $GtCO_2eq$], representing the greater causes of GHG emissions until now and expected to remain the major contributors towards 2050.

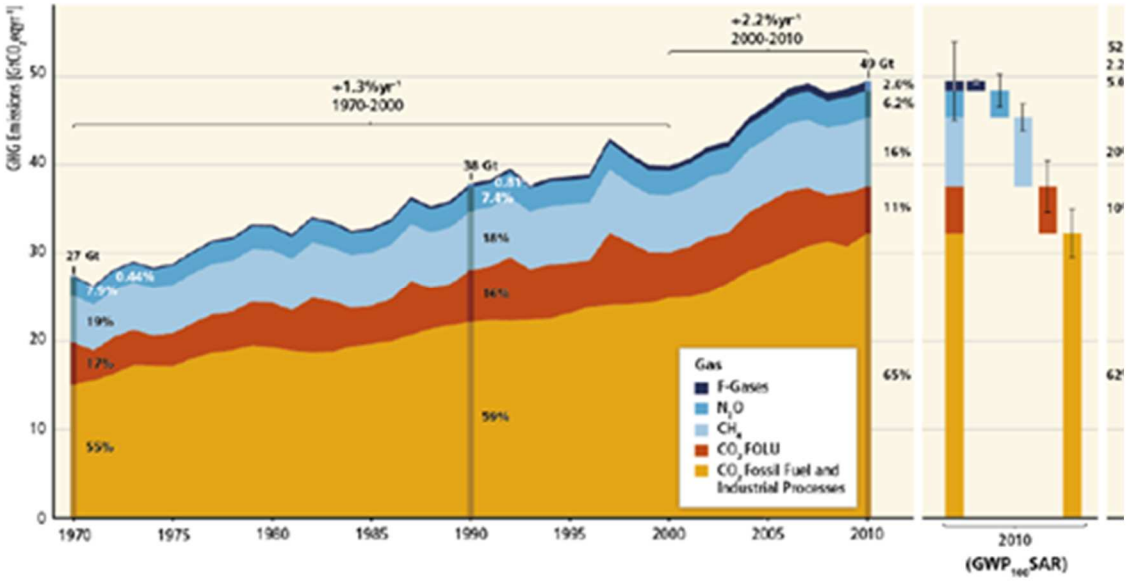

Figure 1.1. Total annual anthropogenic emissions by gases 1970-2010 [IPCC, (2014c)]

Although the CO_2 emissions increasing trend from the previous decades is evident, it is very unclear how this trend would be modified according to scenarios for multiple pathways for CO_2 emissions reduction, as shown in Figure 1.2 for alternative economic scenarios and climate policies. Representative Concentration Pathways (RCPs) are used in the IPCC projections; RCP2.6 being a scenario to keep the average global temperature increase below 2 degrees Celsius when compared to pre-industrial levels [IPCC, (2014c)].

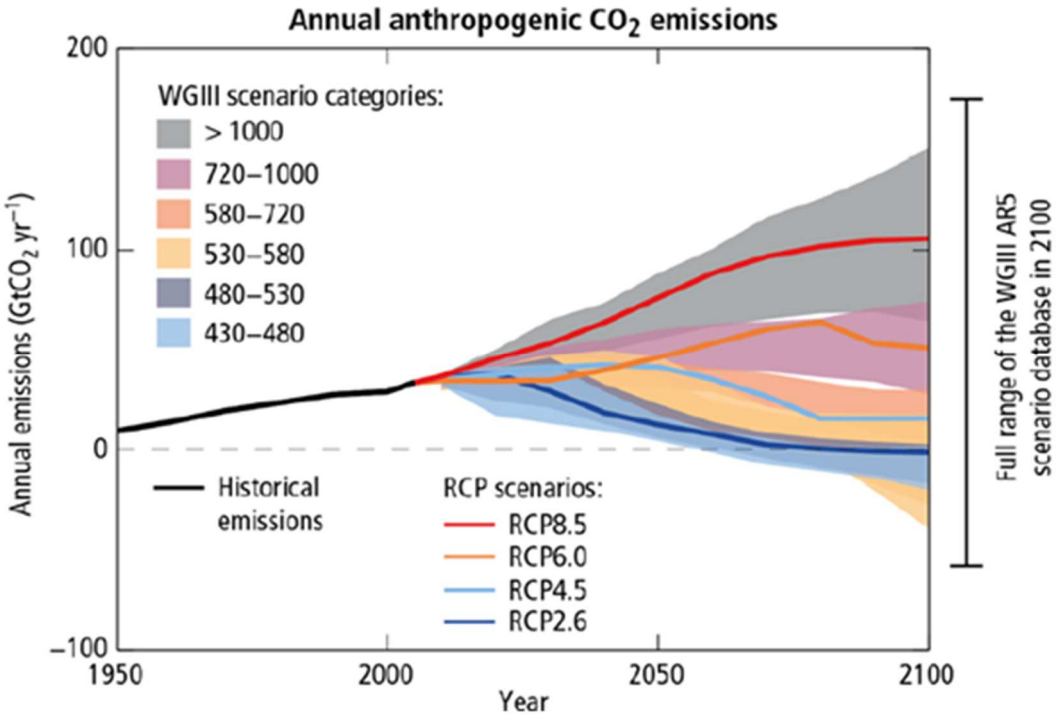

Figure 1.2. Annual anthropogenic CO_2 emissions for 1950-2100 scenarios [IPCC, 2014c)]

RCP2.6 (in dark blue in Figure 1.2) would be equivalent to the IEA 2DS for average global temperature increase, with CCS deployment required at scale to avoid an increase of global average temperature above 2 degrees Celsius through stabilisation of CO_2 levels in the range of 430-480 ppm of CO_2eq by 2100 [IPCC, (2013); IPCC, (2014b)]. In Figure 1.3, multiple CO_2 emissions pathways for 2030 and 2050 are shown.

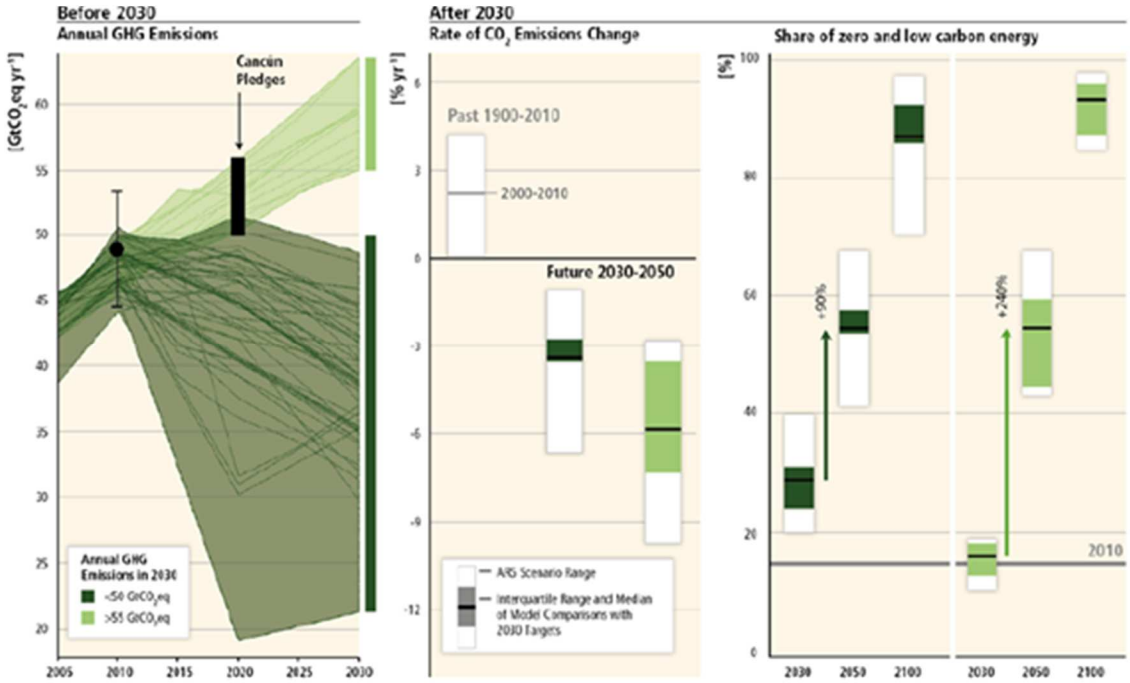

Figure 1.3. Pathways to 2030 and 2050 Low carbon Economy context [IPCC, (2014c)]

There is a limited carbon budget available in a quasi-static system where the pace of emissions is significantly higher than natural abatement, also affected by deforestation. According to IPCC the amount of CO_2 emitted until 2100 could range between 630 to 1180 Gt (billion tons) of CO_2 in a 2DS scenario [IPCC, (2013)]. Delaying GHG emissions reduction before 2030 would make it mandatory to accelerate the rate of emissions reduction in order to meet 2050 targets [IPCC, (2014b)]. The problem is that this estimation would vary depending on the technologies and policies pathways applied, as shown in Figure 1.3. The pathways for GHG emissions reduction by 2030 are quite variable, with substantial uncertainties from 2010 levels and Cancun pledges towards 2020 as seen in left hand side of Figure 1.3 [IPCC, (2014c)]. What it is really important from this figure is that the average reduction rate for emissions (central part of the graph) will have to increase notably (close to -10 % on a yearly basis) if no action to reduce emissions is taken ahead of 2030.

According to the IPCC "*The arrows in the right panel show the magnitude of zero and low-carbon energy supply up-scaling from 2030 to 2050 subject to different 2030 GHG emissions levels. Zero and low-carbon energy supply includes renewables, nuclear energy, and fossil energy with carbon dioxide capture and storage (CCS), or bioenergy with CCS (BECCS)*" [IPCC, (2014c)]. Hence, CCS and BECCS play an essential role for decarbonisation and the 2020-2030 decade is critical for the technology development to accelerate CO_2 emissions reductions and meet 2050 and 2100 targets for a carbon neutral economy.

1.1.2. CCS in the Low Carbon Economy (LCE) context

CCS has been closely linked to the future of the fossil-fuel industry in the Low Carbon Economy (LCE) context. If CCS was to be implemented at the scale required for 2DS, the annual investment rate in CCS could reach almost US$30 billion/year in 2020, with cumulative investment above US$3.6 trillion by 2050 [The Global Commission on the Economy and Climate, (2014)], equivalent to Germany's GDP for 2014 in current international dollars [IMF, (2014)]. Coal and natural gas as fuels in the power sector can remain relatively cheap in the coming decades but if CCS was not available, many coal and natural gas investments would be locked due to limited carbon budget for 2DS. The risk of having stranded assets without CCS available [Clark and Herzog, (2014)] has led to many power generation companies to stopping investment in a new coal fleet and advancing decisions on coal power station closures. In Europe this has been initially driven by the Large Combustion Plant Directive (LCPD) regulating sulphur dioxides (SO_2), nitrogen oxides (NO_x) and other particulates emissions and that has been replaced by the more stringent Industrial Emissions Directive (IED) from 2015. In the UK's aging fleet, the need for investing in flue gas desulphurisation (FGD) and other treatment plants to comply with IED when the CO_2 emissions framework is still unclear has made early decommissioning of unabated plants popular among usually conservative utilities. Thus the IED will further challenge the UK's remaining coal fleet that will close in the early 2020s except for the very few converting to co-firing biomass [Pöyry, (2013)]. Divestment from fossil-fuels has accelerated recently but fossil fuel assets are about US$5 trillion worth at 2014 valuations with 275 coal firms valued at US$233 billion [BNEF, (2014)]. Volatility in '*front month future prices*' of crude oil, over US$100/barrel (bbl) in the summer of 2014 to below US$50/barrel (bbl) in January 2015 for both West Texas Intermediate and Brent contracts [US EIA, (2015)] and consequent harm to the shale industry caused by the uncertainty in prices shows the

importance of developing clear market mechanisms alongside technology in order to hedge investments that usually have a investing framework over 20-30 years. If CCS was available it could reduce the negative effect on the value of fossil-fuel assets in a Climate Change mitigation scenario [IPCC, (2014c)]. It is important to know which type of CCS would be available as not all CCS is equal in terms of the potential climate benefit [Gibbins and Chalmers, (2011)].

More recently, the potential for developing Bio-CCS or Bioenergy with CCS (BECCS) gives further interest to this Ph.D. thesis research work in oxy-biomass as a negative carbon emissions energy technology option in the Low Carbon Economy (LCE). In fact, BECCS could possibly be displacing fossil fuels such as coal in the future if a sustainable supply of biomass was in place. In Table 1.1 bio-energy and CCS are shown as key elements for containing Climate Change mitigation costs.

Table 1.1. Mitigation cost increases significantly if no CCS is deployed [IPCC, (2014c)]

	Mitigation cost increases in scenarios with limited availability of technologies[4] [%increase in total discounted[5] mitigation costs (2015-2100) relative to default technology assumptions]				Mitigation cost increases due to delayed additional mitigation until 2030 [% increase in mitigation costs relative to immediate mitigation]	
2100 concentrations (ppm CO_2-eq)	*no CCS*	*nuclear phase out*	*limited solar/wind*	*limited bioenergy*	*medium term costs (2030-2050)*	*long term costs (2050-2100)*
450 (430-480)	138 % (29-297%) 4	7 % (4-18%) 8	6 % (2-29% 8	64 % (44-78% 8	44 % (2-78%) 29	37 % (16-82%) 29
500 (480-530)	N/A	N/A	N/A	N/A		
550 (530-580)	39 % (18-78%) 11	13 % (2-23%) 10	8 % (5-15% 10	18 % (4-66% 12	15 % (3-32%)	16 % (5-24%)
580-650	N/A	N/A	N/A	N/A		

Symbol legend – fraction of models successful in producing scenarios (numbers indicate the number of successful models)

: all models successful

: between 50 and 80% of models successful

: between 80 and 100% of models successful

: less than 50% of models successful

Table 1.1 from the IPCC Synthesis Report, (2014) included in the Summary for Policymakers (SPM), shows that if CCS was not available as a mitigation technology then the cost of mitigating Climate Change will more than double (increase by 138 %) for 2DS. The results with no CCS are consistent with other studies that previously have suggested the need for CCS to lower the cost of reducing CO_2 emissions [e.g. ZEP, (2013)]. However, some parts of the international community remain sceptical with regard to CCS or the use of sustainable

bio-energy with CCS. But according to the IEA in their latest Energy Technology Perspectives Report of 2014 [IEA ETP, (2014)] cited by the Global CCS Institute [GCCSI, (2014)], CCS would be responsible for 14 % of the CO_2 emissions reductions if deployed to meet CO_2 targets for 2DS as shown in Figure 1.4.

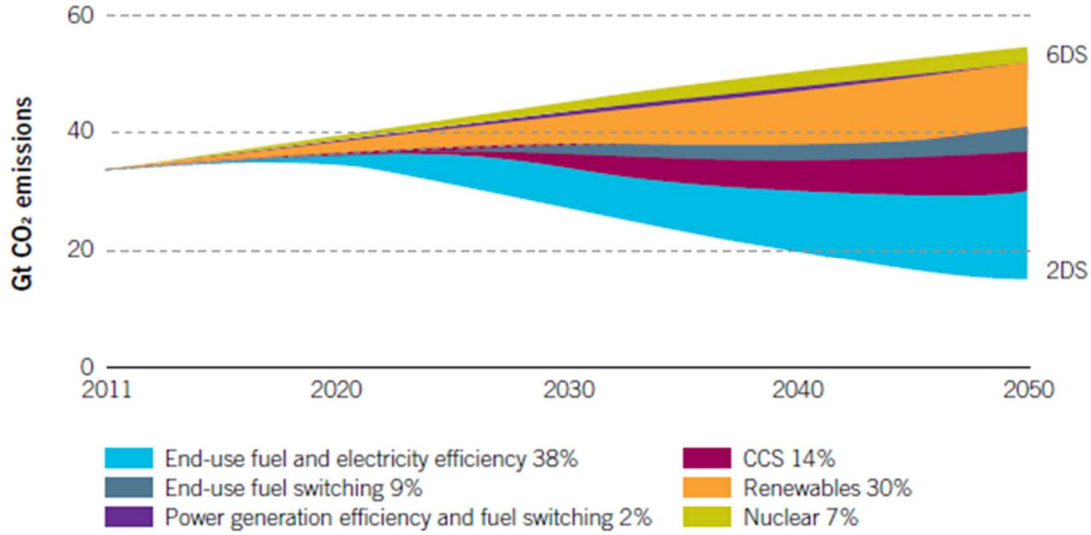

Figure 1.4. CCS contribution in reducing cumulative CO_2 emissions by 2050 in 2DS compared to "business as usual" [IEA, (2014), GCCSI, (2014)]

The significant amount of a 14 % share of total CO_2 emissions reduction is consistent with the potential for these emissions decline if CCS was deployed across multiple sectors in the low carbon economy in applications that other low carbon energy technologies could not replace.

For example, the role of industrial-CCS is critical in decarbonising energy-intensive industries where other options are not available. The earlier deployment of CCS in the power sector should help to develop the technology that would help to decarbonise heavy industries like cement, iron and steel, refineries, chemicals, paper and other structural elements of advanced economies that cannot otherwise be decarbonised at the pace required for 2DS without CCS. The IEA in the CCS Roadmap report [IEA, (2013)] shows in Figure 1.5 the variety of industry sectors where CCS can have a direct impact on CO_2 captured and stored ($MtCO_2/yr$).

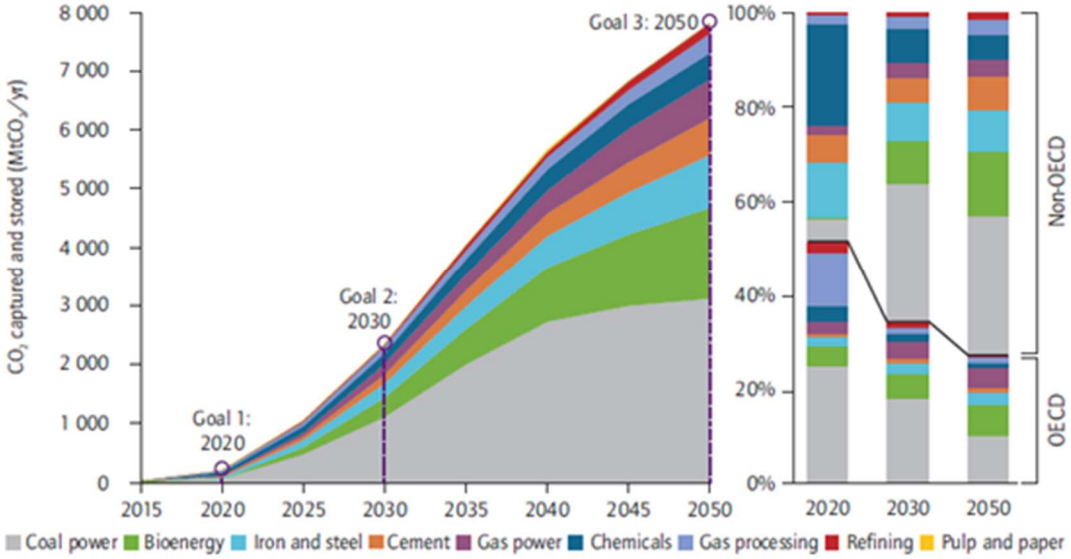

Figure 1.5. CCS deployment in the power and industrial sectors in the 2DS [IEA, (2013)]

In the learning process of CCS technologies roll-out, there is a need for a demonstration phase, currently on-going. Commercialisation in the 2020s could come if CCS has been successfully demonstrated in the numbers required. Hence, there is value in having two learning cycles from two tranches of CCS projects before a global roll-out is implemented according to Figure 1.6 [Gibbins and Chalmers, (2008)].

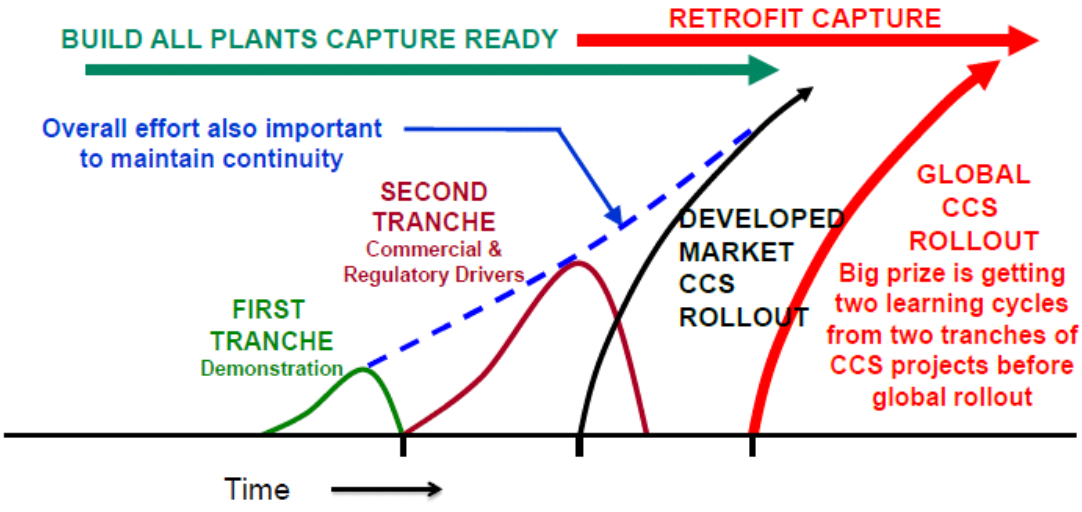

Figure 1.6. CCS sequencing deployment required [adapted by Gibbins from Gibbins and Chalmers, (2008)]

The involvement of Governments is required for an urgent CCS roll-out. In Europe, the UK Government has been leading the way towards policies that support early demonstration of CCS with current R&D funding programme (£125 million for 2011-2015 period) and the flagship UK CCS Commercialisation Programme (£1 billion), with the Department of Energy and Climate Change (DECC) in charge of coordinating the competitive process [DECC, (2013a)]. The Electricity Market Reform (ERM) [DECC, (2014a)] and the Energy Bill made Energy Act in 2013 [DECC, (2013c)] estimated over £110 billion of investment is needed in the UK energy sector before 2020. Delaying decarbonisation target commitments after 2016 is preventing investment decisions from happening in the UK. EMR makes important contributions for developing potential funding mechanisms, principally a Feed in Tariff (FiT) with Contracts for Difference (CfD). Other options, such as an Emissions Performance Standards (EPS), are also included but this may not be effective in incentivising the deployment of technologies like CCS and hence deliver competitive electricity prices in a LCE. According to the Energy Technology Institute (ETI) and cited by the Carbon Capture and Storage Association (CCSA), CCS could reduce the wholesale price of electricity by 15 %, which would result in a £82 reduction per household electricity bills per year (by 2030) [TUC and CCSA, (2013)].

At the European Union (EU) level, The European Union's Emissions Trading Scheme (EU ETS) based on a "cap and trade" system has been under consideration for reform due to the lack of effective mechanisms to avoid making polluting cheaper than implementing carbon abatement technologies. The European Commission (EC) in 2014 opened a consultation period on the evaluation of the CCS Directive from 2009 [EC, (2014a)] and will present a report to the European Parliament by the time this thesis is submitted in Q1 2015. It is important to understand from a European perspective on CCS that on-shore storage of CO_2 does not have a clear framework to incentivise public acceptance, making CCS controversial in key European countries. The lack of a clear European wide CO_2 storage strategy [Shogenova et al., (2014)] has left only the UK (with post-combustion technology at Peterhead [Royal Dutch Shell, (2015) and SSE, (2015)] and oxy-fuel technology at White Rose [Capture Power Limited, (2015)]) and the Netherlands (with post-combustion technology at ROAD [E.ON and GDF Suez, ROAD Project, (2015)] as the two major countries with alive large-scale CCS projects plans as of the start of 2015. Off-shore CO_2 storage potential in the North Sea is the differentiating factor when compared to storage issues around CCS deployment in the continental power sector (e.g. Germany). The European

Commission has also opened a consultation on reforming the EU ETS Directive [EC, (2014b)] and a previous consultation on the EU CCS Directive. CCS project funding mechanisms have to be bankable [DECC, (2013b)] for the companies to be able to borrow capital at investable rates and to include the additional revenue stream on their balance sheets.

1.1.3. CCS as cohesion technology

CCS has a mixed perception among stakeholders [Johnsson et al., (2010)]. However, if CCS was not implemented in the UK Economy alone *"the cost of a low-carbon energy mix in 2050 would increase by 1 % of GDP or £30-40 billion per year"* [TUC and CCSA, (2013)]. If CCS is deployed in the UK gas and coal power stations, then its levelised cost of electricity (LCOE) could be around £100/MWh by the early 2020s, and at a cost significantly cheaper in the second tranche of the technology deployment thereafter, which means that CCS can be cost competitive with other forms of low carbon electricity [DECC, (2013b)].

Industry and jobs would be secured if CCS was to be applied at large scale as a low carbon technology option. With estimates of 10 to 20 GW of CCS installed capacity for 2020-2030 period in the UK [DECC EMR, (2014a)], *"assuming 20 plants, average construction employment would therefore be in the region of 24,000 a year. Longer-term operational jobs are anticipated to reach between 3,750 and 6,250 jobs/yr by 2030 (250 per installation), resulting in a total estimate of annual employment in excess of 30,000 by 2030 for 20 GW"* [TCU and CCSA, (2013)]. If 20 GW of CCS were installed by 2030, *"the cumulative value would reach £34.5bn with an annual market value of £5.8bn"* [TCU and CCSA, (2013)].

CCS is complementary to renewables and other Climate Change mitigation technologies. CCS is critical for decarbonising the power generation sector in a sustainable way where base-load dispatchability remains essential in a scenario with higher renewable penetration in order to contain wholesale electricity prices, as previously indicated. A good understanding of CCS cost estimates [e.g. Rubin, (2012)] is required. According to Morgan Stanley, (2014), if CCS is developed then levelised cost of electricity (LCOE) values, for projects starting in 2030, might be between £96/MWh for Advance Supercritical Coal (ASC) with oxy-combustion (cheapest for coal-CCS) and £108/MWh for Combined Cycle Gas Turbine (CCGT) with oxy-combustion (the most expensive for gas-CCS) as shown in Figure 1.7:

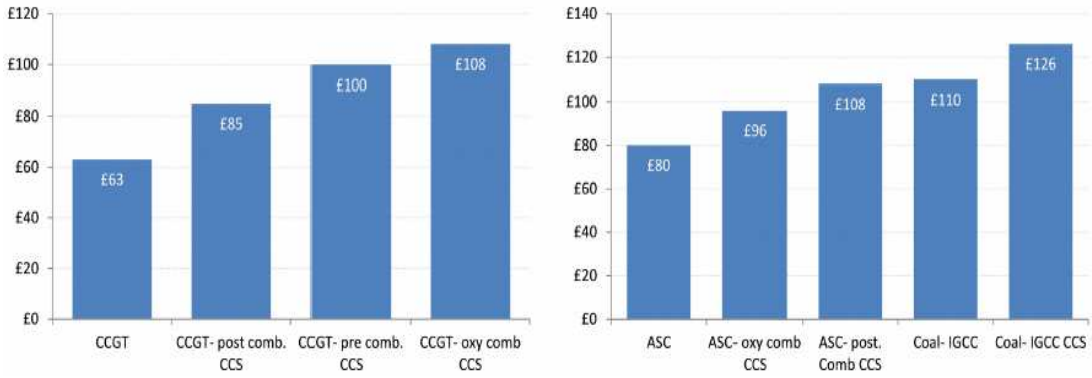

Figure 1.7. Levelised cost of electricity (LCOE) in £/MWh for new built gas (left) and coal (right) power stations in the UK in 2030 [Morgan Stanley, (2014)]

This is one of the examples of LCOE calculations, where an investment bank does not endorse any policy but gives an idea of CCS technology costs comparable to others at a critical point in time on the way to 2DS.

What is more important is the role that CCS can have in adaptation and potential impact on resilience building to Climate Change, an area that is usually neglected not just by policymakers but also by a significant part of the CCS community. Citing the IPCC, (2014c), report summary for policymakers, adaptation *"can reduce the risks of climate change impacts"*, and *"more immediate adaptation actions will also enhance future options and preparedness"* [IPCC, (2014c)]. Adaptation [IPCC, (2014a)] to Climate Change is becoming one of the major issues around member states willing to increment resilience on impacts of Climate Change and potential effects on increases in temperature, sea levels, food scarcity, weather anomalies and other catastrophic events. For instance, making mandatory the building of Carbon Capture Ready (CCR) plants [Gibbins et al. for IEA, (2007)] from 2015/2020 for adaptation to climate mitigation scenarios in the future would increase the resilience of economies willing to implement CCS in a later phase via retrofit [Gibbins et al. for IEAGHG, (2011)] if required for meeting climate targets or if a catastrophic event happened. Although completely non-related to Climate Change impacts, the Fukushima accident in Japan in 2011 showed how an energy system can come under unexpected stress if a primary energy source becomes unavailable, with the consequent need to turn to resources available at the time, in this case, unabated fossil-fuels to keep the economy going. This tragic event in Japan shows the key role for CCS in a limited nuclear energy and stringent climate scenario for sound energy and climate policies [Selosse et al., (2013)]. Building adaptation and resilience with CCS as part of the solutions equation is a

particularly interesting area that requires further work for capacity building collaboration between developed and developing countries in the context of Post-Paris agreement.

1.1.4. CCS in a new climate agreement

The 21st session of the Conference of the Parties to the UNFCCC (COP 21) and the 11th session of the Meeting of the Parties (CMP 11) to the 1997 Kyoto Protocol (COP 21 / CMP 11) will meet in Paris in late 2015 to draw up a new climate agreement after the late Kyoto Protocol (KP) first commitment period ended in 2012 and the proposed second commitment period by the Doha Amendment. Negotiations are currently on-going in the Ad Hoc Working Group on the Durban Platform for Enhanced Action (ADP), a body created as a mandate from decision 1/CP.17 in Durban COP 17 / CMP 7 in 2011. ADP negotiations are *"to adopt protocol, another legal instrument or an agreed outcome with legal force at the twenty first session of the Conference of the Parties and for it to come into effect and be implemented from 2020"* [UNFCCC, (2011)]. ADP has delivered a draft negotiating text [UNFCCC, (2015)] from COP 20 / CMP 10 in Lima 2014 and February 2015 Parties' negotiations at the Climate Change Conference in Geneva.

Member states are to announce pledges and their intended nationally determined contributions (INDCs) in the course of 2015. At the moment of writing this thesis the legal form of the actual document that will be delivered by the Parties in Paris is unclear and also the role of technology. However, the facts contained should be based on the science [IPCC, (2014c)] and an open framework is required for when CCS technology is ready for delivery because INDCs commitments are framed beyond 2020, when the second tranche of CCS should be deployed after the demonstration phase to meet 2DS. Negotiations are inclusive and require flexibility for each case and scenario, which means that leaving the door open for CCS with short-term drivers such as CO_2-EOR and BECCS [Zakkour et al., (2014)] in the 2020s is an option that could be valuable if exercising it is desired by some parties in the climate negotiations process. The narrative has to change with CCS as a legitimate option for a transition towards 2050 and beyond that should be kept open for constituencies willing to do so. Technology development in the 2020s would help implementation in the 2030s and should support the transition to a carbon neutral economy, compatible with economic growth and sustainable development, in the second half of this century.

Paris 2015 should be the first step in the right direction for delivering ambitious 2030 and 2050 targets on Climate Change mitigation, adaptation and resilience. Wider UN system involvement, by the International Monetary Fund, World Bank, and Central Banks to help in developing the right economic framework beyond the Green Climate Fund (GCF), for funding member states and collaboration between developed and developing countries according to common but differentiated responsibilities (CBDR) paying attention to their respective capabilities (RC), is much needed to solve the climate conundrum beyond this year's agreement.

1.2. Background to oxy-fuel combustion

There are three main Carbon Capture Technologies (CCT): pre-combustion, post-combustion and oxy-fuel, which are described in the literature [e.g. IPCC, (2005); Lucquiaud, (2013)]. The work described in this thesis would contribute to pulverised fuel oxy-fuel combustion safety and although some of the climate mitigation background has been discussed for CCS, this thesis will not attempt to cover pre-combustion or post-combustion. Oxy-fuel is the focus and the main characteristics of this technology are briefly explained in this section.

1.2.1. Introduction to pulverised fuel (PF) oxy-fuel combustion

The basics of PF oxy-fuel technology have been comprehensively reviewed in the literature [e.g. Wall et al., (2009); Toftegaard et al., (2010); Scheffknecht et al., (2011); Chen et al., (2012); Fujimori and Yamada, (2013)]. Oxy-fuel is a CCT that is based on coal/biomass combustion in enriched oxygen (O_2) atmospheres (generally assumed to be produced in a cryogenic Air Separation Unit (ASU) that also separates the nitrogen (N_2) which is not introduced in the oxy-fuel combustion atmosphere). The N_2 in the air in conventional PF boilers is replaced by CO_2 that is recycled back to the boiler from the flue gas, constituting the recycled flue gas (RFG). By recycling CO_2 the flame temperature is controlled in the combustion process but also CO_2 is concentrated which makes its separation downstream from other gases easier due to the higher partial pressures of CO_2 being present when compared to post-combustion technology. Oxy-fuel can be carried out in relatively conventional pulverised fuel (PF) or circulating fluidised bed (CFB) boilers. But as this thesis is focused on PF oxy-fuel from now on, all work will refer to this type of CCT. The CO_2 after a compression and purification unit (CPU) is expected to be of more than 95 % v/v purity with

an expected net efficiency penalty about 8-12 percentage points requiring between 21-35 % more fuel consumed for the same output [Scheffknecht et al., (2011)].

In Figure 1.8, a simplified (without De-NO_x unit) process flow diagram (PFD) for PF oxy-fuel is shown [Trabadela et al., (2012)].

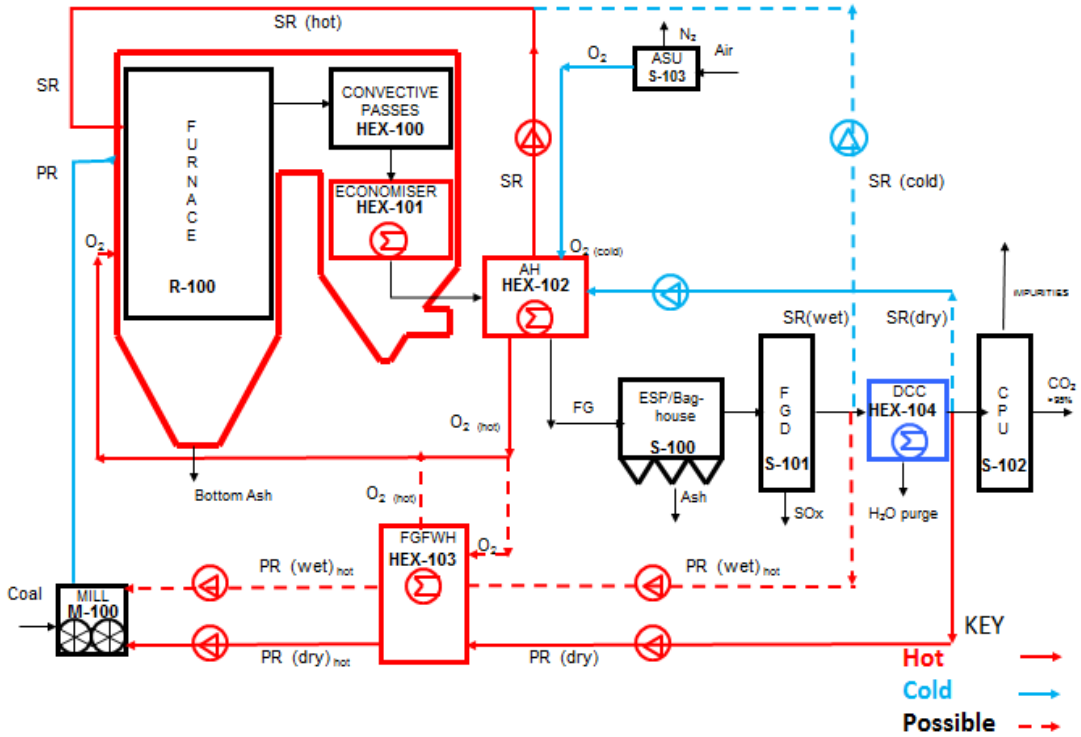

Figure 1.8. Oxy-fuel PFD with PF mill and primary recycle variability [Trabadela et al., (2012)]

The variability of options for recycling flue gas back to the boiler provides additional operational flexibility for PF oxy-fuel when compared to the air combustion case. After the flue gas ash has been separated in an electrostatic precipitator (ESP) or Bag-house filter, according to sulphur content *("0.2 wt. % to 11 wt. %"*) of the PF [Ahn et al., (2011), in most cases a flue gas desulphurisation unit (FGD) will be present to separate sulphur oxides (SOx) from the main flue gas stream. Immediately after the FGD a condenser or direct contact cooler (DCC) is placed for elimination of water. There is the possibility of recycling back a fraction of the flue gas directly into the boiler and this is named the secondary recycle (SR). SR can be recycled back at higher temperatures after (SR_{dry}) or before the DCC (SR_{wet}) using an air heater (AH) to improve heat integration. The main difference is that SR can be at higher temperatures, while the primary recycle (PR), which is going through the mill island

back to the boiler, will have a limited upper temperate due to fire risks and safety concerns in the PF milling stage. Key differences between the oxy-fuel and air case are not only the possibility of recycling flue gas, primary recycle (PR) versus primary air which is taken directly from the atmosphere, while controlling the temperatures but also the possibility of having higher O_2 level in PR passing through the milling stage, as discussed in section 1.2.3 of this thesis.

In oxy-fuel PF combustion, due to the presence of CO_2 and water vapour (H_2O) mixture when compared to N_2 in the air combustion case, CO_2 has a higher specific heat capacity and it is expected to have different heat radiation and absorption behaviour than air and the recycled flue gas (RFG) ratio and temperature adjustment it is the way to optimise firing operation in the PF oxy-boiler [Scheffknecht et al., (2011)]. Hence, this research on O_2 levels for milling in PF oxy-fuel has an indirect impact on oxy-burner and oxy-boiler behaviour for design and operation options.

The higher concentrations of NO_x and SO_x in oxy-fuel , 4-6 times greater for SO_3 according to Ahn et al., (2011), is another important characteristic of the technology that requires attention for the CO_2 purification and storage stages. Due to minimal levels of N_2 in the combustion atmosphere, net reduction of total NO_x produced is possible. However it is important to limit the NO_x concentrations due to higher lifetime exposure from RFG that can cause the corrosion of materials. A way to do this, that would avoid a Selective Catalytic Reduction (SCR) process, is reburning the NO_x which can achieve reductions between 50 and 80 % of the recycled NO_x [Normann et al., (2011)]. Reburning is more sensitive to temperature in oxy-fuel so controlling the combustion temperature and fuel characteristics will be important [Normann et al., (2011)]. In oxy-fuel, SO_x formation is affected by the presence of higher O_2 levels than in air combustion. SO_3 concentration is higher than in air combustion [Stanger and Wall, (2011)]. In the case of PF oxy-coal combustion pilot tests the concentrations of SO_3 and SO_2 were found to significantly higher than in air combustion [Ahn et al., (2011)] due to recycle and absence of N_2. The change in behaviour of mercury (Hg) and higher concentrations exhibited in flue gas [Jang et al., (2014)] with CO_2 recirculation causes Hg concentration, with consequent corrosion of heat exchangers and other equipment [Ting et al., (2014)]. Mercury management is also another important challenge in oxy-fuel when compared to air combustion that has been studied in the literature [e.g. Gharebaghi et al., (2011); Jang et al., (2014); Stanger et al., (2014) and López-

Antón et al., (2015)] to reduce its impact in the process. Mercury captured in a bag-house filter by ash reduces total Hg emissions [Spörl et al, (2014)] and the CPU can drastically reduce total Hg emissions downstream but it might be necessary for mercury to be mostly removed upstream to avoid corrosion damage in the compressors of the CPU [Mitsui et al., (2011)].

1.2.2. Key stages in PF oxy-fuel combustion

As for other CCTs, oxy-fuel has some key stages that define the technology development and the efficiency penalty associated with capture. The ASU and CPU are together the main penalty of CO_2 capture in oxy-fuel. In the case of oxy-fuel, the air separation process in the ASU is estimated to cause up to two thirds of the penalty and the remaining third would be caused by the compression and purification of CO_2 in the CPU [Perrin et al., (2015)]. For example, for a 500 MW_e power plant about 10,000 tonnes of O_2 would be needed to be produced on a daily basis [Higginbothan et al., (2011b)].

The Air Separation Unit, (ASU) is generally based on cryogenic separation of O_2 from N_2 and the process is well described in the literature [e.g. Dillon et al., (2005a); Dillon et al., (2005b)]. Energy requirements for the ASU will depend on the O_2 purity desired for the same amount of oxidant production. The O_2 needed is of low purity and at atmospheric pressure. O_2 is considered of low purity below 97 % when most N_2 is separated but argon (Ar) is present [Higginbotham et al., (2011)]. Ramping rates of the ASU for flexible oxy-fuel mode will also depend on the O_2 purity required. ASU technology is developing fast. In 2005 the power consumption for production of O_2 of 95 % purity at 1.6 bar (a) was 201.3 kWh/t [Dillon et al., (2005); Higginbotham et al., (2011)]. According to Perrin et al., (2015), separation with energy use of 140 kWh/t is to be achieved this year if heat integration is applied. The target for 2020 is 120 KWh/t as shown in Figure 1.9 [Perrin et al., (2015)].

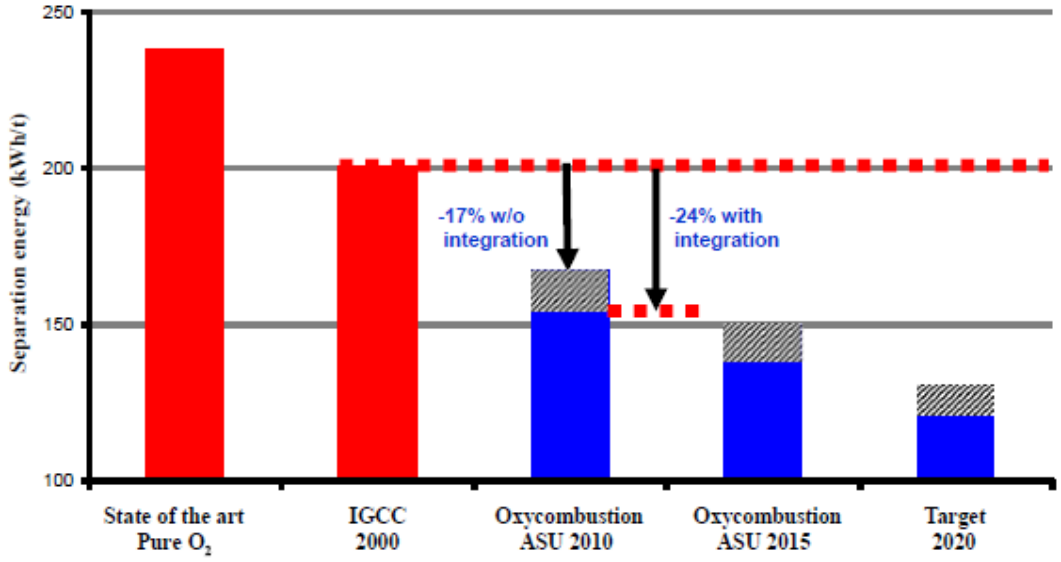

Figure 1.9. Improvements on energy efficiency in cryogenic ASU for oxy-fuel [Perrin et al., (2015)]

It is not the purpose of this thesis to comprehensively describe or study the ASU. However, it is considered important to show evidence that one of the most energy intensive processes in oxy-fuel combustion, O_2 production, has been progressing and it is expected to achieve greater energy reduction targets that will improve the overall efficiency of oxy-fuel for commercialisation in the 2020s. Beyond cryogenic production, Allam, (2009), described a new process for O_2 production with metal oxide ceramic membranes at high temperature (700°C) with the integration of a gas turbine at high pressure and temperature. Furthermore, new oxygen transport membranes (OTMs) for ceramic membrane separation methods for O_2 production are being developed and evaluated in studies [e.g. Castillo, (2011); Lobera et al., (2011); Schreiber et al., (2013)] for a later generation of oxy-fuel capture plants.

The Compression and Purification Unit, (CPU), is where the CO_2 after FGD and DCC stages is finally purified above 90 % v/v purity and compressed for further transport in supercritical conditions and subsequent storage. One of the interesting options becoming available is to compress CO_2 up to 30 bar in two stage compressor and use columns *"to remove SO_x and NO_x from the raw CO_2 stream by controlling the formation of acids, potentially saving expensive upstream"* separation options and consequences from corrosion [White et al., (2013)]. White et al., (2013) describe the sour process in Figure 1.10 in their paper directly

quoted: *"2-stage diaphragm compressor with an interstage cooler and condensate separator is used to raise the pressure of the flue gas to 15 bar, where it enters the first column. This 15 bar column is a packed column with condensate from the bottom being cooled and recirculated to the top of the column, to allow residence time and vapour liquid contacting for the sour compression reactions to occur. Additionally there is a small fresh water makeup stream entering the top of the column. The flue gas stream from the top of the column is then compressed in a single stage diaphragm compressor to 30 bar, before entering the second column also arranged with condensate recirculation and makeup water addition. On leaving the top of the 30 bar column the stream is dried in a Temperature Swing Adsorption unit (TSA) and passed to the low temperature part of the process"* [White et al., (2013)].

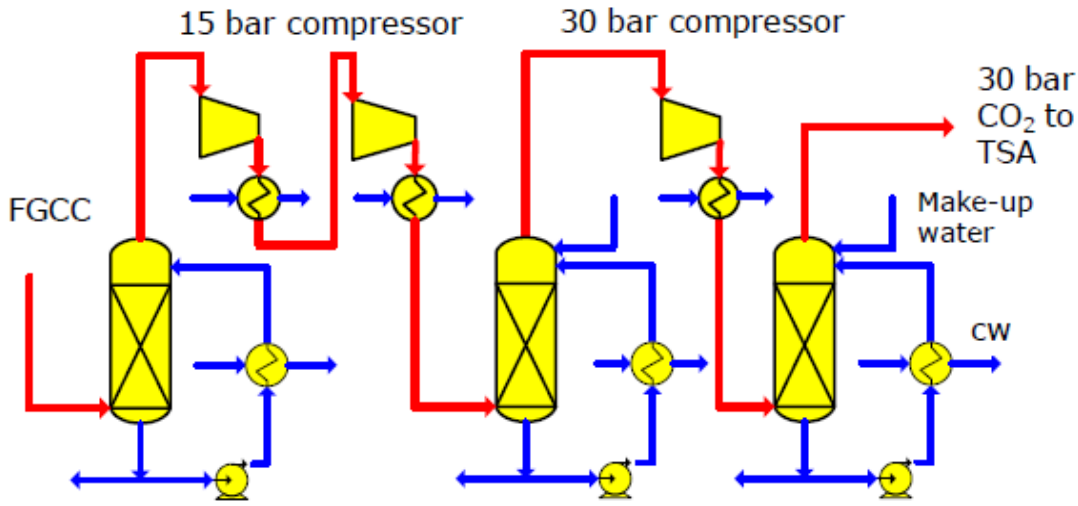

Figure 1.10. Sour Compression to 30 bar in CO_2 CPU developed by Air Products [White et al., (2013)]

The obvious potential given CPU developments is that by having this configuration SO_x and NO_x can be separated from CO_2 with potential savings on FGD/SCR units if no slagging risk is increased. In addition, after the CO_2 has been dried and compressed to 30 bar, the CO_2 can be purified with partial condensation using CO_2 as refrigerant instead of ammonia, introducing potential power reduction savings with the Auto-Refrigerated CO_2 Purification concept used in the Schwarze Pumpe Pilot plant in Germany [White et al., (2013)].

According to experience from a newly installed CPU at the Callide Power station retrofit in Australia, in general in oxy-fuel the reduction of the amount of flue gas to be treated (N_2

replacement by CO_2), allows for the FGD, if existing, to be downsized. NO_x emissions can be reduced because of the gas recirculation and decomposition of the NO_x in the reburning process as well as there being the option of removing it in the CPU [Komaki et al., (2014)]. The CPU in Callide was designed by Air Liquide to treat 75 tonnes of CO_2 on a daily basis [Lockwood et al., (2014)]. For larger scales, Air Liquide has developed the concept of coupled cryogenic purification combined with the use of a special ultra-CO_2 selective polymer membrane on the non-condensable phase of the gas treated to reduce O_2 and N_2 permeation in CO_2 processed in CPU. *"CO_2 permeates through the membranes and is then recycled to the main flue gas compression chain of the CPU in order to be condensed in the cold box with a recovery of 98 % for CO_2".* [Lockwood et al., (2014); Perrin et al., (2015)]. *"Increasing CO_2 recovery at CPU from 90 % to 98 % only increases marginally the cost of the CPU"* but could save between 5-10 % cost per ton of CO_2 captured [Perrin et al., (2015)].

PF combustion under oxy-fuel conditions is significantly different to the air case due to PF ignition and devolatilisation behaviour with the recycled streams in the oxy-fuel furnace. Modified air burners designs for oxy-fuel are under development and Fujimori and Yamada, (2013), described a swirling burner system developed by IHI. Direct O_2 injection is possible but the flame stabilisation will be mainly defined by fuel ingress through the burner with O_2 being injected on the boundary between PR and SR to reduce ignition delay and achieve stable combustion [Fry et al., (2011); Fujimori and Yamada, (2013)]. A two-stage hot gas recirculation flows scheme is shown in Figure 1.11, where "*the inner recirculating flow is formed inside of the outer recirculating flow by the swirling secondary combustion gas flow, and hot combustion gas is recirculated into the combustion chamber. The injected pulverized coal is preheated through mixing with the hot recirculating gas in the chamber. Through this preheating, the devolatilisation and the ignition are enhanced*" [Fujimori and Yamada, (2013)].

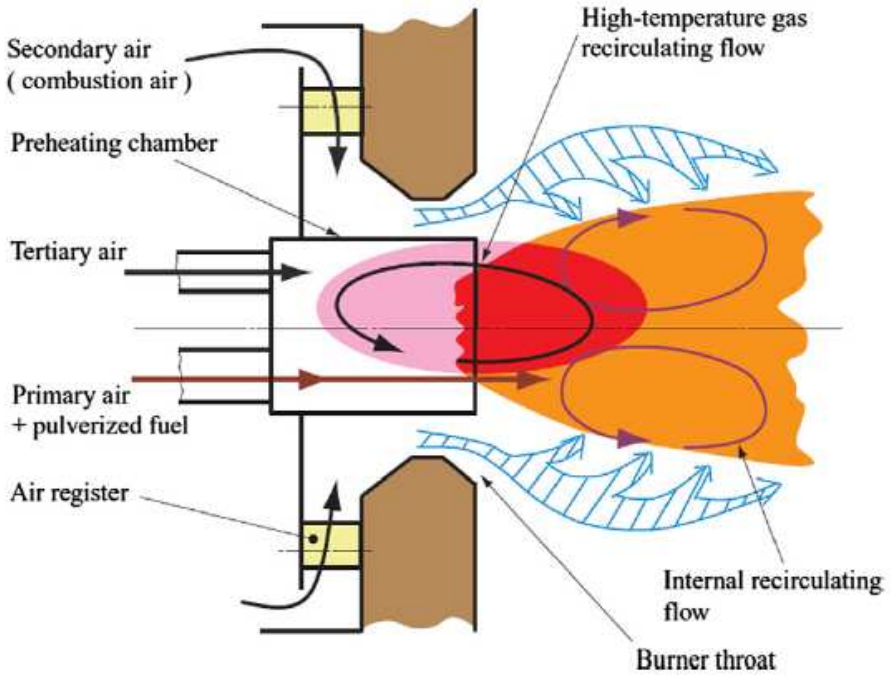

Figure 1.11. Schematic burner section of IHI high-temperature gas recirculation burner. [Fujimori and Yamada, (2013)]

Adiabatic flame temperature (AFT) is reached when all heat released from chemical reaction heats the combustion products and therefore the AFT value is directly affected by the final composition of the combustion products plus the heating value of the fuel and the amount of O_2 present [e.g. Liu et al., (2011)]. Theoretically a PF power plant with oxy-fuel combustion could operate at the same heat transfer rate as in air mode but would require changes in gas flow rate when compared with air firing, lower AFT and lower flue gas exit temperature, based on CFD modelling [Liu et al., (2011)]. Changes in the heat capacity (CO_2 presence versus N_2) and a higher gas emissivity in oxy-fuel impact the heat transfer in the combustion process but the objective in the oxy-fuel plant must be to match the heat output as in the air case by varying the recycle ratio (RR) to control AFT. It is not the purpose of this thesis to evaluate the operation of the oxy-fuel boiler but it is important to pay attention to theoretical AFT values expected when increasing O_2 levels in the combustion process. Liu et al., (2011) used CFD to calculate theoretical AFT for oxy-combustion upon recycle ratio (RR) of flue gas recycle. In Figure 1.12 theoretical variability of AFT upon flue gas recycling ratio (wet/dry) is shown.

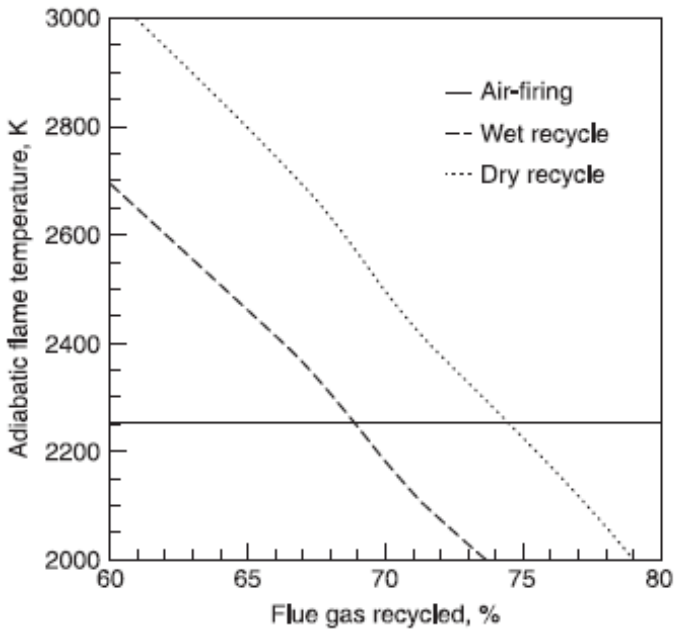

Figure 1.12. Adiabatic flame temperature (AFT) in oxy-fuel combustion upon flue gas recycling ratio (wet/dry) compared to air combustion case [Liu et al., (2011)]

As expected, dry recycle leads to higher AFT values. AFT monotonically decreases from above 3,000 K to below 2,000 K for a change in RR from 60 % from 80 % (Liu et al., (2011)] due to the heat capacity of CO_2 present at higher partial pressure in the furnace. A second order effect on the AFT is the potential temperature increase of RFG reintroduced with secondary recycle (SR) and further heat recovery when compared air combustion case. Bejarano and Levendis, (2008), reported theoretical calculations of Adiabatic Flame Temperature (AFT) for bituminous coal in air and oxy-fuel and compared them to experiments in a drop tube furnace (DTF) in O_2/N_2 and O_2/CO_2 varying O_2 partial pressure with wall temperatures between 1,400 and 1,600 K. Theoretical AFT were higher than these experimental values due to heat losses during measurement with a pyrometer [Bejarano and Levendis, (2008)]. A comparison by Bejarano and Levendis, (2008), of calculated adiabatic flame temperature and average measured volatile flame temperatures for 45–53 µm bituminous coal particles burning in O_2/N_2 and O_2/CO_2 is shown in Figure 1.13.

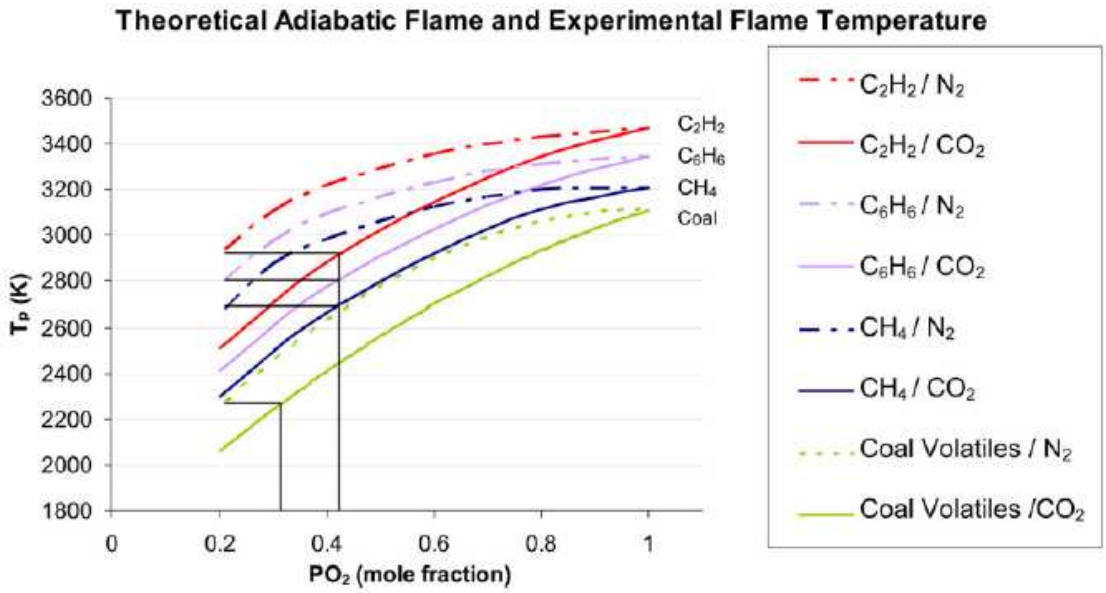

Figure 1.13. Comparison of calculated adiabatic flame temperature and average measured volatile flame temperatures for 45–53 µm bituminous coal particles burning in O_2/N_2 and O_2/CO_2 at $T_{furnace}$ = 1,400 K including AFT for methane (CH_4), acetylene (C_2H_2) and benzene (C_6H_6) as surrogate pyrolysis gases [Bejarano and Levendis, (2008)]

From the Bejarano and Levendis, (2008) figure above, the most relevant conclusion for PF oxy-fuel case, specifically for bituminous coal combustion and further ignition research in this thesis, is as cited by [Fujimori and Yamada, (2013)] that *"The flame temperature of the test coal in 21 % O_2 of a CO_2/O_2 mixture was 200–250 K lower compared to that in air, and the temperature in 30 % O_2 of the CO_2/O_2 mixture was equivalent to that in air*" [Bejarano and Levendis, (2008); Fujimori and Yamada, (2013)].

1.2.3. Safety in PF oxy-fuel combustion

As described by Trabadela et al., (2014), *"in oxy-fuel power plants the PR composition can vary significantly from one plant to another depending on a range of factors including chosen recycle strategy and interactions with other plant components. Fires in pulverised fuel (PF) mills are relatively common events in air-fired PF power plants. An important consideration in assessing combustion safety at power plants burning PF is, therefore, the potential for suspended PF ignition (colloquially known as a 'puff' in the UK) during milling (particularly during mill shut-down), which could lead to overpressurisation of mills and/or pipework"* [Trabadela et al.,(2014)].

Improved understanding of PF ignition under different conditions, comparing air and O_2/CO_2 atmospheres for a selected range of fuels including coal and biomass, is targeted in the present study. The objective is to *"determine which oxy-fuel power plant operating options provide process safety that is, at least, equivalent to conventional primary air PF milling in air-fired plants"* [Trabadela et al., (2014)]. The simplified PFD with PR for oxy-fuel with coal as a fuel is shown in Figure 1.14.

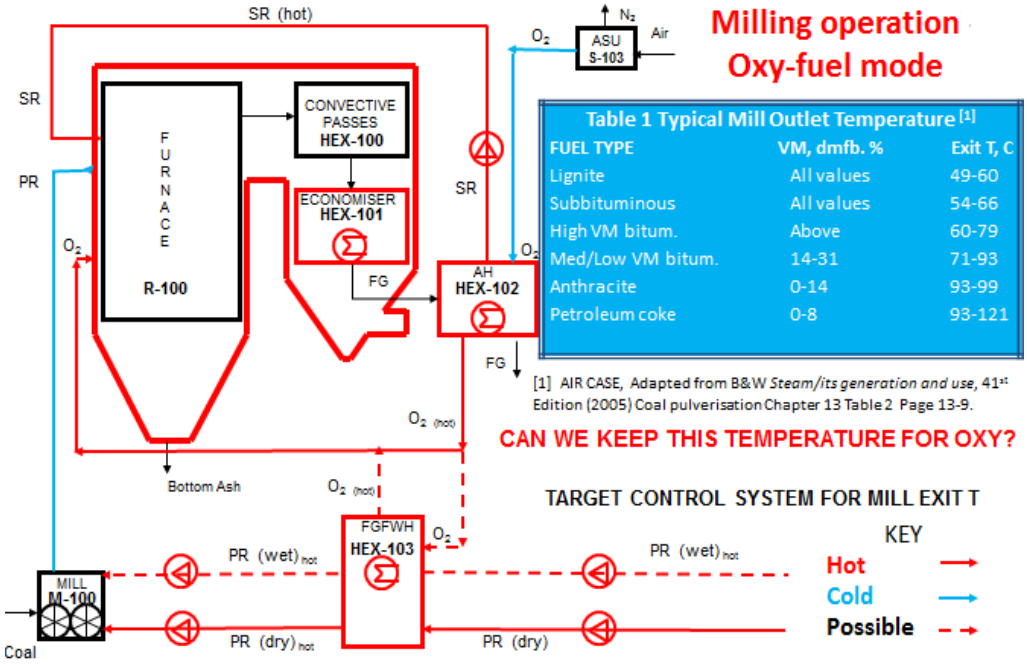

Figure 1.14. Oxy-fuel PF mill island with typical mill outlet temperature for air combustion [Trabadela et al., (2012)]

In air combustion PF power plants, the mill outlet temperature is measured as an indicator for potential fires in the mill operation. Typical mill outlet temperatures for air combustion case are shown in Figure 1.15 [B&W, (2005)]. These vary with coal rank, for instance, for higher rank fuels mill exit temperature could be in the range of 93-121 degrees Celsius. However, if the fuel was lignite, with higher volatile matter content, then the maximum temperature to operate safely would be 60 degrees Celsius. Biomasses mill exit temperature in PF milling in air are below those for lignite due to higher volatile content (>70 % VM). However, there is uncertainty as to whether temperatures would be the same for PF milling in oxy-fuel mode.

The main research problem in this thesis is therefore to experimentally determine the conditions of PF concentration, particle size and O_2 levels under oxyfuel conditions that give positive ignition at constant volume comparable to that in air (or which exhibit lower tendencies for ignition) in order to define conditions for the PF milling stage under oxy-fuel conditions that give comparable (or lower) ignition risks when compared to the air combustion case.

1.2.4. Flexibility and optionality in oxy-fuel

Flexibility in the electricity output from CCS systems is desirable to match electricity demand with a certain level of CO_2 emissions. Chalmers, (2010) and Chalmers et al, (2010), among others, have shown the importance of valuing CCS flexibility, in particular (for post-combustion capture plant) operational flexibility with solvent storage and CO_2 capture bypass options. Chalmers et al., (2010) specifically discuss "'*built-in' flexibility"* for investors when considering retrofitting a CO_2 capture system to a coal plant based on post-combustion capture versus unabated plants. Bruce et al., (2014), have shown the *non-linear interactions between flexible CCS plants and other energy vectors* for the British market case, where thermal plants with CO_2 capture will have to increase their operational flexibility requirements [Bruce et al., (2014)].

When comparing flexibility on CCT, Roeder et al., (2013) have shown that for a conventional 600 MW_{th} hard coal fired power station (600 °C and 285 bar steam), the plant net efficiency decreases with loading (45.2 % full load versus 41.6 % at 40 % load). When comparing CCT for 90 % capture rate and at least 96 % CO_2 purity compressed to 110 bar, for the same plant, oxy-fuel had a net efficiency of 36.6 % full load versus 34.7 % in PCC with MEA. Oxy-fuel plant exhibited 32.3 % net efficiency versus 30.2 % of PCC with MEA [Roeder et al., (2013)]. The difference in net efficiency in part load operation compared to other capture technologies is not very significant but oxy-fuel also exhibits the potential of energy storage with O_2 storage from the ASU introducing additional flexibility in the power generation with CO_2 capture when compared to the unabated plant. Potential for energy storage with liquid oxygen storage (LOX) from the ASU and CPU by-pass at high electricity prices adding operational flexibility in oxy-fuel has been described in the literature. For example, Perrin et al., (2015) described an energy storage solution being developed by Air Liquide, which mainly takes advantage of the unique opportunities in oxy-fuel for energy storage with multiple ASU in operation in combination with cryogenic liquids [Perrin et al., (2015)].

Specifically on oxy-fuel operational mode, Kuczynski et al., (2011) have shown with dynamic modelling work that oxy-fuel *"may provide an opportunity to improve plant flexibility and both primary and secondary response, a capability which is of increasing importance as the mix of conventional, nuclear and renewable generation changes"* [Kuczynski et al., (2011)]. Fuel flexibility with the higher O_2 available in oxy-fuel improving combustion of a broader range of fuels than in air is also a clear example of specific technology flexibility. Pressurised oxy-fuel, where fuel and oxidant streams are pressurised to increase heat transfer while reducing size of equipment [e.g. Hong et al., (2010); Clements et al., (2011)] can also be ideally flexible to thermal load, with increased heat recovery while keeping supercritical operation over a wide range of operational loading [Zebian and Mitsos, (2014)].

Optionality is an economic and financial concept accounting for capital expenditure (CAPEX) and operational expenditure (OPEX) where both of them play a decisive role in order to make an investment decision among a range of different choices (options) available. Options can be used to evaluate or hedge investment opportunities in a context of uncertain future scenarios in energy prices, energy policy and climate policy and some work has been published in the literature for power generation [e.g. Yang et al., (2008)]. Generally, flexibility changes in each capture technology, i.e. oxy-fuel, in a broader market context, and optionality is project specific in a local market. Differences between both concepts are summarised in Table 1.2 where a trade-off between engineering and economics is required before a project is built.

Table 1.2. Flexibility versus optionality in an oxy-fuel plant [Trabadela et al., (2012)]

FLEXIBILITY	OPTIONALITY
• Engineering term.	• Economic/financial term.
• Capture plant operation.	• Accounts for CAPEX/OPEX.
• Electricity output.	• Investment decision (options).
• Variable to each capture technology.	• Project specific.
• Broader market context.	• Local market.
FLEXIBILITY FACTORS:	OPTIONALITY RESTRICTIONS:
1) Recycles.	1) Capital: public or private.
2) Process Safety.	2) Market regulation (revenue from CO_2 capture).
3) Ramp rates.	3) Plant location (CCUS/EOR).
4) Transient operation.	
5) CO_2 Capture levels.	
Engineering/Economics trade-off is required.	

A particular example of options is where location should not be an applicable restriction, and it is up to a utility company to make a decision about building a new capture ready plant or a new built plant with CCS. It will be down to restrictions of capital (CAPEX availability) and market regulation to go for the first option, OPEX affordable, or the latter, OPEX affordable and less restrictions on CAPEX and regulation.

1.2.5. Key Oxy-fuel projects in the world in the early 2010s

At the end of the decade 2000-2010, the Global CCS Institute (GCCSI) estimated that only about 10 % of the active CCS projects were oxy-fuel projects, numbering 14 projects in total [GCCSI, (2009); Wall et al., (2011)]. The main oxy-fuel active pilot plant projects have been described by Wall et al., (2011). At the start of 2015, the global picture of active large scale oxy-fuel projects [GCCSI, (2014)] has not changed much but progress has been made with a pilot 30MW_{th} lignite oxy-fuel in Schwarze Pumpe, Germany and a 30 MW_e retrofit PF oxy-fuel boiler in Callide, Australia. Future large scale projects, such as the proposed new build PF oxy-fuel in White Rose, UK, are expected to change the trend in the oxy-fuel technology roll-out.

Schwarze Pumpe CCS plant, owned by Vattenfall Europe, started operation with a "*30 MW_{th} OxyCoal^{TM} burner designed, manufactured, installed, commissioned"* and tested by Doosan Power Systems [Sturgeon et al., (2013)]. The progress of the project has been described in the literature [e.g. Strömberg et al., (2009); Anheden et al., (2011)] with interesting results on FGD performance, showing that CO_2 higher partial pressure (>90 % v/v dry) did not have any major impact on high removal rates of SO_2 [Faber et al., (2011)]. The Callide Oxy-fuel Project [Wall et al., (2009); Uchida et al., (2013)] is a retrofit of an existing coal power plant of 30 MW_e capacity, with the capacity of producing 330 tonnes of O_2 per day (with two ASU) and compressing/purifying 10 % of the total flue gas, i.e. 75 tonnes of CO_2 per day in one CPU [Komaki et al., (2014); Lockwood et al., (2014)]. At Callide RFG was used to dry and transporting the coal (3 mills and six burners, with 2 mills and 4 burners normally in operation), with a supplementary dehydration system in the PR to prevent low acid dew point corrosion [Komaki et al., (2014)]. Although it is possible to increase mill outlet temperature in oxy-fuel and avoid having to add a dehydration process, at Callide this was not the preferred option [Komaki et al., (2014)], in addition no O_2 was added to the PR but only to the SR, so O_2 present in the milling stage is just the excess O_2 in the RFG from after the combustion process, to lower risk of ignition in the mill [Spero, (2013)]. Presumably

partially to offset the lack of O_2 in the PR, direct O_2 injection into the flame was possible with O_2 lances [Komaki et al., (2014)].

The FutureGen 2.0 project was being developed in Illinois (USA) by "the Alliance", Ameren Energy Resources as a retrofit to an existing coal fire power station. FutureGen 2.0 would have had 168 MW_e output when coal-fueled oxy-combustion technology was implemented. High-sulphur bituminous coal from Illinois (60 per cent) and low-sulphur Powder River Basin coal from Wyoming (40 per cent) blends would have been fired in the system. The capture plant was expected to capture at least 90 per cent of the CO_2, totalling 1.1 Mt per year of CO_2 [GCCSI, 2015)]. The captured CO_2 was to have been compressed and transported via a new 45 km / 28 mile, 10-inch diameter underground CO_2 pipeline from the Meredosia Energy Center to the geologic storage area in eastern Morgan County. The estimated purity level of the CO_2 is at least 97 per cent. Unfortunately at the time of submitting this thesis, the US Department of Energy (DOE) had recently announced the suspension of the federal funding for FutureGen 2.0.

The White Rose Carbon Capture and Storage Project (White Rose CCS Project), [Capture Power Limited, (2015)], at the time of writing this thesis, was being developed in Selby, Yorkshire (UK), by Capture Power Limited, with Alstom, Drax and BOC as project partners in the consortium. White Rose was selected as preferred bidder by DECC as one of the two projects for the UK CCS Commercialisation competition [DECC, (2013a)], and the only one in the NER 300 EU funding scheme. Capture Power signed the Front End Engineering Design (FEED) study contract with DECC in December 2013. The Final Investment Decision is expected in late 2015 [Capture Power Limited, (2015)].

White Rose plans consist of a 426 MWe gross output new coal-fired ultra-supercritical (279/52 bar, 600/620 °C) coal fired power plant [Levasseur et al., (2014)], with the option of co-firing biomass, that is linked to a full CCS chain. National Grid would build and manage the operations of the CCS Humber cluster pipeline, transporting CO_2 over 100 miles to off-shore storage in a deep saline formation in the North Sea [Capture Power Limited, (2015)]. It is expected that above 300 MW_e clean power will supply electricity to 630,000 homes with 100 % flue gas treated, 90 % CO_2 capture rate with a total of 2 million tonnes per year. The project infrastructure for CO_2 transport and storage would develop a transportation and storage network in the Yorkshire and Humber area, with a trunk line sized for 17 Mt per year CO_2 enabling the start of a CO_2 cluster in the Humber region which emits 60 million

tonnes of CO_2 per year or 20 % of all UK CO_2 [Hackett, (2014)]. The White Rose CCS project lay-out next to Drax Power station and ultra-supercritical boiler are shown in Figure 1.15 and Figure 1.16 respectively.

Figure 1.15. Indicative illustration of Drax Power Station (left) and the White Rose CCS project (right) [Capture Power Limited, (2013)]

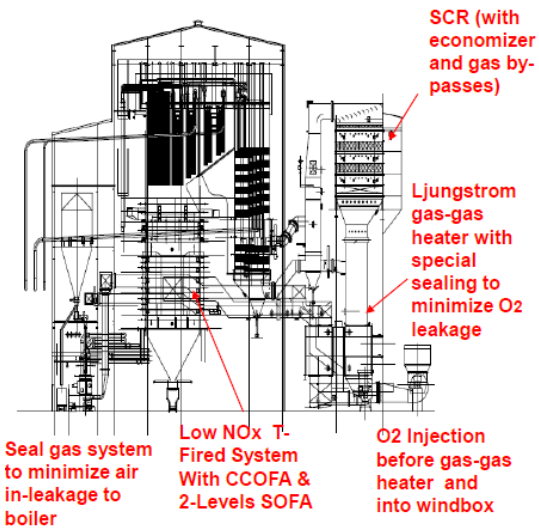

Figure 1.16. Boiler design by Alstom expected at White Rose [Levasseur et al., (2014)]

The project is expected to be decisive, as the first new built full CCS chain project with oxy-fuel to prove CCS technology at commercial scale, and would demonstrate oxy-fuel as a competitive form of low-carbon power generation and as an important technology in tackling climate change [Capture Power Limited, (2015)].

From the perspective of the research presented in this thesis, at the time of submission the FEED was not finished for this project and no information was available due to commercial sensitivity. If results arising from this PF mill safety research could be developed on site and applied in future stages (e.g. to PF milling strategy) in the White Rose project to develop a final design of the plant and provide useful information of potential operating mode of PR with potential addition of O_2 in safe operation in the new oxy-fuel plant, that would notably increase the research impact of this work, which is briefly presented in the final section of this chapter.

1.3. Academic contribution and Research Impact.

1.3.1. OxyCAP UK project

The Oxy-fuel Academic Programme for the UK (OxyCAP UK) was a £2 million research consortium (2009-2014) co-sponsored by the Engineering and Physical Science Research Council (EPSRC), (grant EP/G062153/1), and E.ON. Seven universities (Cambridge, Cranfield, Edinburgh, Imperial College, Kent, Leeds, Nottingham) and other industry stakeholders were among the research project partners. The main objective of the project was to develop fundamental research capability for oxy-fuel combustion as a carbon capture technology in five key areas: 1) new experimental techniques for oxy-fuel combustion; 2) advanced computer modelling techniques; 3) experimental data on coal ash and boiler material behaviour under oxy-fuel conditions; 4) UK capacity in oxy-fuel fluidized bed combustion; and finally 5) training and development of new researchers [EPSRC-E.ON, (2009); Chalmers et al., (2014)]. The Project met biannually for reporting on progress and activities to a Project Advisory Board. For the author this was an experience that enhanced the learning process in the Ph. D. studies.

Chalmers et al., (2014), describe the main highlights and results of the OxyCAP UK project up to late 2014, with emphasis on being able to operate under close to real operational oxy-fuel conditions at the "*developed a 250 kW Combustion Test Facility (CTF), … part of the*

UK CCS Research Centre PACT (Pilot-scale Advanced Capture Technology)" [UK CCS Research Centre PACT, (2015)] and the "*100kWth coal/biomass rig at Cranfield University that is also part of the UKCCSRC PACT facilities"* [Chalmers et al., (2014)]. Academic impacts of the OxyCAP UK project were qualitatively explained by Trabadela, (2012) in Figure 1.17.

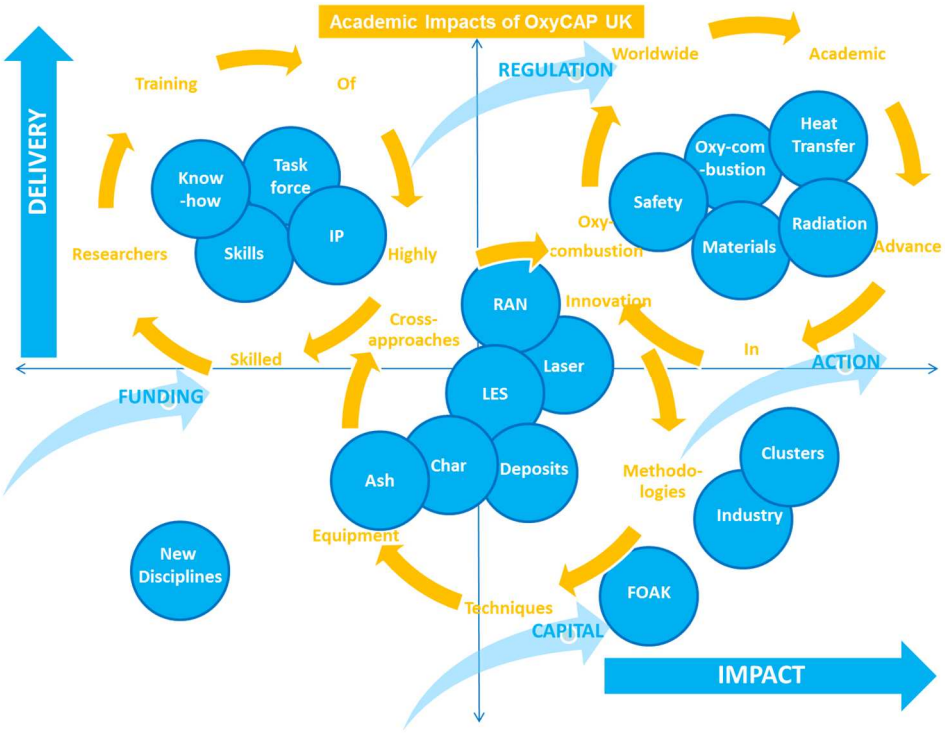

Figure 1.17. Academic Impacts of OxyCAP UK project [Trabadela, (2012)]

There are three main areas affecting OxyCAP UK Academic Impacts:

a) Worldwide academic advances in oxy-combustion, for example, safety studies, heat transfer improvements, new materials development, and understanding of radiation and oxy-fuel combustion fundamentals [e.g. Balusamy et al., (2013); Jurado et al., (2013); Farrow et al., (2013); Trabadela et al., (2014)]. This area should lead to a second generation of oxy-fuel combustion technology to be deployed in power stations around the world in the next decade.

b) Innovation, methodologies, techniques, equipment and cross-cutting approaches, examples being: ash properties studies, char analysis, deposits evaluation, RAN, LES and Laser imaging [e.g. Black et al., (2013); Franchetti et al., (2013), Hossain et al., (2013);

Clements et al., (2015)]. Most of them are the core of the new IP and know-how that could be shared and exported.

c) Training of highly skilled researchers, which leads to a task force with a set of transferable skills and know how (IP) that can be hardly replaced and that represents the competitive advantage of the country in a privileged position in the global oxy-fuel technology roll-out. Hence, the OxyCAP UK project has put in place a taskforce of researchers for coming oxy-fuel projects.

The level of delivery and impact of all the above is extremely variable and depends upon: continuation of public funding, clear and stable technology regulation, private capital investment and immediate and steady action by all stakeholders involved. If there is a close interaction with industry, new disciplines can be advanced that will enable the First of a Kind (FOAK) oxy-fuel plant in the UK (White Rose) and consequent development of the oxy-fuel and carbon capture industry. A key strategic approach for a decisive and successful action is the creation of clusters in order to concentrate projects where industrial clusters will have to necessarily be complemented by technology hubs or centres (the UKCCSRC being an example) where research output is maximised and international cooperation with strategic partners is possible.

On the particular case of the individual research presented in this thesis, the highlights for impact are:

1) To the author's knowledge these are the first results published on biomass ignition in oxy-fuel atmospheres in a constant volume ignition chamber (a specific purpose built and designed 20 litre design (R-20) for PF oxy-fuel milling safety, with the development of an additional 30 litre ignition chamber (R-30)).

2) The science behind the dust experimental methodology in ignition chambers is being evaluated with the potential in the future to develop a system that could provide additional information for oxy-burner development.

For the impact to be enhanced, it is desirable that this work would be continued under realistic plant operation conditions complemented by modelling work and with broader collaboration between the coal dust science experts and the oxy-fuel community.

1.3.2. BECCS and Bio-CCS

According to the IEA by 2050 bioenergy could provide about 8 % of world electricity generation or 3,100 TWh of electricity [IEA, (2012)], while bioenergy is estimated by the International Renewable Energy Agency (IRENA) to be providing about 60 % of the total final renewable used by 2030 [IRENA, (2014)]. The global biomass supply could be in the range of 97-147 Exajoules (EJ) per year [IRENA, (2014)]. According to the IEA in their 2014 World Energy Outlook (WEO), bioenergy could provide 1,933-2,535 million tonnes oil equivalent (Mtoe) by 2040, representing a similar primary demand to coal, in their 2DS or 450 ppm CO_2 scenario [IEA WEO, (2014)].

Biomass and bioenergy future demand gives the potential to deploy bio-CCS [e.g. Arasto et al., (2014); Tanaka et al., (2014)] and bioenergy with CCS or BECCS [e.g. Vergragt et al., (2011); Laude and Jonen, (2013)] for achieving negative CO_2 emissions. But the benefits of Bio-CCS have further implications. For instance, specifically on oxy-biomass, Pickard et al., (2013) showed the potential for not just achieving negative CO_2 emissions but "*reducing NO_x emissions"* with "*higher combustion efficiencies"* in experimental tests in a 20 kW furnace when co-firing coal and biomass [Pickard et al., (2013)]. "*Biomass can be co-fired with coal in PF boilers or, usually with some derating, on its own. Currently, only conventional air-firing is used, but in the future carbon capture and storage (CCS) may be applied to biomass utilisation in order to obtain potentially negative emissions"* [IEAGHG, (2011); Trabadela et al., (2014)]. Further details on the oxy-biomass technology are discussed in Chapter 2 of this thesis.

From the author's perspective, the technical challenges are there and they can be tackled. However, if a sustainable supply of biomass feedstock is not achieved, the potential for Bio-CCS and BECCS will be much reduced to limited markets where indigenous biomass would be available. This is much discussion around the CO_2 emissions due to biomass transport and deforestation and to land-use. IRENA showed in Figure 1.18 the supply and demand framework for bio-energy, where "*biomass energy comes from two different sources. One is primary bioenergy, which uses farmland or forests to produce biomass and the other is biomass residue, which is generated as a by-product of food or wood products throughout their supply-consumption chain*" [IRENA, (2014)].

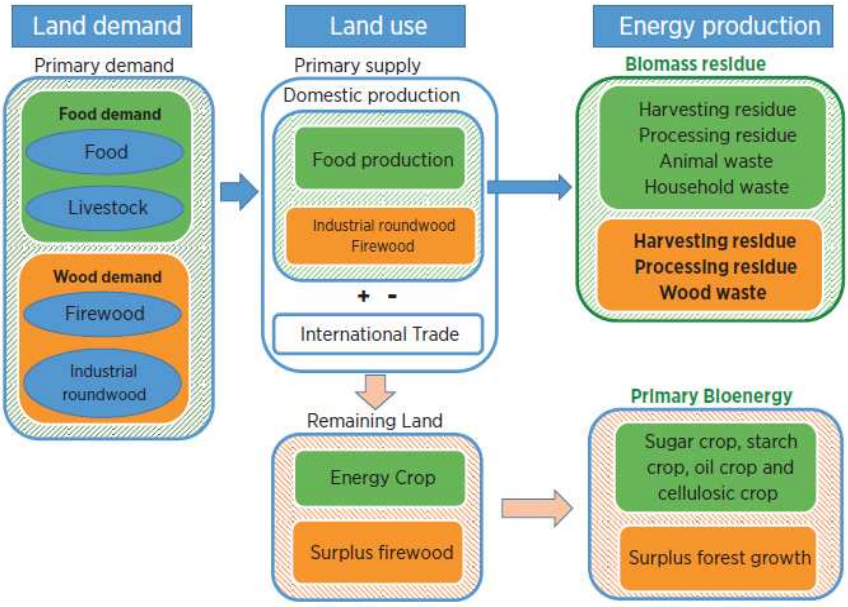

Figure 1.18 Supply and demand framework of bio-energy [IRENA, (2014)]

Land use and deforestation is a major factor in Climate Change that has to be carefully taken into account when assessing biomass options in the power sector that could compete with the CO_2 emissions reduction from forestry activity and with the food supply industry as they use the same land. This is why, from the author's perspective, a combination of vertical farming [Despommier, (2010); Despommier, (2013)] with BECCS (VF-BECCS) would help to create sustainable BECCS alternatives to the use of fossil fuels in the power sector with the potential for CO_2 utilisation. VF-BECCS is clearly out of the scope of this thesis but the author reserves the right to detail this concept in coming publications as a way to securing feedstock, reducing biomass carbon footprint, large scale CO_2 utilisation, achieving negative CO_2 emissions and enhancing economic and societal synergies in the food and energy sectors, both critical for Climate Change adaptation, mitigation and resilience.

Finally, if it was not because of the bigger picture that has been explained in this chapter, there would be not much economic and societal interest beyond the scientific scope of this work. Designing and building a new type of 20 litre ignition chamber (R-20) extensible to 30 litre (R-30) for applied science on coal and biomass dust ignition experiments under O_2/CO_2 atmospheres to safely developing oxy-fuel as one of the technology options available for CCS for Climate Change mitigation is the fundamental objective of this work.

2. Coal and biomass as pulverised fuels in the power sector

In this second chapter the importance of coal and biomass as pulverised fuels in the current power sector and in the future decades is briefly explained. The International Energy Agency (IEA) in their World Energy Outlook (WEO) latest report published in 2014 affirms that *"the power sector is leading the transformation on global energy"* [IEA WEO, (2014)]. Electricity produced is growing faster than any other form of energy and 7,200 Gigawatts (GW) of capacity are expected to be built by 2040 to replace 40 % of the ageing fleet and to cope with the increasing demand [IEA WEO, (2014)]. There is a motivation to move away from unabated coal by switching to biomass for achieving near neutral CO_2 emissions or potentially negative if CCS is deployed for Climate Change mitigation, as explained in the previous chapter. Despite worldwide changes in power generation, and it being the sector in the economy responsible for the major reduction in the share of fossil fuels [IEA WEO, (2014)] with the renewables penetration, coal is still expected to be widely used in the power generation sector [IEA WEO, (2014)]. In Figure 2.1 different IEA scenarios, depending on the energy and climate policies, are presented.

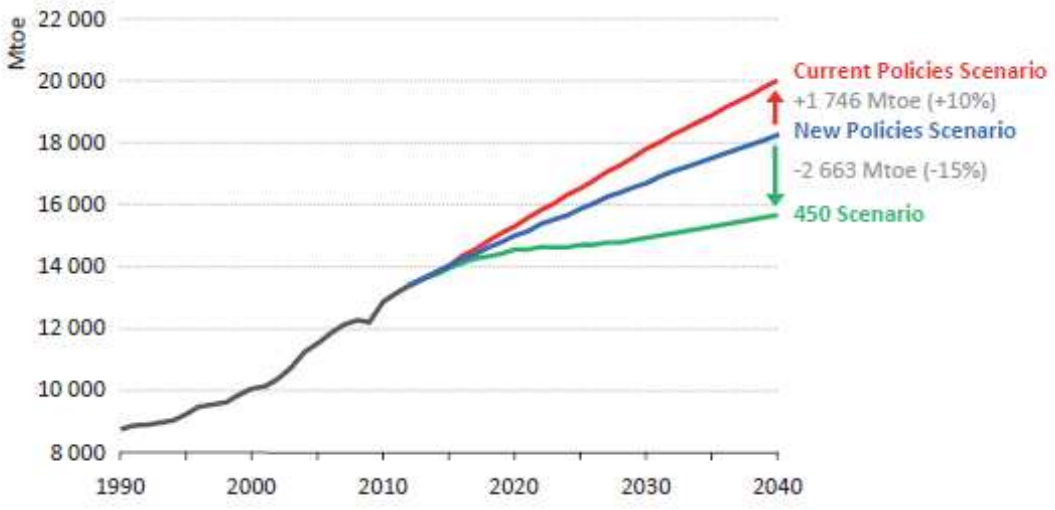

Figure 2.1. World total primary energy demand by scenario [IEA WEO, (2014)]

Current Policies Scenario is the business as usual case, the 450 Scenario is the most strict with CO_2 concentration according to 2DS, and takes into account the limited budget of approximately 1,000 Gigatonne of CO_2 that can be emitted from 2014 onwards [IPCC, (2014c), IEA WEO, (2014)]. This budget would be completely used by 2040 according to the

New Policies Scenario by IEA. In Figure 2.1 [IEA WEO, (2014)] a significant decrease in the demand of primary energy can be observed for the 450 Scenario.

The share of fossil-fuels in the last three decades has remained constant and, despite it being expected to fall in all three scenarios considered, fossil fuels will still be dominant in 2040. In all of the scenarios evaluated by the IEA, the share of fossil fuel is too important to be ignored. *"Their share falls from 82 % in 2012 to 80 % in the Current Policies Scenario, to 74 % in the New Policies Scenario and to below 60 % in the 450 Scenario"* [IEA WEO, (2014)]. If CCS was not implemented the transition to a low carbon economy would be significantly more difficult as complete fuel switching from fossil-fuels will not happen before 2040. Table 2.1 below shows that even in the most restrictive scenario for emissions with ambitious climate policies, 2,590 million tonnes of oil equivalent (Mtoe) of coal would be used by 2040 [IEA WEO, (2014)]. It is important to note the significant demand increase of bio-energy up to 2,535 (Mtoe) for best case scenario, as it is very relevant for potential impact of this research on oxy-biomass ignition for the development of bioenergy with CCS (BECCS).

Table 2.1. World total primary energy demand by fuel and scenario in Mtoe (million tonnes of oil equivalent), [IEA WEO, (2014)]

		New Policies		Current Policies		450 Scenario	
	2012	2020	2040	2020	2040	2020	2040
Coal	3 879	4 211	4 448	4 457	5 860	3 920	2 590
Oil	4 194	4 487	4 761	4 584	5 337	4 363	3 242
Gas	2 844	3 182	4 418	3 215	4 742	3 104	3 462
Nuclear	642	845	1 210	838	1 005	859	1 677
Hydro	316	392	535	383	504	392	597
Bioenergy*	1 344	1 554	2 002	1 551	1 933	1 565	2 535
Other renewables	142	308	918	289	658	319	1 526
Total	13 361	14 978	18 293	15 317	20 039	14 521	15 629
Fossil fuel share	*82%*	*79%*	*74%*	*80%*	*80%*	*78%*	*59%*
*Non-OECD share***	*60%*	*63%*	*70%*	*63%*	*70%*	*63%*	*68%*

* Includes traditional and modern uses of biomass. ** Excludes international bunkers.

In Figure 2.2 from the same IEA report, proven coal reserves are available for the longest when compared with uranium for nuclear power, oil and natural gas. Reserves of coal as of 2012 are over 1,000 billion tonnes for over 135 years at the current rate of coal consumption [IEA WEO, (2014)] and the total remaining recoverable resources are in the

range of thousands of years. The lifetime of coal in the power sector and our current economic model is not depending on scarcity but on the Climate Change problem and whether or not coal can be used in a sustainable way with CCS in a transition towards a carbon neutral economy.

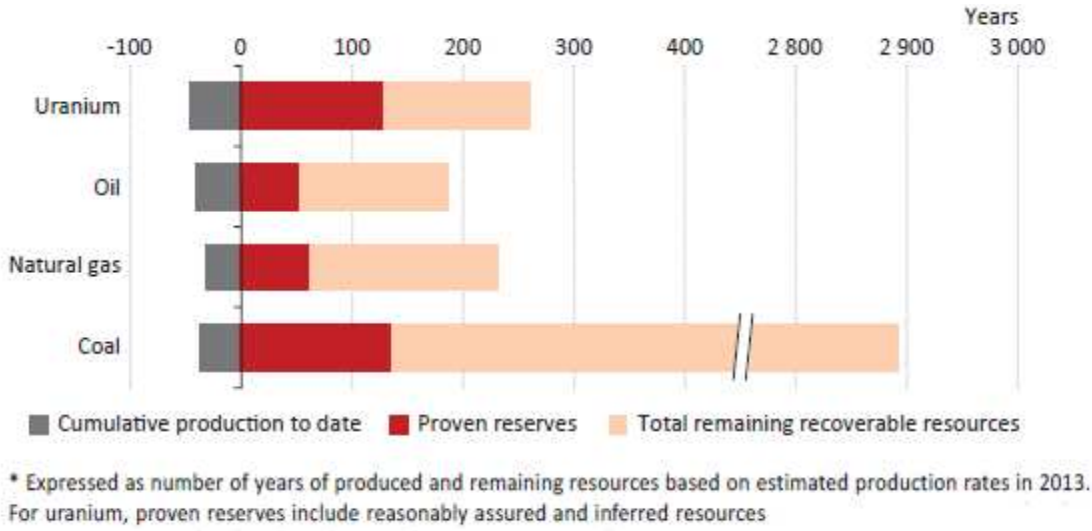

Figure 2.2. Lifetimes of fossil-fuel and uranium resources [IEA WEO, (2014)]

There is abundant coal available for the future, the question is if the market for pulverised fuel power plants in the electricity generation sector will be shaped by the Climate Change problem. For the moment, many countries have decreased the amount of coal used in their power sector (e.g. USA) using renewables and natural gas and others such as China have announced that they will *"replace coal usage with alternative energy sources in heavily polluted areas"* [Reuters, (2015)] and *"reduce emissions per unit of economic output by 3.1 %"* [The Climate Group, (2015)].

2.1. Coal and biomass markets as pulverised fuels in the power sector

In this section, a brief update on coal and biomass markets for electricity generation in the world and in the UK is given, with particular attention, to the expected share of coal in the generation mix.

2.1.1. Coal market as pulverised fuel in the power sector

Coal remains the world second largest energy fuel (after oil) representing a 29 % share of the global primary energy mix, increasing 5 percentage points in the period (2003-2013) [IEA WEO, (2014)]. The continuation of the use of coal will depend on how CO_2 emissions

are tackled. Coal demand is expected to growth 15 % by 2040, "*but almost two-thirds of the increase occurs over the next ten years"* [IEA WEO, (2014)].

Coal markets have changed substantially in the last two decades with many countries switching to cleaner fuels or renewables sources for power generation. China has become the largest user of hard coal for electricity generation (53 %), second in 1990 (18 %), while the USA first in 1990 (28 %) now only accounts for 9 % of the total use of hard coal for electricity generation [DECC, (2014c)]. Figure 2.3 shows the change in the use of hard coal for electricity generation from 1990 to 2012 [DECC, 2014c].

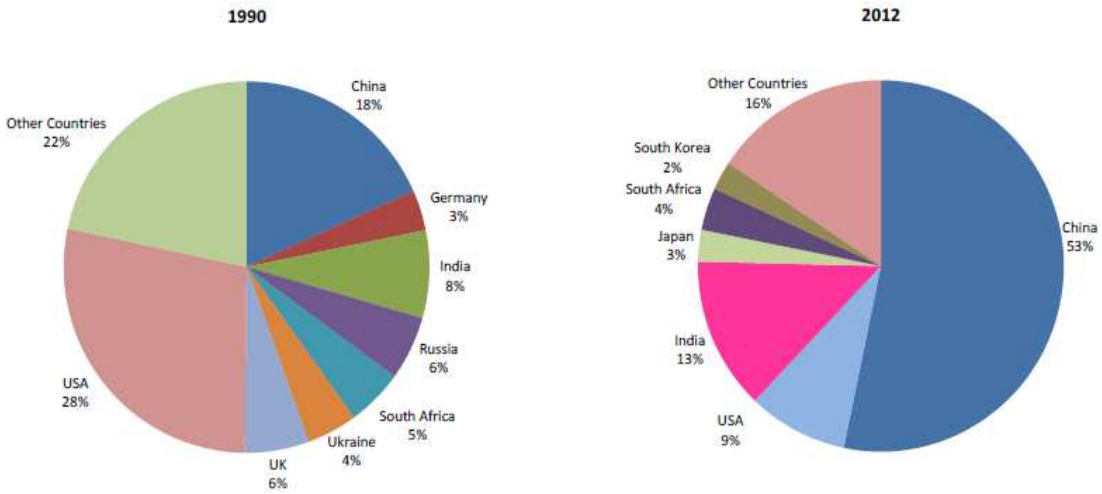

Figure 2.3. Comparison of global hard coal used for electricity generation in 1990 and 2012 [DECC, (2014c)]

China is expected to reach a plateau around 50 % of global coal consumption, fall after 2030 and to be surpassed by India as the world's larger coal importer before 2040 while the United States demand as well as that of the other OECD countries will continue to decline [IEA WEO, (2014)]. Prices are shaping the current markets, with current low prices adding pressure on producers to reduce costs of production. However, "*the shedding of high-cost capacity and demand growth are expected to support an increase in price sufficient to attract new investment. China, India, Indonesia and Australia alone account for over 70 % of global coal output by 2040, underscoring Asia's importance in coal markets."* [IEA WEO, (2014)].

Many countries in Europe with subsidised coal mining industries will lead in the closure of high cost coal production areas. In 2013, the most recent full year of DECC statistics at the

time of submitting this thesis, for the UK electricity generation market (85 GW total capacity), coal represented 36 % (132 TWh) of total demand (317 TWh) reduced from previous year, mainly due to an increase in share of renewables (15 %) and the closure of several power stations (e.g. Cockenzie and Didcot A) [DECC, (2014d)]. About 50 million tonnes of coal were used in 2013 by UK power stations to produce the amount of electricity supplied but indigenous coal production in the UK fell to a new low record in 2013 (12.8 million tonnes) while imports increased 10.1 % from the previous year to a total of 49.4 million tonnes, being the highest level since 2006 [DECC, (2014e)].

2.1.2. Biomass market as pulverised fuel in the power sector

Biomass markets are more difficult to establish and analyse than those for coal or natural gas. In any case, biomass is considered a key part of the primary energy demand portfolio and significant bioenergy share growth is expected towards 2040 [e.g. IEA WEO, (2014)], where biomass availability will play a key role in decarbonising the power sector while potentially achieving negative emissions. The International Energy Agency Greenhouse Gas Programme (IEAGHG) has identified in a 2011 report [IEAGHG, (2011)] the technical potential for achieving these negative emissions, calculated up to 10 Gt CO_2 eq. per year or 3.5 Gt CO_2 if economic potential is conservatively estimated [IEAGHG, (2011)]. The technology routes considered by IEAGHG are post-combustion capture co-firing biomass with coal (PC-CCS), circulating fluidised bed (CFB) with post-combustion capture dedicated (CFB-CCS), integrated gasification combined cycle (IGCC) with CCS (IGCC-CCS), biomass IGCC with CCS, bioethanol and Fischer-Tropsch (FT) biodiesel production. PC and IGCC have greater potential but all will depend on sustainable biomass supply, for which each technology will compete for land use with food and energy crops (biomass feedstock's sustainability as discussed in Chapter 1). In Figure 2.4 an estimation of BECCS potential by IEAGHG is shown, differentiating between limitations for technical potential with respect to energy demand, deployment rate and capital availability (realisable potential) and price of biomass with a certain CO_2 price for electricity production (economic potential) [IEAGHG, (2011)].

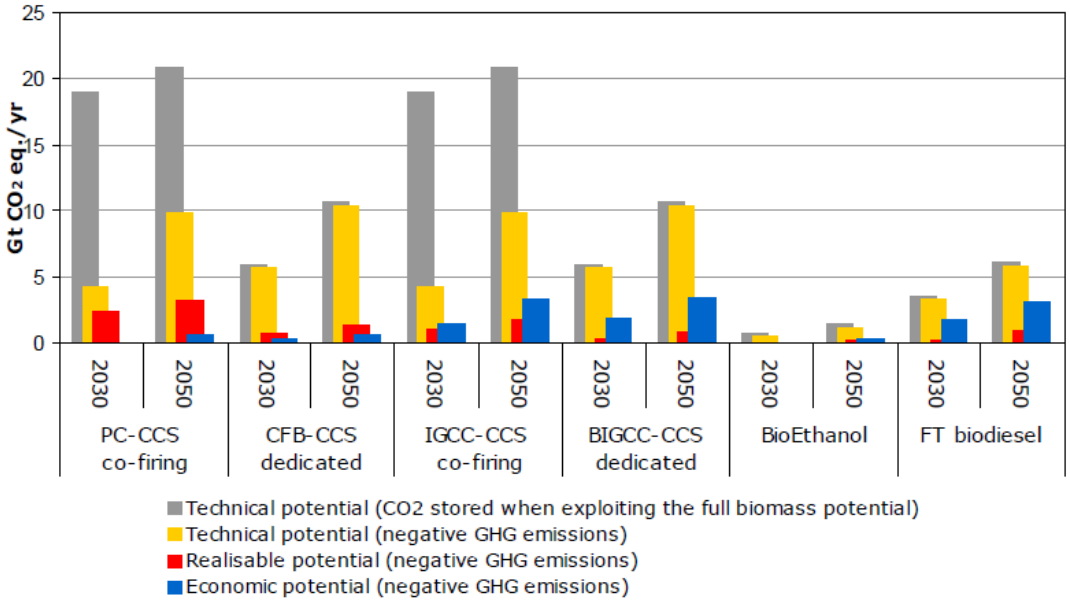

Figure 2.4. Estimation of BECCS potential for GHG emission reduction (Gt CO_2 equivalent per year) 2030 and 2050 [IEAGHG, (2011)]

Biomass potential in the power generation sector is widely recognised [e.g. IEA WEO, (2014); IRENA, (2014);] and it is important to reiterate that it has become too important to be ignored in any comprehensive strategy for CCS roll-out due to the unique role of BECCS according to IPCC, (2014c) as mentioned in Chapter 1.

For the local market of this experimental oxy-biomass programme, in the UK, while renewables accounted for a record of 15 % share for electricity produced [DECC, (2014e)], bioenergy contribution to electricity generation (including co-firing) has experienced a sustained increase in the recent years according to DECC as shown in Figure 2.5. Biomass accounted for about 3 % of the total electricity generated in the UK in 2012 as indicated by the UK bioenergy strategy [DECC, (2012)], where the combination of CCS and biomass is considered a matter of urgency for achieving negative emissions according to the Committee on Climate Change (CCC) [DECC, (2012)]. So far most of the bioenergy deployed in power generation has been on *"co-firing and conversion of existing coal power plants"* (e.g. Drax) with the funding support of the Renewables Obligation [DECC, (2012)].

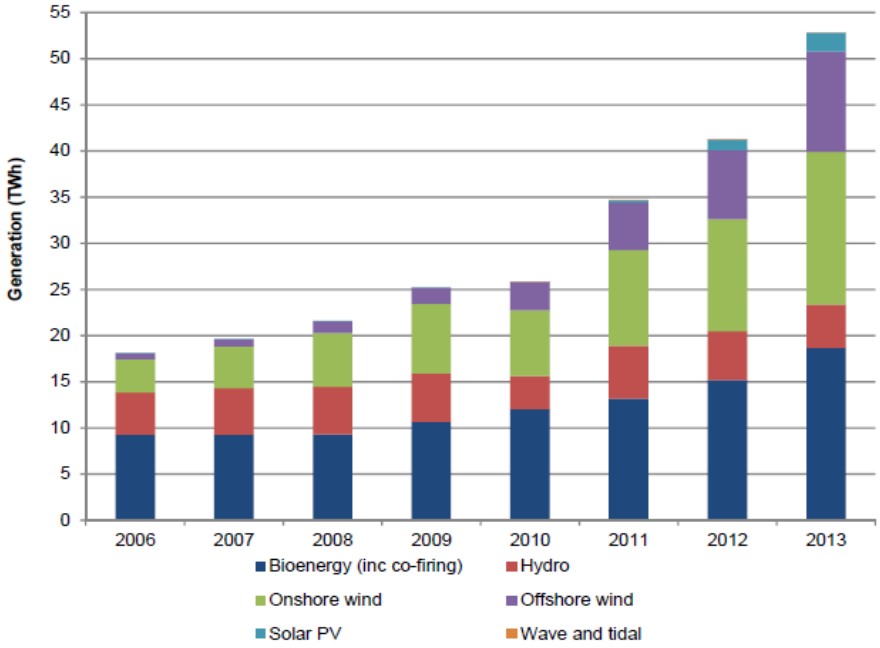

Figure 2.5. UK electricity generation from renewables including Bioenergy [DECC, (2014e)]

With the current criteria, around *"624 kg of CO_2/MWh of power generation"* can be saved with coal conversion to biomass [DECC, (2012)]. However, new dedicated biomass is expected to have *"a limited role as part of a wider energy mix"* [DECC, (2012)]. The same reports cites CCC work to re-affirm that low-carbon bioenergy will have to account for 10 % of the total primary energy demand for the UK to meet 2050 targets as shown in Figure 2.6:

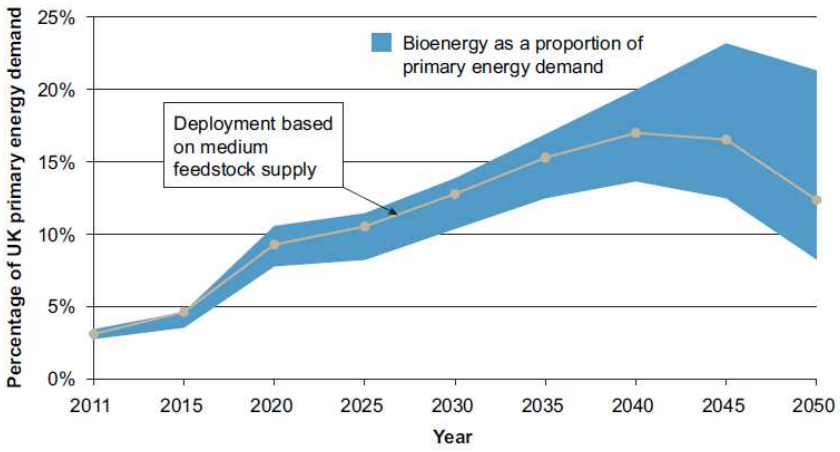

Figure 2.6. UK primary energy demand with potential Bioenergy contribution pathways [DECC, (2012)]

If that 10 % for bioenergy share for primary energy demand is not met, with part coming from BECCS, then, and citing textually: *"meeting the overall 2050 emission targets will be extremely difficult (even if Carbon Capture and Storage (CCS) is available). Similarly, recent analysis from the Energy Technologies Institute (ETI) indicates that the removal of biomass from the energy mix could increase the costs of decarbonising our energy system by £44 billion in 2050*" [DECC, (2012)]. The cost estimation of not having CCS available is £42 billion in 2050 [DECC, (2012)]. Consequently the combination of bioenergy and CCS (BECCS) has the potential to be a key cost effective mitigation option, with two technology options that are mutually dependant on each other success. This option is too important to be ignored (given sustainable feedstock availability) and the work under this research programme is focused on contributing to the safe development of oxy-biomass combustion for BECCS.

2.2. Coal and biomass preparation as pulverised fuel in a power station

In this section fundamental aspects related to this research programme regarding coal and biomass milling in the power station are briefly explored.

2.2.1. Coal handling and milling operation

Coal sources are underground coal mines or surfaces mines and the flexibility in its production is critical for the sector competitiveness versus other fossil fuel alternatives (such as natural gas) with lower CO_2 emissions in the power generation sector. In this section, the critical steps undergone by coal in the PF power station are briefly discussed. Equipment for coal handling, grinding and milling has been described comprehensively in the literature [e.g. B&W, (2005)] and its evaluation is not the objective of this literature review nor this thesis.

Rotary breakers, roll crushers and hammer mills with different design options are among the equipment commonly employed to reduce coal particle size while limiting the amount of fines produced [B&W, (2005)]. A cleaning plant can be used to remove foreign material, ash, sulphur and moisture from coal, with an estimation of 70 % of the coal mined for electricity generation being cleaned [B&W, (2005)]. During coal transportation coal particle size degradation has to be taken into account when considering fuel particle size specifications with an upper limit supplied to a PF power station [B&W, (2005)]. When the

coal is at the power plant, raw coal handling has to be done carefully with particular attention to the pulverisation stage due to the potential for fires.

Coal pulverisation is the critical stage of the PF power plant process that is directly impacted by the outcome of this research programme. Deflagration events in PF milling in air are relatively common. Fires are not infrequent in mills where hot spots of coal can be burning in a smouldering fire or in hot surfaces after a mill trip [B&W, (2005)]. Mill exit temperature is monitored to indicate if a fire might have started. Temperature monitoring is slow but reliable. In mills at fixed coal feed rate with primary air in automatic mode, i.e. the same air/coal ratio, a significant difference between mill inlet and mill exit temperature when comparing multiple mills, might be the indication of a fire [B&W, (2005)].

Start-up, shut-down, feed interruption and transient operation of mills [Carini and Hules, (1987)] are the critical phases when an explosion might happen. Air coal mixture changes from fuel lean to fuel rich (start-up) and this makes the mixture to go through coal dust concentrations that are ideal for developing a dust explosion in the mill if an ignition source such as sparks or hot surfaces is available [B&W, (2005)]. Common PF mill exit temperatures for different coal types have been referred to in Chapter 1 for explaining the PF oxy-fuel mill safety case.

There are studies in the literature reporting explosions in coal pulverisers although many of these events are kept private by the utilities. Carini and Hules, (1987) reported on a research sponsored by the Electric Power Research Institute (EPRI) in the U.S. in the early 1980s, where one explosion for each utility steam generator would happen on average every three years [Carini and Hules, (1987)]. Coal type (volatility) *"has a clear influence on the explosion frequency"*. It is important to know that explosion term here includes *"severe puffs (structure deformation) and true explosions (containment breaching)"* [Carini and Hules, (1987)]. The authors found with a statistical caveat regarding explosion frequency that pulveriser age was not important while type was relevant, attrition pulverisers are safer than ball mills and ball mills are safer than spindle pulverisers; pressurised pulverisers were safer than suction operation pulverisers; explosion frequency was *"independent of pulveriser capacity"*; if a boiler had multiple milling units then "*explosion frequency increased with an increasing number of pulverisers per unit"*; on coal type, subbituminous coals caused twice the explosions of bituminous coals, i.e. *"explosion frequency increases with an increase in volatility content"* and moisture and ash content increases did not seem

to have a clear impact on explosions in mills [Carini and Hules, (1987)]. Coal type was found to be a *"major factor in explosions frequencies"* and *"all explosions were initiated thermally"* [Carini and Hules, (1987)]. Mechanical sparks are also reported to be a frequent ignition source in mills [Eckhoff, (2003)].

Eckhoff, (2003), reports a plant for grinding and drying coal that uses CO_2 for inerting the potential explosion as shown in Figure 2.7 below:

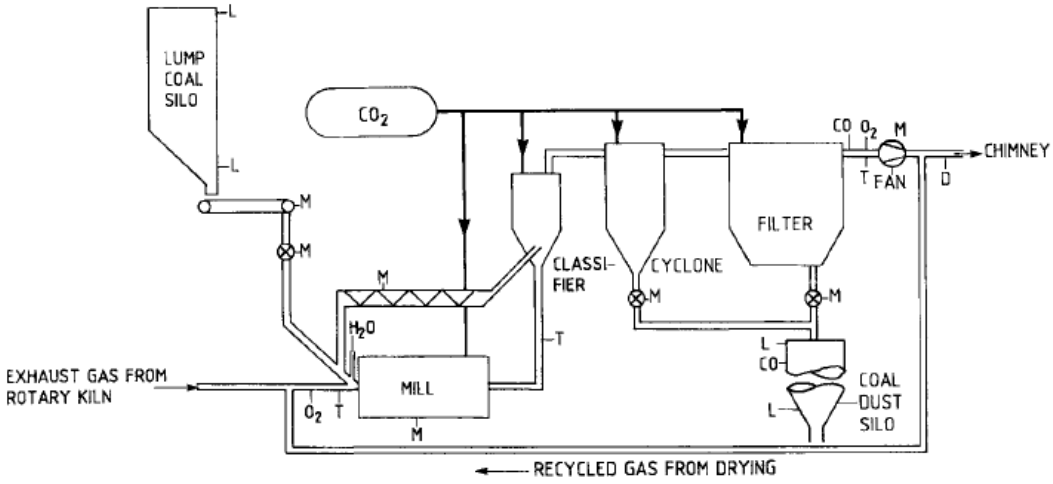

Figure 2.7. Coal milling and drying process with CO_2 as explosion inerting option [Eckhoff, (2003)]

This example case of inerting strategies in coal pulverisation is particularly interesting since in oxy-fuel primary recycle (PR) the presence of recycled CO_2 can be expected to partially inert the potential ignition of pulverised fuel for some cases when compared to air operation, as shown in the experimental results reported later in this study.

Coal storage is required for typically 90 days to secure power production through any interruption of supply. Storage strategy is based on economic considerations due to market conditions and it is proportional to the plant power output [B&W, (2005)]. However, coal storage considerations are not particularly related to the output of this research on PF ignitability.

2.2.2. Biomass milling operation

Biomass milling in the power station is different from the coal case, mainly due to the specific characteristics of pulverised biomass. The biomass can reach the power station

with greater variability than coals: as wood, Miscanthus, straw, food residues, recycled litter, etc. For instance, wood chips are mixed with coal before milling [Henderson, (2015)]. The variety makes the biomass handling and milling operation quite specific for each plant and a comprehensive description of it would fall outside the immediate goals of this research. The assumption made here is that the biomass will reach the power station as pellets, as the form most widely used, with high co-firing ratios, and will be milled separately from coal [Henderson, (2015)]. Three of the four biomass types supplied and tested in the oxy-biomass ignition experimental programme included in this thesis were supplied in pellet form.

The biomass generally used in the UK for pulverised fuel firing is white wood that has been pelletized and with lower calorific value and density than coal [EA, (2013)]. Torrefied biomass is also an alternative fuel being demonstrated that can be used, where the biomass has been thermally treated by pyrolysis at 200-300 °C to increase its calorific value, making the fuel hydrophobic and with the advantage of requiring minimal changes to the power plants being converted to biomass [Henderson, (2015)]. Torrefied biomass's higher energy intensity and characteristics has the benefit of reducing the economic costs of transport, storage and milling with the potential of a high energy yield (90-95 %) [Henderson, (2015)].

The Environment Agency (EA) recommends best available techniques (BAT) principles for handling woody biomass in power stations [EA, 2013]. The key from, this research perspective, is to ensure that ignition sources are not available and, if that is not possible, are at least minimised [EA, (2013)]. Elimination of moisture and shortening the handling and storage time with as much automation in the process as possible is also recommended [EA, (2013)].

Milling of the biomass from pellets can be done in standard coal mills if operating in co-firing or converting an existing plant since the mills are very robust requiring low maintenance [Livingston, (2013)]. Depending of the type of mill some modifications might be required. Potential modifications for ball and ring mills include to the mill throat to control air velocities and baffle addition inside the mill or classifier vanes for biomass throughput optimisation [Livingston, (2013)]. Some types of mills can be more sensitive to tramp material, causing much higher maintenance costs *"depending on the fuel quality"* [Livingston, (2013)]. The fuel pelletisation process is a very relevant stage as most of the crushing processes in the mills give similar size distributions to the original biomass through

breaking the pellets back into their source material. Torrefied biomass can, however, yield finer size distributions [Livingston, (2013)]. Dedicated biomass milling is an option if economics allow but the key for safety in any of the milling cases is to maintain control of the mill exit temperatures to control the risks of fires and potential explosions.

Higher volatile content in the biomass requires that the primary air temperatures are kept sufficiently low [EA, (2013)], operating with cold primary air if required and derating by around 50-80 % the heat output from the plant when compared to coal [Livingston, (2013)]. In any case, generally, controlling mill operating temperatures (inlet and exit) lower than for most coal cases at an appropriate level for biomass dust is the objective for ensuring mill safety [Livingston, (2013)]. Flow rates also have to be kept high enough to prevent any dust settling out of the mill exit towards the boiler [EA, (2013)]. In addition, suppression and inerting systems (steam/water misting) for explosions can be installed if required by clients [Livingston, (2013)] but gas inerting is preferred to water deluge to manage potential fires [Henderson, (2015)].

Magnets to remove tramp metal, explosion vents, etc., are used in mills in some cases as described by Amyotte et al., (2009). The event of an explosion is likely for instance in hammer mills, so they are *"designed to withstand the overpressure resulting from a dust explosion"* [Amyotte et al., (2009)]. An alternative is to relieve that overpressure to avoid damage to other process units [Amyotte et al., (2009)].

On biomass storage, EA recommends users to carry out specific risk assessments for *"silos, bunkers, hoppers and other containment less than 10 m^3 volume"* [EA, (2013)]. Covered storage of biomass is recommended with special protection for water and with gas extraction systems and monitoring of carbon monoxide (CO) and CO_2 levels [EA, (2013)]. Thermal imaging and other temperature measurement techniques are recommended for surface temperature monitoring [EA, (2013)]. Inerting gas injection, such as N_2 is recommended, combined with foam and water deluge [EA, (2013)].

2.3. Coal dust ignition in air

In this section, the science behind the studies on dust ignition for underground coal mining is explained, highlighting the most relevant parameters for the research on pulverised fuel safety in coal and biomass power plants with oxy-fuel for CO_2 capture. It is important to

note the change in terminology when referring to dust instead of pulverised fuel. Dust refers to a broader range of solids, usually employed in normal practice in mine safety work; while fuel in this thesis will be only coal and biomass, type of dusts for which ignitability and explosibility have been evaluated for power generation with CCS. Reference to other dusts in this section is used to illustrate differences in the ignition behaviour when testing ignitability with different experimental conditions.

Coal dust ignition has been a continuous concern for the coal mining industry. The United States Bureau of Mines (USBM), now NIOSH (National Institute for Occupational Safety and Health) is a world class reference in this science and their work is widely recognised. They started their research activities in 1911 in the experimental mine in Bruceton, Pennsylvania, U.S. although the first mine explosion in the U.S. is recorded in 1810 in Virginia [Verakis and Nagy, (1987)]. The USBM carried over 4,200 explosion tests in the Bruceton Experimental Mine up to its closure in the mid-1980s [Verakis and Nagy, (1987)] and the research continued in the Experimental Lake Lynn Mine, which unfortunately also closed recently. The large scale research work was complemented with laboratory research, including the work carried out with the 20 litre ignition chamber, PRL-20 [e.g. Cashdollar, (2000)].

2.3.1. Literature review on coal dust ignition in air

The literature review begins with the basic theory of dust explosions and follows on with the main parameters for the PF oxy-combustion case and consequently for the design of experiments. Secondary order parameters affecting the combustion process in an enriched CO_2 atmosphere are also briefly discussed here.

a) Dust ignition and explosion theory background

A dust explosion involves the rapid chemical oxidation of dust particles dispersed in a combustion atmosphere that leads to a rapid energy release. That increases the system temperature so rapidly that it translates into a pressure increase in the system [Hertzberg and Cashdollar, (1987)]. For a dust explosion to happen five elements of the dust explosions pentagon are required: fuel, ignition source, oxidant, dispersion/mixing and confinement [Stephan, (1990); Cashdollar, (2000)]. As the products from explosions are gases, according to the ideal gas law:

$$pV_\circ = \left(\frac{m}{M}\right) RT \qquad \textbf{Equation [2.1]}$$

Where:

V_o : system volume

p: system absolute pressure

T: system absolute temperature

m: mass of gas

M: molecular weight

R: universal gas constant

According to Hertzberg and Cashdollar, (1987), most of the internal chemical energy of the fuel is released as heat, increasing the temperature of the system which will translate into a pressure increase following the proportionality shown in Equation 2.2.:

$$\frac{p_{max}}{p_o} \approx \frac{T_b}{T_0} \qquad \textbf{Equation [2.2]}$$

Where:

P_{max}: maximum absolute pressure in the system from explosion

P_0: absolute pressure in the system before explosion

T_b: burned gas temperature from explosion

T_0: initial temperature in the system before explosion

Hertzberg and Cashdollar, (1987), explain that in a 20 litre (L) spherical chamber where dust is centrally ignited and assuming that *"spherical combustion waves… are generated by flame fronts that propagate outward from a central ignition point at subsonic velocities"* with rapid flames or deflagrations [Hertzberg and Cashdollar (1987)]. This assumption follows the classical combustion theory [Lewis and von Elbe, (1961)] cited by Hertzberg and Cashdollar, (1987):

$$\frac{[p(t)-p_o]}{p_{max}-p_o} = k\frac{V(t)}{V_o} \qquad \textbf{Equation [2.3]}$$

Where "*p(t) is the pressure time evolution in a constant volume, spherical explosion is related to the fractional volume, V(t), occupied by the fireball during the time of propagation, t"* and *"k is a correction factor related to the difference in compressibility between burned and unburned gases"* [Hertzberg and Cashdollar, (1987)]. Developing Equation 2.3 for the case of spherical propagation from ignition source:

$$\frac{V(t)}{V_o} = \left[\frac{r(t)}{r_o}\right]^3 = \left[\frac{S_b t}{r_o}\right]^3 \qquad \textbf{Equation [2.4]}$$

Where r(t) is the radius at time t, S_b is the flame speed defined as the density ratio (at constant pressure) of unburned to burned gases (ρ_u/ρ_b) times the burning velocity (S_u):

$$S_b = \frac{dr(t)}{dt} = \left(\frac{\rho_u}{\rho_b}\right) S_u \qquad \textbf{Equation [2.5]}$$

The maximum pressure in the explosion (P_{max}) is reached when the spherical combustion wave overtakes the last fraction of unburned gas close to the wall of the chamber and these are then transformed in the combustion products, i.e. $r(t) \rightarrow r_o$. At that instant k=1 and the following Equation 2.6 is obtained if Equation 2.3 is differentiated respect to time and Equation 2.4 is substituted in Equation 2.5 to confirm the previous affirmation that the maximum pressure rise rate will happen when the wave touches the wall of the chamber [Hertzberg and Cashdollar, (1987)]:

$$\frac{dp(t)}{dt} = 3(p_{max} - p_o)\left(\frac{\rho_u}{\rho_b}\right) S_u \frac{r(t)^2}{r_o^3} \qquad \textbf{Equation [2.6]}$$

If in a sphere $r(t) = r_o = \left(\frac{3V_o}{4\pi}\right)^{1/3}$ and assuming $\frac{\rho_u}{\rho_b} \cong \frac{T_b}{T_o} \cong \frac{p_{max}}{p_o}$, Equation 2.7 for the "cubic law" to generate K_{st} values (st for "staub", which means dust in German) can be obtained [Hertzberg and Cashdollar, (1987)]:

$$\left[\frac{dp(t)}{dt}\right]_{max} V_o^{1/3} = K = 4.84\left(\frac{p_{max}}{p_o^{-1}}\right) p_{max} S_u \qquad \textbf{Equation [2.7]}$$

This expression for the "cubic law" is based on the assumption that the 20 litre pressure vessel volume is large when compared to the ignitor flame and the dust flame thickness [Cashdollar, (2000)]. According to Equation 2.7, the burning velocity (S_u) is the driving force

that determines the combustion rate. S_u is directly affected by the turbulence, accelerating the rate of the explosion as S_u increases with turbulence [Hertzberg and Cashdollar, (1987)]. The rapid pressure rise and burning velocity in the rapid oxidation of the fuel can reach sonic velocities (detonation) but for the fuel dusts cases sub-sonic is the most common case, i.e. deflagration [Cashdollar, (2000)]. In the dust ignition experiments in the combustion chamber(s) presented in later sections of this thesis, turbulence is controlled by the gas inlet pressure and dispersion nozzle design. Turbulence has been kept as constant as possible in the series of experiments, by keeping the same method for dust dispersion method into a cloud, and so it is expected that the propagation of ignition is approximately spherical as the "*turbulence level reached in this type of experiments is moderate"* [Hertzberg and Cashdollar, (1987)].

In the dust ignition experiments in this experimental programme for PF mill safety, pressure ratio (P/R) defined as maximum pressure during ignition (P_{max}) divided by the initial pressure (P_0) is taken as the key parameter for determining positive ignition.

Dust ignition at constant volume has been previously described in the literature according to the physical phenomena happening in the process. Hertzberg et al., (1982), defined the sequence as:

1) Heating and devolatilisation of the dust particles, to the point of vaporisation or pyrolysis [Cashdollar, (2000)].

2) Mixing of the volatiles released with the combustion atmosphere.

3) Gas-phase [i.e. homogeneous] combustion of the volatiles-oxidant mixture.

The flame propagation from ignition source competes with two processes: *"a) Natural-convection or buoyancy, through the mechanism of flame stretch, and b) conductive-convective heat losses to dust particles"* acting as heat sinks [Hertzberg et al., (1982)]. When the dust cloud in the gas mixture is able to propagate the ignition then it can be said that the dust is flammable or explosible, although historically flammable has been use only for gases while explosible is used for dusts [Cashdollar, (2000)]. According to Cashdollar et al., (1989) and citing textually: *"The overall mechanism of flame propagation in explosions of carbonaceous dusts in air appears to be primarily, or even entirely, homogeneous gas phase combustion of the volatiles. There is little or no contribution to the flame propagation*

process from the heterogeneous surface oxidation of the char, fixed carbon, or graphite. Instead, these components actually inhibit flame propagation by acting as heat sinks" [Cashdollar et al., (1989)]

For the PF mill safety case, then the release of volatiles from the fuel and subsequent combustion to develop the flame from ignition is the critical phase and for biomass it is expected that, with higher volatile matter content this step will also be critical. As in the milling plant a wide range of fuel dust concentrations are seen at different operational phases, it is important to pay attention to the lower end of dust concentrations and their effect on ignition as well as to higher dust loadings.

b) Dust concentration effect on dust ignition

Dust concentration affects ignitability of the fuel-oxidant mixture. In PRL-20 the flame propagation from ignition with a given ignition energy is limited if too much dust is present. Lean Flammable Limit (LFL) or Minimum Explosible Concentration (MEC) refers to the minimum dust-oxidant mixture concentration where ignition is sustained in an explosion at ambient temperature and pressures [Hertzberg et al., (1982)]. LFL for Pittsburgh coal dust has be found to be of 90 ± 10 g/m^3 with a P/R of 2 and K_{st} above 1.5 bar m/s criteria [Hertzberg et al., (1988)]. If testing a low volatile bituminous coal then the MEC was found to be 125 g/m^3 in PRL-20 tests and for lower volatile coals can increase up to 200 g/m^3 [Cashdollar, (2000)]. Explosibility variability for Pittsburgh high volatile coal dust is shown in Figure 2.8 [Cashdollar, (2000)].

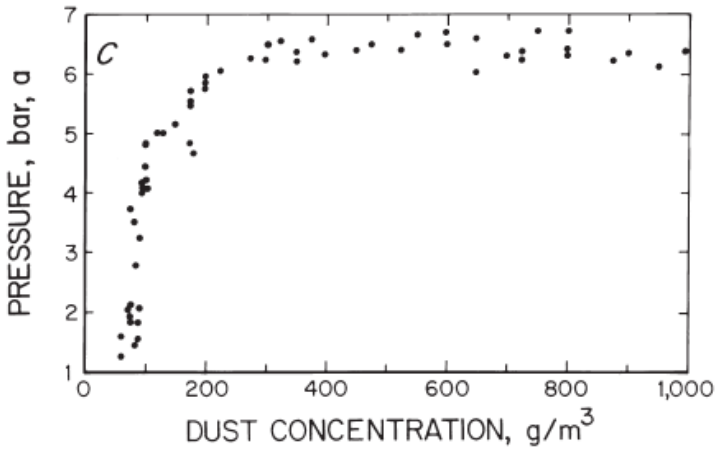

Figure 2.8. Explosibility trend for Pittsburgh high volatile coal dust [Cashdollar, (2000)]

This figure confirms MEC for Pittsburgh coal at around 80 g/m^3 [Cashdollar, (2000)]. When determining positive or negative ignition, pressure values exhibit a plateau and then descend when too much dust is present for the same oxidant mixture available as shown in Figure 2.9. According to Cashdollar, (2000), K_{st} values present more scatter than pressure values, *"typical of dusts"*, so P/R has been selected as the key parameter to use in this study to determine if ignition is positive or negative. For coal dusts, maximum pressure (P_{max}) usually peaks at dust concentrations of 200-300 g/m^3, a level at which all the O_2 in the chamber is consumed [Cashdollar, (2000)]. It is expected than in oxy-fuel atmospheres the peak values would be found at slightly higher fuel rich concentrations as more oxidant would be present if testing ignitability in above 21 % O_2 v/v balance CO_2. Figure 2.9 shows a decrease in pressure from ignition for very high dust concentrations of high volatile bituminous coal (solid curve) versus polyethylene (higher volatile) dusts (dotted curve) [Cashdollar, (2000)].

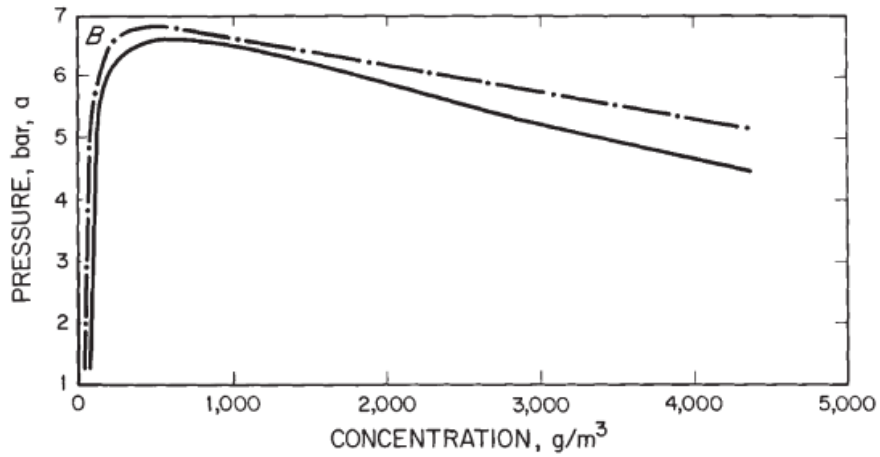

Figure 2.9. Comparison of Explosibility trend for Pittsburgh high volatile coal dust (solid curve) and polyethylene dust (dotted curve) [Cashdollar, (2000)]

According to Cashdollar, (2000), dusts can explode at concentrations above 4,000 g/m^3 but higher amounts of dust acting as heat sink cause a decrease in pressure rise and consequently in P/R values. In the PF milling safety case, all the concentrations are seen during operation of the mill. The interest lies in the vicinity above the lean limit with rich oxidant as for concentrations above 600 g/m^3 a plateau or decrease in P/R is expected due to self-suppression effect on ignition as explained in later sections of this chapter [e.g.

Sapko et al., (2000)], were omitted from the experimental programme to save time and dust (some samples of which e.g. the PPC sample, were in limited supply).

c) Dust type (volatiles) effect on dust ignition

Dust type and volatiles content has a critical effect on explosibility in pulverisers as shown previously [e.g. Carini and Hules, (1987)]. Minimum autoignition temperatures (AIT), the lowest temperature at which a dust cloud will spontaneously ignite [Abrahamsen, (1987)], are also quite interesting for evaluating the explosion potential of dusts when above the lean flammability limit. When the strength of the ignition source is adequate to heat up the dust particles surrounding the source, the propagation of the flame and subsequent explosions due to volatiles combustion is dependent on fuel characteristics. Conti and Hertzberg, (1987) used thermal autoignition temperatures determined in a 1.2 litre furnace to evaluate the potential for explosions. Hertzberg (1991) continued the work for different coals and determined minimum autoignition temperatures for a range of fuels as summarised in Table 2.2:

Table 2.2. Minimum Autoignition Temperatures (AIT) for various dusts in air as measured in the 1.2 litre furnace

Dust Type	Proximate volatility (%)	Particle diameter D_s (µm)	Particle diameter D_w (µm)	Minimum AIT (°C)
Graphite	<1	28	43	925
Anthracite coals				
Reading	5	6	9	780
Pennsylvania	8	6	9	760
Bituminous coals				
Pocahontas	16	16	59	635
Sewell	29	22	44	560
Pittsburgh	37	28	48	540
Subbituminous coals				
Western (10 % H_2O)	35	25	71	475
Western (dried fully)	39	25	71	450
Lignite coals				
North Dakota (26 % H_2O)	33	43	115	600
North Dakota (dried fully)	43	43	115	555
Wood, treated	70	30	64	450
Beulah, ND (27 % H_2O)	30	15	29	440
Beulah, ND (dried to 8 % H_2O)	41	15	29	425
Gilsonite	85	20	50	480
Lycopodium	85	27	28	435
Polyethylene	100	27	37	400
Cornstarch	87	18	21	400
Decane (liquid)	100	Not applicable	Not applicable	275

Adapted from [Conti and Hertzberg, (1987) and [Hertzberg, (1991)]

According to [Conti and Hertzberg, (1987)] the data shown in Table 2.1 leads to a general assumption that the minimum AIT values for coals and other carbon dusts are mainly affected by the volatile yield during the pyrolysis of the dust as it is ignited [Conti and Hertzberg, (1987)]. Citing literally: *"The lowest AIT values for the coals were in the lower rank, finer particle coals in their dried states. Those coals also display the greatest intrinsic tendency for self-heating, and it is therefore not surprising that the subbituminous coals have been the most troublesome for coal pulverisers in utility plants"* [Conti and Hertzberg, (1987)].

In Figure 2.10 the rank impact on AIT for the same dust concentration is seen when comparing anthracite to Pittsburgh bituminous coal.

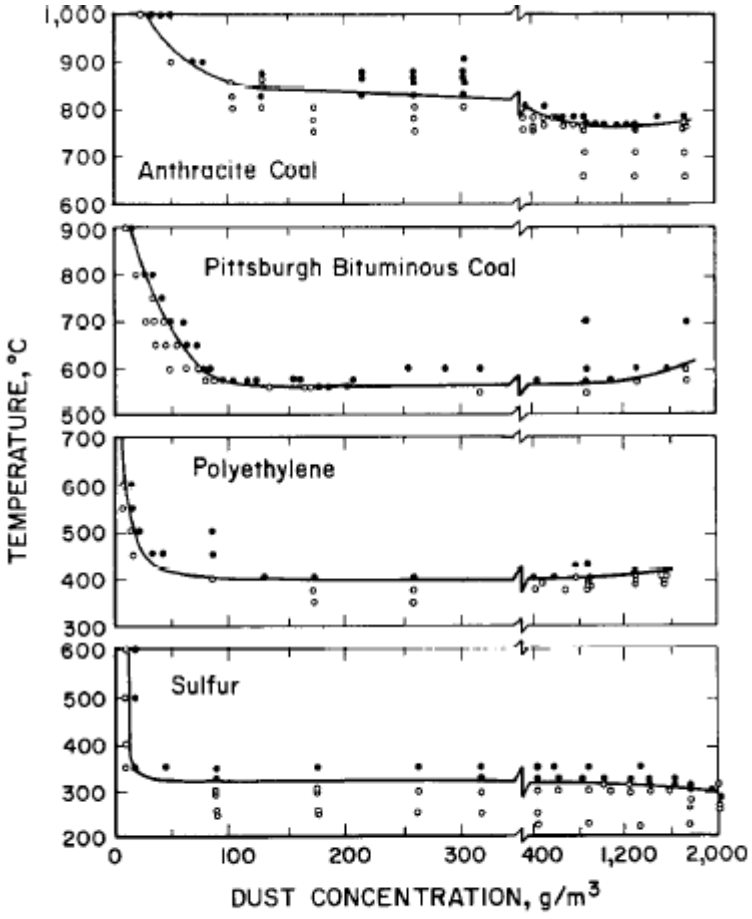

Figure 2.10. Minimum autoignition temperatures (AIT) comparison [Hertzberg, (1991)]

For coal dust ignition in air and for other dusts the minimum AIT is a good indication of how likely the particles surrounding the ignition source would be to ignite with the rapid heating of the volatiles released and support the flame propagation along the bulk of the fuel dust. Fuertes et al., (1993), have tested the ignition temperatures in air for 60 µm mean size pulverised coal particles using a heated wire mesh technique. They found, that temperatures reached "*ranged from 685 °C for a high volatile bituminous coal to 1,090 °C for metallurgical coke"* [Fuertes et al., (1993)]. El Cerrejon coal reached temperature of 690 °C for coal and 725 °C for char particles, leading to the conclusion that the differences between temperatures *"for high-volatile coals indicate that the influence of volatile matter on the ignition mechanism cannot be ignored"* [Fuertes et al., (1993)].

Cashdollar, (2000), showed the impact of dust concentration and thermal ignitability of the coal dust, as in Figure 2.11 when compared to methane gas.

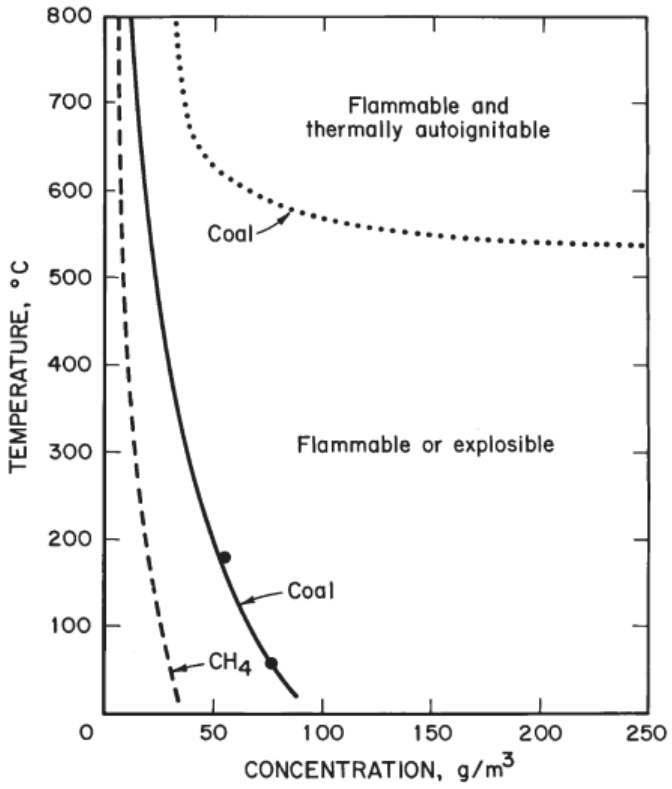

Figure 2.11. Thermal ignitability of coal dust compared to methane, [Cashdollar, (2000)]

The dotted curve for coal shows the boundary region where coal dust would thermally autoignite according to concentration variability. In the coal and biomass dust ignition experimental programme undertaken in the present study, AIT is expected to have a critical

role for dust ignition behaviour differentiation between coal and biomass ignition cases. Biomass dust particles with hither volatile content surrounding the ignition source can be expected to ignite at lower temperatures than coals. Temperatures reached during the ignition and combustion process vary. For example, Cashdollar and Hertzberg, (1983), measured the Pittsburgh coal dust ignition temperatures in the 8 litre ignition chamber and, of particular interest for oxy-fuel operation, this included temperatures for O_2 concentration of 50 % v/v balance N_2. Figure 2.12 shows the variation of P/R and temperature with dust concentration for very fine Pittsburgh coal (5 µm) for air and 50 % O_2 v/v respectively.

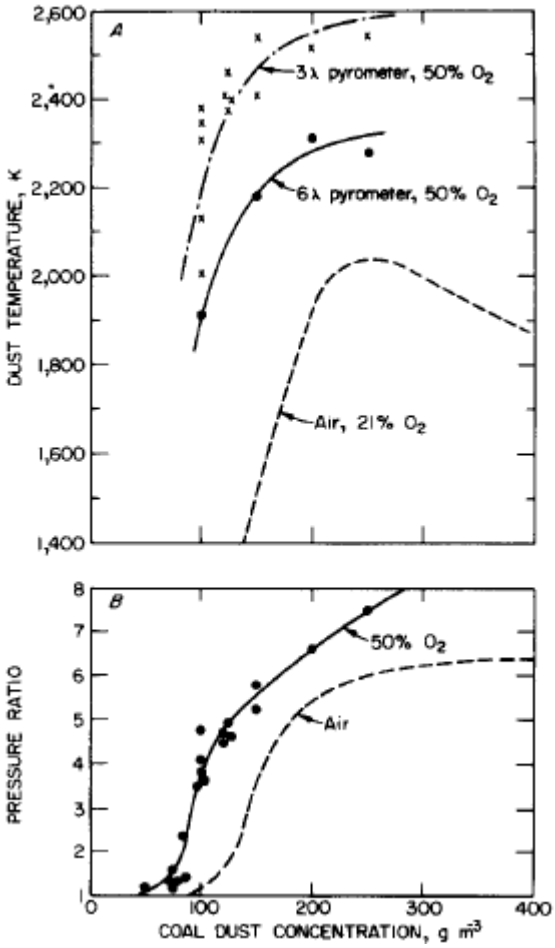

Figure 2.12. P/R and temperature evolution with loading, PPC [Cashdollar, (2000)]

The temperatures of the particles in 50 % v/v/ O_2 were much higher than in the air case, probably with higher amounts of volatiles generated and released during the ignition and combustion process at the higher heating rates of the higher oxidant flame, causing the LFL

to be lower than in the air case [Cashdollar and Hertzberg, (1983)]. Cashdollar and Hertzberg, (1983), also found that *"gas temperatures were significantly higher than the dust particle temperatures*" for all the experiments. These gas temperatures were found to be similar to the adiabatic flame temperature of *"typical gaseous hydrocarbon fuels"* [Cashdollar and Hertzberg, (1983)].

More recently, Amyotte et al., (2003), have tested Colombian coal (36 VM % wt.) with Powder River Basin coal (39.9 VM % wt.) and petroleum coke (17 VM % wt.) among other fuels in air in a 20 L Siwek chamber. They found that petroleum coke, mainly due to its lower volatile content, or any blend of the other fuels with it was inherently safer than Colombian coal [Amyotte et al.,(2003)]. This is important in confirming volatile content relationship with fuel reactivity in order to evaluate potential ignition risks for biomass when compared to coals in the experimental programme. In addition, a concentration of 750 g/m^3 was found the average optimum for the fuels tested for giving peak pressure and K_{st} values [Amyotte et al., (2003)].

d) Particle size effect on ignition

Particle size is a very important parameter to take into consideration in dust ignition experiments. It is expected that the finer the dust particles the easier would be the volatile release for combustion and flame propagation after ignition. When compared to pre-mixed gas explosions, the dust-oxidant mixture is not homogeneous and the dynamic behaviour of the heterogeneous mixture will be critically affected by the particle size when defining the fuel concentration [Hertzberg et al., (1988)].

Hertzberg et al., (1982), found while testing narrow size distributions of several dusts in an 8 litre ignition chamber that:

-If the dust particle diameter is below a certain *"characteristic diameter"* (specific to each fuel) the lean flammability limit (LFL) or minimum explosible concentration (MEC) were insensitive to particle size [Hertzberg et al., (1982)]. In that insensitivity case, the flame propagation rate is controlled by the gas-phase combustion of the volatiles-oxidant mixture where quenching is mainly impacted by the natural convection of the flame stretching along the ignition chamber [Hertzberg et al., (1982)]. "*For fine particles, limits are essentially independent of particle size because finer particles can fully devolatilize within the flame front"* [Hertzberg and Zlochower, (1990)]. However, *"a particle size dependence*

appears at the characteristic diameter" where the rate control of propagation moves from gas-phase combustion of volatiles to phase 1 where the mixing of these volatiles released during ignition become the rate controller for the process, with the natural buoyancy still present as a quenching mechanism [Hertzberg et al., (1982)].

-As dust particle size increases, LFL rises significantly and above a certain diameter, called the *"critical diameter",* the coarse size makes the dust non-flammable for any concentration at standard pressure and temperature [Hertzberg et al., (1982)]. Above the critical diameter the dust-oxidant mixture becomes non-flammable since the combustion process is controlled by the mixing of the volatiles released with the oxidant and now quenching is enhanced by flame buoyance and also by conductive-convective heat losses to those large dust particles that act as a heat sink [Hertzberg et al., (1982)].

Later Hertzberg and Zlochower, (1990) confirmed this, citing textually: "*a size dependence appears for coarser particles above some characteristic diameter (50 µm for the coal), because total particle devolatilisation is not possible within the flame front. Lean limit concentrations increase rapidly above those characteristic diameters because more dust per unit volume is needed to compensate for the smaller fraction of each dust particle that contributes volatiles to the flame. As diameters increase still further, a critical size is soon reached above which the dust is nonexplosive. The particle size dependence for the minimum explosive concentration is thus determined by the devolatilisation rate process"* [Hertzberg and Zlochower, (1990)].

Dust particle size has also an important impact on minimum autoignition temperature (AIT). Hertzberg et al., (1982) have reported minimum AIT values for Pittsburgh coal (35 % volatile) and Pocahontas (16 % volatile) as shown in Figures 2.13 and 2.14. Pocahontas coal shows a tendency for steadily increasing minimum AIT with increasing particle size and that trend is less steep than for Pittsburgh coal, as shown in Figure 2.14, probably due to the difference in volatile content between the two coals.

From figure 2.14 below it can be seen that the minimum AIT becomes independent of particle size for Pittsburgh coal at particle diameters below 50 µm [Conti and Hertzberg, (1987)].

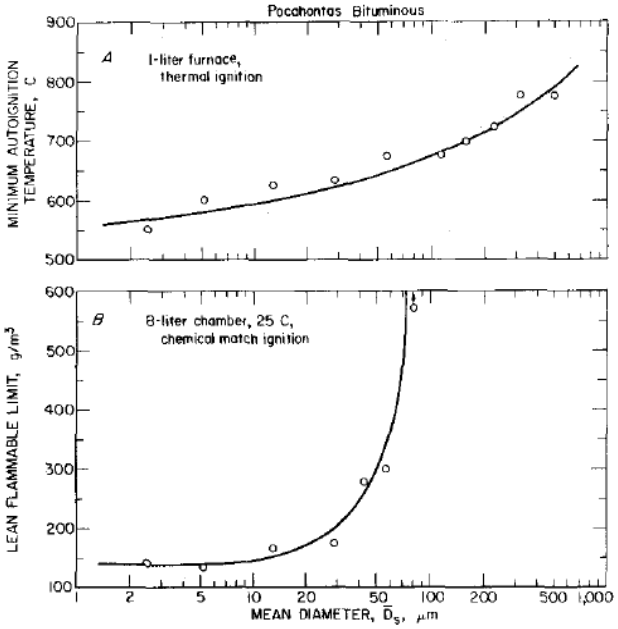

Figure 2.13. Lean flammable limits (LFL) and minimum autoignition temperatures for Pocahontas coal dust tested in 1 litre furnace and 8 litre chamber as reported [Hertzberg et al., (1982)].

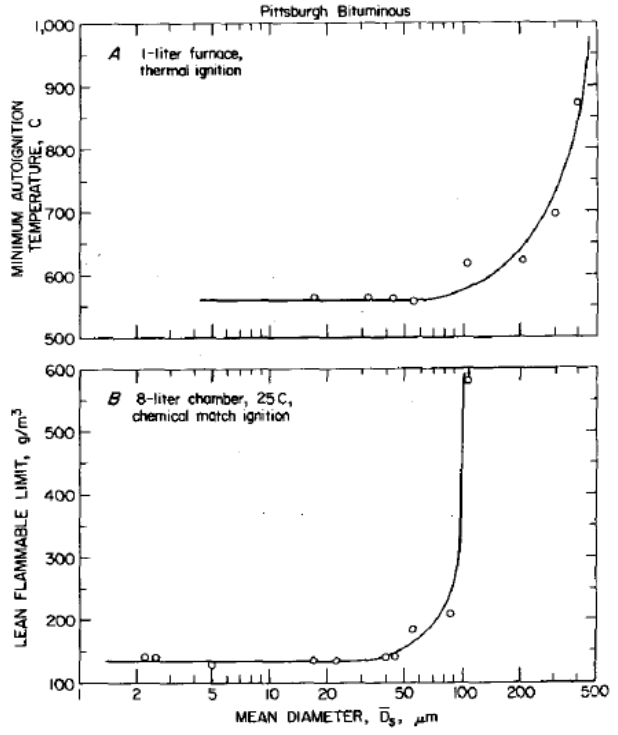

Figure 2.14. Lean flammable limits (LFL) and minimum autoignition temperatures for Pittsburgh coal dust tested in 1 litre furnace and 8 litre chamber as reported [Hertzberg et al., (1982)].

In more recent studies for broader range of coals, a complex effect of particle size in coal ignition was found. *"Increasing the amount of fine particles beyond a limit did not improve ignition significantly but removing them worsened the ignition process dramatically"* [Gibbins and Man, (2005)]. For this research programme on PF mill safety, particle size interest is in the <75 µm distributions for coal while for biomass characterising particle size is attempted with a different approach and a different particle size range is employed as described in Chapter 4.

e) O_2 content effect (ignition atmosphere) on dust ignition

The O_2 content in the combustion atmosphere has a direct impact on the LFL or MEC values for dust explosions. Hertzberg et al., (1982) have reported that characteristic diameter and critical diameter *"were observed to increase monotonically with increasing dust volatility and O_2 content"* in the combustion atmosphere (Hertzberg et al., 1982). In the same paper, when testing Pittsburgh coal in 8 litre ignition chamber (Figure 2.13), as O_2 % v/v increased, the LFL value decreased, propagating the flame into an explosion. For 50 % v/v O_2 LFL stayed below 80 g/m^3 for mean diameter particle sizes up to 100 µm. In O_2 concentrations of 21 % v/v. as in the air case, the LFL went up to 140 g/m^3. Critical diameters for Pittsburgh coal dust varied significantly with O_2 concentration as shown in Figure 2.15:

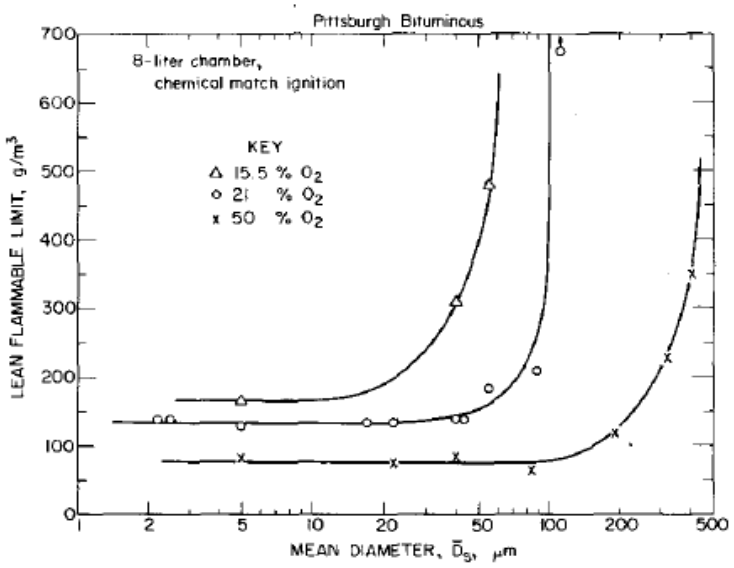

Figure 2.15. Lean flammable limits (LFL) for 15.5 % v/v, 21 % v/v and 50 % v/v O_2 in air for Pittsburgh coal [Hertzberg et al., (1982)].

This trend of O_2 content dependence for coal ignition was observed previously by Hertzberg et al., (1981)]. The O_2 content effect on LFL is particularly important in the oxy-fuel case, where up to 30 % v/v O_2 balance CO_2 is considered relevant for PF oxy-fuel plant operation. In the experimental programme with the ignition chambers presented, the effect on the critical diameter of oxy-fuel atmosphere is evaluated for coal dust samples. For biomass cases, this relationship has to be evaluated with more caution due to the different characteristics of biomass dusts, but the impact of higher O_2 levels is also evaluated. In addition, the CO_2 presence is important because of its greater ignition inerting effect when compared to N_2 in the air case.

f) Ignition energy effect on ignition on dust ignition

Ignition energy is a critical issue for coal and biomass dust combustion in suspension. When determining "*true flammability limit*" the results should be independent of ignition energy [Hertzberg et al., (1988)]. However, there is evidence that there is a direct effect of ignition energy strength in ignition tests undertaken using coal dust with inert rock dust. According to Hertzberg et al., (1988), before 1910, due to the misunderstanding of the impact of ignition source strength, it was thought that coal dust was nonexplosive and that the disasters in coal mines where just caused by methane gas [Hertzberg et al., (1988)].

Dust ignition tests in a 20 litre ignition chamber are usually triggered by pyrotechnic chemical ignitors or sparks. In the following table, typical values of energy strengths for relevant ignition sources are shown according to Hertzberg et al., (1988).

Table 2.3. Ignition source strengths

Source	Stored electrical energy, J	Nominal calorimetric energy, J	Pressure rise, Δp, mbar	Effective energy, J
Electric spark	17	-	8.5	1.6 ± 0.2
Sobbe Chemical Ignitor	-	500	50	255 ± 45
	-	1000	110	570 ± 80
	-	2500	250	1280 ± 160
	-	5000	420	2120 ± 220

Adapted from [Hertzberg et al., (1988)].

The pyrotechnic igniters were selected for use in the PF mill safety research programme due to the low ignition energy available from a spark system. But it is important to take into account the effective energy input from igniters as shown in Table 2.3.

Chemical igniters in the higher energy end of the range (2,500 J, 5,000 J and 10,000 J for some cases) were chosen for the experimental programme, since it was expected that ignition would not happen with lower energy igniters if it did not occur when a higher energy igniter was employed. The chemical igniters (shown in Chapter 3) are manufactured by Fr. Sobbe in Germany and develop a *"strong exothermic reaction…capable of generating an adiabatic flame temperature of 3,870 K"* [Hertzberg et al., (1988)]. Going et al., (2000), when testing dusts in PRL-20 and $1m^3$ chambers found that overdriving occurs in PRL-20 and that using 2,500 J in the 20 litre chamber was equivalent to using 10,000 J igniters in $1m^3$ chamber [Going et al., (2000)]. Overdriving it is defined in this context as the effect caused in the flame from ignition due to preconditioning at the start of the experiment and the pressure rise from the igniter. Using CFD, Cloney et al., (2013) *"found that for 10,000 J igniters with an assumed 50 % efficiency, polyethylene particles under 50 µm reach 400 K"* [Cloney et al., (2013)]. Hence, the real temperatures in the ignition process are expected to be much lower than those theoretical if adiabatic flame temperature theory was considered. In addition, variability in chemical igniter efficiency introduces another experimental factor affecting flame propagation that must be taken into account when analysing dust ignition results. Due to the ignitor detonation dust particles might be displaced from the centre of the chamber increasing local dust concentration [Cloney et al., (2013)]. However, overdriving in 20 litre chamber would give a LFL that is lower than the actual one [Going et al., (2000)], which should not be a problem if just evaluating MEC values for the PF milling safety case.

In Figure 2.16, for Pittsburgh coal samples with 50 µm mean diameter, flammability evolution according to pressure ratio is shown for different ignition energies. As it can be seen, the trend for LFL or MEC versus concentrations (g/m^3) for the same coal varies significantly depending on the ignition energy used. As ignition energy increases, LFL values are reduced making the risk of ignition higher [Hertzberg et al., (1988)]. In Figure 2.18 the effect on LFL from ignition energy is shown, with values for that particular coal becoming close to independent of igniter energy above 2,500 J for both ignition criteria.

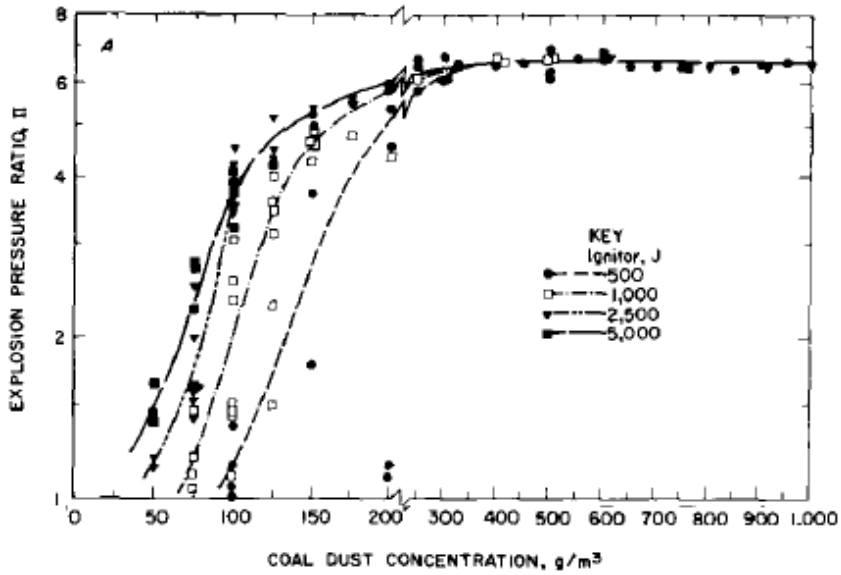

Figure 2.16. Flammability data showing pressure ratio (P/R) values with different chemical ignitors (500 - 2,500 J) for Pittsburgh coal [Hertzberg et al., (1988)].

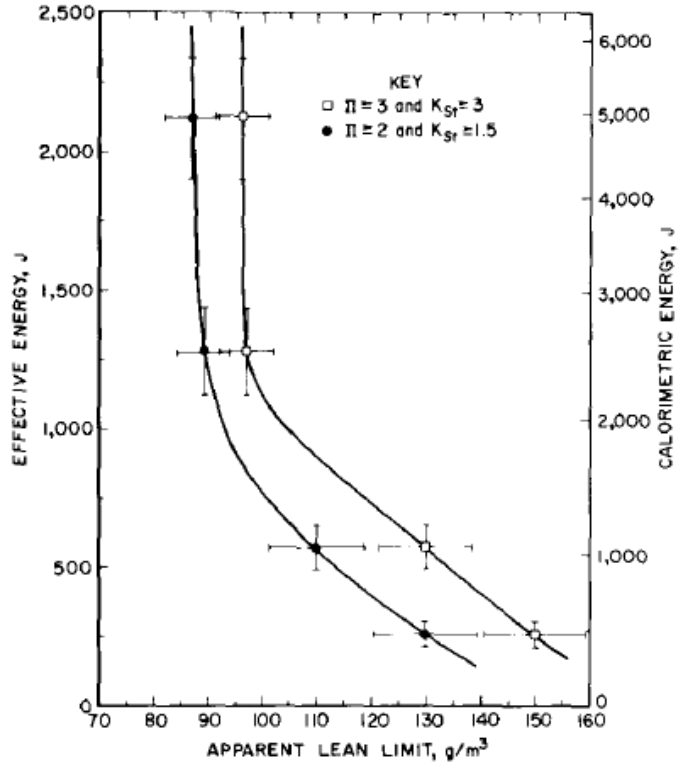

Figure 2.17. Effect of ignition energy on the apparent lean flammability limit (LFL) for coal dust with different ignition propagation criteria [Hertzberg et al., (1988)].

Kuai et al., (2013) have studied the role of ignition energy on dust explosion behaviour from a series of experiments in a Siwek 20 litre ignition chamber. The main conclusion is that "*inappropriate ignition energy will cause under-/over driving in the thermodynamic/kinetic characteristic measurements"* [Kuai et al., (2013)]. In addition, the impact of ignition energy strength on LFL was more significant for carbonaceous dusts than for metal dusts, in particular for fuels with lower volatile content [Kuai et al., (2013)].

Thus is can be seen that dust ignition phenomena are substantively more complex than gas ignition. For the coal and biomass dust ignition experimental programme for PF milling safety reported in this study, dust concentration, dust type (volatile content), dust particle size, O_2 content in the ignition atmosphere and ignition energy are considered as first order parameters and their effects are evaluated based on the P/R values obtained. Flame propagation from ignition and additional information that might have been provided by K_{st} values were considered less relevant for the identification of positive ignition in a 20 litre ignition chamber for the safety case.

To illustrate the theory explained in the above sections, Figure 2.18 [Cloney et al., (2013)] is used. This shows the idealised ignition process and flame propagation for dust explosions in the case of electrical activation.

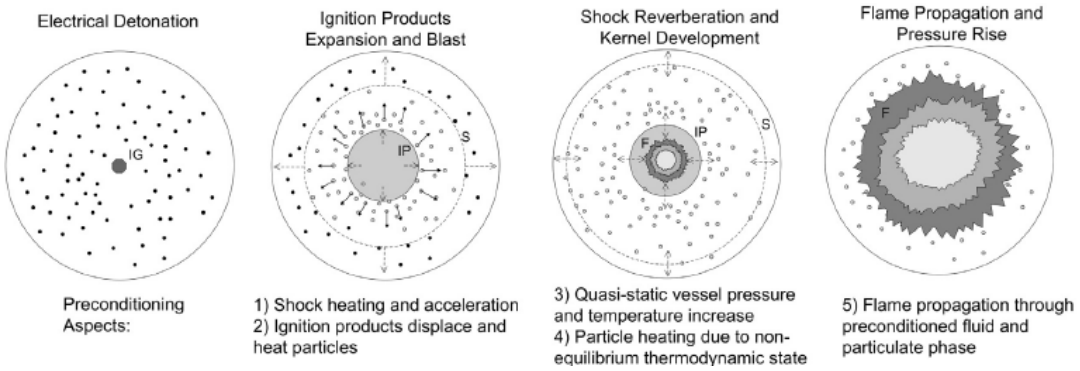

Figure 2.18. Idealised ignition process with flame propagation stages [Cloney et al., (2013)].

The key for ignition is achieving the devolatilisation process that will produce the combustion products to heat up the dust particles in a core area or kernel, releasing more volatiles and reaching the volatiles gas combustion mixture where flame propagation

develops a pressure rise at constant volume inside the ignition chamber. For flame propagation mechanisms and ignition understanding, inerting and dust ignition suppression studies are very useful in the underground coal mining safety case as developed by NIOSH. The author had the opportunity to contribute in the experimental programme with PRL-20 for characterising inerting dust particle size effects in ignition suppression [Trabadela, (2012)].

g) Dust ignition suppression and inerting

The aim of the research on coal dust explosions for underground coal mine safety is to prevent explosions and casualties in the industry. In 2010, NIOSH published a report reviewing the requirements for inerting and suppressing dust ignition [Cashdollar et al., (2010)]. Work by NIOSH [e.g. Sapko et al. 2000] showed that the amount of rock dust required for inerting increases with the coal volatile content of the dust and also depends on coal particle size, requiring more dust for finer coals [Cashdollar et al., 2010]. *"NIOSH recommends a new standard of 80 % total incombustible content be required in the intake airways of bituminous coal mines in the absence of methane"* [Cashdollar et al., (2010)]. According to the same publication, particle size *is "the single most influential factor controlling coal dust explosion propagation"* [Cashdollar et al., (2010)]. Sapko et al., (2000), assumed in NIOSH work rapid devolatilisation of the dust took place in the area near to the edge of the flame [Sapko et al., (2000)]. It was found that when the dust particle size is small enough, (<34 μm for coal and <14 μm the inerting rock dust) then it can be assumed that the ignition is independent of dust particle size [Sapko et al., (2000)]. In the case of the experiments carried out with pulverised Pittsburgh coal (PCC) (VM 36 % daf), it was observed that 20-L chamber and Lake Lynn Experimental Mine (LLEM) experiments required around 74 % and 80 % respectively (76 % and 82 % including ash and moisture) of limestone rock dust inerting material to suppress ignition (20L chamber) or suppress propagation of an explosion (mine) [Sapko et al., (2000)]. The rock dust amount required in the mine is slightly higher than in the chamber due to caking and dispersion effectiveness of the inerting dust. When inerting in the PRL-20 chamber, the results are obtained from runs at fuel loadings that give the highest peak pressures (e.g. 220 g/m^3 of PCC) and employing a moderate-energy ignition source (e.g. 5,000 J chemical igniter) in order to test the concentrations which would produce violent explosions in the combustion chamber but without excess fuel. This is distinct from the case of fuel-rich conditions at higher coal dust

concentrations (i.e. >500 g/m^3) where the maximum rate of pressure rise can reach a peak value but peak pressures are slightly lower. The general trend is that explosion intensities increase as fuel concentration is raised up to certain limit, where coal loading corresponds to the volatiles/air stoichiometric ratio limit; beyond this point the excess coal dust itself suppresses ignition, which means that less inert dust is required [Cashdollar et al., (2000)].

Dastidar et al., (1997), when testing rock dust inerting levels, found that the higher values of peak pressures and pressure rise rate were obtained with 2,500 J - 5,000 J igniters for most cases, but it could be possible that the properties of different inerting solids would change this pattern. In addition, the effect of a 5,000 J igniter in the PRL-20 combustion chamber was similar to a 2,500 J igniter in the Siwek 20-L chamber. Hence, depending on the geometry (nearly or complete spherical) and coal dust dispersion system, with lower or higher level of turbulence respectively, more rock dust inert material can be required. Interestingly, the Pocahontas and Pittsburgh coals despite having different volatile contents required similar amount of inerting dust [Dastidar et al., (1997)]

Dastidar and Amyotte, (2002), continuing on the dust explosions suppression work, compared new work on a 20 Siwek litre chamber with a 1m^3 ignition chamber. They attempted to find a minimum inerting concentration (MIC) for a range of fuels with the 20 litre vessel, demonstrating that there is a strong dependence on the strength of the igniters used to determine the amount of rock dust required for suppressing the explosion [Dastidar and Amyotte, (2002)]. This is particularly relevant for the oxy-fuel ignition experiments campaign in this study, as choosing an appropriate ignition strength is critical when testing a new range of pulverised fuels such as biomass. Furthermore, as the dust concentration increases in the ignition chamber, a lesser amount of rock dust was required to inert the explosion [Dastidar and Amyotte, (2002)]. This is consistent with [Sapko et al., (2000)] among others. Consequently, the range of fuel concentrations for the experimental programme will be in the lean end of dust concentrations to determine LFL for milling safety in the start-up process.

More recently, Man and Harris, (2014) worked on defining rock dust particle size requirement for effective ignition suppression with PRL-20, 1m^3 chamber and comparing them to LLEM data. Particles up to 841 µm can be found in limestone samples and particles larger than 75 µm *"offer almost no protection as inhibitor against coal dust explosions"* [Man and Harris, (2014)]. Coal dust explosion severity is controlled by particle size, with the

fines being the critical element in LFL/MEC values [Man and Harris, (2014)] and consequently particle size of inerting dust is relevant for suppression effectiveness.

h) Other parameters affecting ignition in 20 litre/30 litre chambers

Dust dispersion effectiveness inside the chambers can affect P/R values from coal and biomass ignition. Kalejaiye et al., (2010) studied the dust dispersion effectiveness and turbulence in the 20 litre Siwek ignition chamber using Pittsburgh coal and one of the dust optical probes from PRL (NIOSH). Dispersion uniformity was found to be independent of the nozzle type. In Siwek's 20 litre ignition chamber, particle size (surface weighted diameter) was reduced 60 % for Pittsburgh coal when dispersing the dust inside the chamber. Hence, dust particles tested in Siwek's chamber could be finer than the dust introduced originally due to the design of the dispersion valve which differs from PRL-20. This effect has not been found in PRL-20 or $1m^3$ chambers [Kalejaiye et al., (2010)]. Consequently, for the R-20 and R-30 designs used in this study it is expected that dispersion and turbulence will be carefully maintained stable between experiments but there was not time available in this experimental programme to use dust probes to check dispersion effectiveness. Preheating of the dust has a direct impact in the devolatilisation rate, where dusts can become more flammable if the temperature is increased at the start of the process [Hertzberg and Cashdollar, (1987)]. The is also a linear dependency on initial pressure in 20 L ignition chamber and LFL for coal dusts, showing higher LFL (g/m^3) as initial pressure increases [Hertzberg and Cashdollar, (1987)]. For this experimental programme in this study the initial pressure and temperatures were kept at atmospheric (in line with pulverised fuel practice) and ambient (to avoid undue experimental complexity and deemed adequate for comparison purposes between fuels, atmospheres etc.) respectively.

Other possible factors in dust ignition such as heterogeneous combustion, water and CO_2 dissociation were judged not to have a major influence in this study but might be investigated in future applications of oxy-fuel in coal and biomass power plants.

2.3.2. Implications for PF oxy-fuel development

In general, there is extensive literature on ignition chamber behaviour for coal dusts but when specific literature on dusts explosions in ignition chambers (e.g. for biomass dust ignition) was not found a broader approach has been taken.

When testing coal dusts for PR oxy-fuel safety in the PF milling operation the experimental methodology and parameters to be considered have been adapted from the underground coal mine safety case. A summary of the experimental characteristics for ignition chambers is included as Table 2.4.

Table 2.4 Dust explosions in mine safety versus oxy-fuel PR safety

	Mine safety	**PR oxy-fuel safety**
Ignition atmosphere	Air/ CH_4 <5 vol. %	Air, 21Oxy-30Oxy
Ignition E / source	1000-2,500 J chemical	2,500 J /5,000 J chemical/ spark
P/R	Threshold at >2	Threshold at >2.5
K_{st}	Confirms positive >1.5	Optional K_{st}
Turbulence	Low in mine gallery	High in PF mill
Overdriving	To be avoided	Desired for safety
Suppression	80 % suppressing dust	Optional
Forensic analysis	TGA	Optional TGA

When testing dusts ignitability in a 20 litre chamber at higher O_2 concentrations in CO_2, P/R has been considered 2.5 based on empirical evidence as an indicator for a valid threshold. K_{st} cannot be considered as a confirmation parameter for positive ignition if overdriving is desired in a safety case. The determination of K_{st} will be valid and optional for sizing venting system options if these are required in a mill. K_{st} values should be determined and contrasted with larger ignition chambers (e.g. 1 m^3) where overdriving is less likely. Turbulence is also a key parameter that has to be controlled, in particular if turbulence is too high it will impact on ignition and not allow devolatilisation and flame propagation. The ignition energy strength will also be a critical factor; in the experimental programme in this thesis, 2,500 J and 5,000 J chemical igniters are considered, with 10,000 J for some specific cases where dusts might be harder to ignite.

2.4. Coal dust ignition in oxy-fuel atmospheres

Relevant literature on coal dust ignition under oxy-fuel conditions is growing. A very important example is the programme of work that Molina and Shaddix have been carrying out in the recent years [e.g. Shaddix and Molina, (2011)]. In particular, high volatiles bituminous coals have been ignited in a furnace with temperatures from 1,130 K to 1,650 K. When testing with 1,130 K temperature, the ignition time was significantly delayed due to the O_2 concentration variability and the substitution of N_2 (air case) by CO_2 (oxy-fuel case). However, when testing with 1,650 K the same fuels, the change in O_2 concentration effect

was negligible and the presence of CO_2 instead of N_2, *"only retarded ignition by a few milliseconds"* [Shaddix and Molina, (2011)]. The retarding effect on ignition seems to be related to the higher heat capacity of CO_2 when compared to N_2, being compensated by higher O_2 concentration when igniting in 30 % O_2 v/v balance CO_2. Citing: *"These effects can be rationalized by applying autothermal ignition theory to describe the ignition of ejected volatiles in the presence of a hot oxidizing gas. CO_2 and H_2O also tend to inhibit ignition because of their chemical influence in reducing the concentrations of highly reactive radical species"*. [Shaddix and Molina, (2011)]. Hence, what happens is that CO_2 and water can compete with other species formed (such as hydrocarbons from devolatilisation), where "*the lower diffusivity of both oxygen and small hydrocarbons in CO_2 compared to N_2 is an important factor"* [Toftegaard et al., (2010)].

According to Toftegaard et al., (2010), devolatilisation is impacted by oxidiser composition, with the surrounding gas temperature around the particles determining the rate of devolatilisation [Toftegaard et al., (2010)]. Particle ignition, "*is a strong function of both the transport properties of the gas phase surrounding the particles as well as the combustion heat release rate and the reactivity of the local fuel-oxidizer mixture"* … "*Ignition times comparable to those observed during air combustion can be obtained by increasing the oxidizer oxygen concentration to 27–35 vol. % and thus the flame temperature"* [Toftegaard et al., (2010)]. When it comes to char combustion, there is a mixed chemical kinetic control (low and intermediate temperatures) and diffusion control (at higher temperatures) [Shaddix and Molina, (2011)]. As oxygen concentration increases, char burnout time is reduced and char particle temperature increases [Shaddix and Molina, (2011)].

Higher concentrations of water (when compared to the air combustion case) and its effect on ignition processes under oxy-fuel conditions has been evaluated by Yi et al., (2014), for several Chinese coals, with water causing a larger ignition delay and faster burnout under oxy-fuel conditions, the effect being more significant for brown coal, and directly related to the heating rate [Yi et al., (2014)].

The work presented in this thesis is an attempt to extend the closely related research by Man and Gibbins, (2011) for coals to biomass dust ignitability under oxy-fuel atmospheres for BECCS. When testing coal dust ignition behaviour under oxy-fuel conditions, Man and Gibbins, (2011) used a 20 litre ignition chamber (PRL-20)) to rank the ignitability of a set of coals and found that the coals with lower volatile matter content were more difficult to

ignite requiring higher ignition energy (2,500 J vs 1,000 J). "*Few coals ignited at 21 % v/v O_2 in CO_2 balance*" at all energies with *"important safety implications"* for PF milling. When coal dusts were ignited in a 30 % O_2 or 35 % O_2 in CO_2 atmosphere they gave similar ignition behaviour to air case [Man and Gibbins, (2011)]. Flower et al., (2010) using the same equipment also found that 30-35 % O_2 in CO_2 gave a similar ignition pattern to the air case. Most importantly, out of the 7 coals tested, "*only a few high volatile coals ignited in 21 %"* O_2 v/v balance CO_2 and these required 2,500 J igniters instead of 1,000 J to achieve positive ignition [Flower et al., (2010)].

Regarding particle size, Man and Gibbins, (2011), did not find a linear behaviour but particles larger than 53 µm were difficult to ignite and below that size they behaved *"almost identically"* to the entire coal sample [Man and Gibbins, (2011)], a sign of finding the characteristic diameter of the dust

2.5. Biomass dust ignition in air and oxy-fuel atmospheres

A brief discussion of biomass ignition behaviour in air and oxy-fuel atmospheres is shown in the following sections.

2.5.1. Literature review on biomass dust ignition in air

Biomass dusts are difficult to characterise since they are fibrous and the particles' aspect ratios makes the spherical idealisation used for coal particles much less appropriate. Volatile and moisture content are significantly higher to those in many coals, and this can be expected to influence biomass dust ignition behaviour in air and in O_2/CO_2 atmospheres. There are some studies in the literature on biomass ignition as single particle and as pulverised fuels in experimental rigs.

Flower and Gibbins, (2009), in a radiant heating wire mesh single-particle apparatus tested biomass combustion in air and found that increased moisture content of single particles of biomass impacted directly by increasing the devolatilisation and burnout times required. However, the mass of the particle was found to be the main factor in determining the ignition and combustion times, with moisture only a secondary effect [Flower and Gibbins, (2009)]. Although the ignition and combustion behaviour is expected to differ somewhat between biomass dusts clouds and single particles, the particle mass, and consequently size

range, needs to be considered as a major variable when planning the biomass dust ignition experimental programme in the ignition chambers.

For biomass dusts ignition in air, Huéscar-Medina et al., (2013), have reported MEC values from modified Hartmann tube apparatus for wood and torrefied biomass and compared this to Kellingley coal. Flame speeds from biomass ignition were 5-10 times higher than for the coal case [Huéscar-Medina et al., (2013)]. Saeed et al., (2014), continued the work in same rig, testing a range of agricultural biomass with the modified Hartmann apparatus and finding that biomass ash content influenced MEC values. Ash and moisture content which is higher in agricultural biomass than in wood tend to inert ignition and to reduce flame temperature while reducing MEC values. The flame speed was about 2.5 m/s. It is important to note that LFL values were comparable to those for wood but much lower than for coal, showing a highly reactive behaviour [Saeed et al., (2014)]

Wilén et al., (1999), reported ignition temperatures for biomass dust ignition in ignition chambers ranged between 300-340 °C for a biomass layer and higher range in 400-460 °C for biomass dust clouds in air. These ignition temperatures are different from self-ignition or minimum AIT which are lower [Wilén et al., (1999)]. This suggests ease of ignition behaviour when compared with coal dust ignition. Biomass dusts have also shown lower AIT in previous literature [e.g. Conti and Hertzberg, (1987); [Hertzberg, (1991)].

One of the pulverised fuels tested in the experimental programme is torrefied biomass. Toptas et al., (2015) have shown that torrefaction of biomass increased the char reactivity during the combustion process for a set of cellulose and animal waste biomass. When blending the torrefied biomass with lignite (1:1 ratio) they found that the blend had a lower ignition temperature than the lignite. Higher char reactivity was a consequence of torrefaction of biomass but no interaction of lignite-biomass was seen in the first stage of co-combustion [Toptas et al., (2015)].

Further literature on biomass ignition and combustion in air is cited in the oxy-fuel section, where it is used to compare oxy-fuel behaviour to air combustion.

2.5.2. Literature review on biomass dust ignition in oxy-fuel atmospheres

The author is not aware of any other studies in the literature on oxy-biomass dust clouds in ignition chambers, apart from Trabadela et al., (2014), which are partial results of this Ph.D. research thesis. However, there are examples of experimental work in the literature of biomass ignition studies under oxy-fuel atmospheres in other systems such as employing single particle apparatus, DTF, TGA and pilot scale rigs for larger scale oxy-biomass combustion evaluation. Many of the experimental cases focus on coal-biomass blends for co-firing studies.

Riaza et al, (2014), tested single particles of pine sawdust and torrefied sawdust among other biomass types in a DTF at 1,400 K in oxy-fuel atmospheres. They found that combustion of the biomass happened in two phases, the first on combustion of volatiles in spherical envelope flames and the second phase involving char reacting with the oxidant mixture [Riaza et al., (2014)]. If 21 % O_2 v/v balance CO_2 was used as oxidant, the intensity of the combustion decreased, with lower temperatures and longer burnout times than in air, that were recovered when using 28-35 % O_2 v/v in CO_2. It is relevant that the role of the volatiles (>70 wt. %, db. for all biomass samples tested) in the combustion process translated into lower soot formation when compared to coals.

Then it is expected that the pyrolysis of the fuel has an impact on the transition from homogeneous combustion of the volatiles to heterogeneous combustion of the char. Yuzbasi and Selçuk, (2011), when testing blends of olive residue and lignite (1:1 ratio) with a TGA have shown that blend samples behaved similarly up to 700 °C with the pyrolysis not significantly affected by O_2 dilution in N_2 (air case) or CO_2 (oxy-fuel case). The combustion process *"was slightly delayed in oxy-fuel"* [Yuzbasi and Selçuk, (2011)] compared to the air case if the same molar O_2 was present. At higher O_2 levels complete combustion was reached at lower temperatures with higher weight loss experienced by the fuels [Yuzbasi, and Selçuk, (2011)].

Follow-on TGA studies Pickard et al., (2014a) showed that higher O_2 levels increased the volatiles and char reactivity for four biomass types, with devolatilisation behaving similarly for two different heating rates but char oxidation being slower at the higher heating rate. It was not that clear the N_2 substitution by CO_2 was having much effect. When testing in 30 % O_2 v/v balance in CO_2, "*combustion was more reactive*" than in air case [Pickard et al.,

(2014a)]. When testing biomass and coal blends with TGA, a similar trend was observed but when "*cofiring three biomasses with coal at 20 kW scale suggest substitution of N_2 with CO_2 significantly reduces temperatures, carbon burnout and emissions of NO while combustion in O_2-enriched conditions has the opposite effects"* [Pickard et al., (2014b)]. Holtmeyer et al., (2012) when using CFD modelling for oxy-biomass have confirmed that delayed devolatilisation in biomass can impact NO formation and that "*Flame envelope length is influenced by volatility and particle size when cofiring"* with the flame being shorter at higher O_2 levels [Holtmeyer et al., (2012)].

According to Farrow et al., (2013), when testing in a DTF and TGA, there is a "*potential catalytic effect of biomass-contained alkali and alkaline metals on coal char burnout"* when co-firing with coal [Farrow et al., (2013)], with this effect being more pronounced in oxy-fuel atmospheres when compared to air. The same effect was observed by Toptas et al., (2015) for air firing. Citing literally from Farrow et al., (2013): "*The DTF biomass/coal char blends from devolatilisation in CO_2 burn off approximately two times faster than those prepared in nitrogen"* [Farrow et al., (2013)]. Thus it is expected that devolatilisation will be significantly faster in oxy-fuel atmospheres for biomass tested in the experimental programme in this study.

2.6. Conclusions for experimental programme

In this chapter the dust ignition theory and previous work required to design an experimental programme on coal and biomass dust ignition under oxy-fuel conditions has been presented. The primary issue has been defining positive and negative ignition cases for enhanced PF mill safety in oxy-biomass. Fuel concentration, particle size, ignition energy and ignition atmosphere (O_2 levels balance CO_2) are established as the key experimental parameters to be analysed in order to increase the understanding of ignition behaviour for the pulverised fuel clouds considered. For that purpose, the design and manufacturing process for two novel ignition chambers of 20 litre and 30 litre volumes (R-20 and R-30 respectively) is comprehensively explained in the following Chapter 3 of this thesis.

3. Ignition chamber(s) (R-20, R-30) design and manufacture process with ancillary equipment for coal and biomass dust ignition experiments

3.1. Relevant existing 20 Litre ignition chambers

A broad range of experimental apparatus has been designed and built in the past to carry out dust suspension ignition experiments. The purpose of the present study was to construct a suitable ignition chamber with improved versatility for a wide range of test conditions within the budgetary constraints of the OxyCAP UK project. The focus in assessing previous chamber designs was on Pittsburgh Research Laboratory (PRL) 20 Litre ignition chamber [Cashdollar and Hertzberg, (1985)] and the Siwek ignition chamber [British Standards BS EN 14034-1, (2004)]. The PRL-20 design was chosen due to familiarity and experience using the chamber and the Siwek-20 chamber because it is the standard design for a 20 litre spherical pressure vessel for dusts explosivity studies in Europe.

3.1.1. Pittsburgh Research Laboratory 20 Litre ignition chamber (PRL-20)

Coal dust ignition and ignition inerting measures to prevent dust explosions in underground coal mines have been comprehensively studied at the US Bureau of Mines (USBM) and its successor organisation the National Institute for Occupational Safety and Health (NIOSH, part of CDC) at the Pittsburgh Research Laboratory, located at the Department of Energy (DOE) Complex in Pittsburgh (USA), most recently under the direction of Dr. Chi Man succeeding Mr. Ken Cashdollar. A 20 litre explosion chamber designed in-house was employed in the research facilities to simulate similar conditions to coal dust ignition that can occur in the galleries of coal mine and related industries. Cashdollar and Hertzberg, (1985), describe how the PRL-20 was designed to permit the use of *"very strong ignitors which are necessary for hard-to-ignite dusts and for dust-inhibitor mixtures"* [Cashdollar and Hertzberg, (1985)]. The idea of building a pressure vessel to carry out constant volume explosions with suppression agents provided new research capabilities to investigate dust explosions propagation. PRL-20 was built with the capability to attach in-house dust-probes [Cashdollar, Liebman and Conti, (1981)] to the vessel to evaluate dust dispersion inside the chamber [Cashdollar and Hertzberg, (1985)].

The PRL-20 (Figures 3.1 and 3.2) is characterised by a non-spherical ignition chamber shape of the bomb, which is has a short cylindrical section with hinged top and domed ends [Cashdollar, (2000)]. This is a very important characteristic of this chamber that makes it different from the Siwek vessel and the R-20 ignition chamber designed at the University of Edinburgh, both of which are perfectly spherical in geometry. PRL-20 is made of stainless steel type 304 and its pressure rating is 21 bar. Ports allow for gas inlet/exit valve connections as well as access for instrumentation [Cashdollar and Hertzberg, (1985)].

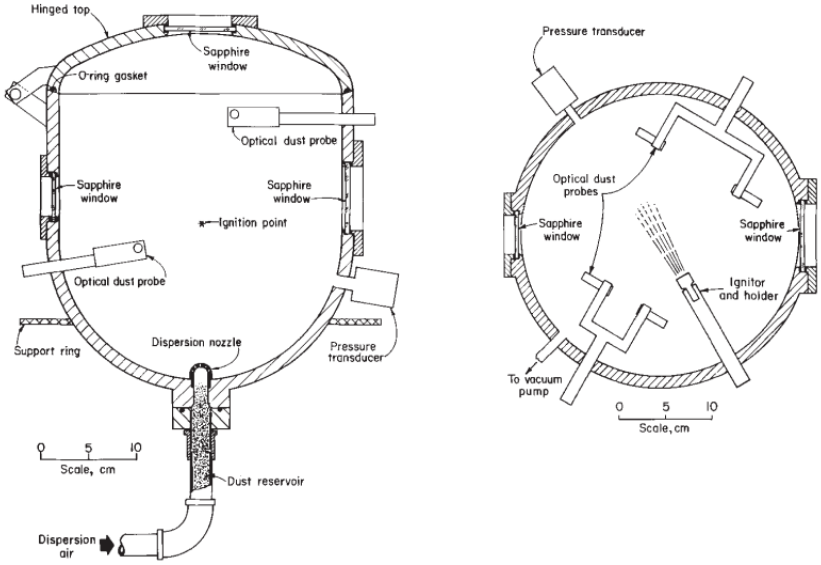

Figure 3.1. Cross sections of 20 L ignition chamber at NIOSH [Cashdollar, (2000)].

Figure 3.2. PRL-20 Ignition Chamber [Man and Gibbins, (2011)].

As described in the previous chapter, oxy-fuel ignition work was developed by Man and Gibbins, (2011) with the PRL-20 combustion chamber. They reported interesting coal dust ignitability data for a set of coals used in the UK and worldwide under oxy-fuel atmospheres. More recently, PRL-20 was employed during an experimental programme that evaluated particle size effects for limestone for ignition suppression in air combustion. This research was carried out in the Fall of 2011 by Trabadela, Green and Man. Part of the results arising from this work also contributed to the publication by Man and Harris, (2014), discussed in Chapter 2.

3.1.2. Siwek 20 L ignition chamber

Ignition chambers employed in Europe to study the safety cases for PF combustion include the design in the British Standards (based on Siwek's 1978 design) shown in Figure 3.3:

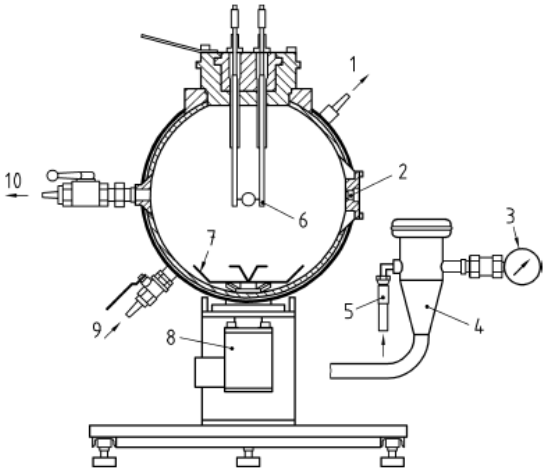

Figure 3.3. Siwek 20 litre Ignition Chamber [British Standards BS EN 14034-1, (2004)].

According to Siwek, (1996), investigation of dust explosibility has to be carried out following standard procedures. The 20 litre chamber was considered to give similar behaviour to a standard 1m^3 chamber and this is why the use of 20 litre chamber in lieu of 1 m^3 was widely extended [Siwek, (1996)]. The Siwek chamber uses 2 x 5,000 J igniters and a rebound dust dispersion nozzle [BS EN 14034-1-4, (2004, 2006, 2008], with 0.1 s ignition delay and 20 bar inlet pressure, causing higher turbulence when compared to PRL-20 [Cashdollar, (1996)].

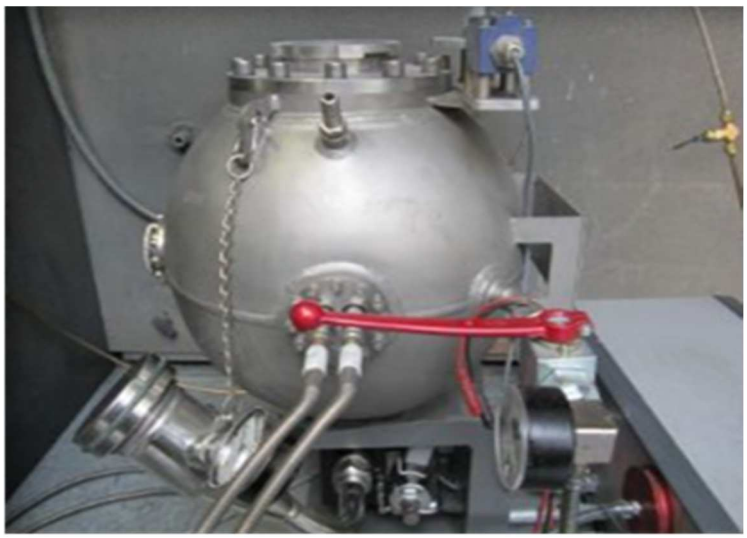

Figure 3.4. Siwek-20 Litre Ignition Chamber [Extracted from http://www.explosivedust.com/dusttest.htm#].

In Figure 3.4 a picture of Siwek type ignition chamber is shown, with its characteristic double ignition source (the two connections in the centre of the image). Access to the chamber is on top and via ports allocated on the sides of the pressure vessel. This less accessible 20 litre chamber design together with there being no possibility of chamber extensions made the Siwek design unsuitable for the OxyCAP UK research project.

3.2. New design for a new 20 Litre ignition chamber (R-20)

After carefully evaluating the options available and checking the advantages and disadvantages of the existing ignition chambers, the choice for a new 20 Litre ignition chamber design (R-20) to be built to carry out a constant volume dust explosions under oxy-fuel conditions experimental programme for CCS was made.

3.2.1. Factors affecting R-20 design options

The process of designing R-20 ahead of the experiments was mainly influenced by the following factors:

1) Safety, the pressure vessel had to be reliable and able to withstand dust explosions within a general laboratory (i.e. without any special blast protection).

2) Economic constrains due to budget plan in the OxyCAP UK project.

3) Technical services machining capabilities within the University of Edinburgh, i.e. maximum of 400 mm external diameter for milling at the time of the vessel construction.

4) Time limit and urgency to start the project as soon as possible to deliver on the OxyCAP UK Consortium meeting project deadlines.

5) Versatility of the pressure vessel to maximise value of the investment, i.e., being able to reuse the apparatus for future research projects involving gases or other fuels at potential higher pressures and operating under different experimental conditions to the current case.

In many respects the ignition chamber design has required finding a balance between operability and enhanced safety, taking into consideration that ignition experiments could not be carried out with other students in the immediate vicinity nor with the operator working entirely alone without adequate monitoring and safety measures to avoid potential accidents.

3.2.2. Principal features of R-20

The principal features of ignition chamber R-20 at the University of Edinburgh are explained in this section. Although specific details are explained in sections below, the purpose of this summary is to explain to the reader the main characteristics of the pressure vessel that forced certain decisions in the design and the construction process. The features are as follow:

1) The need to have a spherical 20 litre ignition chamber. R-20 is a perfect sphere and this was decided in order to be able to use a standard geometry [British Standards BS EN 14034-1, (2004)] as well as to ensure that the distance from ignition point (centre) to the walls of the pressure vessel would be the same in all directions. The latter cannot be assumed for the PRL-20 design due to the cylindrical section and domed top of the chamber. It is important that the combustion chamber is spherical so as to be able to assume that the maximum rate of pressure rise occurs at the time a symmetrically-expanding flame front contacts the vessel.

2) Overdesigned. The chamber as shown in the section below was voluntarily overdesigned, not just in terms of pressure and temperature rating in order to be well within safety limits for the current programme but also to facilitate possible use of the chamber for other applications in future research projects. The use of stainless steel as design material was

the option made even if corrosion is not a major issue in the type of experiments carried out. The approach of having a spherical shape inside but not outside gives the design two major characteristics, first, it provides additional strength due to extra metal thickness and second, the chamber manufacturing process was easier and cheaper than if the outside surface would also have been spherical (as in Siwek-20 design).

3) Ease of access. R-20 can be opened at its centre to be cleaned and to collect the dust samples after ignition experiments. This is a very important characteristic for any dust, as opposed to gas, ignition chamber.

4) Potential multiple configurations. The pressure vessel R-20 is made of four independent parts that are not permanently joined or welded in any way. They can be taken apart from each other for revision or individual substitution. Any potential thermal effects on the metal during the welding process are also avoided. The most important reason for the independent parts option is the need to be able to extend the volume of the chamber beyond 20 litres while changing the geometry of the pressure vessel. This would involve inserting a tube section between the two hemispheres that form R-20. The operator can then easily adapt the instrumentation to continue the dust ignition explosions research programme in a larger vessel without having to duplicate auxiliary equipment (see further details on R-30 in Section 3.4). This method has the disadvantage of not being able to operate multiple chambers at the same time. The potential multiple configurations of the chamber(s) include even larger volumes not built in this research project and the ability to undertake ignition experiments at constant pressure. As far as the author is aware this example of an extendable chamber for carrying out dust ignition experiments under oxy-fuel conditions is a novel contribution to the field that adds value to the outcome of this Ph.D. research.

5) Can be operated by just one person. There was a need for the ignition chamber experiments to be able to be run by the research student without permanent additional technical support. Finally, robustness combined with versatility are characteristics of the ignition chamber(s) R-20 and R-30 one of the most important strengths of the first of a kind design in Edinburgh.

3.3. Edinburgh University 20 Litre ignition chamber (R-20)

The process of designing and building a new ignition chamber at the University of Edinburgh was a major part of the research programme. The steps taken forward after careful consideration of alternative options are presented in the sections below.

3.3.1. Basic parameters for R-20 ignition chamber

R-20 as a sphere inside the pressure vessel requires some basic calculations before determining the final design of the chamber.

a) Basic dimensions

Attending to the formula for the volume of a sphere for a 20 litre ignition chamber:

$$V = \frac{4}{3}\pi \cdot r^3 \qquad \textbf{Equation [3.1]}$$

$$r = \left(\frac{3 \times 0.02}{4 \cdot \pi}\right)^{1/3} = 0.16839\,m \leftrightarrow 168.4\,mm \therefore D = 336.8\,mm \qquad \textbf{Equation [3.2]}$$

For a volume of 20 litres a in the R-20 oxy-fuel ignition chamber a spherical cavity of 336.8 mm internal diameter (ID) is required. Respective diameters for 150 litres and 200 litres are 659.2 mm and 725.6 mm.

Given the construction and operational constraints mentioned before it can be seen that, although it could be attractive to have a 200 litres spherical ignition chamber, at the time of building the first pressure vessel for the experiments the standard option of 20 litres volume was selected since dimensions for R-150 and R-200 meant they were far too large to be machined in-house. Subsequently it was decided that even the R-20 would need to be machined by an external contractor, Lazer Engineering, in Musselburgh, Scotland.

b) Coal and biomass dust loading

It was expected to have to work with similar coals and types of biomass that covered examples of fuels burnt in power plants in UK. Experimental coal/biomass concentrations and loadings most likely to be used upon volume of ignition chamber variation are shown in Table 3.1:

Table 3.1. Experimental coal/biomass concentrations and loadings												
Bomb	**20 L**	**30L**	**40L**	**60L**	**80L**	**100L**	**120L**	**140L**	**150L**	**160L**	**180L**	**200L**
Conc., g/m^3	**Coal/biomass loading, g**											
100	2	3	4	6	8	10	12	14	15	16	18	20
150	3	4.5	6	9	12	15	18	21	22.5	24	27	30
200	4	6	8	12	16	20	24	28	30	32	36	40
250	5	7.5	10	15	20	25	30	35	37.5	40	45	50
300	6	9	12	18	24	30	36	42	45	48	54	60
350	7	10.5	14	21	28	35	42	49	52.5	56	63	70
400	8	12	16	24	32	40	48	56	60	64	72	80
450	9	13.5	18	27	36	45	54	63	67.5	72	81	90
500	10	15	20	30	40	50	60	70	75	80	90	100
550	11	16.5	22	33	44	55	66	77	82.5	88	99	110
600	12	18	24	36	48	60	72	84	90	96	108	120

The pulverised fuel (PF) loading is considered up to a concentration of 600 g/m^3; for higher concentrations for the same ignition source, dust can self-suppress the ignition propagation acting as a heat sink. However, fine dusts like PPC coal can explode even at concentrations beyond 4,000 g/m^3 despite uncertainty on dust dispersion effectiveness [Cashdollar, (1996)]. As the loading increases in terms of weight, it makes it more difficult to disperse the dust in cloud formation before ignition as well as making it more complicated to deal with samples in the pre and post-experiment phases. Moreover, a major focus of this research programme is determination of the lean flammable limit (LFL) for ignition at constant volume. Although a wide range of dust concentrations, including above 600 g/m^3, can be expected in PF milling plant during normal operation it is the lower end of dust concentrations in air or O_2/CO_2 that needs to be considered for possible explosion during mill start-up/shut-down if an ignition source is available (e.g. PF smouldering fire, sparks from damaged components).

c) Combustion atmospheres for experiments

In order to study the gas or combustion atmosphere effect on PF ignition, up to 5 different cases were considered, as shown in Table 3.2:

Table 3.2. Combustion atmospheres		
Cases		
Gas mixture	**O_2 vol.%**	**N_2 vol.%**
1	21	79
Oxy-atmosphere	O_2 vol.%	CO_2 vol.%
2 (21 Oxy)	21	79
3 (25 Oxy)	25	75
4 (30 Oxy)	30	70

Based on previous studies [e.g. Man and Gibbins, (2011)] 30 Oxy is particularly interesting when comparing data to air combustion case at least for coal behaviour. Case 3, 25 Oxy, is also an important addition to show the effect of atmosphere between 21 Oxy and 30 Oxy when compared to other dusts ignition studies in O_2/CO_2 mixtures [e.g. Man and Gibbins, (2011)]. Higher O_2 concentrations than 30 %, although potentially of interest, could not be carried out under this research programme due to site-specific safety concerns.

3.3.2. Determination of limit operational conditions for R-20 and other design considerations

For R-20 design constraints, it was important to determine the expected limits for experimental conditions in coal dust ignition tests under oxy-fuel conditions, in particular the peak design temperature and pressure.

Mathematical formulation of combustion phenomena can be complex in the oxy-fuel case, but for a safety study it could be assumed that the adiabatic flame behaviour is the worst case scenario and calculate the maximum temperature and pressures from it for each fuel.

a) Design temperature

When considering constant volume adiabatic flame temperature (T_{ad}), it can be assumed that the maximum temperature reached during the combustion process is in the flame and that temperature is considered to be constant along all the dimensions of the flame. T_{ad} simplification for dust ignition can be used with the following assumptions:

1. Ideal Gas Law is held in the ignition process.
2. The dust-ignition source mixture is ignited and the ignition energy source effect (pressure rise and volume) is negligible.

3. The flame front velocity is below speed of the sound (deflagration).

4. The pressure increase in the chamber due to ignition is considered uniform in the pressure vessel.

5. Burning time in the flame front is short, so combustion is completed in a thin flame.

The approach taken to be used to determine possible T_{ad} and P_{max} for a broad range of cases is:

1. Assume complete combustion case, calculating T_{ad} following standard method of enthalpies with reactants and products in Gaseq version 0.79 [Morley, (2005)]. T_{ad} (and P_{max}) are determined by Gaseq software.

2. Assume detonation case (not realistic, only deflagration expected) to determine with Gaseq T_{ad} and P_{max} with Chapman-Jouguet detonation option where it is assumed that the chemical reactions are instant within the shock and the wave velocity generated is "*only dependent on the physical and chemical properties"* of the reactants [Brüls et al., (1994)].

3. Compare Tad or P_{max} values obtained from simulations with those available from literature in key publications. Then the higher T_{ad} leading to maximum pressure P_{max} is taken as the worst case scenario for safety design purposes.

A set of typical coal data was selected from Technical data on fuel [Rose and Cooper, (1977)] to "simulate" in Gaseq and estimate T_{ad} and P_{max} during pulverised fuel the ignition tests (Table 3.4). In the case of oxy-combustion, with the presence of water vapour and dissociation effects, it is a simplification to simulate coal as mixture of graphite, liquid water and gaseous hydrogen, the same assumption as if Dulong formula for calorific value of the coal [Rose and Cooper, (1977)] is applied.

Coal = graphite, H_2O (liq) +H_2 (g) **Equation [3.3]**

From technical data on fuel [Rose J.W. and Cooper J.R., (1977)] for a coal as reactants an illustrative example is shown:

C: 85.0 85/12=7.08 atom mol **Equation [3.4]**

H: 5.3 5.3 atom mol **Equation [3.5]**

O:7.1 7.1/16=0.44 atom mol **Equation [3.6]**

And for products:

H: 5.3-2 × 0.44=4.4 atom mol **Equation [3.7]**

H_2: 4.4/2= 2.2 atom mol **Equation [3.8]**

Mass in = 17.74 moles ×20.05 g/mole (From Gaseq)= 355.67 g **Equation [3.9]**

Fuel in = 355.67-8.1 × 32g/mol O_2 = 96.47 g **Equation [3.10]**

Results for T_{ad} and P_{max} for each potential type of coal are presented in Table 3.4. Screenshots of Gaseq software with an example for adiabatic temperature and composition calculation at constant volume for coal 601 for equilibrium and detonation cases are shown in Figures below. Note the significant difference between P_{max}, with detonation case nearly doubling the equilibrium value. Similar procedure for all coals in Table 3.3 was followed to build data shown in Table 3.4. At the time R-20 ignition chamber was designed only evaluation of coals was considered; requirements for biomass experiments came in later stages of the OxyCAP UK project.

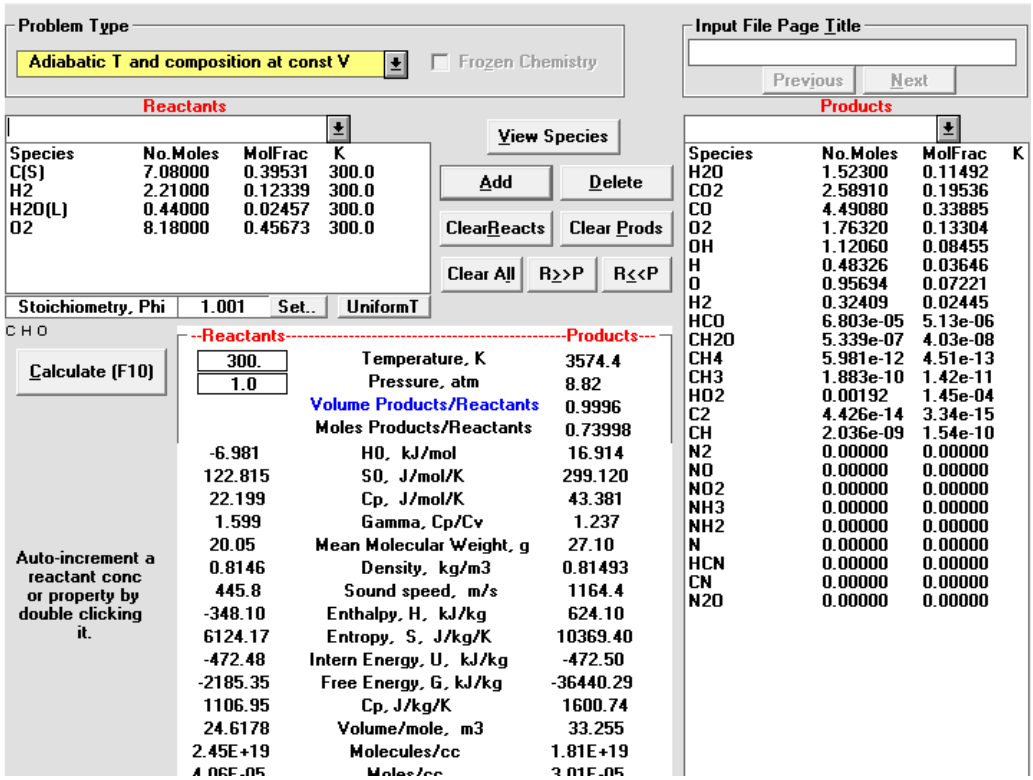

Figure 3.5a. Screen capture of Gaseq for T_{ad} and P_{max} calculation for coal 601.

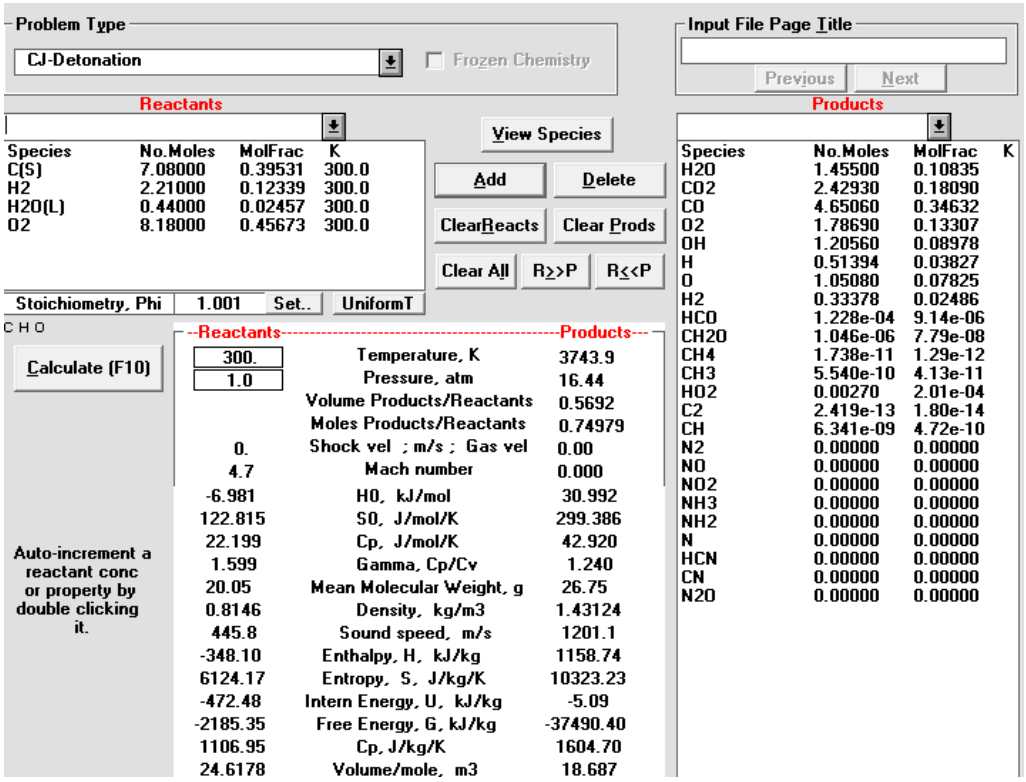

Figure 3.5b. Screen capture of Gaseq for T_{ad} and P_{max} calculation for detonation - coal 601.

Table 3.3. Coal data																		
Coal Type	**Anthracite**		**Dry Steam coal**	**Coking Steam Coals**		**Medium volatile Coking Coals**		**Heat-altered Coals**		**Very strongly caking**	**Strongly caking**		**Medium caking**		**Weakly caking**		**Very weakly caking**	**Non-caking**
National Coal Board Rank Code	101	102	201	202	204	301a	301b	302H	303H	401	501	502	601	602	701	702	802	902
Moisture content, %																		
Air-dried coal	2	1	1	1	1	1	1	1	2	2	2	3	4	4	5	5	8	10
At 96% relative humidity and 30ºC	4	2	1	1	1	1	1	2	3	2	3	4	6	5	6	7	11	13
Properties of dry, mineral matter free coal																		
C, %	94.4	93	92.4	92	91.6	90.4	89.3	88.8	87.8	87.5	86.8	85.2	85	84.5	84.5	83.5	82	81
H, %	2.9	3.7	4	4.2	4.5	4.9	5	5	5.1	5.3	5.3	5.4	5.3	5.5	5.2	5.4	5.3	5.1
N, %	1.1	1.3	1.4	1.4	1.4	1.5	1.5	2	1.7	1.9	1.7	1.8	1.8	1.8	1.8	1.7	1.7	1.6
S, %	0.7	0.7	0.9	0.7	0.7	0.6	0.8	0.8	0.1	1	1	0.9	0.8	0.9	0.8	1	1	0.7
O, %	0.9	1.3	1.3	1.7	1.8	2.5	3.4	3.4	4.4	4.3	5.2	6.7	7.1	7.3	7.7	10	10	11.6
VM, %	5	7.5	11.5	14	18	23	30	25	28	35	35	37.5	35	37.5	35	39	39	40
GCV, kJ/kg	35800	36250	36500	36650	36750	36750	36400	36300	35950	36050	35700	35450	34900	34900	34400	33750	33750	32800

[Extracted from Rose and Cooper, (1977)]

Table 3.4. Adiabatic flame temperature (T_{ad}) and maximum pressure (P_{max}) determined with Gaseq																		
Coal type	101	102	201	202	204	301a	301b	302H	303H	401	501	502	601	602	701	702	802	902
C	7.87	7.75	7.70	7.67	7.63	7.53	7.44	7.40	7.32	7.29	7.23	7.10	7.08	7.04	7.04	6.96	6.83	6.75
H	2.90	3.70	4.00	4.20	4.50	4.90	5.00	5.00	5.10	5.30	5.30	5.40	5.30	5.50	5.20	5.40	5.30	5.10
O	0.06	0.08	0.08	0.11	0.11	0.16	0.21	0.21	0.28	0.27	0.33	0.42	0.44	0.46	0.48	0.63	0.63	0.73
H_2	1.39	1.77	1.92	1.99	2.14	2.29	2.29	2.29	2.28	2.38	2.33	2.28	2.21	2.29	2.12	2.08	2.03	1.83
H_2O	0.06	0.08	0.08	0.11	0.11	0.16	0.21	0.21	0.28	0.27	0.33	0.42	0.44	0.46	0.48	0.63	0.63	0.73
O_2	8.565	8.635	8.66	8.665	8.1	8.1	8.1	8.54	8.46	8.48	8.395	8.24	8.1	8.18	8.1	8	7.845	7.665
Moles in	17.9	18.2	18.4	18.4	18.0	18.1	18.0	18.4	18.3	18.4	18.3	18.0	17.8	18.0	17.7	17.7	17.3	17.0
MW, g/mole	20.05	20.05	20.05	20.05	20.05	20.05	20.05	20.05	20.05	20.01	20.02	20.02	20.05	19.99	20.11	20.1	20.1	20.22
Mass in, g	358.53	365.61	368.12	369.55	360.57	362.57	361.74	369.72	367.45	368.62	365.93	361.16	357.56	359.25	356.78	354.93	348.30	343.03
Fuel in	84.45	89.29	91.00	92.27	101.37	103.37	102.54	96.44	96.73	97.26	97.29	97.48	98.36	97.49	97.58	98.93	97.26	97.75
Fuel/kg react	0.2355	0.2442	0.2472	0.2497	0.2811	0.2851	0.2835	0.2609	0.2632	0.2638	0.2659	0.2699	0.2751	0.2714	0.2735	0.2787	0.2792	0.2850
Gaseq T Adiabatic T at cnt. V, K	3647.9	3633.5	3629.4	3623.8	3620.2	3610.4	3603.7	3603.4	3594.5	3593.8	3587	3575.8	3574.4	3570.5	3570.3	3552.2	3551	3540.1
Gaseq P Adiabatic T at cnt. V, atm	8.907	8.908	8.912	8.904	8.909	8.899	8.885	8.89	8.87	8.87	8.85	8.83	8.82	8.814	8.8	8.76	8.757	8.71
Gaseq P Adiabatic T at cnt. V, bar	9.0250	9.0260	9.0301	9.0220	9.0270	9.0169	9.0027	9.0078	8.9875	8.9875	8.9673	8.9470	8.9369	8.9308	8.9166	8.8761	8.8730	8.8254
Gaseq CJ Detonation T, K	3825.2	3809	3804.4	3798.2	3794.2	3783.4	3776	3775.6	3765.9	3765.1	3757.7	3745.4	3743.9	3739.7	3739.4	3719.7	3718.3	3706.4
Gaseq P CJ Detonation, atm	16.593	16.597	16.605	16.594	16.603	16.588	16.564	16.56	16.53	16.541	16.508	16.459	16.443	16.44	16.414	16.34	16.328	16.25
Gaseq P CJ Detonation, bar	16.813	16.817	16.825	16.814	16.823	16.808	16.783	16.779	16.749	16.760	16.727	16.677	16.661	16.658	16.631	16.557	16.544	16.465

From Table 3.4, it can be observed that there are discrepancies among maximum pressures and temperatures calculated. The adiabatic flame temperature at constant volume approach (Gaseq) is complemented with detonation case which is not going to happen during the ignition test due to just deflagration is expected. Although some of the assumptions above might not be entirely correct for an ignition case, which is not complete combustion, for the purpose of designing R-20, detonation for 101 coal is taken with a T_{ad} value of 3825.2 K.

Finally, the pressure vessel walls are thick enough to include an adequate safety margin accounting for uncertainties in the prediction of adiabatic flame temperature as well as to act as heat sink to absorb the temperature increase from the ignition experiments without risks to the chamber operator.

d) Design pressure

Following the indications in the BS EN 10034, (2004), it can be assumed that the maximum pressure reached inside a closed spherical or cubic vessels of size ≥20 dm^3 it is nearly independent of the volume of the vessel (this also has implications from the experimental programme).

The design pressure is a very important aspect of the entire mechanical design; the test chamber has to be able to withstand at least 10 % above the maximum pressure conditions in the process [DTI, (2005)]. The design pressure in this case has not been considered as the maximum pressure before relief devices activate, which are set at lower pressure for a different vessel failure mode explained in further sections.

Gaseq calculations were used as indication of potential experimental conditions and the final design pressure and design temperatures for R-20 were decided according to the material selection and the insurance process.

d) Materials of construction

The materials used for building pressure vessels vary depending on several factors that can affect the behaviour of the chamber in the short and longer term. Although in many cases, carbon steels and other alloys of steel are used, there are also examples of pressure vessels made of different materials such as plastics or glass. Key factors taken into account for R-20 construction were:

1) Prevention of catastrophic consequences if ductile failure of the chamber happens.

2) Design variables for operation, including design pressure, design temperature and potential for corrosion.

3) Avoiding contamination of dust samples.

4) Physical and mechanical properties of the material in order to meet safe operating requirements.

5) Cost of the material, if suitable alternatives are available.

In the case of the oxy-fuel ignition bomb (R-20) it was decided to use a stainless steel as the main material in order to help ensure there are no thermal or chemical problems related to the material choice when operating the vessel. Hence, in the following sections a justification of which alloy of stainless steel to use is presented. Special attention was paid to nominal design stress with thermal and corrosion properties for each option considered.

e) Nominal design stress

The nominal design stress has to be decided for design purposes to determine the maximum allowable stress that is required to be supported by the material of construction. This is determined by applying a suitable "design stress factor" or "factor of safety" to the maximum stress that the material could be expected to withstand without failure under standard test conditions.

Nominal design strength (f_N) can be determined. For this purpose, the nominal design strengths listed in the standard [BS PD5500, (2009)], for a range of materials and temperatures are shown in Tables 3.5 and 3.6:

Table 3.5. Nominal design strength for some Austenitic Stainless Steels above 700ºC

Stainless Steel	Rm, N/mm^2	Re, N/mm^2	T_{max}, ºC	f_N	Design lifetime, h
Type 304	490	230	720	28	100,000
Type 316 S51-S52	510	240	720	23	100,000
Type 321 S51	490	190	700	26	100,000
Type 347 S51	510	240	700	23	100,000

[**Extracted from British Standards BS PD5500, (2009)]**

Table 3.6. Nominal design strength for some Austenitic Stainless Steels at 500°C					
Stainless Steel	**Rm, N/mm^2**	**Re, N/mm^2**	**T_{max}, °C**	**f_N**	**Design lifetime, h**
Type 304	490	230	500	86	100,000
Type 316 S51-S52	510	240	500	93	100,000
Type 321 S51	490	190	500	77	100,000
Type 347 S51	510	240	500	119	100,000

[**Extracted from British Standards BS PD5500, (2009)]**

Where:

R_m: Minimum tensile strength of material concern at room temperature

R_e: Minimum value of specific yield strength at room temperature

f_N: Nominal tensile strength

f) Welded joint efficiency

Here there is another important mechanical design aspect. The strength of a welded joint depends on the type of joint and the quality of the welding. The soundness of welds can be checked by visual inspection and by non-destructive testing (radiography). The possible lower strength of a welded joint compared with the virgin plate is usually allowed for in the design by multiplying the allowable stress for the material by a "welded joint factor" J. The value of the joint factor used in design will depend on the type of joint and amount of radiography required by the design code [Sinnott, (2008)].

Taking the factor as 1.0 implies that the joint is equally as strong as the virgin plate; this is achieved by radio-graphing the complete weld length, and cutting out and remaking any defects. The use of lower joint factors in design, though saving costs on radiography, will result in a thicker and heavier vessel [Sinnot, (2008)]. For illustration purposes to give an example of the preliminary design calculations for R-20, a joint factor for the mechanical design of 0.8 has been used.

Finally, despite taking into account the welding factor in these preliminary calculations, it was decided that R-20 would not to have any welding work on it to avoiding potential heat effects in the pressure vessel. Economic costs related to having to pay for external coded welding not available in the School of Engineering (University of Edinburgh), was another factor taken into account for this decision.

g) Corrosion allowance

The corrosion allowance is the additional thickness of metal added to allow for material lost by corrosion and erosion or scaling. Corrosion is a complex phenomenon and it may be hard to predict its effects over extended periods of time. Generally, it is important to choose a reasonable extra thickness looking for a balance between reliability and economic costs. Corrosion allowance minimum is equal to 1 mm unless a protective lining is employed [BS PD5500, (2009)].

In the case of the oxy-fuel ignition bomb (R-20) there is not an expectation of strongly corrosive materials being present, although some acids (e.g. Carbonic, Hydrochloric, Sulphuric) can be formed due to the relative higher water content when compared to air combustion. Carbon dioxide is an acid gas which can form carbonic acid (a weak reducing acid) when dissolved in water but stainless steels are satisfactory resistant to carbonic acid. In addition, at higher partial pressures of carbon dioxide such as during the oxy-combustion process, carburization happens at temperatures above 500 °C [Kranzmann et al., (2011)]. Humidity at concentrations higher than 1,500 ppm is expected to corrode all steels with Chromium (Cr) content below 12 % [Kranzmann et al., (2011)]. For the oxy-fuel ignition bomb (R-20) case, in terms of overdesigning the vessel for safety purposes a minimum allowance of 2.0 mm is used. It is important to note that this is a voluntary corrosion allowance for the calculations, since a stainless steel with higher Cr content was chosen.

h) Vessel Wall Thickness

The wall thickness of the oxy-fuel ignition bomb (R-20) it is very important in order to ensure safe operation and to prevent catastrophic events during the experimental activity. As has been mentioned before, the British Standard PD 5500, (2009) was used as design code guidance and the calculations below are based on its information. In order to calculate the minimum shell thickness required with the existing internal pressure, for spherical shells the formulae are:

$$e = \frac{p \cdot D_i}{4 \cdot f \cdot J - 1.2 \cdot p}$$ **Equation [3.14]**

$$e = \frac{p \cdot D_o}{4 \cdot f \cdot J + 0.8 p}$$ **Equation [3.15]**

Where:

D_i or ID : inside diameter of shell.

D_o or OD: outside diameter of shell.

e: minimum calculated thickness of shell wall

f: nominal design stress.

p: design pressure.

J: welded joint factor.

Hence by applying equation 3.15, because the internal diameter ID is known (fixed by the design volume) and assuming J=0.8 (as safety case although welding was not relevant in this ignition chamber machined from a forged billet) and for the worst case of 720 °C metal temperature (non-realistic case due to limited pulverised fuel loading), for stainless steel 304 the example calculation for 50.5 bar or 5.05 N/mm^2 design pressure is shown:

$$e = \frac{5.05 \times 336.78}{4 \times 28 \times 0.8 - 1.2 \times 5.05} = 20.36mm + 2mm \approx 22.36mm$$ **Equation [3.16]**

Table 3.7. Vessel wall thickness-Case 1; T=700 ºC

Stainless steel	**304 S51**	**316 S51-52**	**321 S51**	**347 S51**
Min Thickness, e_{min}, mm	20.36	25.18	22.05	25.18
Corrosion allowance, mm	2	2	2	2
Thickness, e	22.36	27.18	24.05	27.18
Negative tolerance, mm	0	0	0	0
OD, mm	381.5	391.1	384.9	391.1

[**Extracted from British Standards BS PD5500, (2009)]**

Table 3.8. Vessel wall thickness Case 2; T=500 ºC				
Stainless steel	**304 S51**	**316 S51-52**	**321 S51**	**347 S51**
Min Thickness, e_{min}, mm	6.32	5.83	7.08	4.54
Corrosion allowance, mm	2	2	2	2
Thickness, e	8.32	7.83	9.08	6.54
Negative tolerance, mm	0	0	0	0
OD, mm	353.4	352.4	354.9	349.9

[**Extracted from British Standards BS PD5500, (2009)]**

As it could be expected, maximum pressure inside the vessel plays a decisive role regarding wall thickness required. Hence, a trade-off between design constrains and capital cost has to be considered in order to make a final decision but always taking into account the safety requirements above all. Accordingly, the type of stainless steel to be employed was decided based on an assumed maximum working pressure of 50.5 bar. This represents overdesigning the combustion chamber to give a high margin of safety given that this pressure will not be reached inside the vessel during normal experimental conditions of PF ignition under air or oxy-fuel atmospheres.

i) Stainless steel AISI 304 grade selection

Type AISI 304 stainless steel was selected for manufacturing R-20 ignition chamber (Cr >18 %). Type 316 stainless steel was also considered but was rejected due to the fact that the oxy-fuel ignition bomb (R-20) was expected to be built or at least upgraded on-site. Special attention was therefore paid to steel machinability in order to get a good balance between pressure vessel weight and making manufacturing processes easier. Type 304 is slightly cheaper than 316 in most cases. Details of the final material used are included in the Appendix.

j) Analysis of stresses

Stress analysis is the process where the relationship between external forces applied to a vessel and the corresponding stresses is studied.

Pressure vessels are subjected to other loads in addition to pressure and must be designed to withstand the worst combination of loading without failure. It is not practical to give an explicit relationship for the vessel thickness to resist combined loads. A trial thickness must be assumed (based on that calculated for pressure alone) and the resultant stress from all loads determined to ensure that the maximum allowable stress intensity is not exceeded at any point. The primary stresses are considered next.

In a sphere longitudinal and circumferential stresses due to pressure are the same (stresses in any two orthogonal circumferential directions are the same) given the equations:

$$r_1 = r_2 = \frac{D_i}{2}$$ **Equation [3.17]**

$$\sigma_r = \frac{P D_i}{4t}$$ **Equation [3.18]**

The applicability of this equation depends on the vessel being “thin-walled,” i.e. r >> e. In practice a pressure vessel is considered to be "thin-walled" if its radius r is larger than 5 times its wall thickness [BS PD 5500, (2009)]. This is the case for the fuel ignition bomb (R-20). At the surfaces of the vessel wall, a radial stress σ_r must be present to balance the pressure there. But the inner-surface radial stress is equal to p, while the circumferential stresses are p times the ratio (r/2e). When this ratio is large, the radial stresses can be neglected in comparison with the circumferential stresses [BS PD 5500, (2009), Sinnott, (2008)]. Calculation results for hoop stress are shown in Table 3.9:

Table 3.9. Hoop stress	
P, kPa	5050
ID, m	0.3368
e (thickness) or t or bc, m	0.0403
σ_r, kN/m^2	10545
σ_r , N/mm^2	10.55

From the result can be concluded that as σ_r << Rm, by approximately a factor of 50, so there is not an issue for material failure due to hoop stress.

In addition, it is useful to check that the axial stress in the spherical section of the vessel is the same to the hoop stress:

$$\sigma_x = \frac{pR}{2b_c}$$ **Equation [3.19]**

Table 3.10. Axial stress (in the sphere)	
P, kPa	5050
R, m	0.1684
e (thickness), m	0.0403
σ_r, kN/m^2	10545
σ_r , N/mm^2	10.55

Hoop stress for the tube section follows the same equation and should be slightly lower due to an increased thickness in the central part of the vessel. However, if the axial stress for the whole vessel is calculated, the equation for cylinder axial stress has to be used and taking into account the total thickness in the longitudinal section:

$$\sigma_r = \frac{pR}{b_c}$$ **Equation [3.20]**

Table 3.11. Axial stress (in the whole cylinder)	
P, kPa	5050
R, m	0.1684
e (thickness), m	0.0403
σ_r, kN/m^2	21090
σ_r , N/mm^2	21.09

Fatigue was not considered due to the specific characteristics of the research project with well below rating pressures and short residence time. This analysis of stresses was complemented by ANSYS simulation work carried out by Prof. Kamenev's team showing the concentration of stresses in the central part of the vessel in the flange area to close the ignition chamber. Thanks to Prof. Kamenev's team for the assistance and advice provided.

k) Wind loading, earthquakes considerations

Wind loading can be an important issue regarding vessel instability when it is located outside. The oxy-fuel ignition bomb (R-20) in most of the possible configurations is not a tall vessel and it was decided to be installed indoor. Consequently, no wind loading was considered.

Possible extra loading due to earthquakes and an adequate seismic design must be considered when the pressure vessel is located in regions with high seismic activity. From the British Geological Survey the seismic activity in Scotland since 1750, shows that no catastrophic earthquakes have been recorded [BGS, (2011)]. Furthermore, it is important to say that as the experiments were run on an batch process, there was no risk of earthquake loading in absence of the operator (as for continuous processes) and obviously in that extreme earthquake case, the experiment would have been immediately stopped and personnel evacuation and safety would be the priority. As a conclusion, no special

arrangements are considered in order to take into account possible but improbable extra loading due to an earthquake in the case of the oxy-fuel ignition bomb (R-20) design located at the University of Edinburgh.

3.3.3. Main drawings

After all the considerations explained in previous sections, R-20 was designed with the help of Solid Edge v.20 software. The initial approach was to have a spherical inner chamber but a non-spherical outside, to make it cheaper in the manufacturing process. The selection of a cylinder as external shape was because of the possibility of readily sourcing cylindrical stainless steel billets that could be machined into the shape needed. The closing system of the vessel would be an adequate number of bolts going through the entire length of the cylinder, as shown in Figure 3.6.

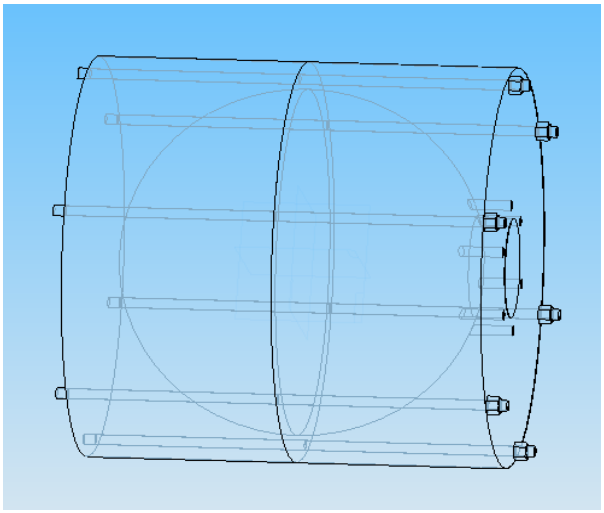

Figure 3.6. Initial design of R-20 ignition chamber.

Consideration of this initial design identified two major problems:

1) The vessel has to be opened, lifted and cleaned after each dust explosion experiment, which could prove challenging with a bolting system that would go through the entire length of the chamber. In addition, the continuously threaded bolts might break with the local accumulation of stresses due to forces imposed during the dust ignition experiment.

2) The need for instrumentation to measure relevant variables during the experiments, not just of this Ph.D. research project but of potential projects in the future. Drilling ports for instrumentation with a different insertion angles could prove difficult.

Despite the simplicity and potential of this design, in order to improve versatility of the chamber, it was considered preferable to change the closing system and external geometry of the vessel.

In Figure 3.7 a modification of the design in Figure 3.6 can be seen. The bolting system is now going through a flange turned in the original steel bar. This makes the threaded bolts shorter and it is also easier to open and close the chamber. When the ignition chamber is subjected to high internal pressure, the chamber can be affected by supplementary radial deformation forming peak stresses in the central area of the ignition chamber [For more details, see the ANSYS simulation in Appendix carried out by Prof. Kamenev's team on R-20, (2011)]. By inserting a chamfer in the flange, stress and deformation effect can be reduced if the joint area between the flange and the main vessel is given a curved fillet radius. Hence, it was decided that the original 200 mm long x 400 mm OD billet would be reduced to 370 mm OD at the top of the vessel and be kept at 400 mm in the bottom, leaving a 15 mm wide flange at each side of the vessel with fillet radius of 5mm [Figure 3.7, and detail B of figure 3.12]. Another important modification introduced in Figure 3.7 from the previous conceptual design is a 45° truncated conical form for the top of the chamber. This conical section around the core of the vessel allows for penetrations and straight ports (not included in Figure 3.7] to be drilled at an angle of 45° through the thicker section of the vessel wall for instrumentation to be used in ignition experiments [detail D of figure 3.13].

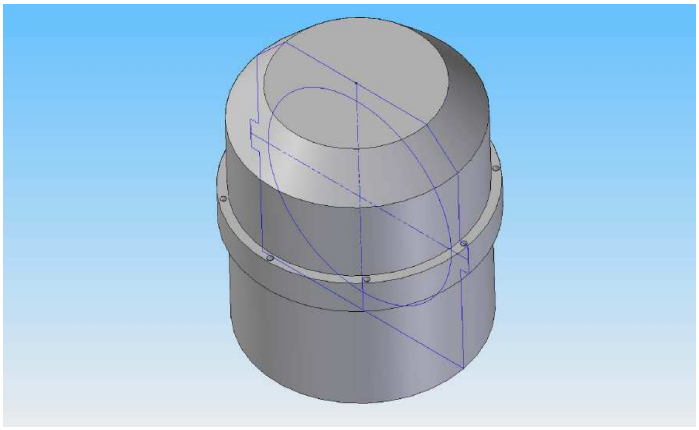

Figure 3.7. Early stages design of R-20 ignition chamber.

However, the design presented in Figure 3.7 has the problem that the new flange is not wide enough to allow for studs or bolts to withstand high pressures. Moreover, it is considered that the versatility of the pressure vessel and operational stability related to

weight distribution decreases if it does not having symmetric finishing. In Figure 3.8, the exploded parts of a near final version of R-20 are shown. Symmetry is reached by designing two hemispheres with a conical section at 45° angle for the insertion of ports for instrumentation (which are not shown in the figure). The closing system of the ignition chamber now is based on two external lock rings located at the centre of the chamber, which allows for an adequate number and size of studs and nuts.

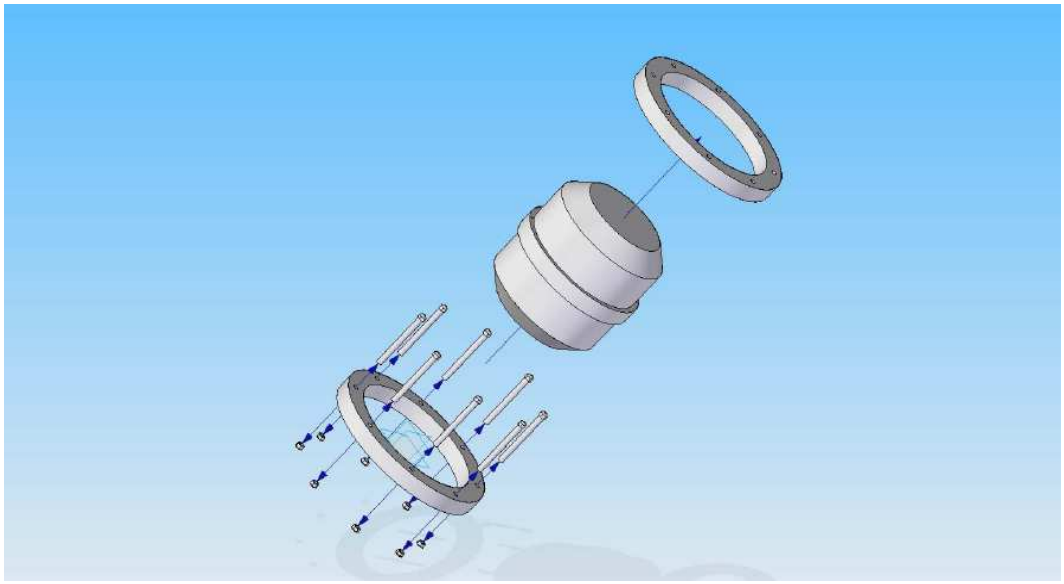

Figure 3.8. Near final design of R-20 ignition chamber.

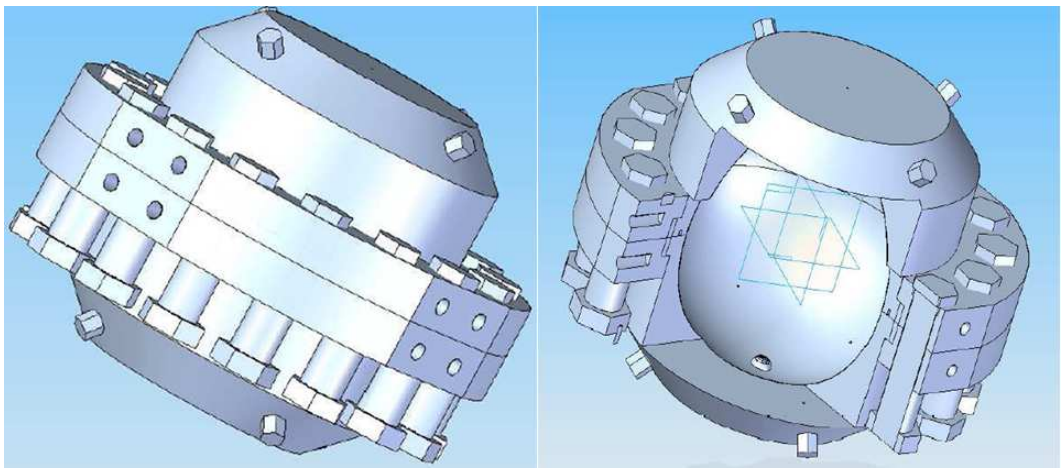

Figure 3.9. Design of R-20 ignition chamber.

In Figures 3.9 and 3.10 the final design of R-20 ignition chamber assembled is shown. The bolts are 16 x M48. Two independent hemispheres join to make the 20 litre spherical

ignition chamber and two independent external lock rings are used with a larger OD to accommodate the total number of bolts required in order to withstand at least 50 bar of internal pressure.

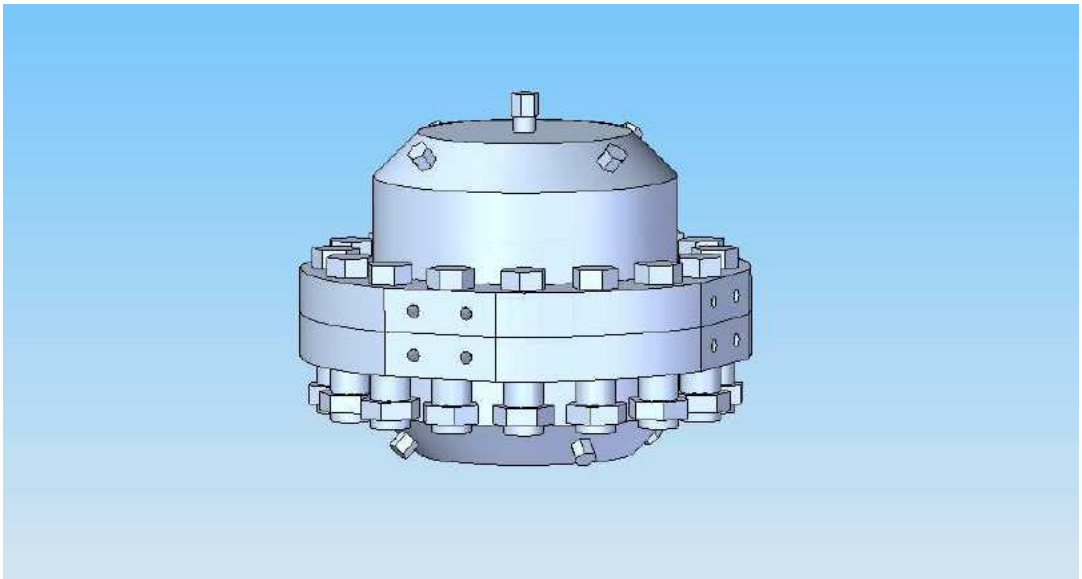

Figure 3.10. Final design of R-20 ignition chamber.

At the top of R-20 a 1 inch female NPT port with corresponding Swagelok male plug can be seen in Figure 3.10. The same type of port is at the bottom hemisphere of the chamber to allow for gas inlet through a dispersion nozzle. Details of these ports can be seen in Figure 3.11 which shows a cross-section of R-20. Eight ¾ inch female NPT ports are added to the ignition chamber to allow for instrumentation access, valves and other potential auxiliary equipment that might be needed. In total there are 10 penetrations to the pressure vessel which are detailed in figures below and in the drawings included in the Appendix.

The section of the pressure vessel (Figure 3.11) shows the key dimensions of the chamber in millimetres. The overall length is 400 mm and the overall width is also 400 mm with an inner sphere of radius of 168.4 mm. R-20 has been milled down to 370 mm except for the flange section allowing for the external lock rings to be allocated at the centre to close the vessel. The 45° conical section provides room for instrumentation and auxiliary ports as mentioned. The external lock rings have holes for 16 M48 bolts and are 550 mm OD and 370/400 mm ID (the inner dimension changes to locate them on the vessel).

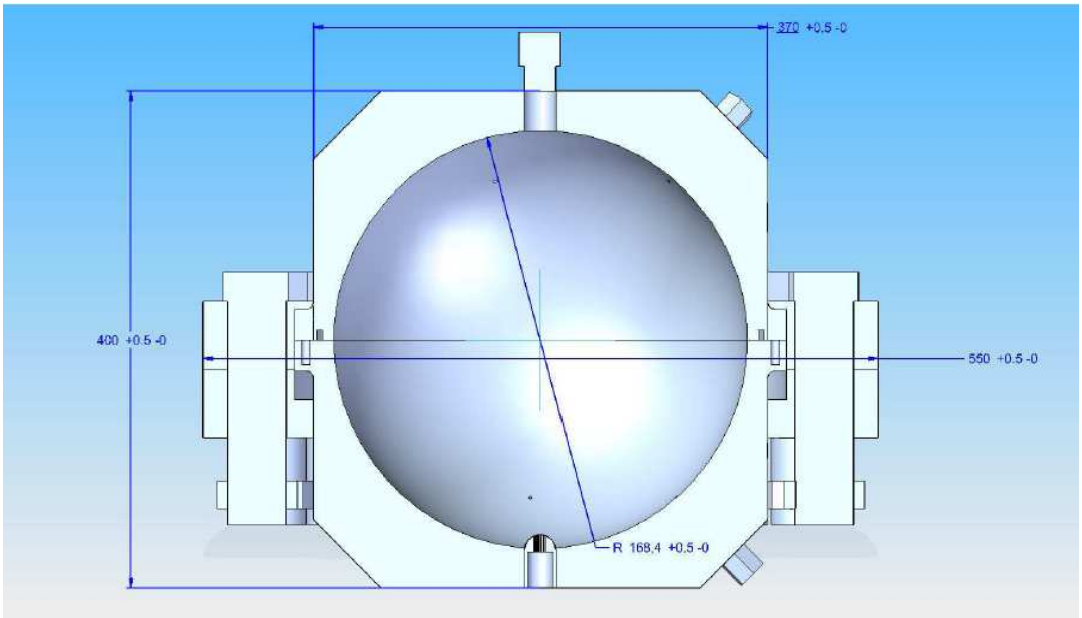

Figure 3.11. Section of final design of R-20 ignition chamber with key dimensions in mm.

Full dimensions with respective tolerances of the chamber and parts can be seen in Figure 3.12 and further drawings are included in the Appendix.

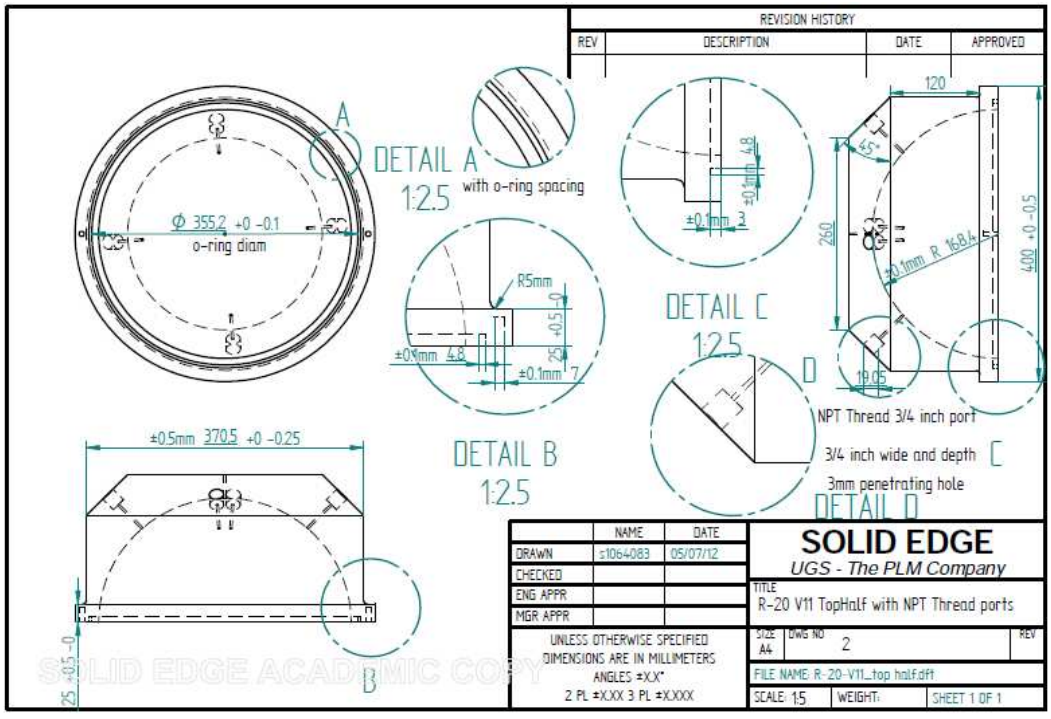

Figure 3.12. Detailed drawing of final design for half of R-20 ignition chamber with dimensions in mm.

From the details in drawing seen in Figure 3.12, it is important to focus on the following:

1) Detail A. The chamber has an O-ring seal to seal the chamber when both stainless steel hemispheres make contact. Further information on the 355.2 mm diameter O-ring seal is in Section 3.5.1.

2) Detail B. As previously mentioned, there is a fillet radius of 5mm on the flange to minimise stress concentrations that internal pressure can exert in the flange of the vessel. Space for a locating clamp of 7 mm diameter is also included to allow for ease of alignment of both hemispherical parts when opening/closing the ignition chamber.

3) Detail C. A depth of 3 mm with 4.8 mm difference between ID/OD for O-ring was used for adequate spacing. It was preferable not to have a very thick O-ring and the version used can be cheaply replaced if worn due to ignition experiments. In the future if required, it is also possible to mill an O-ring groove with a larger OD and depth if needed for higher pressures and temperatures in the experiments.

4) Detail D. Instrument ports with a ¾ inch female NPT thread to a limited depth and a 3mm final penetrating hole in order to maintain as smooth an internal surface as possible for the spherical inner chamber, with a minimum of features that could distort the dispersion of the dust during the ignition experiments. A penetration of 3 mm is adequate for the currently-used pressure transducer and other measurements. If in the future further instrumentation is required, the diameter could be enlarged, an analogous similarly to the approach taken to O-ring spacing design. Subsequently this was modified to be a 1 inch NPT thread during manufacture, to secure stainless steel billet when milling. A similar 1 inch NPT port can be seen in detail in the Appendix A.1, drawing for bottom half of R-20 ignition chamber.

3.3.4. R-20 manufacture

After discussing in detail the key dimensions and features of R-20 in the previous drawings, in this section, pictures of the manufacturing process are shown [Burns, (2012)]. Despite having planned to build the ignition chamber in-house and therefore conditioning some of the larger dimensions to the machining limitations in the School, some external factors affecting technical staffing in the School and the time constrains well advanced the Ph.D. project, it was decided to ask an external contractor to build the pressure vessel at Lazer Engineering Ltd., in Musselburgh, under the direction of Mr. Chris Burns.

Figure 3.13. AISI 304 200 x 400mm billet being drilled.

Figure 3.14. Milling of hemisphere of 336.8 mm ID.

In Figure 3.13 one of the 2 stainless steel billets with 200 mm length x 400 mm diameter is drilled with the mill in to start making the centre-hole for a hemisphere of 336.8 mm of internal diameter (Figure 3.14).

Figure 3.15. AISI 304 Cutting of hemisphere for R-20 ignition chamber.

Figure 3.16. Cutting and milling of AISI 304 plasma cut plate for 550 mm OD 370/400 mm ID and 50 mm depth lock ring(s).

The cutting of stainless steel AISI 304 can be seen in Figure 3.15. The machining of a hemisphere can be challenging particularly if the outside is spherical outside too; this is why it was preferred to have it made spherical only inside. In Figure 3.16 manufacturing of one of the lock rings is shown. The ring is cut from stainless steel AISI 304 plasma cut plate, 550 mm OD and 55 mm depth. Although could have been possible to attach these lock rings to the vessel it has been preferred not to in order to keep versatility of the ignition chamber. Figure 3.17 shows one of the hemispheres that forms the ignition chamber. Note the 1 inch

NPT port at the centre of the hemisphere which has been used for either insertion of the dispersion nozzle to create the dust cloud inside the pressure vessel pre-ignition or, in the top half of the vessel, to locate a viewport or for lifting the vessel with an eye bolt as needed. In Figure 3.18, one of the external lock rings to close the vessel is finished.

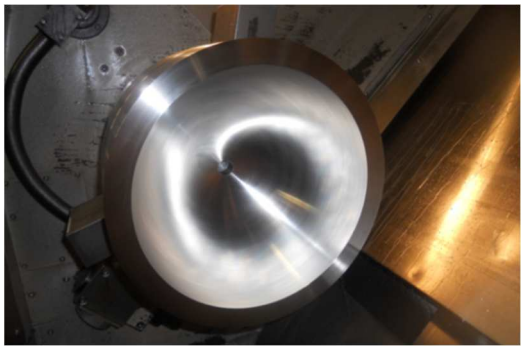

Figure 3.17. AISI 304 R-20 hemisphere finished with central port.

Figure 3.18. AISI 304 Lock ring with ID step for flange accommodation and 16 M48 holes for bolts and nuts.

Figure 3.19. Components of R-20 ignition chamber made of AISI 304. Note O-ring space in bottom half for sealing chamber.

.

Figure 3.20. Half of core of R-20 with details of ¾ inch FNPT port (x8) and 1 inch FNPT (x2) at the bottom/top of the chamber.

The four independent parts forming the R-20 ignition chamber are seen in Figure 3.19 as received at the University of Edinburgh. In Figure 3.20 half core of the pressure vessel is shown, with one of eight threaded ¾ inch FNPT ports at the front and the one of two 1 inch FMNT at the bottom/top of the bomb.

3.3.5. R-20 assembly

The R-20 ignition chamber when assembled is supported on a steel frame made in house that is placed on top of a lift table with wheels that makes the R-20 portable to different locations. Figure 3.21 shows the chamber assembled. *"It is made of stainless steel 304L in two hemispheres, held together by bolted lock rings. When assembled these parts form a perfect spherical test cavity with suitable wall thickness for withstanding 50 bar (a) or 5,000 kPa (a) pressure and beyond if needed for other type of tests"* [Trabadela et al., (2014)]. Sixteen M48 12.9 grade bolts with the lock rings closed the vessel. The nuts for the M48 bolts cannot be seen; they are below the locking ring, spot welded to the plate supporting the chamber, not to the lock rings, to secure them against rotation during opening and closing sequences.

Figure 3.21. 20 L ignition chamber at the University of Edinburgh (R-20) [Trabadela et al., (2014)]

Further details dedicated to closing system for R-20 ignition chamber are included in Chapter 4. In Figure 3.21 above the R-20 ignition chamber can be seen with exhaust line. Lines made of Swagelok ½ inch pipe are attached to the ¾ inch FNMP ports with a ¾ to ½ inch adapter. At the top of the vessel a viewport is seen. Full description of ancillary equipment is included in section 3.5 of this chapter.

3.3.6. R-20 safety aspects and insurance (Zurich Engineering)

R-20 had to be tested and insured before being used during the experimental campaign: *"All autoclaves and other pressure vessels…must be notified to the University's Engineering Insurers, who will inspect each item at the statutorily required interval"* [University of Edinburgh, Health and Safety Department (2010)]. For fulfilling these requirements, the Inspecting Authority, Zurich Engineering, part of Zurich Insurance Group Ltd. has assisted in the project.

The process of approval and insuring R-20 ignition chamber, undertaken with the valuable help of Mr. Alan Harrison from Zurich Engineering, was as follows:

1) Check of preliminary design calculations and design drawings for the 20 litre ignition chamber.

2) Evaluation of experimental methodology proposed, with assessment of potential hazards with special attention to R-20 lifting devices, overpressure relief valves, bolts tightening system and escaping routes in case they could be needed during the experiments.

3) Approval of the design with recommendations for design pressure and design temperatures.

4) Inspection of material and certificates after approval of the design, when the material is stamped by engineer from insurance company. This visual inspection also has to happening at the moment of reception of the material by the manufacturer to avoid confusion with parts and other steel available on-site.

5) Hydraulic test

Hydraulic or hydrostatic testing was completed by filling the chamber with water at up to 1.5 times the pressure which is the design pressure for the ignition chamber for a minimum of 15 minutes while remaining constant (Figure 3.22). In the case of R-20 the test was performed at 1,100 psi (75 Bar - Figure 3.23) and R-20 held pressure without leaks for over an hour. While knowing that the current design of R-20 could withstand much higher pressures due to being overdesigned, R-20 was officially rated at approximately 50 bar or 725 psi. Other relevant components in experimental set-up such as relief valves, also had to be rated and certified for insurance purposes.

Figure 3.22. R-20 assembled and fully closed during hydrostatic pressure test witnessed by Zurich Insurers

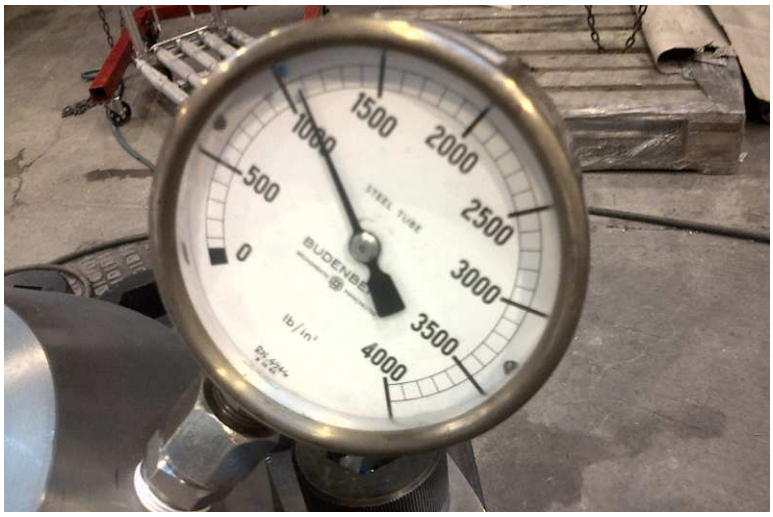

Figure 3.23. Pressure gauge indicating 1,100 psi withheld at least for 15 minutes during R-20's pressure test.

6) Certificates and stamp

After all the conditions had been adequately fulfilled, the 20 L Chamber (R-20) was approved by Zurich Engineering for use within the School of Engineering at the University of Edinburgh. The design code according to standards followed in R-20 is PD5500 Category 3 [BS EN PD5500, (2009)].

The maximum design pressure was set to 50 bar (725 psi), as sufficient for the purpose of the oxy-fuel ignition experiments at the planned fuel loading. The maximum design temperature was set at 288 °C, instead of 500 °C used in the calculations in accordance to recommendations from the insurers. The metal thickness provides an adequate heat sink for the small amounts pf transient heat input expected. Therefore, the use of external insulation and cladding to prevent operator burns is not required for this experimental programme. In Figure 3.24 the plate or in this case the label with main design parameters and key information of R-20 ignition chamber at the University of Edinburgh is shown.

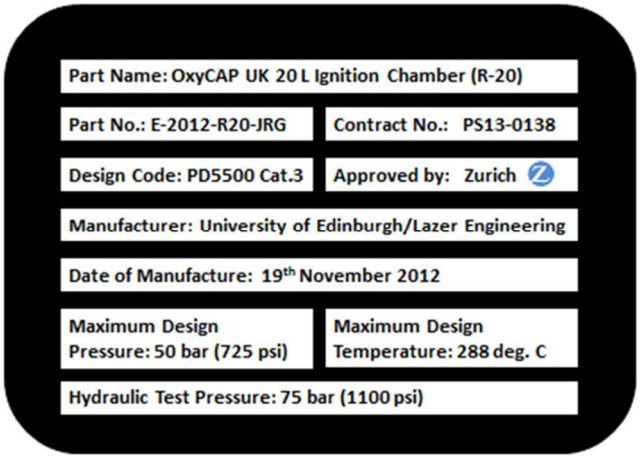

Figure 3.24. R-20 ignition chamber plate with key design information.

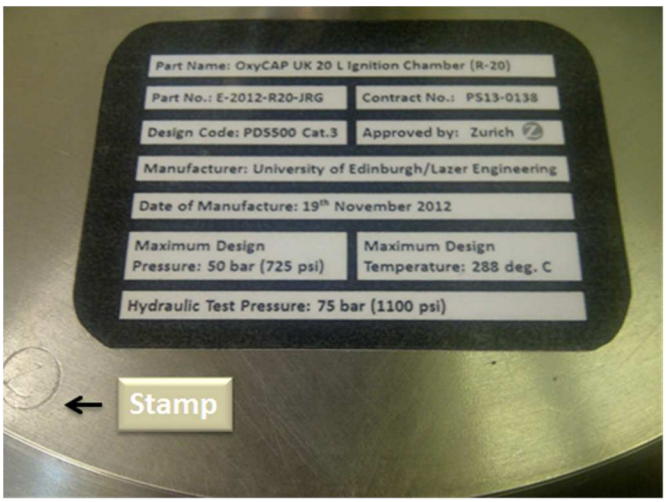

Figure 3.25. R-20 with plate with information and Zurich stamp after approval.

This label is attached to the pressure vessel for ease of identification and then the chamber is stamped by Zurich to formalised inspection and approval for use (Figure 3.25). Zurich Engineering forms and certificates of approval for the ignition chamber(s) for use are included in the Appendix.

3.3.7. R-20 novelty and versatility

The value of this Ph.D. research project is substantially increased because instead of copying existing ignition chamber designs, a new design for a spherical pressure vessel, the R-20 ignition chamber at the University of Edinburgh, to carry-out dust ignition experiments has been developed. This option of building a new improved design has added novel operating capabilities and also gives versatility to recycle existing research techniques in new aspects that might be of interest for CCS in the near future, such as oxy-gas experiments.

1) The novel operating capabilities of the R-20 design arise because it is a spherical chamber with full access to the inside for dust sample collection and chamber cleaner (when compared to Siwek's 20 litre chamber). But not having a spherical outer shape facilitates the insertion of ports and auxiliary instrumentation.

2) The versatility of the R-20 arises from capabilities that include:
R-20, being formed of four independent parts of stainless steel, can be easily dismantled and attached to other experimental rigs.
Having the pressure vessel overdesigned, leaves space for future research programmes.

As discussed in subsequent sections, the design can be extended to give a larger test volume while reusing most of the equipment in the current vessel.
With suitable addition the R-20 could also be used to carry out constant pressure ignition experiments.

3.4. Edinburgh University 30 Litre ignition chamber (R-30) design

As already noted, the initial concept in the OxyCAP UK project was to have a large volume pressure vessel to carry-out ignition experiments; 150-200 litres was the volume range considered. Time and logistics constrains made this option unfeasible. Moreover, the interest on dust ignition experiments shifted mostly to biomass under oxy-fuel conditions, rather than previous interest in just coal combustion. Knowing some of the experimental challenges confronted by researchers using the larger ignition chambers, it was decided to go for a slightly larger vessel of 30 litres volume.

3.4.1. Factors affecting R-30 design options

When the R-30 design was being developed some key factors influenced the pressure vessel configuration adopted. These included:

1) Changes in volume and geometry. R-30 had to provide a change in volume for the ignition experiments. A change of internal geometry from perfect sphere to a non-spherical shape was also an important consideration.

2) Easy of operation. The pressure vessel should be operated by just one researcher and with similar auxiliary equipment so as not to duplicate effort.

3) Dust dispersion and other experimental aspects. Dust dispersion inside the chamber should be easy and the experimental set-up similar to that existing for R-20. However, the additional option with R-30 of having the ignition source at different points was also an advantage compared to the R-20 design.

4) Constant pressure ignition experiments. The option of adding an extension tube to the lower half of the pressure vessel and leaving the other end open would allow constant pressure dust ignition experiments in the future.

5) Economic and time constraints. Lack of time due to delays in development of R-20 and also economic constrains for the OxyCAP UK project, made the option of a 30 litre vessel more feasible compared to completely new designs with larger volumes (150-200 litre) and left time for a successful experimental programme.

3.4.2. Design option taken for R-30

It is important to note that successful operation of the 20 litre (R-20) ignition chamber was verified during an experimental campaign before deciding to go ahead with the option of extending the pressure vessel. It would have been a failure to have built both chambers simultaneously and then discover operational issues in the smaller chamber. Once it was confirmed that the R-20 design behaved as expected there was a sound basis to enhance it with an extension in volume of the chamber and also a change in geometry (from a perfect sphere to an ellipsoidal geometry).

R-30 is formed from the R-20 rig and with the addition of 10 litres of extra volume in a cylindrical AISI 304 stainless extension piece (550/530mm OD, 336.8 mm ID, same ID as R-20) 112.3 mm long located between the two hemispheres. Drawings are included in further sections and further details are given in Appendix A.2. Closing of the vessel system is achieved by using existing lock rings with longer M48 12.9 grade bolts. This section was relatively easy to manufacture but it was found to be critical was to align M48 bolts so they perfectly match with the profile of the existing lock rings. Material was acquired in the form of plasma cut plate (as for the manufacture of the lock rings).

3.4.3. Basic parameters

If the additional volume required is 10 litres and the diameter is kept the same to R-20 then a cylinder length of 112.7 mm is required.

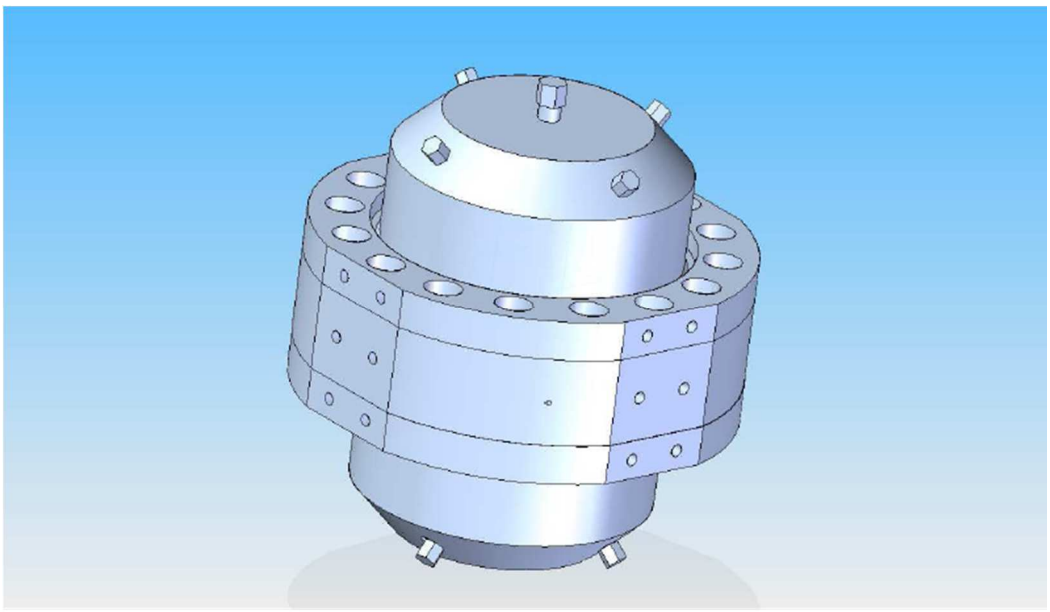

Figure 3.26. Final design of R-30 ignition chamber.

R-30 can be closed with the existing external lock rings using longer M48 bolts. The disadvantage of this design was having to use different length bolts. There is also the option of using a double set of two lock rings at each end of the cylinder, an approach that would also allow the chamber to be extended to larger volumes (e.g. 50 litres) with longer tube sections in the future and this option is still open. Nevertheless, for the research in the OxyCAP UK project 30 litre was considered to be sufficient volume and the other option would have required additional lock rings to be manufactured at extra cost. The cross section of R-30 with key dimensions is shown in Figure 3.27.

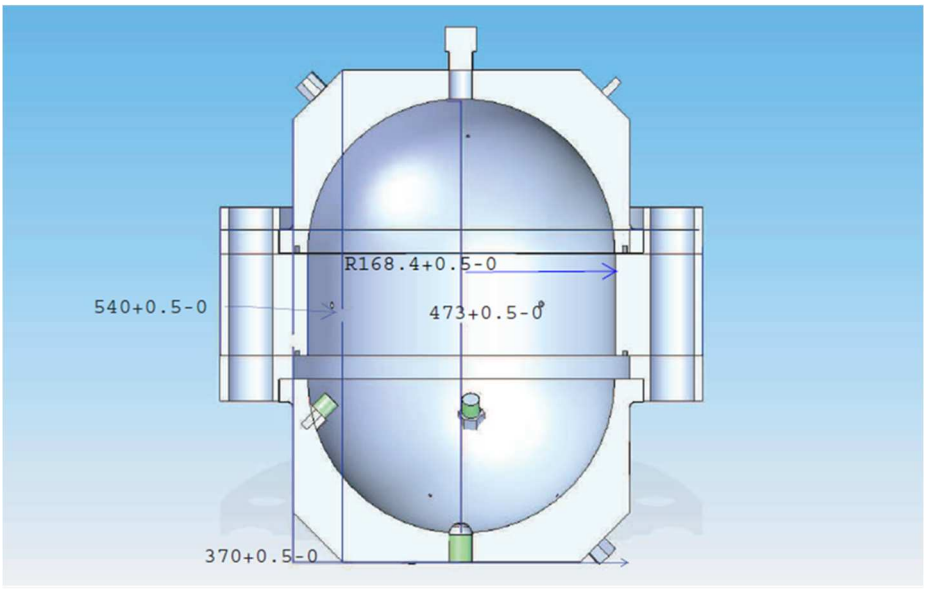

Figure 3.27. Section of final design of R-30 ignition chamber with key dimensions in mm.

The details of the tube section for the additional 10 litre volume are described in Figure 3.28 overleaf.

1) Detail A. Similar to R-20, R-30 has O-ring spacing to seal the chamber when both stainless steel hemispheres make contact. Details of the 355.2 mm diameter O-ring seal are in section 3.5 of this chapter.

2) Detail B. Two ¼ inch female NPT ports are added to the 112 mm long central ring of R-30 ignition chamber. These ports are just 6.25 mm OD towards the inside of the wall with the full thread penetrating for just 25mm so as not to unnecessarily weaken the vessel.

3) Detail C. Basis dimension of one of the ¼ inch female NPT ports and its location can be seen. Note that the two ports are at right angles from each other for access for instrumentation. Further ports can be drilled in the ring if required. These ports are sealed, with ¼ inch Swagelok plugs, when not in operation with ¼ inch fittings.

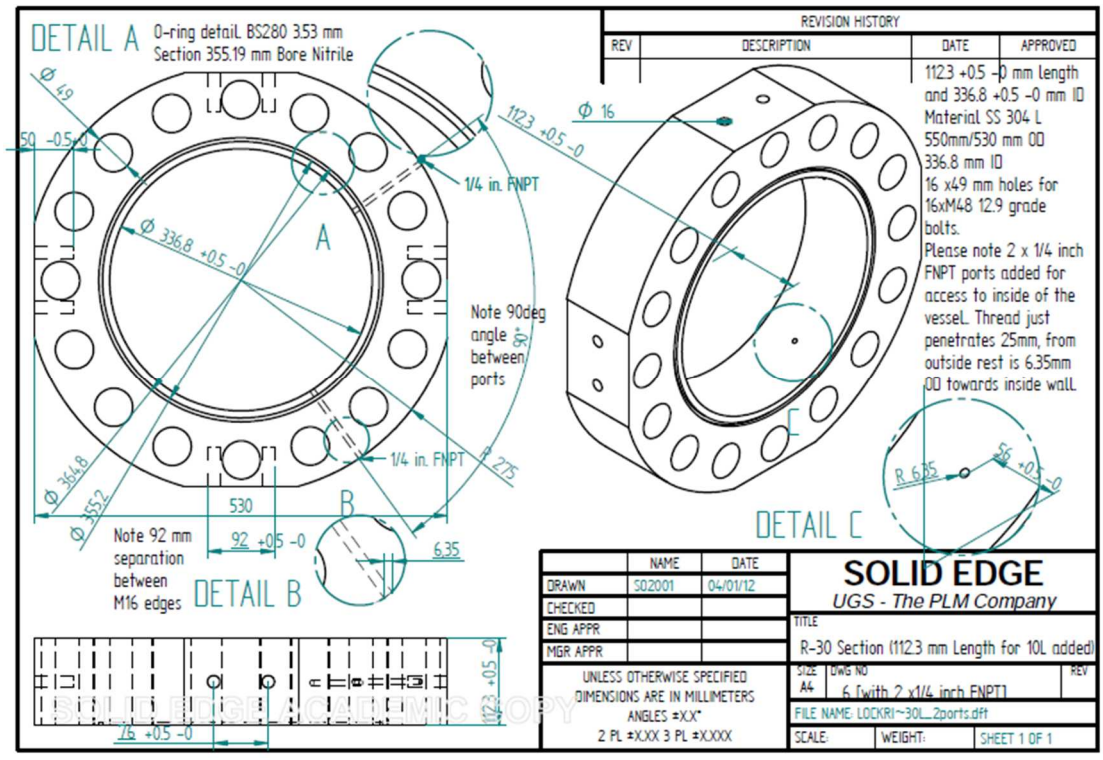

Figure 3.28. Detailed drawing of final design for half of R-30 ignition chamber with dimensions in mm.

The great advantage of this design for R-30 is that the addition of a thicker tube section to R-20 does not weaken the 20 litre ignition chamber. Therefore, by having that robust piece of steel, the chamber it is overdesigned again for potential future applications. The part is relatively easy to manufacture and the addition of ports is possible due to extra thickness when compared to requirements for the design pressure. The great disadvantage is the extra weight added to the vessel. Despite this, R-30 is still a movable ignition chamber that can be operated by one researcher.

3.4.4. R-30 manufacture

In this section, pictures of the manufacturing process at Lazer Engineering are shown [Burns, (2013)].

The stainless steel AISI 304 plasma cut plate is being cut and milled with an inside diameter of 336.8 mm (Figure 3.29) and when the diameter is finished, the groove for O-ring sealing, similar to the R-20 case, is added to the R-30 vessel section (Figure 3.30).

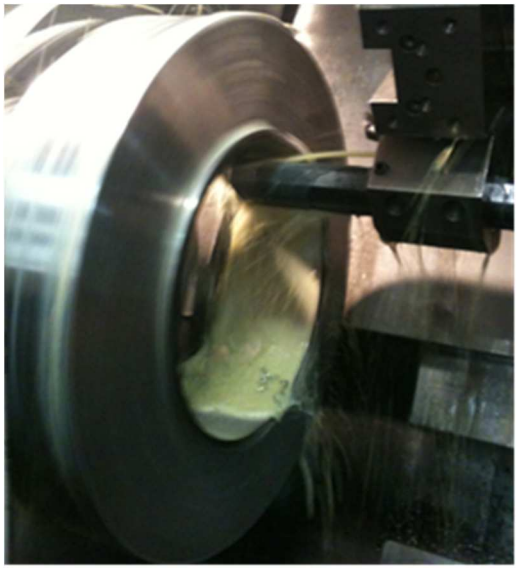

Figure 3.29. Cutting of AISI 304 R-30 10 litre ring for R-20 extension from a cut plate.

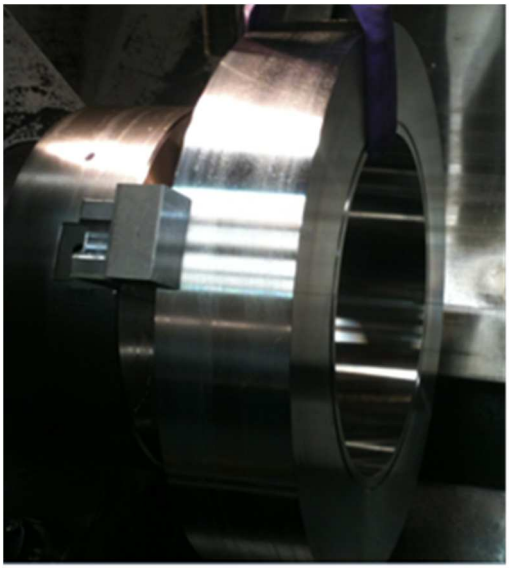

Figure 3.30. AISI 304 10 litre ring with spacing for O-ring seal being added.

Figure 3.31. R-30 extension of 10 Litre finished at Lazer Engineering.

The last stage of the process is the addition of the holes for 16 M48 bolts and two ¼ inch ports that can be used for instrumentation. On the front side of the section (Figure 3.31) there are two holes for M16 bolts that could be used to handle the vessel in a steel frame supporting structure if needed in future applications.

For this research programme, both R-20 and R-30 have been supported in a lifting table and crane, both having a capacity of 500 kilogrammes.

3.4.5. R-30 safety aspects and insurance (Zurich Engineering)

The R-30 insurance process with Zurich Engineering followed the same steps as for R-20. Hydrostatic testing was carried out on-site and the vessel held the 1.5 times 50 bar over 15 minutes while witnessed by Alan Harrison from Zurich. After the design was approved and the test passed, the vessel had added a new plate or label with key information shown in Figure 3.32.

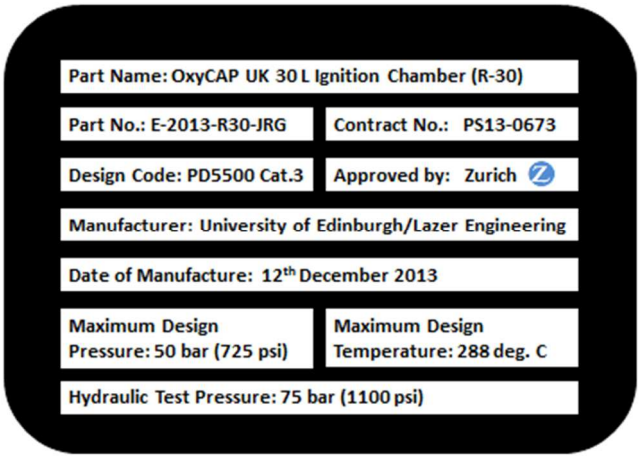

Figure 3.32. R-30 ignition chamber plate with key design information.

It is important to say that although the vessel does not need to be insured twice, these are two different vessels with legal effects, which means that in order to cover both when working with them individually R-30 has to be treated as a new item. Pressure vessels have to be inspected every year and R-20 and R-30 will be inspected as independent pressure vessels.

R-20 and R-30 have been designed with a failure mode that is intended to avoid catastrophic events. As both chambers are overdesigned, the failure sequence for progressively higher pressure levels would be:

1) Relief valves activate and release overpressure beyond set-point.

2) O-ring seal fails due to overpressure.

3) Bolts stretch and leak starts.

4) Lock rings deform and pressure in the vessel is relieved by leaks.

Relief valves are set at 35 bar while failure steps 2), 3) and 4) are not expected to happen below 50 bar.

3.4.6. R-30 assembled

R-30 is assembled when 5 independent parts, 2 hemispheres, two lock rings and central section ring, are joint with 16 new M48 bolts of 180 mm length. In Figure 3.33 the pressure vessel is shown on top of the support frame on the lift table. On top of the vessel, an eye bolt as previously mentioned is used for handling the chamber and lifting it when opening and closing during the experiments. A wooden box was built around R20 and R30 to avoid getting underneath when lifting the chamber and any trip hazard for the operator.

Figure 3.33. R-30 ignition chamber designed and built at Edinburgh University

In Figure 3.34, R-30 is shown with a round perforated coal injection nozzle and an igniter in the igniter mounting. Note that the igniter is not centrally located in the chamber, as discussed in Chapter 4.

Figure 3.34. R-30 ignition chamber with round perforated nozzle and igniter in place.

3.5. Ancillary equipment

R-20 and R-30 require the use of auxiliary equipment when having to set-up both chambers to carry out the dusts ignition experimental programme. The dust to be ignited is placed on top of the dispersion nozzle pre-ignition and the igniter at the centre of the chamber (or in other positions, depending on the experiment). Then, the vessel is closed and sealed with an O-ring which avoids any pressure leak. When the chamber is closed, it is evacuated with a vacuum pump up to an adequate level and then a blast of air (or O_2/CO_2 mixture) enters the vessel through the nozzle. The gas blast with the pulverised fuel on the nozzle creates a dust cloud that is ignited with the activation of the pyrotechnic igniter with a certain delay. Pressure in the chamber is recorded for key parameters determination.

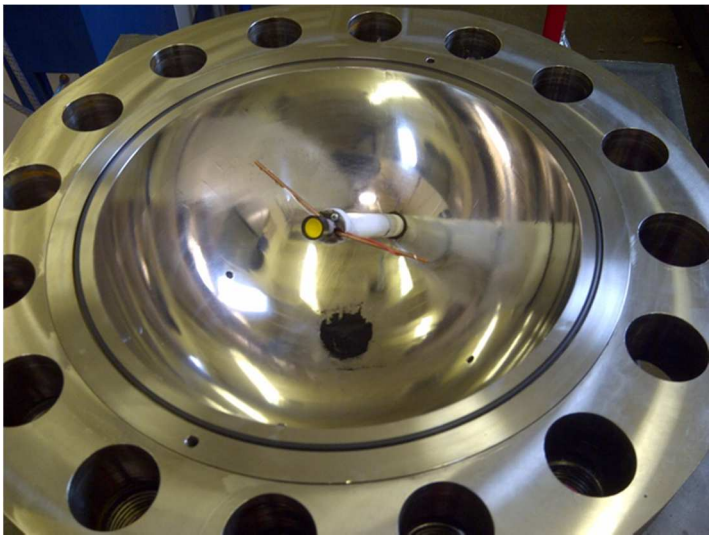

Figure 3.35. Bottom half of R-20 ignition chamber at Edinburgh University with O-ring Seal, Teflon igniter mounting, igniter and coal dust in place ready for the experiment.

The main elements in the experimental set-up for coal dust ignition experiments are briefly described in the following sections.

3.5.1. O-ring seal (R-20/R-30)

Due to the vessel design, there will be some joints metal to metal that cannot be perfectly sealed without the use of additional material due to the metal properties. Hence, the use of O-rings is required. An O-ring *"is a torus, or doughnut-shaped ring, that has been moulded from an elastomer"* [Parker, (2014)]. They can be used for sealing as in the R-20 case, but also as light-duty, mechanical drive belts. According to Parker Handbook, O-rings *"seal over*

a wide range of pressure, temperature and tolerance"; do not require torque or tightening avoiding potential structural damage in the pressure vessel; O-ring failure can be identified relatively easily and they are also cost effective [Parker, (2014)]. An example of O-ring is show in Figure 3.36:

Figure 3.36. O-rings [Extracted from: http://www.parker.com/]

R-20 and R-30 both use the same type of O-ring. The ID of the pressure vessels is 336.8 mm. Dimensions of the O-rings have to be in accordance with the ID of the vessel and the expected tolerances required. The correct O-ring for R-20 was chosen following relevant literature [Parker, (2007); British Standards BS ISO 3601-1, (2008)]. It was decided to use BS-280 with 355.19 mm nominal diameter (d_1) and cross section diameter (d_2) of 3.53 mm class B, as indicated in portion of table below [British Standards BS ISO 3601-1, (2008)].

Table 4 — Size code, size, inside diameter and inside diameter tolerances of class A and class B O-rings for general industrial applications — Cross-section diameter, d_2, of 3,53 mm ± 0,10 mm (0,139 in ± 0,004 in)

Size code	Size	d_1 nom.	Tolerance mm		d_1 nom.	Tolerance in		Volume ref.	
		mm	Class A	Class B	in	Class A	Class B	cm^3	in^3
280	355,19 × 3,53	355,19		± 2,49	13,984		± 0,098	11,033	0,673 3

Figure 3.37. Part of table extracted from British Standards for O-ring size selection [BS ISO 3601-1, (2008)].

The O-ring, with a rating of 200 ^{o} C was chosen to be the second point of failure in case of excessive pressure and temperature conditions inside R-20 and R-30 for the ignition experiments as described in Section 3.3.2. This is to avoid any catastrophic failure of the vessel. It is important to mention that the O-ring could fail not only because of high pressure or temperature. More likely, in the case of R-20/R-30, failure would be caused by a problem in the bolt tightening process that would cause the O-ring seal to be displaced and

deformed. Replacement of the O-ring seal was required once during over 1,000 experiments with R-20/R-30 chambers.

3.5.2. Teflon igniter mounting and pyrotechnic igniters

Igniter mounting was located inside ignition chamber R-20/R-30 through one of the ¾ inch MNPT ports. The mounting was made of Teflon bar as material having good electrical resistance and low surface friction. Low friction is useful to have minimum interaction with solid phases during the ignition experiment and consequent ignition propagation. Wires and connections were made of copper rod inside the Teflon to have increased material resistance to any breaking when access for handling/cleaning. This copper rod replaces the lighter wiring and clips used in the PRL-20 igniter mounting design which needed to be replaced after a certain number of experiments and occasionally required the manufacture of an entire new piece of the mounting. In addition a two part assembly mounting allows for ease of access and detachment of the mounting to be located in any of the other ports in the chamber. A picture of the igniter mounting (IM-A) is shown in Figure 3.38.

Figure 3.38. Igniter mounting (IM-A) for R-20 made of Teflon and copper rod.

Chemical igniters used in the ignition experiments are manufactured by Fr. Sobbe, Germany, in 500-10000 J energy range. Their chemical composition is 40 wt. % zirconium, 30 wt. % barium nitrate and 30 wt. % barium peroxide. After ignition (in the centre of the chamber) these chemicals will become part of the process residues as barium and

zirconium oxides. There is, however, a minimal associated gas volume generated with the hot particles [Cashdollar, (2000)].

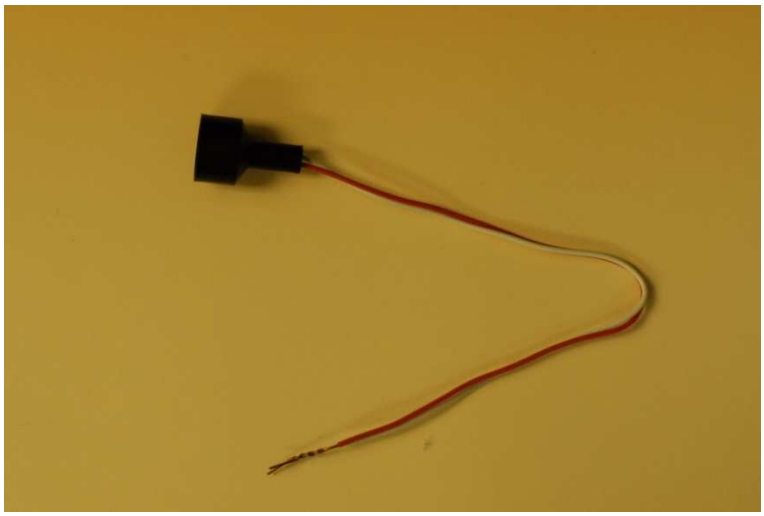

Figure 3.39. Pyrotechnic igniter manufactured by F.r. Sobbe.

The igniters require careful handling and must not to be exposed to ignition sources. For safety, they were stored in a dedicated location for hazardous substances and chemicals and not in the main laboratory. During the experimental programme, igniters are activated controlled by LabVIEW^{TM}. Blank experiments just with igniters were carried out in order to determine the pressure rise due to the ignition source. Average values were of 5.275 psi (a) (36.369 kPa (a)) and 8.023 psi (a) (55.317 kPa (a)), including noise in the measurement, for 2,500 and 5,000 J respectively. These pressures were subtracted in the software programme from the measured values obtained in the chamber. Hence, the results are normalised taking into account the igniter effect.

Igniters placed in the igniter mounting are activated with a 0.4 seconds delay after dispersion of the dust cloud in the chamber with the air/oxy-fuel mixture. This delay is consistent with experiments completed with PRL-20. Other time delays were tested (e.g. 0.04 s) but it was decided to follow the same time delay as experienced at NIOSH. In addition, although there are other types of ignition sources available for these experiments (e.g. spark), it was decided to use the chemical igniters from F.r. Sobbe to follow similar ignition procedures when compared to the PRL-20 chamber. The reasons for this were to have a reliable experimental procedure in the short time available while also being able to compare results with those obtained with PRL-20 where appropriate.

3.5.3. Dispersion nozzles (R-20/R-30)

The target is to have a well dispersed cloud of dust (coal/biomass) to be ignited by pyrotechnic igniters inside the R-20/R-30 ignition chambers. It is very important to control dispersion with suitable turbulence as it has a significant effect in ignition and subsequent ignition propagation [Hertzberg and Cashdollar, (1987)]. For R-20/R-30, a perforated round nozzle and flat nozzle have been designed and built. In Figure 3.40 the drawing for the design of the perforated round nozzle is shown.

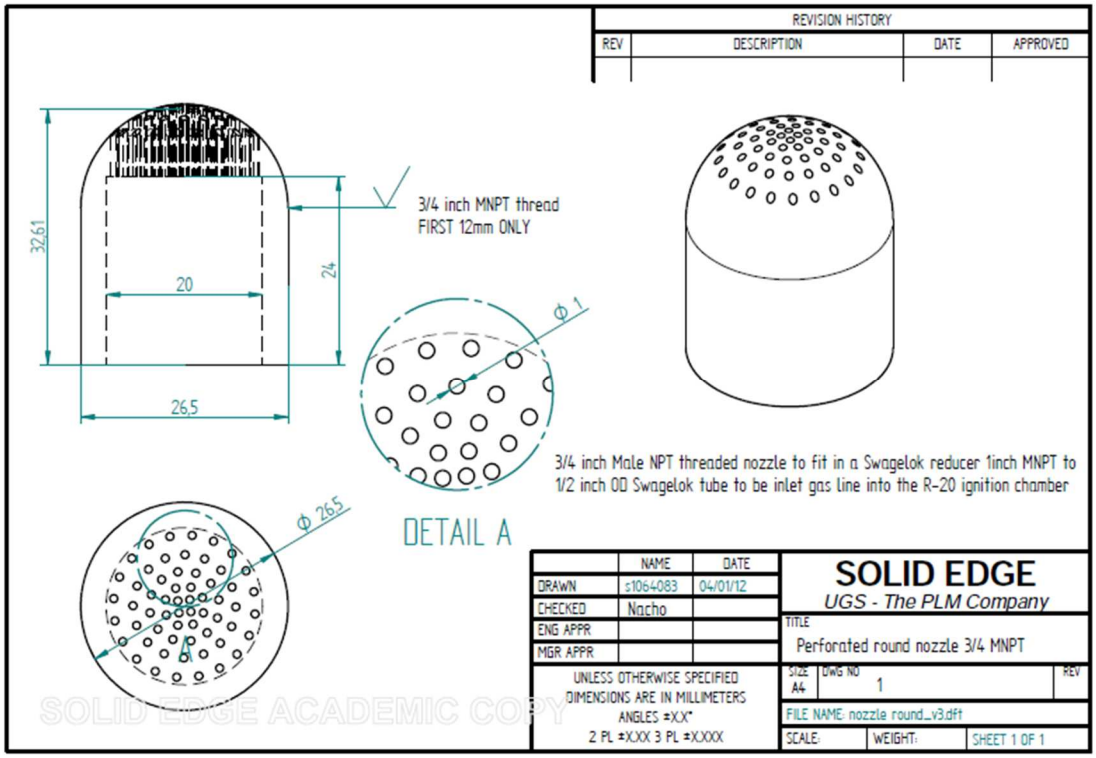

Figure 3.40. Drawings for perforated round nozzle ¾ inch MNPT.

The nozzle is hemispherical like the nozzle used at NIOSH with PRL-20. However the design is modified to adjust to the R-20/R-30 configuration. Made of stainless steel 304, the nozzle is long enough to be slightly above the bottom level of the ignition chamber. The ¾ inch MNPT threaded nozzle fits in a Swagelok reducer that adapts the 1 inch MNPT port to a ½ inch OD Swagelok pipe used as gas inlet to the pressure vessel. The thread in the nozzle goes deep enough to fit in the port (12 mm). The holes in the nozzle are 1 mm ID. A modification of the round nozzle uses flat instead of hemispherical ends, the design is included in the Appendix. Dispersion nozzles designed for use in ignition experiments are shown in the Figures 3.41 and 3.42, the perforated hemispherical nozzle (right hand side of

Figure 3.41) the flat nozzle (left hand side of same Figure); the latter was not, however, used in this experimental programme.

Figure 3.41. Perforated round (right) and flat (left) nozzles.

Figure 3.42. Nozzles with ¾ inch MNPT to a 1 inch Swagelok MNPT for R-20/R-30 ports.

The double threaded shanks seen in Figure 3.42 serve to locate the nozzle on the Swagelok fitting and then the fitting in the 1 inch port. This is an important feature so the nozzles can be threaded to a ¾ inch fitting and also located in any of the ¾ inch MNPF fittings in R-20/R30 if required in future research. In Figure 3.43 the perforated hemispherical nozzle can be seen in its regular configuration in the ignition chambers R-20/R-30. A detail of the nozzle, showing slightly above the surface of the chamber is seen in Figure 3.44.

Figure 3.43. Perforated round nozzle in R-20.

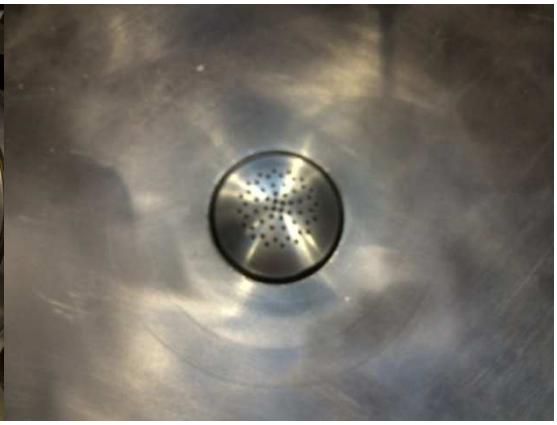

Figure 3.44. Detail of perforated round nozzle in R-20.

The idea of having two nozzle designs was to evaluate the influence of nozzle design on turbulence and dust dispersion. However, this would have required the use of dust probes that unfortunately could not be manufactured within the scope of this research programme. It is useful to have them available, however, for subsequent research on dusts ignition in oxy-fuel.

3.5.4. Gas cylinder reservoir and gases (R-20/R-30)

A Gas Sample Cylinder (CYL-102) was supplied by Swagelok 304L-HDF8-1GAL. Rated up to 2300 psi, this cylinder acts as the gas reservoir for air and O_2/CO_2 mixtures that will enter ignition chamber (R-20) as a blast of gas released by solenoid valve when the set pressure is reached. The air released, disperses the coal dust placed in the dust reservoir. It is very important to control the initial pressure in the system to achieve good turbulence before ignition. This pressure was set at 140 psi for all the experiments (coal and biomass) versus values of 115/120 psi used in PRL-20 for coal. The reason for this is to secure good dispersion of biomass dust for the same time delay 0.4 s for ignition. The sample cylinder was connected via ¼ inch Swagelok pipe to air-O_2/CO_2 gas cylinders and on the other end to a ½ inch Swagelok tube straight to adaptor attached to 1 inch MNPT port at the bottom of R-20/R-30 chambers.

Gases mixtures used in the experiments were supplied in cylinders by BOC. The mixtures were prepared off site by BOC because it was not possible to have a gas mixing system in the laboratory, mainly due to safety concerns. The O_2/CO_2 mixtures in the cylinders were not entirely accurate and a deviation of up to 1 % v/v in O_2 content could be found although relatively infrequently. For instance, for 21 Oxy, calibrated concentration ranged between 20.77 % and 22.88 % v/v O_2 in CO_2. These deviations will have a small impact on the results from experiments and also reflect the difficulty of achieving a precise O_2/CO_2 mixture in the real power plant scenario. It is recommended for future research programmes that a better O_2/CO_2 mixtures system is employed in-house to try to reduce this variation and also the experimental costs.

3.5.5. Vacuum pump (R-20/R-30)

A vacuum pump (P-101) supplied by Edwards Pumps XDS5 is attached to vacuum system in the R-20 ignition chamber in order to evacuate chamber with to a reduced pressure before

dispersing the coal dust cloud with blast of gas from the gas cylinder reservoir. Thus the coal dust is well dispersed during the 0.4 s interval before the igniters are activated.

3.5.6. Pressure Relief Valves

High-Pressure Proportional Relief Valves, 1/2 in. MNPT (SS-R4M8S8), identified as V-104 and V-105 in diagrams, and springer kit 177-13K-R4-B for 25-50 bar range were used for safety. Both items were supplied by Swagelok. Pressure relief valves were located in the gas inlet line and the chamber in order to prevent any overpressure in the system that could lead to catastrophic failure.

3.5.7. Solenoid and other valves (R-20 and R-30 set-up)

A Solenoid valve VXD2150A-06F-5DO1 activated with 12VDC (V-101) and supplied by SMC was connected to LabVIEW^{TM} software to be opened to actuate the blast from the gas reservoir into the ignition chamber. An advanced control system set-up with LabVIEW^{TM} coordinates the timing of the solenoid valve actuation with the igniter relay before the actual ignition of the dust is started.

A non-return valve or check valve (V-107) supplied by Swagelok. Model SS-58S8 Lift Check Valve, 2.20 Cv, 1/2 in was included in gas inlet line in the proposed system to prevent the effect of any backpressure coming from ignition in R-20 that could damage the solenoid valve or any other component upstream in the experimental set-up. The gas line is made of ½ inch Swagelok tube. Additional ball valves are included to manually open exhaust and vacuum lines when required. A needle valve is used in inlet gas line to release pressure from the gas reservoir as required.

3.5.8. Pressure transducers (R-20/R-30)

Three types of pressure transducers supplied by Cole Parmer are used to record pressure in the ignition experiments. A transmitter VAC/30P ¼ MNPT part number SN-68900-62 identified as PT-103 is used for pressure measurement in the gas vacuum line. A transmitter 300PSI ¼ MNPT part number SN-68334-46 (response time <2 ms), identified as PT-101, is used for recording peak pressure and pressure rise rate in R-20/R-30. It is important to take into account that this transducer should not be placed in ports located at the bottom of the chamber to prevent dust accumulation from experiments plugging the transducer. Finally, a

transmitter 200PSI ¼ MNPT part number SN-68900-68, identified as PT-102, is used for controlling pressure in gas cylinder (gas reservoir) as explained in Chapter 4. The settings of the transducers are controlled with LabVIEW^{TM} and pressures recorded are stored in a file by the software. A set of pressure gauges are also placed in the gas inlet line and vacuum line to support visual inspection of pressures by the operator. All transducers are cleaned regularly.

3.5.9. Viewport (R-20/R-30)

Sapphire windows are used in PRL-20 to have visual access to the coal dust ignition experiment. Experience with this type of window can be useful when using the right imaging techniques. For the purpose of determining positive ignition in the OxyCAP UK project, imaging analysis is not required. However, it was considered useful to have the option of attaching a viewport to one of the 1 inch MNPT ports in case some visual inspection was required. For this a Metaglas disc supplied by Visilume (Type 61) was acquired [Figure 3.45]. The port has 1 inch NPT male thread x 28 mm thick with 22 mm viewing diameter. The materials are duplex stainless steel 1.4462 for the metal housing and borosilicate glass following standard DIN 7080/7079 for the window. The maximum operating pressure is 100 bar and maximum operating temperature 280 °C.

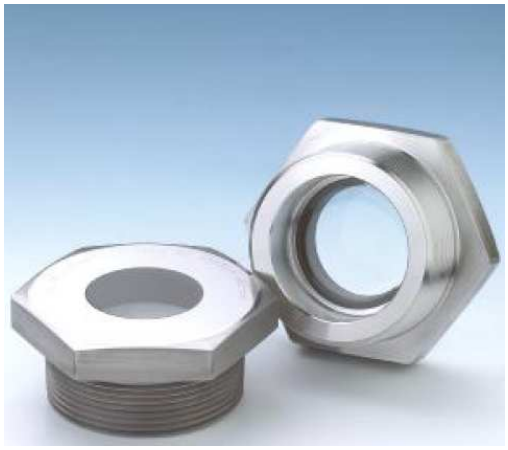

Figure 3.45. Viewport by Visilume [Visilume, (2012)].

3.5.10. M48 Bolts and nuts with Torc Gun for R-20/R-30 closing with lifting device for R-20/R-30

The closing and lifting system for R-20 and R-30 ignition chambers have been carefully evaluated. The objective was to have a pressure vessel that was portable, extendable and that could be opened and closed in a reasonable time due to the large amount of experiments expected. Initially there were some calculations to determine the characteristics and amount of bolts required for design pressure. However, the option decided was not based on the preliminary calculations but was overdesigned to leave open the possibility of using the vessel for higher pressures while also being able to modify the closing and lifting system of the vessel. The M48 bolts selected are of the type shown in Figure 3.46.

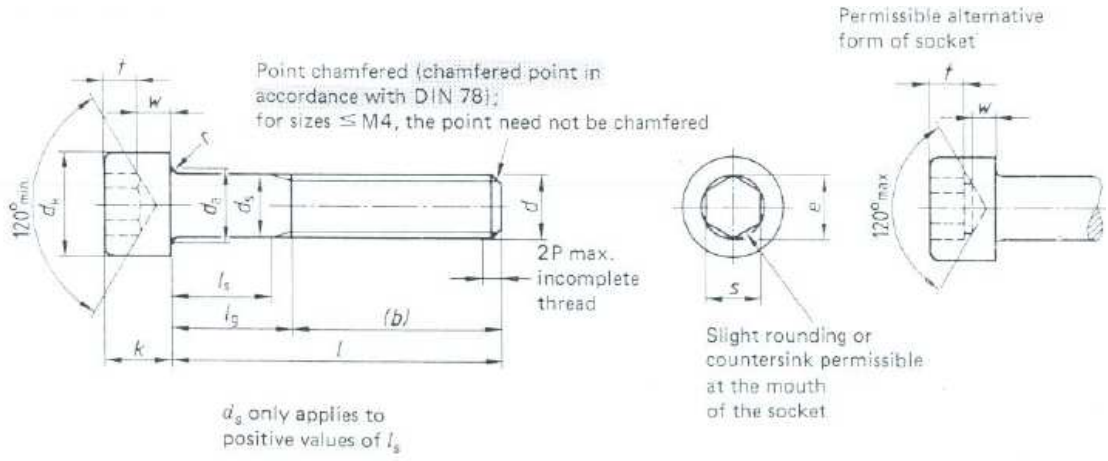

Figure 3.46. Hexagon socket head cap screws DIN912 [Kirk, (2012)].

Sixteen bolts 12.9 grade high tensile alloy steel 48mm x 180 Socket Head Capscrew Self Colour are used for closing R-20. The screws have tensile strength up to 1250 N/mm^2 with Rockwell Heat Treatment [Kirk, (2012)]. Hexagon full nuts are used in combination with the bolts. These nuts are spot welded to the lower steel place from the frame that supports R-20/R-30 on top of the lifting table. The idea of welding the nuts to the plate and not to the lock rings of the vessel is to avoid any heat effects from welding to any parts of R-20/R-30. Coded welding is necessary for any welding on the insured pressure vessel but is not needed for welding on a support frame made in-house that is not part of the chamber(s).

For the case of R-30, as the chamber now has the ring section in between the two hemispheres, longer bolts are required. 16 M48 x 300 Socket Head Cap 12.9 Grade Self Colour DIN 912 were employed in R-30. The same nuts welded to the frame have been used for closing R-30.

R-20 and R-30 are closed using a compressed air Torc Gun supplied by Hytorc. The gun can adjust easily the tension on the bolts to precise value with the aid of a regulator and pressure gauge. A tension of 40 N/mm^2 is used as sufficient for the expected 10 bar for most ignition experiments and well below the tensile strength of the bolts. The use of the gun significantly reduces, to a few minutes, the opening and closing time of the chamber(s). The gun has to be handled carefully by a trained operator to prevent any accidents. Both hands have to be on the gun simultaneously, one on the trigger and the other on the back lever of the gun. This design for operation avoids any accident that could injure the operator's fingers. Hearing protection is used to avoid exposure to the high noise level from the gun. For lifting R-20 and R-30 the combination of a lift table and an O-bolt with an electric power hoist is satisfactory for all the lifting work required. An electric power hoist up to 500 Kg, manually operated, is employed in the experiments.

3.5.11. Control of experiments (manually and LabVIEW™)

Control of experiments was carried out manually with the exception of the opening of the solenoid valve to release the blast of gas and the ignition of the coal/biomass sample after 0.4 seconds delay. For ignition, pressure indication and recording and data acquisition LabVIEW™ by National Instruments is used. All the software programming and hardware design has been carried out by Mr. Douglas Carmichael, technical staff at the University of Edinburgh with long-term experience on LabVIEW™ and officially qualified as a developer. His contribution to this research programme is sincerely acknowledged.

In figures below, NI Compact DaQ with modules for data acquisition are shown (Figure 3.47). A hardware box with power supply for LabVIEW™ modules and a 12 V supply for the igniters were used (Figure 3.48).

Finally, it was decided that the control of the experiments would be a hybrid of manual and automatic control of the system. The main reason for that was to keep the critical phases in the hands of the operator so as to be able to use the chamber alone. If the was a complete

automatic control of the chamber via software it would be more difficult to secure safety in the process. A similar control strategy is used for the R-30 configuration.

Figure 3.47. NI LabVIEW™ modules with Compact DaQ.

Figure 3.48. Hardware and power supply for LabVIEW™ and igniter.

Data was displayed in a personal computer (PC) with LabVIEW™ file shown in Figure 3.49.

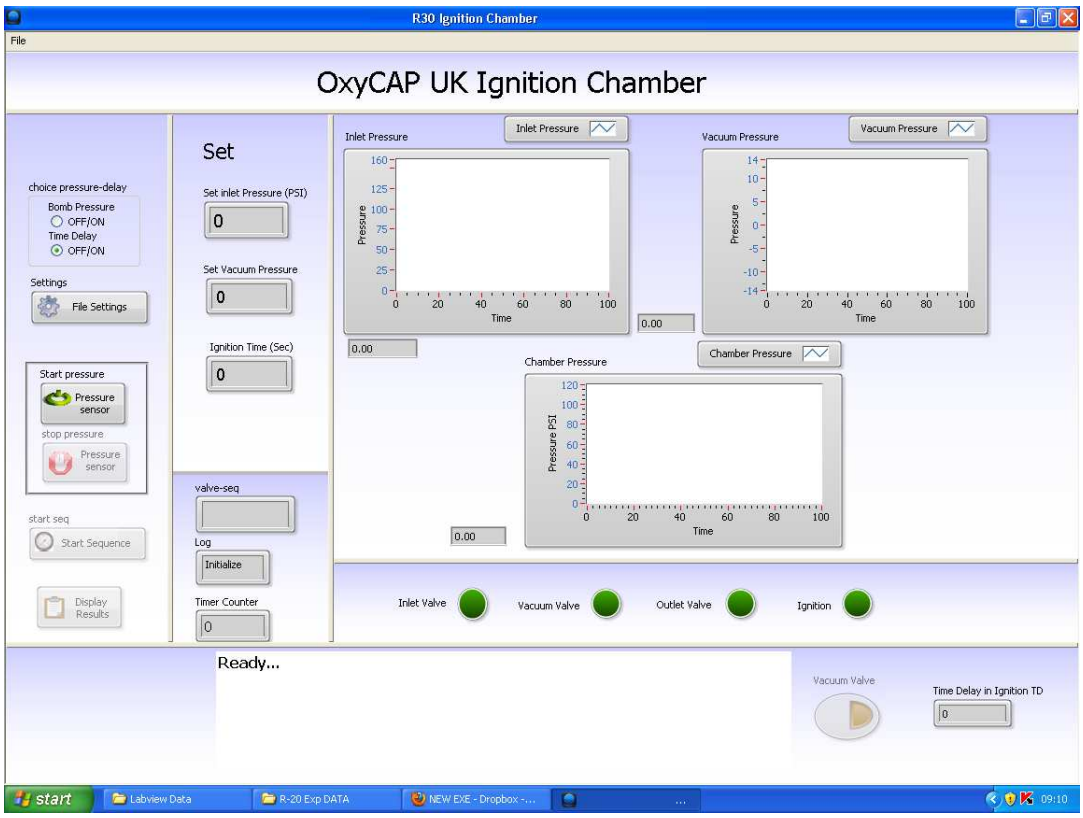

Figure 3.49. PC Screen capture of LabVIEW™ front panel for R-20/R-30 data acquisition.

The pressure evolution in the inlet line, vacuum line and chamber(s) are shown in graphs during the experiment. Light indicators for inlet valve, vacuum valve, outlet valve and ignition were also included in the display. When the sequence is activated the lights will turn from green to red. The pressure recording was prepared separately with a pressure sensor icon from the start sequence icon. This was considered to increase safety while being able to record pressure pre-post ignition at all times. From LabVIEW^{TM} was possible to set inlet pressure (gas reservoir, set at 140 psi) and ignition time delay (set 0.4 seconds). An important characteristic of the set-up is that LabVIEW^{TM} allows starting ignition either with a time delay or when a certain pressure is reached in the chamber pre-ignition. This was prepared in case pressurised air and oxy-fuel dust ignition experiments are of interest in the future.

4. Experimental methodology and set-up for coal and biomass dust ignition experiments

4.1. Coals used

A set of coals relevant in the UK and the global markets are used for the ignition experiments in air and oxy-fuel atmospheres. The selection of coals was made based on current availability in the UK for use in power plants and on the previous experience with the types of coals selected. The coals were supplied in pulverised form.

4.1.1. Pittsburgh Pulverised Coal (PPC) as reference coal for ignition experiments

Pittsburgh pulverised coal (PPC) is the Pittsburgh type coal that has been used for many years at NIOSH for ignition experiments in PRL-20 [e.g. Cashdollar, (2000)]. The coal is available from the mines that were active in the seams around Pittsburgh, including in the vicinity of the former Bureau of Mines research facilities. The key characteristic of NIOSH's PPC is that around 80 % of the particles are below 75 µm or 200 mesh. Currently, the availability of this coal is less common than in the past due to running out of the stock after the closure of the mines. During the experimental programme of coal dust ignition suppression with limestone carried out in 2011 [Trabadela, (2012)], coal was "prepared" with other sources of PPC collected from the bag-house filter used in the milling process. These particles are significantly finer than other coal samples collected from different parts of the mills and the mine itself.

The preparation of PPC is intended to replicate conditions inside underground coal mines where the fine particles of coal are suspended in the atmosphere and can form an ignitable fuel-O_2 mixture. For the milling safety case, the motivation for using PPC as reference coal is that to the percentage of particles below 75 µm is close to the operating conditions required for mill output in a power plant operation.

PPC is currently used as reference coal for the ignition experiments in PRL-20 due to the extensive experience in handling this coal and similarities to other US bituminous and sub-bituminous coals that are relevant to the work done by NIOSH. For the purpose of R-20/R-30 work, PPC is used to compare the results from coals of interest in the UK with the results published in air and oxy-fuel conditions from PRL-20. PPC analysis is shown in Table 4.1.

Table 4.1. Pittsburgh coal, proximate and ultimate analysis			
PROXIMATE %		**ULTIMATE, % (daf)**	
Moisture	1.8	**Moisture**	-
VM	35.4	**C**	84.0
FC	57.5	**H**	5.5
Ash	5.3	**S**	1.2
VM % daf	38.5	**Cl**	0
GCV, MJ/kg (daf)	-	**N**	1.7
	-	**O**	7.7
		Ash	-

[Man and Gibbins, (2011)]

4.1.2. El Cerrejon as reference coal for OxyCAP UK project (R-20/R-30)

Colombian coal from El Cerrejon widely traded and currently used in the UK was employed. Due to the closure of UK mines and the need for importing overseas coal it was decided during the OxyCAP UK project advisory board meeting that the reference coal for the project was to be El Cerrejon IC G145. The idea of having a reference coal within the project is useful to compare data when operating several rigs in operation. In addition, the coal is currently used by power generators in the UK, hence the potential for increasing research impact if providing data that can be transferred to industry.

El Cerrejon coal was supplied by Durrans Ltd. Coal is produced (typically at 45 °C) and after production there is a waiting period (3 to 7 days) before shipment for the temperature of the product to fall to 24 °C. Pulverised coal is packed into a special paper bag so that it can cool without condensation and with no issues on self-heating [Brown, (2012)]. Coal is packed in 3 ply paper bags (25 kg per bag) in two different formats, IC Grade 100 and IC Grade 145. Oxidation was controlled keeping coals in sealed bags. IC Grade 145 was decided to be used as the coal for ignition experiments in R-20 and R-30 due to a larger amount of particles below 200 mesh or 75 µm. However, it is important to take into consideration that finer particles below 75 µm are in lower quantities than in the PPC case (Table 4.9.). El Cerrejon IC G145 it is a quite reactive coal due to the amount of volatiles (Table 4.2.). This makes this El Cerrejon coal a quite interesting dust to evaluate its ignitability. As El Cerrejon IC G145 is the reference coal for the project, this coal was used in

a wider variety of experimental conditions when compared to the other dusts selected such as scarce PPC and less widely used UK coals.

Table 4.2. Cerrejon coal, proximate and ultimate analysis			
PROXIMATE %		**ULTIMATE, % (daf)**	
Moisture	5	**Moisture**	-
VM	40	**C**	69.2
FC	58	**H**	4.40
Ash	3	**S**	0.58
VM % daf	-	**Cl**	-
GCV, MJ/kg (daf)	-	**N**	1.42
		O	9.98
		Ash	-

[Durrans, (2012), Hochgreb, (2015)]

4.1.3. Other relevant UK coals used for ignition experiments (R-20/R-30)

In order to complement the work done on R-20 and R-30 chambers, Thoresby and Kellingley were selected as indigenous coals in the experimental programme, both being coals that have been used in the past for other research projects in the coal industry. They were also available via the BCURA coal bank and being some of the few coals with active mines in the UK, made them very good candidates to complement data obtained from El Cerrejon as reference coal.

Table 4.3. Thoresby coal, proximate and ultimate analysis			
PROXIMATE %		**ULTIMATE, % (daf)**	
Moisture	5.6	**Moisture**	-
VM	34.2	**C**	84.3
FC	55.3	**H**	4.6
Ash	4.9	**S**	1.12
VM % daf	38.7	**Cl**	0.67
GCV, MJ/kg (daf)	34.68	**N**	1.83
		O	7.9
		Ash	-

[BCURA, (2012]

Table 4.4. Kellingley coal, proximate and ultimate analysis			
PROXIMATE %		**ULTIMATE, % (daf)**	**daf**
Moisture	4.7	**Moisture**	-
VM	37.1	**C**	85.1
FC	53.2	**H**	5.9
Ash	5.0	**S**	0.84
VM % daf	41.6	**Cl**	0.41
GCV, MJ/kg (daf)	35.44	**N**	2.12
		O	5.7
		Ash	-

[BCURA, (2012)]

4.1.4. Coal samples preparation

Coal samples are prepared as received when particle size selection is not required for a certain set of experiments. Pulverised coal samples received from the suppliers follow the handling sequence below:

1) Drying and moisture control. Coals are not dried with any heat source. However, particles are isolated from contact with atmospheric moisture by keeping them inside a desiccator for at least for a day in the laboratory pre-weighting them in the balance. If the research purpose would have been to study the moisture content effect on ignition of dusts, the option of pre-heating and drying would have been preferred. As the objective is to study ignitability with similar conditions to PF in the mills of the power plants, then the moisture control strategy adopted is considered adequate in this case.

2) Weighing process for coal samples. Coal samples are weighed in a 300 g Steinberg Systems laboratory precision balance with milligram precision. As most of the samples are required in the 2-18 grams for 100-600 g/m^3 concentration range in R-20 or R-30 ignition chambers, accuracy to the milligram is not required for this type of dust ignition experiments. However, it is important to note the exact amount for comparing with collected dust from ignition when undertaking weight comparisons and other loss measurements from ignition.

3) Coal particle size selection with Ro-Tap®. In the case of El Cerrejon coal, particle size was selected for a set of experiments to evaluate the effect of particle size on ignition in air and in oxy-fuel atmospheres. The particle size distributions considered of interests were: >75 µm (200 mesh), 75-53 µm (270 x 200 mesh) and <53 µm (270 mesh) respectively. Particle size distributions below 53 µm were considered of less interest, avoiding the need for 38 µm or 400 mesh sieving for this set of experiments. In order to have a narrow particle size distribution between the two mesh sizes selected, coal particles are sieved with the use of a Ro-Tap® RX-29-E manufactured by W.S. TYLER™. The test sieve shaker is shown is Figure 4.1 below.

Figure 4.1. Ro-Tap® RX-29-E manufactured by W.S. TYLER™.

El Cerrejon G145 samples are placed at the top of 200 mesh sieve and the Ro-Tap® RX-29-E is closed with the sieves sequenced from top to bottom (200 mesh, 270 mesh, collecting plate/separator, 200 mesh, 270 mesh, collecting plate). The coarse analysis is done continuously for 20 minutes. After the 20 minutes, samples from collecting plates or finer particles are retrieved. The process starts for another 20 minutes and then samples are collected again. The sequence of 20 minutes stops at the moment that no newer fine

particles (below 270 mesh) are observed in the collecting plates. For narrowing the coal particle size cut between 75 µm and 53 µm, the sieve is regularly taken out before re-starting the process, placed on top of a white sheet of paper and the contents of the sieve are manually sieved with a lid in a fume cupboard to check that no new fine particles go through the sieve. This process is quite time consuming, and the narrower the particle size distribution, the longer takes the sieving. However, it is very important to be sure that the finer particles (<53 µm) do not stay in the 75 µm - 53 µm particle size distribution.

4.2. Biomass used

In the case of biomass used in the research programme, there was no previous experience in the use of the ignition chamber for oxy-biomass conditions (this is part of the novelty of this Ph.D. thesis). Hence, there was no analogy to PPC as in the coal dust ignition case for comparison with previous experience in a 20 litre chamber.

4.2.1. Biomass from E.ON

Biomasses used in the OxyCAP UK were supplied by E.ON and by the University of Cranfield. The assistance of Dr. Susan Weatherstone from E.ON is gratefully acknowledged. Ignitability of Torrefied Spruce Pellets, I2 White Wood Pellets, Miscanthus Pellets and Cereal Co-product has been evaluated. These are of interest in the UK power generation sector and their analyses (wt. %) are shown in Tables 4.5, 4.6 and 4.7.

Table 4.5. Torrefied Spruce biomass analysis

%	As received	%	Dry
Moisture	3.1	**Moisture**	-
VM	73.9	**Ash**	0.7
FC	22.4	**CV, MJ/kg**	22.196
Ash	0.6	**%**	**daf**
GCV, MJ/kg (daf)	21.510	**VM**	76.7
S	0.01	**CV, MJ/kg**	22.340
Cl	0.01	-	-
H	5.50	-	-
NCV, MJ/kg	20.236	-	-

[Weatherstone, (2014)]

Table 4.6. White wood biomass analysis			
%	**As received**	**%**	**Dry**
Moisture	9.1	**Moisture**	-
VM	75.5	**Ash**	1.2
FC	14.3	**CV, MJ/kg**	20.166
Ash	1.1	**%**	**daf**
GCV, MJ/kg (daf)	18.320	**VM**	84.1
S	0.02	**CV, MJ/kg**	20.400
Cl	0.01	-	-
H	5.37	-	-
NCV, MJ/kg	16.950	-	-

[Weatherstone, (2014)]

Table 4.7. Miscanthus biomass analysis			
%	**As received**	**%**	**Dry**
Moisture	11.6	**Moisture**	-
VM	71.8	**Ash**	2.9
FC	14	**CV, MJ/kg**	19.227
Ash	2.6	**%**	**daf**
GCV, MJ/kg (daf)	17.000	**VM**	83.7
S	0.03	**CV, MJ/kg**	19.810
Cl	0.07	-	-
H	5.11	-	-
NCV, MJ/kg	15.597	-	-

[Weatherstone, (2014)]

4.2.2. Biomass from cereal as reference biomass for OxyCAP UK project

Cereal-coproduct supplied by Cranfield University was employed as reference biomass for the OxyCAP UK project to be used in different rigs in analogy to El Cerrejon coal. Biomass was received sieved through 180 µm instead of in pellets. Ms. Nelia Jurado from Cranfield University is acknowledged for supplying the biomass. Analysis (wt. %) of Cranfield biomass is in the Table 4.8 below.

Table 4.8. Cereal Co-product biomass, proximate and ultimate analysis

PROXIMATE %	As received	ULTIMATE, %	As received
Moisture	8.10	**Moisture**	-
VM	70.8	**C**	43.3
FC	-	**H**	5.8
Ash	4.2	**S**	0.16
VM % daf	-	**Cl**	0.17
GCV, MJ/kg (daf)	17.610	**N**	2.7
NCV, MJ/kg	16.340	**O**	35.57
		Ash	-

[Jurado, (2014)]

4.2.3. Biomass samples preparation for ignition experiments (R-20/R-30)

1) Particle size. For biomass particle size selection, the use of the Ro-Tap® RX-29-E was discarded due to the different particle aspect ratio of biomass when compared to coal, makes sieving not the best option. Preparation of biomass samples was approached differently upon reception of the biomass. Torrefied Spruce, I2 White Wood and Miscanthus, received as pellets, were ground first with a regular coffee grinder and later on with *"an ultra-centrifugal Retsch® ZM 200 apparatus with a high speed rotor mill at 8,000 revolutions per minute (rpm) and a 0.25 mm stainless steel ring sieve"* [Trabadela et al., (2014)]. Cereal co-product, when used as received, after being sieved through 180 µm originally, was also ground with the Retsch® ZM 200. The apparatus is shown in Figure 4.2.

Figure 4.2. Retsch® ZM 200 apparatus.

For the larger biomass particle size distributions, Torrefied Spruce, I2 White Wood and Miscanthus were ground with a 0.5 mm stainless steel ring sieve in the Retsch® ZM 200. However, Cereal co-product samples, when used in larger particle size distribution, were directly ignited as received from Cranfield University. Note that from now onwards, biomass particles ground with a 0.25 mm ring will be identified as 0.25G and particles ground with a 0.5 mm ring will be identified as 0.5G.

Figure 4.3. Biomass particles after grinding with a regular coffee grinder.

Figure 4.4. Biomass sample after grinding with a 0.25 mm sieve in the Retsch® ZM 200 grinder.

From Figures 4.3 and 4.4 above, a visual difference in particle size of biomass from regular coffee grinder and Retsch® grinder is observed. It is important to mention that, when operating Retsch® grinder, accumulation of particles in the sieve must be avoided, since agglomeration can decrease the performance. Higher rotor velocities cannot be used and grinding has to be done in stages with pauses to prevent the dust from overheating.

2) Drying and moisture control. Moisture content and control of exposure of the biomass is more difficult when compared to the coal case. Although the biomass samples were kept in sealed bags to avoid contact with atmospheric humidity, this contact could not be prevented when grinding the samples. Also, there is a clear difference between torrefied and non-torrefied biomass. Moisture has been reduced during the torrefaction process but *"thermally treated biomass is important from an experimental perspective because it is more friable and less fibrous, so it can be used to give a check on the adequacy of dust dispersion in the chamber with untreated biomass samples"* [Trabadela et al., (2014)].

3) Weighing of samples. The process in this case is similar to coal samples. An analytical balance with milligram precision has been used for weighing samples for up to 600 g/m^3 in R-20 and R-30. Final weights are noted for each sample.

4.2.4. Coal and biomass particle size analysis

Coal and biomass particle size analysis is a key element of the research programme that can be improved in the future work. The major issue is that coal and biomass particles have different shapes and characteristics which makes comparison quite challenging if using the same type of analysis method. In addition, when coal has been used, there is broader experience in particle size analysis by using manual sieving, sonic shifter or a laser diffraction particle analyser, such as the Beckman Coulter LS 13 320. The three methods mentioned have been used by Trabadela, Green and Man during experimental programme at NIOSH [e.g. Trabadela, (2012)]. However, the same approach is not useful with biomass samples due to agglomeration with sieves and non-spherical aspect ratio or lack of realistic models on particle shapes used for laser diffraction methods of analysis. Knowing these limitations, it has been decided to carry out tests for all relevant samples with a Beckman Coulter apparatus to have at least a representative idea of the size of particles.

In Table 4.9, particle size analysis results from representative samples of each fuel dust used in the experiments are shown.

Table 4.9. Particle size analysis of coal and biomass used in R-20/R-30 experimental programme									
Sample	**10% < Size, µm**	**25% < Size, µm**	**50% < Size, µm**	**75% < Size, µm**	**90% < Size, µm**	**Mean, µm**	**Median, µm**	**Mean/ Median ratio**	**Specific surface, cm^2/g**
1000 PPC Coal	5.89	16	40.8	72.7	104	48.08	40.8	1.179	5307
1222 Torrefied Spruce 0.25G	10.3	30.2	76.5	154	250	109.6	76.52	1.433	3438
1223 Torrefied Spruce 0.25G	10.1	28.6	68.9	137	219	97.38	68.85	1.414	3,541
1310 I2 White Wood 0.25G	10.9	37.1	114	262	491	180.7	113.8	1.589	2,856
1313 I2 White Wood 0.25G	11.9	41.1	128	285	479	192.9	128.1	1.506	2,705
1400 El Cerrejon coal 53µm<s<75 µm	9.02	35.6	62.4	87.5	110	62.04	62.44	0.994	3,488
1401 El Cerrejon coal >75 µm	77.6	114	171	260	432	216.5	171.1	1.265	1,690
1402 El Cerrejon coal <53 µm	3.66	9.37	23.5	42.4	58.3	29.4	23.5	1.253	7,918
1403 El Cerrejon coal G145 A.R.	7.51	29.5	84.6	201	428	144.5	84.6	1.709	4,048
1404 Thoresby A.R.	4.77	20.1	65.9	131	188	82.7	65.9	1.254	5,604
1405 Kellingley A.R.	10.5	33.1	82.4	148	209	102.0	82.4	1.237	3,178
1406 Cereal Co-product 0.25G	12.8	46.8	172	408	719	273.6	171.7	1.593	2,242
1407 Cereal Co-product A.R.	16.1	75	343	1087	1584	591.8	343.1	1.725	1,988
1408 Torrefied Spruce 0.5G	12.8	48.9	152	319	495	203.6	152.3	1.337	2,772
1409 I2 White Wood 0.5G	39.1	125	369	798	1296	523.2	369.4	1.416	1,253
1410 Miscanthus 0.25G	13.3	53.8	154	319	522	229.5	154.4	1.487	2,545
1411 Miscanthus 0.5G	29.9	122	348	695	1075	453.6	348.3	1.303	1,536
1412 El Cerrejon G100 A.R.	23.6	71.8	168	315	453	206.7	168.4	1.228	2,076

[Mennim, (2014)]

Particle size analysis tests shown in Table 4.9 were carried out by Ms. Ann Mennim at the School of Geosciences, University of Edinburgh, and her contribution is gratefully acknowledged. Errors associated with this methodology are assumed, particularly in the specific surface values reported. According to the analysis, some of the samples were quite fibrous so the particles were showing up at the high end of the range [Mennim, (2014)]. This is an important problem when analysing biomass particle size with laser methods. PPC as received is the coal with the lowest mean and median values for particle size. Also 90 % of the particles are below 104 µm and 75 % below 72.7 µm. About 25 % of the particles for PPC are below 16 µm, representing a typical amount of ultrafine particles in a PPC coal sample. Specific surface values are shown to have an indication of the surface available to enter in contact with the O_2 during the ignition and propagation but they must be treated with caution due to inaccuracies in the analysis technique employed. Similar interpretation on the values shown can be done for the rest of the samples included in the table. For the narrow particle size distributions selected for El Cerrejon, there is a clear difference in the amount of fines between the three distributions. It is important to note for the biomass that although the sieve for the grinder is half the size that does not translate to a halving in the key values (mean, median, specific surface) when comparing 0.5G and 0.25G samples, showing the non-homogenous particles resulting from the biomass grinding process. Further considerations of sample particle size effects are included in the results and discussion chapters.

4.3. Configuration of experiments

4.3.1. Primary experimental set-up

The primary experimental set-up for controlling and monitoring variables during ignition experiments is discussed in this section. Although mostly described for R-20, the same strategy is used when operating the R-30 ignition chamber. A major part of the system operating strategy was the manipulation of the inlet-outlet flows in the chamber(s), using a valve system in the piping. Most of them are common ball valves, but in addition, a fast acting valve (V-101) is installed in the feed of the ignition chamber (R-20/R-30) to ensure effective coal dust dispersion from the reservoir/bottom of the chamber into R-20/R-30.

The initial configuration of R-20 and auxiliary units for the coal dust ignition tests programme is shown in Figure 4.5. Simplicity has been the objective, some units initially considered have not been included but if necessary they could be added in the future (e.g. additional pressure gauges/transducers).

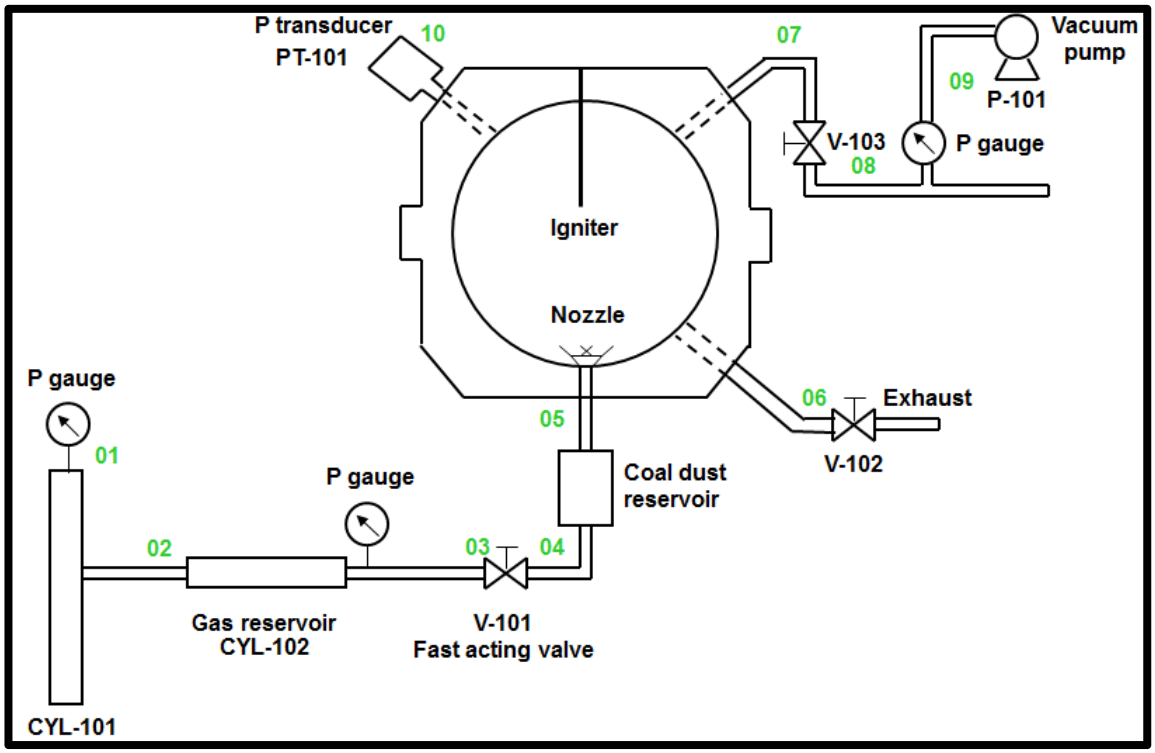

Figure 4.5. Schematic configuration of R-20 and auxiliary units with primary monitoring set-up.

The following abbreviations and symbols have been used in the configuration scheme:

Table 4.10. Configuration abbreviations

Abbreviations	
CYL-1XX	Gas cylinder/reservoir.
V-1XX	Flow Valve
P-1XX	Flow Pump
R-X0	Reactor or combustion chamber
PT-1XX	Pressure Transducer
T	Temperature Indicator
CA	Composition Alarm

Pressure gauge units are strategically located in order to monitor the pressure in the extremes of the process lines.

4.3.2. Advanced experimental set-up

The main objective of the advanced experimental set-up with monitoring system for R-20/R-30 is to maintain the specified operating conditions in the ignition chamber and to correct the effects due to possible disturbances in:

Feed flow-rate, composition and temperature.

Pressure and temperature in R-20 and the streams involved in the ignition/combustion process.

Ambient conditions, which could cause changes in the operating conditions.

The monitoring system of the ignition bomb R-20 has to ensure that the process variables (e.g. pressure, temperature and flows) are maintained during operation. For this purpose it is important to talk about manipulated variables and controlled variables. In the R-20 the controlled variables are:

Composition of inlet stream 5 (Figure 4.5), i.e., coal/biomass dispersion line. Pressure within the combustion chamber R-20.

Pressure in other lines (e.g. vacuum system).

Temperature in the combustion chamber R-20 (optional, not used in this research programme).

Composition of the exhaust gas, in particular, CO alarm presence for lab safety (optional).

On the other hand the manipulated variables are the ones which are regulated to certify that the controlled variables are constant and approximate to the values required for the success of the operation. These manipulated variables follow:

- Gas reservoirs (CYL-101, CYL-102) inlet/outlet pressure(s).
- Fast acting valve (V-101) opening and closing times.
- Vacuum system pressure (P-101, V-103).

- Stream 6 flow rate (exhaust) (V-102).

In Figure 4.6, the chosen configuration for an advanced monitoring system is shown. Due to independent pressure relief systems installed (V-104, V-105 and optional V-106), pressure controllers (PC) in R-20 and vacuum lines are not installed initially. The short duration of the experiments reinforces the option of not having a completely automated process as shown in Figure 4.6 below.

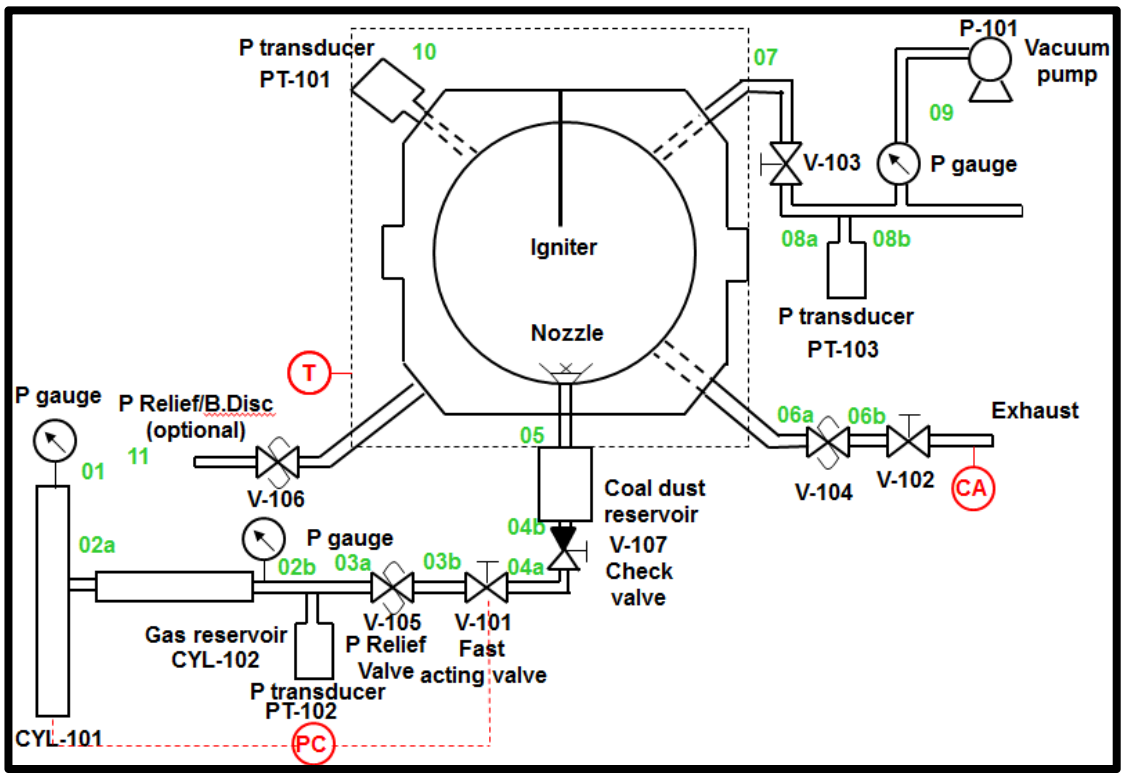

Figure 4.6. Schematic configuration of R-20 and auxiliary units with advanced monitoring set-up.

Pressure transducers (PT-101, PT-102 and PT-103) are strategically placed in R-20/R-30, gas inlet and vacuum lines to monitor pressure development in ignition experiments. The optional temperature indicator (T) for temperature monitoring in R-20 and concentration alarm (CA) in the exhaust line for carbon monoxide levels are considered for future experimental programmes.

Parts of the experimental set-up with R-20 is shown in Figures 4.7 and 4.8.

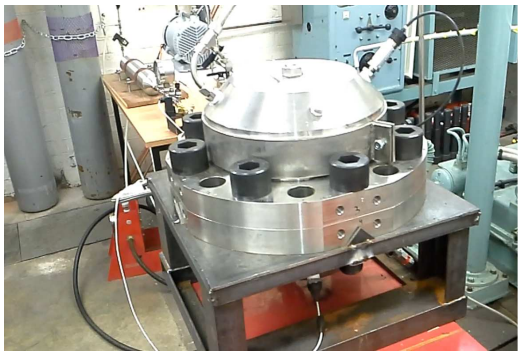

Figure 4.7. R-20 Experimental set-up.

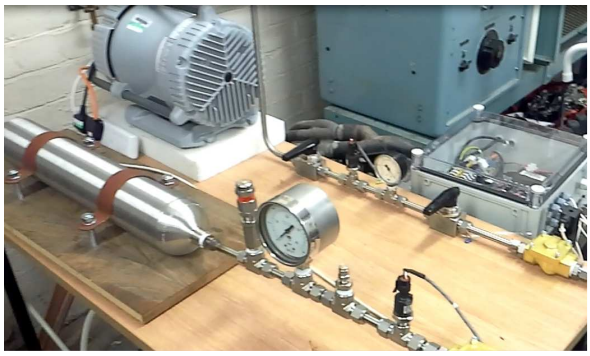

Figure 4.8. Detail of R-20 Experimental set-up.

4.4. Experimental procedure

The experimental procedure is summarised in this section, following on from the description of the auxiliary equipment and set-up required for the experimental programme in Chapter 3. Mr. George Cairns and Mr. Gordon Paterson, Technical Staff at the School of Engineering, are gratefully acknowledged for their essential contribution with the set-up of R-20 and R-30.

4.4.1 Summarised methodology

The critical steps in the coal/dust ignition experiments are:

1) Dust. Place pulverised fuel (coal or biomass) on top of the round nozzle. It is essential to put dust on top of the nozzle rather than in the optional dust reservoir upstream of the nozzle to avoid any plugs forming in the nozzle openings, particularly when using biomass.

2) Ignition source. A pyrotechnic igniter is placed inside the ignition chamber. For R-20, the igniter was centrally positioned. For R-30, igniter mounting was not moved from the same ¾ inch port as in R-20, which means that now the igniter was not centrally placed. This arrangement was used for simplicity and to investigate the geometry/volume effect on P/R values from ignition propagation. A sketch of igniter placement is shown in Figure 4.9.

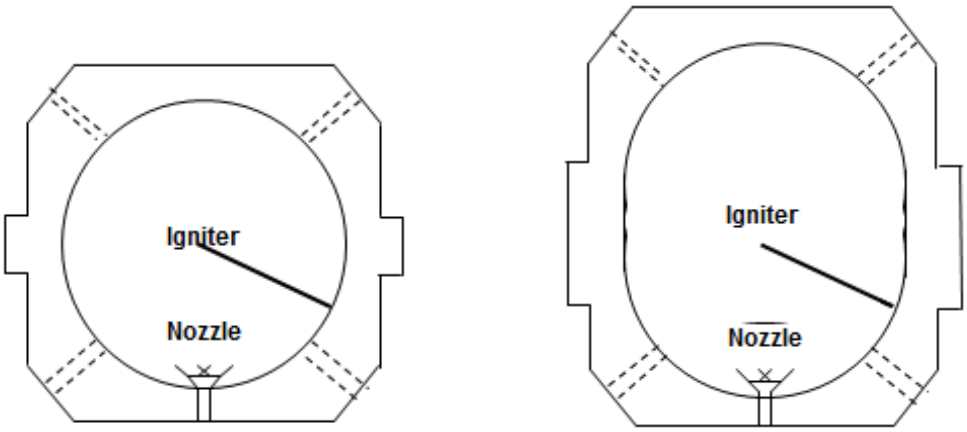

Figure 4.9. Sketch of igniter location, centred in R-20 (left) and non-centred in R-30 (right).

3) The ignition chamber (R-20/R-30) is closed with the bolting system using a Torc Gun.

4) Ignition atmosphere. The pressure in the gas reservoir is set at 965.3 kPa (140 psi) for air and O_2/CO_2 mixtures. The value is higher than used in PRL-20 tests in order to provide higher turbulence for good dispersion of biomass dust. For the air case, is not necessary to purge atmosphere in R-20/R-30 after closing the chamber. For oxy-fuel cases, R-20 and R-30 are first evacuated from its air, then pressurised over 2 bar with mixture from gas cylinder and then the exhaust line is opened to bring back the pressure down to atmospheric. This way nitrogen (N_2) is purged leaving inside chamber mostly O_2/CO_2 selected mixture.

5) Partial vacuum below 0.9 bar is pulled to cause a difference in pressure between chamber pressure and inlet pressure that will facilitate dust cloud formation inside the ignition chamber.

6) The solenoid/control valve opens with LabVIEW™ software starting the sequence completely automatically. A dust cloud is formed inside the pressure vessel.

7) The igniter is activated with 0.4 seconds delay after the control/solenoid valve opens.

8) Pressure data is acquired and recorded in a LabVIEW^{TM} file and exported to Excel. P/R is calculated with P_{max} and an average of 5 pressures recorded in the interval between opening the control/solenoid valve and ignition.

9) The ignition chamber (R-20/R-30) is opened using the Torc Gun. Dust residues are collected and the chamber is cleaned to avoid sample contamination when proceeding with another experiment.

The main steps for the dust ignition experiments are summarised in Figure 4.10.

Figure 4.10. Experimental methodology summarised for R-20/R-30 [Adapted from Trabadela et al., (2013)].

4.4.2. Start-up/shut down sequence in R-20/R-30 experiments

In coal/biomass dust ignition experiments, start-up is considered to be up to the point when peak pressure is recorded in the ignition chambers(R-20/R-30) after igniter activation. Shut-down procedures include char sample collection, R-20/R-30 cleaning and steps towards leaving chamber in a safe condition. A wooden/steel box was built with appropriate dimensions to prevent access of the body of the operator underneath or too close to R-20/R-30. For safety reasons, procedures are tabulated and placed next to the experimental area for reference and within the records for insurance purposes. Start-up and shut-down procedures are shown in Box 4.1 and Box 4.2.

These start-up and shut-down procedures was reviewed by insurers and safety advisers before proceeding with the ignition experiments. It is recommended to review this procedure particularly in case of changes in location or operator of R-20/R-30.

Box 4.1. START-UP R-20/R-30 Ignition chamber

1) Initialise control system in computer/remote device (LabVIEW^{TM}).
2) Check all air/gas valves are closed (V-101…3) while safety devices in place (V-104…7).
3) Check all (8+2) NPT ports in ignition chamber (R-20/R-30) are closed as required.
4) Check igniter shunt (supply) is off.
5) Check pressure transducers (PT-101…3) are in place with no change/recorded pressures.
6) Locate prepared dust sample on top of dispersion nozzle.
7) Place igniter in igniter mounting (wear goggles/face mask and gloves). R-20/R-30 bottom is away from top (not underneath then) to prevent unnecessary handling under R-20/R-30 top that could fall from stand/crane/beam support.
8) Close ignition chamber (R-20/R-30) by putting top of R-20/R-30 on bottom part with electric hoist. Lower part of operator body remains always outside safety perimeter (*box*).
9) Tight, following sequence (opposite bolts), 16 M48 bolts for rated pressure with Torc Gun. Up to 40 N/mm^2 is applied on bolts.
10) Start vacuum pump (P-101) in vacuum line but leave V-103 closed (check PT-103).
11) Open/close cylinder valve (CYL-101) and build pressure in (CYL-102) up to requirements.
12) Check PT-102 records pressure (140 psi) in CYL-102 for controlled turbulence in dust dispersion. Note this pressure can vary upon nozzle configurations and chamber volumes.
13) If ignition is not in air but oxy-fuel atmosphere, pressurise R-20/R-30 up to twice atmospheric and then open exhaust bringing back pressure in chamber to atmospheric in order to purge air in R-20/R-30.
13) When pressure in CYL-102 is set, open V-103 in vacuum line and manually close it when PT-101 records set vacuum in R-20. Note not much vacuum is needed.
14) Close vacuum line (V-103). Stop vacuum pump (P-101).
15) Check everything in the system is in place and V-102 in exhaust is closed.
16) Switch on igniter shunt (red light should be shown).
17) From a safe distance and wearing face mask, light igniter by pushing red light of igniter shunt (manually or with LabVIEW^{TM}). V-101 opens, dust cloud forms, ignition in 0.4 sec.
18) Pressure during experiment in system is recorded (PT-101…3)/displayed in LabVIEW^{TM}.

Box 4.2. SHUT-DOWN R-20/R-30 Ignition chamber

1) Switch off igniter shunt (red light should NOT be shown).
2) Open valve (V-102) in exhaust line to release pressure in R-20/R-30.
3) Check rest of air/gas valves are closed (V-101-3) while safety devices in place (V-104…7).
4) Check all (8+2) NPT ports in ignition chamber (R-20/R-30) are closed/plugged as required.
5) Check pressure transducers (PT-101…3) are in place.
6) Un-tight, following sequence (opposite bolts), 16 M48 bolts with Torc Gun.
7) Raise top of R-20/R-30 with electric hoist on beam to open chamber and take it away from top of fixed top of R-20/R-30. Do not enter safety perimeter (*box*).
8) Keep lift table underneath top of R-20/R-30 to hold it just in case it could fall from the stand. Stay outside safety perimeter (*box*).
9) Collect char samples with brush (when required) from R-20/R-30.
10) Remove rests of used igniter (i.e. plastic) from igniter mounting.
11) After top R-20/R-30 is cleaned, leave it held on back-up lift table.
12) Clean both hemispheres with a cloth to remove any residue from ignition experiment.
13) Close V-102 in exhaust line.
14) Check igniter mounting is centrally positioned in R-20 bottom half.
15) Get samples for further analysis as required.
16) Check LabVIEW™ has recorded experimental data before starting next test.
17) Check levels of dust are acceptable before next test (extraction system).
18) Go back to START-UP.

4.4.3. Examples of sample behaviour and appearance during experiments

Examples of sample behaviour during the experiments are shown in this section. In Figure 4.11, the R-20 ignition chamber is ready to be closed to start the experiment. Note the dust placed on top of the nozzle to avoid plugging and that the chamber is perfectly cleaned from previous experiment. On the right hand side (Figure 4.12) there is an example of R-20 "dirty" after dispersion of the dust in the test with a negative result for ignition. Note that in this picture is from an experiment where the igniter mounting is used in an alternative configuration without the top cap for the igniter (IM-B).

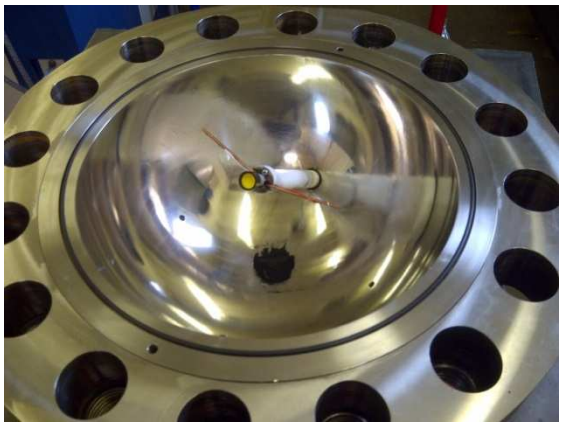

Figure 4.11. R-20 with coal and 2500 J igniter ready for test.

Figure 4.12. Coal dust dispersed inside R-20 for negative ignition test.

Figure 4.13. Coal char formed during positive ignition test with R-20.

Figure 4.14. Detail of coal char formed during positive ignition test with R-20.

The test, when positive, yields readily-identifiable coal char formed from ignition (Figure 4.13). In Figure 4.14 a detailed view of this coal char formed is shown. Note that pictures where taking immediately after the test and some smoke from ignition is still leaving after opening R-20 and that is the reason for the slightly fogged view.

Another example, of a negative ignition test for coal in R-20 with 2,500 J igniters, is shown in Figure 4.15. The coal particles around the round perforated nozzle present similar morphology as pre-ignition, with maybe some agglomeration, and the yellow cap of the igniter is barely touched. In contrast, in Figure 4.16 the coal char formed with the positive ignition test is clearly visible and on the left hand side edge of the picture the deformed cap of the ignitor, completely blackened, can been seen.

Figure 4.15. Dispersion nozzle with coal dust and 2,500 J igniter yellow cap for negative ignition test.

Figure 4.16. Dispersion nozzle with coal char and 2,500 J igniter cap (left) for positive ignition test.

In Figure 4.17 some biomass that has partially ignited and the remaining biomass dispersed around R-20 can be seen. As indicated by the nearly untouched yellow igniter cap, this ignition experiment was only partially positive. On the right hand side in Figure 4.18 an example of biomass dispersed for a negative test is shown. Note that this biomass was particularly large in particle size and how some particles have attached to the igniter mounting. Finally two examples of positive ignition tests for biomass are shown in Figures 4.19 and 4.20.

Figure 4.17. Biomass dust partially ignited with 2,500 J igniter for weak positive ignition test.

Figure 4.18. Biomass dust dispersed in R-20 for negative ignition test.

Figure 4.19. Dispersion nozzle with unburnt biomass yield for weak positive ignition test.

Figure 4.20. Biomass char formed and dispersed dust for positive ignition test.

In Figure 4.19, the biomass has ignited with partial accumulation of the char residue formed. In Figure 4.20 ignition of a lower concentration of biomass dust for the same ignition energy and O_2 level yielded mostly char formed during the experiment. The difference observed between these two pictures is an example of how ignition magnitude

can be visually assessed for lower P/R value (Figure 4.19) and higher P/R (Figure 4.20) from the test residues.

Work on improved imaging and char analysis from ignition are recommended as part of forensic studies that could be considered in future research programmes. It is interesting that an experienced operator can manage to identify positive from negative ignition for a significant amount of tests in lieu of instrumentation, which might help for experiments *in situ* or analysis of accidents in industry.

For the OxyCAP UK project, coal and biomass dust ignition experiments have been considered positive when the P/R value from an experiment is above a 2.5 threshold value. As noted in previous sections, the ignition can be designated as positive when P/R is above 2 and K_{st} as defined is above 1.5 [e.g. Cashdollar, (2000)]. The critical difference is that here the experiments are done with the need to "overdrive" the R-20 ignition chamber with higher energy igniters. The case for underground coal mining is different to PF milling in an oxy-fuel plant with higher O_2 levels and the presence of CO_2 in the mixture. The use of 5,000 J igniters is intended to ensure that if ignition does not happen with that energy source then it should not happen with 2,500 J or lower energy igniters. Further details on experiments are included in Chapters 5 and 6 dedicated to results and discussion arising from the experimental programme.

5. Results and discussion from R-20/R-30 coal ignitability experiments in air and oxy-fuel

The ignition experiments results presented in the following two chapters (Chapter 5 and Chapter 6) are for the identification of positive ignition with P/R values for the PF mill safety case in air and oxy-fuel atmospheres. Time constraints for R-20 calibration and limitations on experimental data acquisition rate with the data logging system meant that it was not possible to report additional data (e.g. K_{st}). However K_{st} values are not required to confirm positive ignition in the flame propagation criteria selected for the mill safety case. For dusts, there is also more scatter in K_{st} values than in pressure data from ignition experiments [Cashdollar, (2000)]. In addition, for a comprehensive report of valid K_{st} values it would have been necessary to compare data from R-20 and R-30 with data from a larger volume ignition chamber, such as $1m^3$, to evaluate impact of overdriving in those K_{st} values [Going et al., (2000)]. Further comments on this are included in Chapter 7 on recommendations for future work.

A set of coals relevant for the UK market at the time of this study have been tested. Details of the samples of coals used have been described in Chapter 4. The OxyCAP UK project selected El Cerrejon IC G145 as the reference coal due to broad international use as well as it being employed in power stations in the UK. As discussed in Chapter 2, there are different parameters that determine whether or not the initial ignition of coal dust suspensions will propagate into a more widespread and self-sustained process. These parameters are:

- Coal dust concentration

- Coal particle size

- Ignition energy

- O_2 concentration in ignition atmosphere

- Coal type (volatile content).

The presentation of these results and further discussion shows examples of lessons learned from ignition experiments.

5.1. Coal dust ignition in air

Coals dust ignition in air in R-20 and R-30 are presented as the baseline for further work using O_2/CO_2 mixtures and also for ignition of biomass later in the research programme.

5.1.1. Coal concentration effect in air

Figures 5.1 and 5.2 show Pittsburgh pulverised coal as received (PPC A.R.) and El Cerrejon Grade 145 as received (A.R.) respectively. For ignition of the PPC in air in R-20 using 2,500 J igniters, as coal concentration increases there was a P/R peak in the 300-500 g/m^3 range and then a plateau where the P/R decreases for the same ignition energy. Note that PPC ignited (P/R above 2.5 threshold) at all concentrations in the 100-600 g/m^3 range. Higher dust concentrations were not considered at this stage due to increased agglomeration affecting dust dispersion effectiveness [Cashdollar, (2000)] and ignition self-suppression effects when too much dust is present acting as heat sink [Cashdollar, (2000)] for the same ignition energy and oxidant mixture.

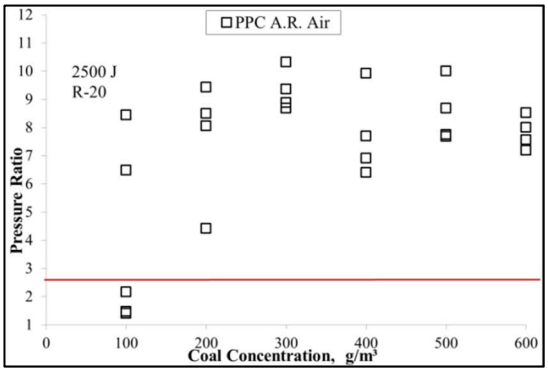

Figure 5.1. R-20 P/R vs. conc. PPC (2,500 J) for air combustion.

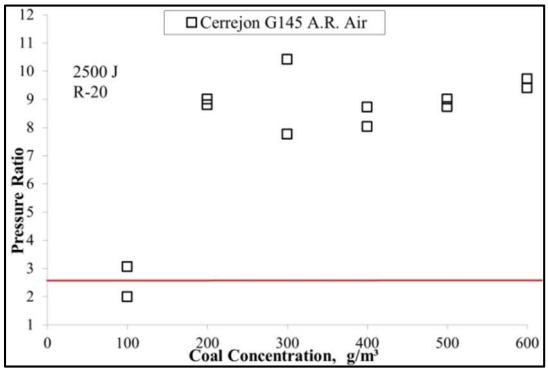

Figure 5.2. R-20 P/R vs. conc. Cerrejon G145 coal A.R. (2,500 J) for air combustion.

For the case of El Cerrejon grade 145 coal as received (G145 A.R.), there was positive ignition for all concentrations in air with 2,500 J in R-20. A peak in P/R value at 300 g/m^3 was found and then another plateau when dust concentration was increased.

When comparing PPC and El Cerrejon behaviour in air, using 2,500 J igniters and in R-20, it seems that PPC gives slightly higher P/R values, therefore a greater extent of combustion of

the sample when it does ignite. This is tentatively ascribed to finer particles in PPC versus El Cerrejon, despite the higher volatiles content in the latter.

In Figure 5.3 ignition of Thoresby coal as received (A.R.) is shown while Kellingley coal as received (A.R.) is shown in Figure 5.4, in both cases with 2,500 J igniters in air in the R-20 ignition chamber.

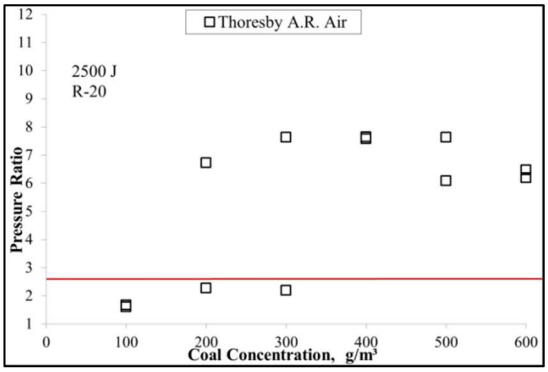

Figure 5.3. R-20 P/R vs. conc. Thoresby coal A.R. (2,500 J) for air combustion.

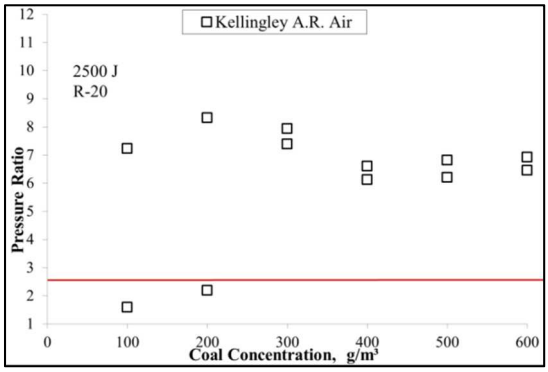

Figure 5.4. R-20 P/R vs. conc. Kellingley coal A.R. (2,500 J) for air combustion.

Thoresby coal A.R. in air with 2,500 J igniter in R-20 did not ignite at 100 g/m^3 concentration when compared with Kellingley coal A.R. which did ignite at all concentrations in the 100-600 g/m^3 range tested. Both coals have shown a plateau in P/R values from 300 g/m^3 concentration and both gave lower peak values when compared to PPC and El Cerrejon. Proximate Volatile Matter content is slightly higher in Kellingley (41.6 % daf.) vs Thoresby (38.7 % daf.) which may account for a slightly higher volatile yield and the ease of ignitability with a positive case for 100 g/m^3 concentration.

5.1.2. Coal particle size effect in air

Coal particle size effects for ignition in air are very relevant for understanding milling operation and further safety consequences if operating in oxy-fuel mode. Comparing ignitability of PPC and El Cerrejon G145 coals (Figures 5.1 and 5.2 respectively), both as received (A.R.), it is very interesting to see how both coals ignited at all concentrations and gave very similar ignition patterns in R-20 ignition chamber. On the contrary, when comparing Thoresby coal A.R. (Figure 5.3) and Kellingley coal A.R. (Figure 5.4), Thoresby did not ignite at concentrations <200 g/m^3. Thoresby A.R. mean particle size was 65.9 µm vs. 82.4 µm for Kellingley, suggesting Thoresby A.R. has more finer particles (<65.9 µm for 50 %

of them) but it seems that the characteristic diameter from which ignition is independent of particle size has not been reached for Thoresby coal.

For milling operation and primary air transport safety, size effects for the same coal is considered. When comparing particle size effect within the same coal, in this case El Cerrejon G145 as reference coal for the OxyCAP UK project, three particle size distributions have been prepared as described in Chapter 4. Igniters of 5,000 J energy have been used to ensure all the conditions for ignition are met and overdrive R-20. The particle size distribution >75 µm (Figure 5.5) had an average size of 171 µm and very low specific surface, resulting in negative ignition in air for all concentrations except for 600 g/m^3. On the contrary, particle size distribution for 75-53 µm (Figure 5.6) with an average particle size of 62 µm, gave positive ignition for all the concentrations tested.

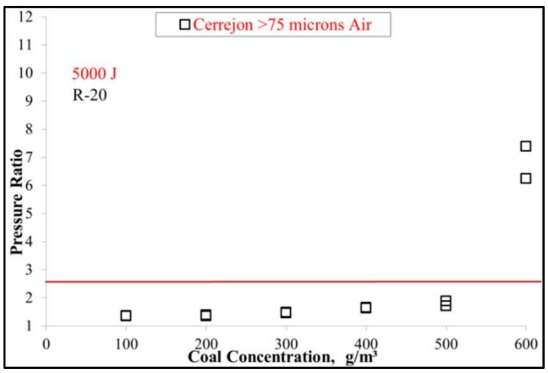

Figure 5.5. R-20 P/R vs. conc. Cerrejon coal >75 µm (5,000 J) for air combustion.

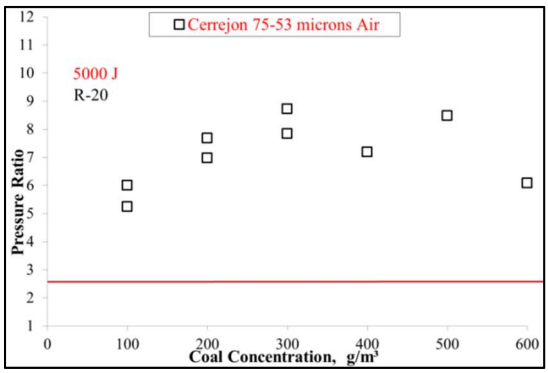

Figure 5.6. R-20 P/R vs. conc. Cerrejon coal 75 µm – 53 µm (5,000 J) for air combustion.

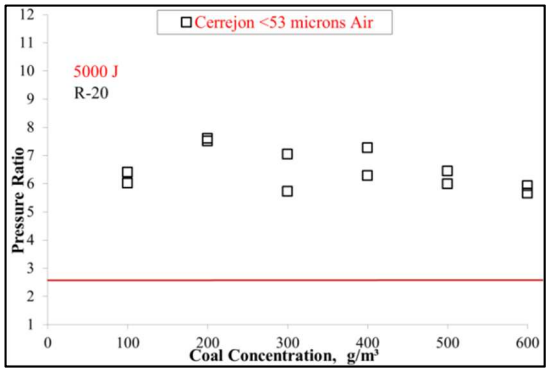

Figure 5.7. R-20 P/R vs. conc. Cerrejon coal < 53 µm (5,000 J) for air combustion.

Shown in Figure 5.7 the finest El Cerrejon case, particle size distribution <53 µm has an average particle size of 29 µm, and gave positive ignition for all concentrations. The

characteristic diameter for the ignition of El Cerrejon coal in air with 2500 J ignition energy is in the size distribution <53 µm. There is not much difference in ignition pattern and P/R between concentrations within this size distribution which means that *"if the dust particles are fine enough, their devolatilisation rates are not limiting"* [Hertzberg and Cashdollar, (1987); Hertzberg et al., (1982)]. Furthermore, not so fine particles between 200 and 270 mesh are key for P/R values from ignition, where volatiles homogeneous combustion is the critical stage controlling ignition propagation and if particles are too fine the amount of volatiles released is tentatively indicated to be more limited in the <53 µm than in the 75-53 µm particle size distribution. Consequently, 75-53 µm particle size distribution yielded in some cases higher P/R values than <53 µm particle size distribution. This is one of the most interesting lessons concluded from R-20 ignition experiments because it was thought that just the fines and ultrafines are the key particles for ignition. The use of lower ignition energy in other experimental programmes [e.g. Cashdollar, (2000)] that did not allow for adequate devolatilisation might have had an impact in that conclusion.

5.1.3. Ignition energy effect in coal ignition in air

Ignition energy effect is very important for PF milling safety. It can be argued that in the 500-10,000 J ignition energy range for pyrotechnic igniters commercially available, 2,500 J and 5,000 J are the most interesting as moderate ignition strength for PF milling safety and burner behaviour in the power plant boiler. Igniters of 2,500 J energy were widely used as ignition energy in the past in 20 litre chamber [e.g. Cashdollar, (2000); Going et al., (2000)] but 5,000 J are now more relevant than lower energy values for tests where overdriving is required for the mill safety case.

Comparison for PPC coal as received (A.R.) was carried out in R-30 to decrease overdriving effect by using an ignition chamber of largest volume available. As shown in Figure 5.8, PPC A.R. did not ignite for 100 g/m^3 concentration with 2,500 J while it gave positive ignition for all concentrations with 5,000 J (Figure 5.9). However, when positive, P/R values were very similar, indicating that the peak pressure reached could be not very different if the bulk of the dust was burnt, irrespective of the ignition energy strength.

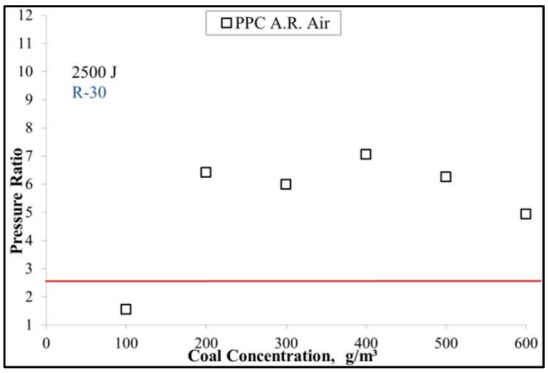

Figure 5.8. R-30 P/R vs. conc. PPC A.R. (2,500 J) for air combustion.

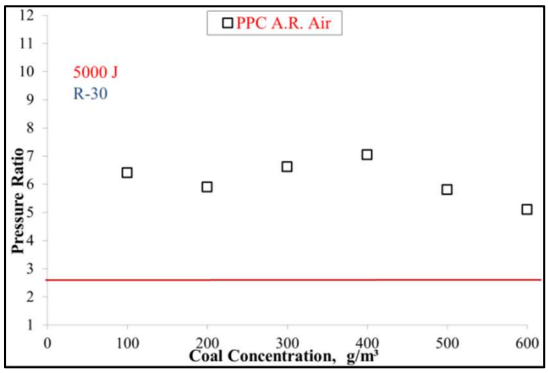

Figure 5.9. R-30 P/R vs. conc. PPC A.R. (5,000 J) for air combustion.

In Figure 5.10, El Cerrejon as received in R-30 gave positive ignition for concentrations above 250 g/m^3 with 2,500 J igniters and above 200 g/m^3 when testing fuel-air mixture with 5,000 J igniters (Figure 5.11). Note the decrease in the LFL value due to the ignition energy effect.

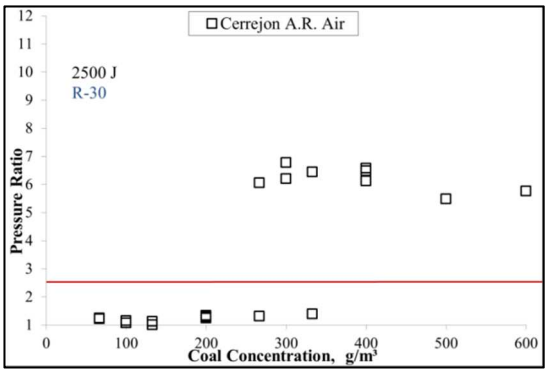

Figure 5.10. R-30 P/R vs. conc. Cerrejon coal A.R. (2,500 J) for air combustion.

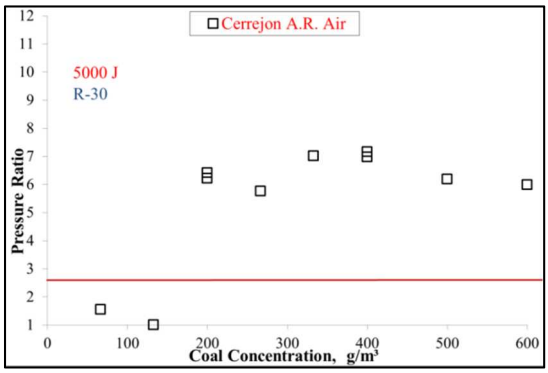

Figure 5.11. R-30 P/R vs. conc. Cerrejon coal A.R. (5,000 J) for air combustion.

In Figures 5.12 and 5.13, Thoresby coal as received (A.R.) in R-30 gave a very different ignition pattern depending on the igniter energy used. While P/R values were positive for all the concentrations tested, only for 500 g/m^3 concentration was ignition positive when using a 2,500 J igniter (Figure 5.12). This significant difference shows the importance of selecting higher ignition energy, 5,000 J, when testing for PF milling safety than the 2,500 J used in the underground coal mining case. LFL or MEC true values should be independent of ignition energy strength but low ignition energy use can underestimate P/R values for the PF mill safety case.

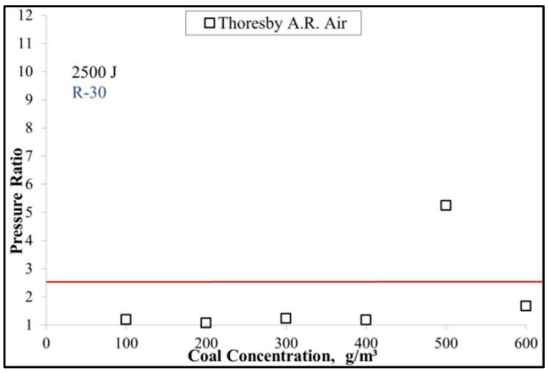

Figure 5.12. R-30 P/R vs. conc. Thoresby coal A.R. (2,500 J) for air combustion.

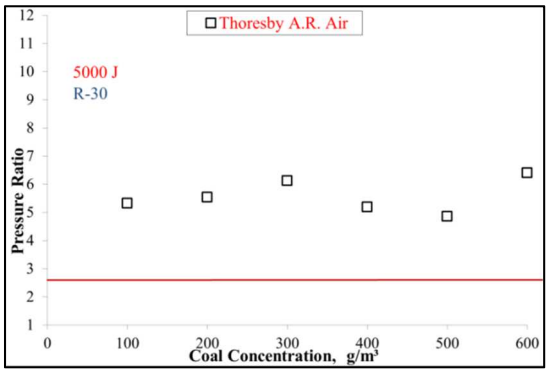

Figure 5.13. R-30 P/R vs. conc. Thoresby coal A.R. (5,000 J) for air combustion.

5.1.4. Coal type effect in air

From this set of experiments, PPC yielded the highest P/R values while El Cerrejon coal was also very reactive. Thoresby and Kellingley coals gave also positive ignition in air for most cases. However, coal type effect (volatile content) was evaluated in detail in further sections of this chapter with all the other ignition atmospheres tested.

5.2. Coal dust ignition in oxy-fuel

Ignition in oxy-fuel is affected by a second order effect, the presence of carbon dioxide (CO_2), which will tend to suppress ignition propagation into a more sustained flame. The higher heat capacity of CO_2 (versus N_2) represents the major atmosphere difference when comparing 21 % oxygen (O_2) v/v balance CO_2 (21 Oxy) with the air case. Oxy-fuel mixtures can have higher O_2 levels than in the air case and this is another major difference that is shown in the results sections. Coals were ignited in 21 Oxy, 25 Oxy and 30 Oxy for most cases with some particular experiments in 23 Oxy. Oxygen concentrations above 30 % v/v balance CO_2 (35 Oxy and 40 Oxy) although of interest, were not employed in this experimental programme due to safety concerns with housing and handling the required gas mixtures in the facilities available.

5.2.1. Coal concentration effect in oxy-fuel

For PF milling safety the key question is if, having favourable conditions for ignition energy and O_2 level, the most favourable concentrations (e.g. during start-up) will cause ignition propagation and trigger an explosion in the mill. For this purpose, Pittsburgh pulverised coal (PPC) as received (A.R.) from NIOSH was tested in R-20 with 2,500 J igniters for 21 Oxy,

similar conditions to tests carried out for underground coal mining safety except for CO_2 presence and higher turbulence introduced with 140 psi inlet gas pressure. Results for PPC A.R. are shown in Figure 5.14.

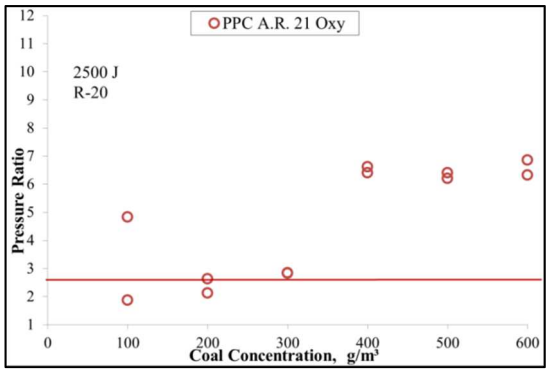

Figure 5.14. R-20 P/R vs. conc. PPC A.R. (2,500 J) for 21 Oxy-combustion.

PPC A.R. ignition experiments resulted in positive ignition for concentrations ≥300 g/m^3. The positive case at 100 g/m^3 is a clear case of scatter that sometimes occurs in these type of tests. At 200 g/m^3 both tests were negative according to P/R values providing additional information for the potential out of trend data for 100 g/m^3. Looking at the complete series is when it is possible to have an idea of PPC ignition patterns in 21 Oxy with 2,500 J in R-20. However, the presence of scatter has to be reflected in the oxy-fuel milling safety case indicating that PPC dusts can give positive ignition below 200 g/m^3, tentatively due to very fine particles present in PPC, so ignition propagation might still happen at lower concentrations. Having more data points for 100 g/m^3 concentrations and below would probably confirm the MEC for 21 Oxy. This experimental inaccuracy shows some of the limitations of this technique. A combination of a broader range of experimental conditions with experienced operators in dust ignition science would provide the best experimental based safety scenarios at a reasonable cost.

In Figure 5.15, El Cerrejon coal (G145 A.R.) ignition tests with 2,500 J in 21 Oxy in R-20 resulted in negative ignition at all concentrations except for 500 g/m^3, which shows an out of trend data point. Probably the scatter caused here was due to an issue with R-20 evacuation that made the ignition atmosphere not entirely 21 Oxy and that was noted in the experiments book. On this occasion, tentatively, it is safe to say that ignition in 21 Oxy

will give a negative result for more concentrations ≤ 600 g/m^3 than in the air ignition case, indicating a safer operation in 21 Oxy mode for this particular coal and ignition energy strength.

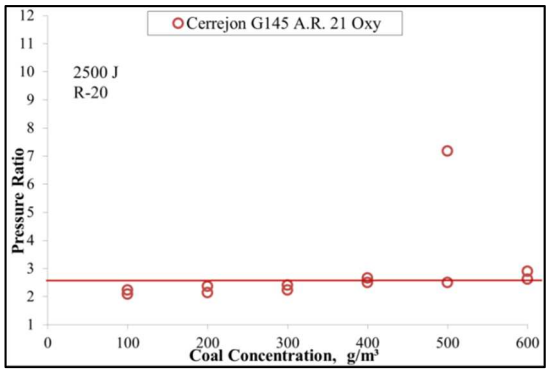

Figure 5.15. R-20 P/R vs. conc. Cerrejon G145 A.R. (5,000 J) for 21 Oxy-combustion.

The importance of interpretation of scatter and results for PPC A.R. and El Cerrejon G145 A. R. shows the need, as previously mentioned, to combine good experimental methodology with experienced researchers and operators to evaluate dust ignitability from these tests.

5.2.2. Coal particle size effect in oxy-fuel

Similarly to the air case shown in Section 5.1.2 included in this chapter, chamber ignition trends for coals PPC A.R. and El Cerrejon G145 A.R. are compared for 21 Oxy, 25 Oxy and 30 Oxy with 2,500 J igniters using R-20 in Figures 5.16 and 5.17.

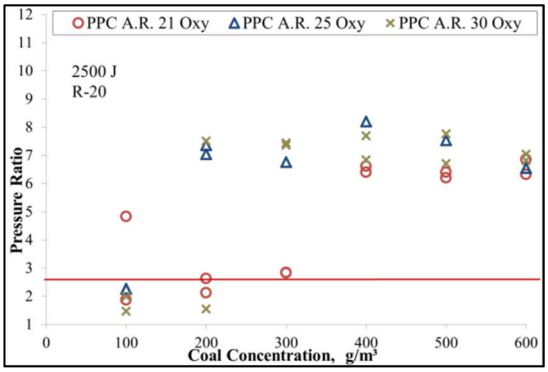

Figure 5.16. R-20 P/R vs. conc. PPC A.R. (2,500 J) for Oxy-combustion.

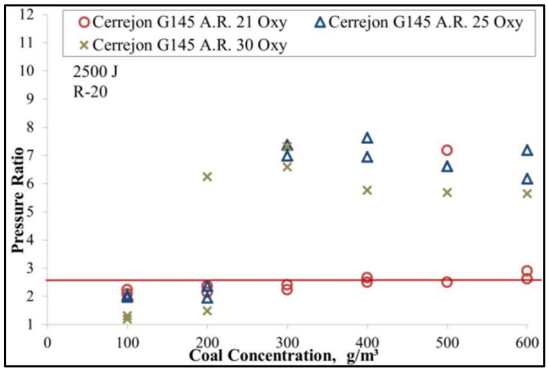

Figure 5.17. R-20 P/R vs. conc. Cerrejon G145 coal A.R(2,500 J) for Oxy-combustion.

Coal PPC A. R. gave clear positive ignition for all concentrations and all oxy-fuel atmospheres used when above 300 g/m^3. When testing 200 g/m^3, ignition was positive for

25 Oxy and 30 Oxy (Figure 5.16). P/R values were relatively similar when using 25 Oxy and 30 Oxy, probably due to similar devolatilisation of finer particles present in the fuel. El Cerrejon G145 A.R. gave negative ignition for all concentrations in 21 Oxy (except for scatter point mentioned before), negative at ≤200 g/m^3 for 25 Oxy and negative for 100 g/m^3 in 30 Oxy (Figure 5.17). Hence, in 25 Oxy El Cerrejon did not ignite at 200 g/m^3 but PPC did. This is attributed to a larger particle size distribution for El Cerrejon offsetting the higher volatile content in the coal. However, this effect is clearly pronounced when looking at P/R values for 25 Oxy and 30 Oxy in El Cerrejon case in Figure 5.17. Surprisingly, in the higher range of concentrations (≥400 g/m^3), P/R values are higher for 25 Oxy than 30 Oxy. This is possibly a sign of a higher proportion of larger particles in some coal samples (sampling errors) causing agglomeration affecting dispersion efficiency. Consequently, despite there being more oxygen available for ignition, the larger particles present in El Cerrejon are more difficult to heat up and cannot access the entire oxidant-ignition source mixture in a devolatilisation control stage. As fuel particle size increases, a decrease in devolatilisation rate can be expected despite higher O_2 levels present in the mixture. It is important to see if this effect is shown with finer coal distributions and for higher ignition energy levels, which might prove that 2,500 J is not a completely adequate ignition energy strength for larger coal particles.

El Cerrejon G145 particle size distributions prepared as described in Chapter 4 were also tested for 21 Oxy, 25 Oxy and 30 Oxy in R-20 and 5,000 J igniters. The reason to overdrive using higher ignition energy is to see if the phenomenon of devolatilisation being suppressed with larger particles present is evident when higher O_2 content in oxy-fuel atmospheres are tested. Also by doing tests with 5,000 J it potentially saves some tests with 2,500 J if the result is negative ignition with 5,000 J. The amount of work that could be undertaken in this area was, however, limited because preparation of the coal size distribution with the Ro-Tap® RX-29-E is time consuming and experimental time was also needed for biomass ignition tests.

As shown in Figure 5.18, the El Cerrejon G145 larger particle size distribution (>75 µm) gave negative ignition for all the concentrations in 21 Oxy and 25 Oxy with 5,000 J in R-20. Ignition was only (partially) positive for 600 g/m^3 concentration in air and 30 Oxy, showing a similarity in ignition pattern between 30 Oxy and air (Figure 5.18).

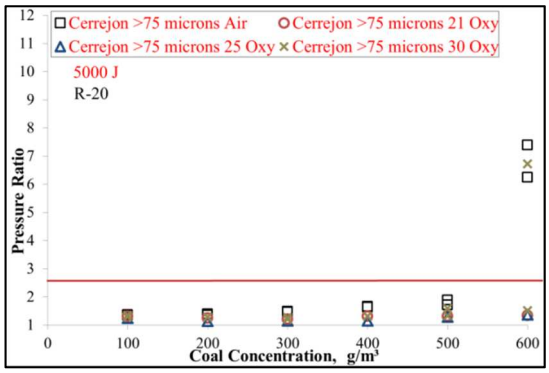

Figure 5.18. R-20 P/R vs. conc. Cerrejon coal >75 µm (5,000 J) for air and Oxy-combustion.

Although not undertaken, as mentioned before, it is likely that ignition tests for larger particle size distribution (>75 µm) would be self-suppressed as dust concentration increases but this affirmation is not certain for the same ignition energy particularly when increasing the O_2 available (e.g. 30 Oxy). Higher loadings with higher O_2 concentrations should be explored in the future.

In Figure 5.19, for the medium range particle size distribution (75 µm-53 µm), ignition was positive for concentrations ≥300 g/m^3 in 21 Oxy, while positive at all other concentrations for 25 Oxy and 30 Oxy cases. The ignition pattern according to P/R values was more similar to air for 30 Oxy than for 25 Oxy, tentatively confirming the need for a higher O_2 level in CO_2 to match air combustion behaviour [e.g. Man and Gibbins, (2011)].

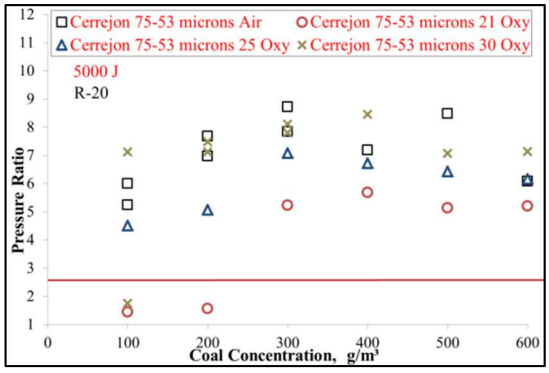

Figure 5.19. R-20 P/R vs. conc. El Cerrejon coal 75 µm – 53 µm (5,000 J) for air and Oxy-combustion.

Interestingly from Figure 5.19, tests with 30 Oxy gave higher P/R values when compared to 25 Oxy, tentatively attributed to a finer particle size distribution that prevents high

agglomeration causing the dust dispersion issues discussed in connection with the results shown previously in Figure 5.17.

In Figure 5.20, tests of finer particle size distribution (<53 µm) for El Cerrejon gave positive ignition for concentrations ≥200 g/m^3 in 21 Oxy and again positive ignition at all other concentrations for 25 Oxy and 30 Oxy cases. A slight peak in P/R values at 200-400 g/m^3 is observed for all oxy-fuel atmospheres and air. It is significant that P/R values for 21 Oxy are above P/R for 25 Oxy for some cases, indicating that at the moment of carrying out the experiments with 25 Oxy there may have been some inconsistencies with the coal samples used. The 30 Oxy ignition pattern gave P/R values above all the other oxy-fuel atmospheres tested and closer to the air ignition case.

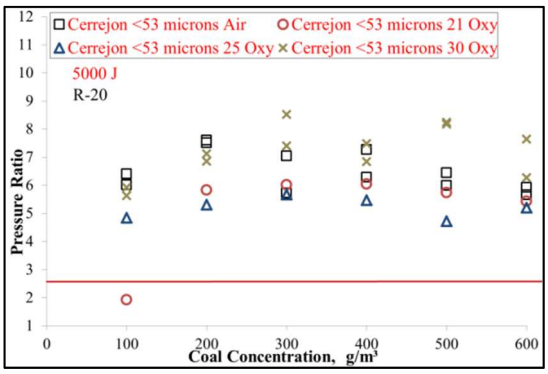

Figure 5.20. R-20 P/R vs. conc. Cerrejon coal <53 µm (5,000 J) for air and Oxy-combustion.

5.2.3. Ignition energy effect in coal ignition in oxy-fuel

Ignition energy effects in oxy-fuel have been evaluated for the two key coals tested: Pittsburgh pulverised coal (PPC) and El Cerrejon. PPC sample availability was limited and so it was decided to test the extremes of the oxy-fuel atmospheres range (21 Oxy and 30 Oxy) in R-20 and compare 21 Oxy with the air case only in R-30 test.

In Figure 5.21, in R-20 tests, PPC did show scatter for 100 g/m^3 with 2,500 J, otherwise the fuel did not ignite at concentrations <300 g/m^3 with 21 Oxy while with 5,000 J igniters PPC ignited for all concentrations except for 100 g/m^3. For tests in 30 Oxy, PPC ignited at all concentrations with 5,000 J but did not ignite at ≤200 g/m^3 with 2,500 J in R-20. This shows the importance of choosing adequate ignition energy when assessing safety during milling in oxy-fuel plant.

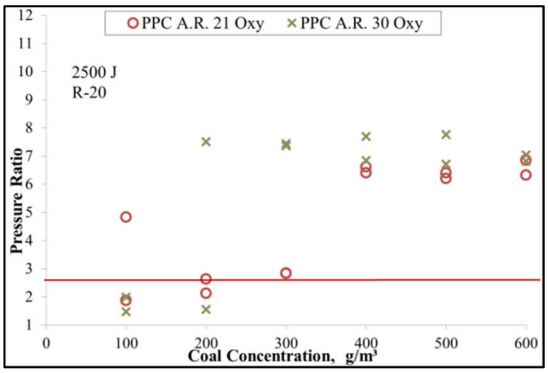

Figure 5.21. R-20 P/R vs. conc. PPC (2,500 J) for 21 Oxy and 30 Oxy-combustion.

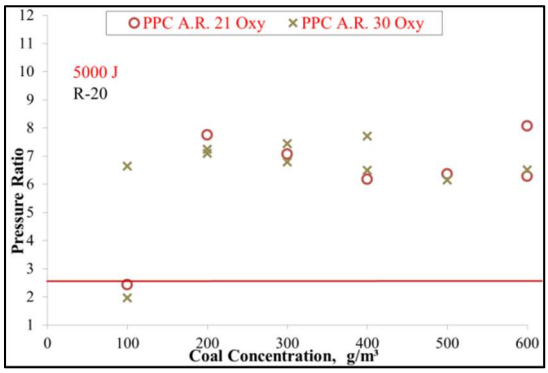

Figure 5.22. R-20 P/R vs. conc. PPC (5,000 J) for 21 Oxy and 30 Oxy-combustion.

When testing PPC in the R-20 ignition chamber with 5,000 J igniters (Figure 5.22) there was a trend for P/R values to be slightly higher than with 2,500 J (Figure 5.21) in cases where ignition was positive in both cases. In Figure 5.23, PPC gave negative ignition for all concentrations in 21 Oxy with 2,500 J but yielded positive ignition with 5,000 J for concentrations ≥300 g/m^3 in R-30 (Figure 5.24). For this case of PPC in R-30, when comparing with air ignition, a very similar ignition pattern was observed except for positive ignition at 100 g/m^3 with 5,000 J (Figure 5.24) that is negative in 2,500 J case (Figure 5.23). Differences in P/R might be a sign that overdriving shows P/R values which are lower if overdriving happens in a small pressure vessel of 20 litre (R-20) but does not prevent a positive ignition that could not happen if not enough ignition energy was put in place (100 g/m^3 case for 30 Oxy, Figure 5.22).

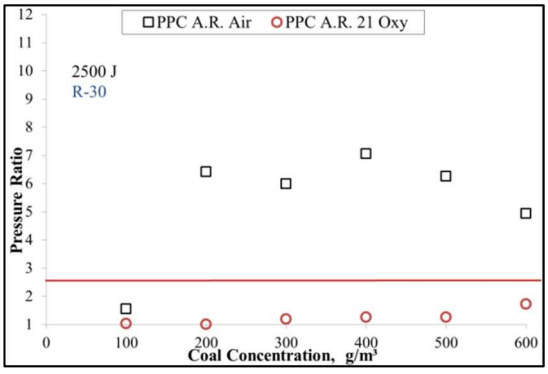

Figure 5.23. R-30 P/R vs. conc. PPC (2,500 J) for air and 21 Oxy-combustion.

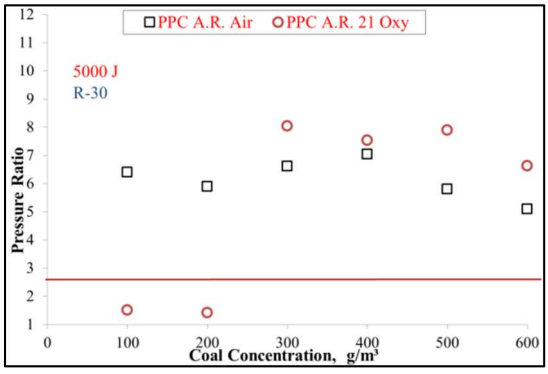

Figure 5.24. R-30 P/R vs. conc. PPC (5,000 J) for air and 21 Oxy-combustion.

Evidence of this tentative conclusion can be seen more clearly when comparing Figure 5.21 results with Figure 5.23 for experiments for PPC in R-30. What is clear is that, for air ignition

with 2,500 J in R-30, P/R values are lower than when compared to R-20 results (Figure 5.1). For 21 Oxy, there is a trend towards higher P/R values (if positive ignition) in R-30 for same ignition energy when compared to R-20, but this is not so evident at the higher concentration end (Figure 5.24 vs Figure 5.22). What this might indicate is:

1) Overdriving R-20 might not be an issue, and in fact it is necessary for experiments to be carried out with the right ignition energy (5,000 J) to avoid potential false negatives

2) When using larger pressure vessels (R-30), not increasing the ignition energy could give negative ignition cases that would be positive in a standard pressure vessel of 20 litre (e.g. 100-600 g/m^3 range negative in R-30 with 2,500 J for 21 Oxy, Figure 5.23, that were positive for R-20 in Figure 5.21.)

Even with increased ignition energy (5,000 J, R-30, Figure 5.24) tests could yield negative ignition (200 g/m^3 in 21 Oxy) that was positive for the same dust concentration for 21 Oxy in R-20 (Figure 5.22). The second inference can be a consequence of common issues around correct dust dispersion uniformity and also ignition atmosphere distribution inside larger ignition chambers. This is a common problem, particularly for fibrous dusts when operating 1m^3 ignition chambers [e.g. Huescar-Medina et al., (2013)]. However, carrying out tests in overdriven larger vessels in combination with R-20/R-30 is an economically viable method for detecting positive ignition tests for PF milling safety. Furthermore, there could be some added value if accurate determination of P_{max} for K_{st} and flame velocity is needed for oxy-burner design or for sizing pressure venting systems. Further comments are included in Chapter 7.

In Figure 5.25, El Cerrejon G145 tested as received (A.R.) gave positive ignition for 400 g/m^3 and 600 g/m^3 concentrations in 23 Oxy with 2,500 J in R-20. In Figure 5.26, for the 5,000 J case, ignition in 23 Oxy was positive for dust concentrations ≥300 g/m^3 in R-20, indicating the ignition energy effect and the need for high ignition energy to really overdrive R-20. For 30 Oxy, ignition was positive for all concentrations tested with 5,000 J in R-20 (Figure 5.26) while for 2,500 J a concentration of 100 g/m^3 gave negative ignition, remaining positive for all the other concentrations (Figure 5.25).

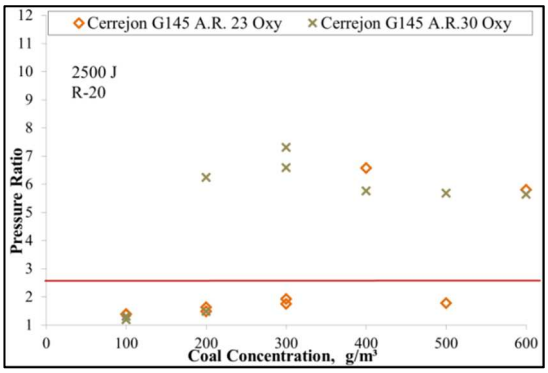

Figure 5.25. R-20 P/R vs. conc. Cerrejon G145 A.R. (2,500 J) for 23 Oxy and 30 Oxy-combustion.

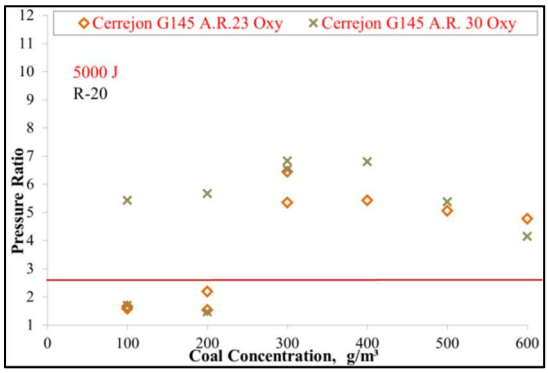

Figure 5.26. R-20 P/R vs. conc. Cerrejon G145 A.R. (5,000 J) for 23 Oxy and 30 Oxy-combustion.

In R-30, with 2,500 J ignition was negative for all concentrations tested in 21 Oxy, 25 Oxy and 30 Oxy (Figure 5.27). However, with 5,000 J (Figure 5.28), ignition was positive for 600 g/m^3 in 21 Oxy, ≥500 g/m^3 in 25 Oxy and ≥300 g/m^3 in 30 Oxy in R-30.

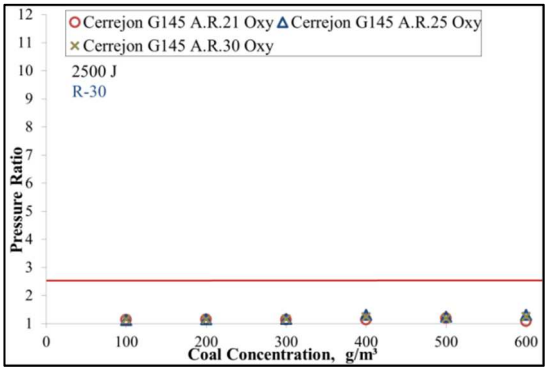

Figure 5.27. R-30 P/R vs. conc. Cerrejon G145 A.R. (2,500 J) for Oxy-combustion.

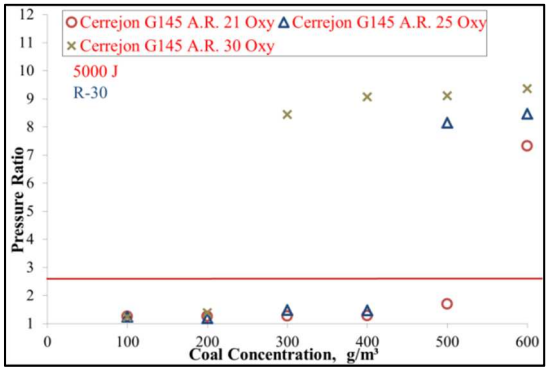

Figure 5.28. R-30 P/R vs. conc. Cerrejon G145 A.R. (5,000 J) for Oxy-combustion.

This behaviour, confirms the need for overdriving the R-30 ignition chamber and therefore suggests a volume and tentatively geometry effect in ignition for the PF mill safety case in oxy-fuel. When ignition was positive in R-30, higher P/R values tentatively confirmed that R-20 might not be ideal for accurate P_{max} determination. Further experiments are required in larger ignition chamber(s) to confirm this.

5.2.4. Atmosphere effect (O_2/CO_2 vol. %) in coal ignition in air and oxy-fuel

After evaluating step by step in separate figures some other effects on coal dust ignition for air and oxy-fuel, in this section a comparison of atmosphere effects on ignition with all the

relevant data available is shown. In Figure 5.29, results for PPC as received (A.R.) with 2,500 J in R-20 are displayed. PPC ignited at all concentrations ≥200 g/m^3 except for 21 Oxy when it did not ignite at 200 g/m^3. Ignition in air gave higher P/R values in the 300-500 g/m^3 concentration range and oxy-fuel P/R values were lower, probably due to the presence of CO_2 in the balance of Oxy atmospheres when compared to lower heat capacity inert (N_2) in air case. For 25 Oxy an ignition pattern close to that for 30 Oxy was observed, indicating that in the case for PPC is not that clear that any of the oxy-fuel atmospheres tested behaved similarly to air ignition mode.

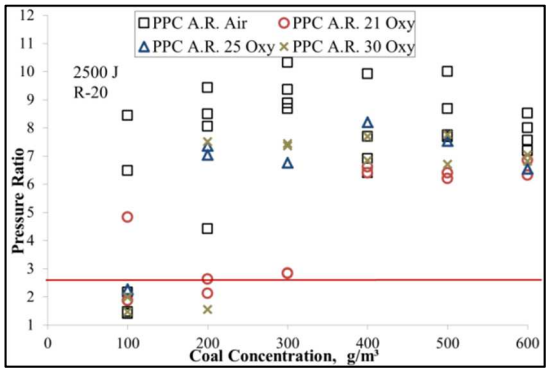

Figure 5.29. R-20 P/R vs. conc. PPC (2,500 J) for air and Oxy-combustion.

El Cerrejon coal G145 as received (A.R.) was tested in air, 21 Oxy, 25 Oxy and 30 Oxy in R-20 and R-30 with 2,500 J and also in R-30 with 5,000 J (Figures 5.30, 5.31 and 5.32). When using 2,500 J in R-20 coal did not ignite in 21 Oxy except for a test at 500 g/m^3. In air, El Cerrejon ignited at all concentrations tested (100 g/m^3 – 600 g/m^3 range) and the same happened for 30 Oxy except for the 100 g/m^3 test. Under 25 Oxy, El Cerrejon ignited at concentrations ≥300 g/m^3 although a more pronounced plateau distanced 25 Oxy from air ignition behaviour at higher coal concentrations (Figure 5.30). In R-30 with 2,500 J El Cerrejon G145 did not ignite at all concentrations for 21-25-30 Oxy (Figure 5.31). El Cerrejon ignited in air for concentrations ≥267 g/m^3. Intervals here in concentrations were narrowed in the area for P/R peak values. This discrepancy with R-20 results is tentatively related to the R-30 ignition chamber larger volume acting as a heat sink and/or chamber geometry effect in dust dispersion causing difficulties in initial ignition when not overdriving.

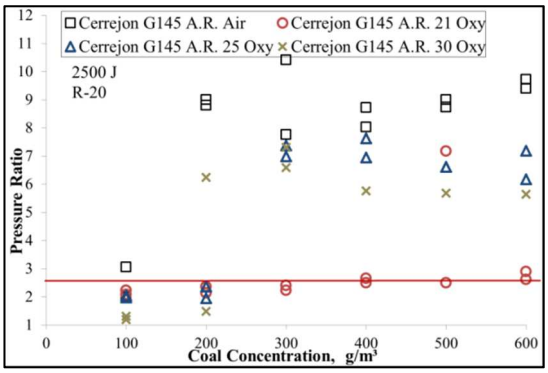

Figure 5.30. R-20 P/R vs. conc. Cerrejon G145 coal A.R. (2,500 J) for air and Oxy-combustion.

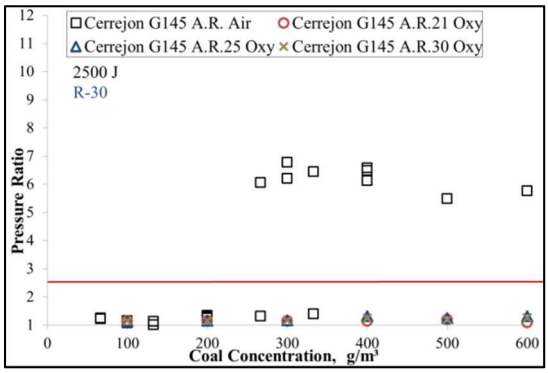

Figure 5.31. R-31 P/R vs. conc. Cerrejon G145 coal A.R. (2,500 J) for air and Oxy-combustion.

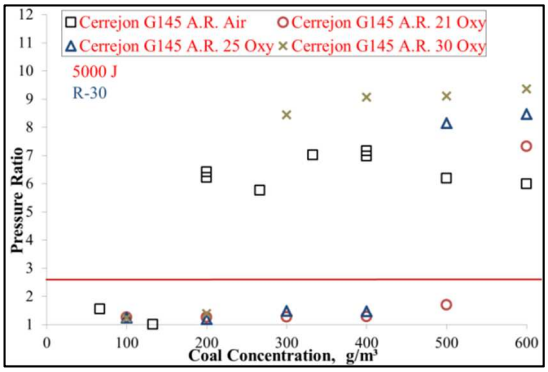

Figure 5.32. R-30 P/R vs. conc. Cerrejon G145 coal A.R. (5,000 J) for air and Oxy-combustion.

As shown in Figure 5.32, testing El Cerrejon in R-30 with higher ignition energy (5,000 J) resulted in more positive ignition tests. When carrying out the ignition test in air, MEC was approximately 200 g/m^3, in 25 Oxy was 500 g/m^3 and in 30 Oxy was 300 g/m^3 in the 100 g/m^3-600 g/m^3 range tested. Results arising from R-30 with 5,000 J are significantly different from R-20 results, shown in Figure 5.19. El Cerrejon has a volatile content around 40 % wt. and this is reflected in high P/R values when ignition is positive with a higher ignition energy that facilitates volatiles release during ignition, homogenous combustion of volatiles being the critical stage for ignition propagation [Cashdollar et al., (1989)]. However, particle size effect limitations for P/R values have been observed when comparing El Cerrejon G145 A.R. with narrower particle size distributions, as shown in previous sections.

In Figure 5.33, Thoresby coal as received (A.R.) with 2,500 J in R-30 yielded low P/R values for negative ignition tests for all concentrations tested (100 g/m^3-600 g/m^3 range) in all oxy-fuel atmospheres tested (21 Oxy, 25 Oxy and 30 Oxy). Only for concentration 500 g/m^3 was ignition positive in an air atmosphere, for all the other coal concentrations ignition was found negative (Figure 5.33). As shown in Figure 5.34, using higher ignition energy (5,000 J) in R-30 resulted in more positive ignition cases, giving positive tests for all concentrations in air. In addition, P/R values indicated positive ignition for concentrations ≥400 g/m^3 in 30 Oxy. Only at 600 g/m^3 was ignition positive when testing in 25 Oxy. Thus it can be seen that there is a clear ignition energy effect in order for the same fuel to use the higher O_2 available in the oxy mixture and propagate ignition. For the same amount of O_2 is available in the ignition atmosphere (e.g. air case) it is significant the effect of the igniter energy on dust ignition. The need for overdriving the ignition chamber to adequately heat up the dust particles and promote the volatiles release is characteristic of the PF mill safety case. Overdriving clearly does not happen in R-30 when using 2,500 J igniters.

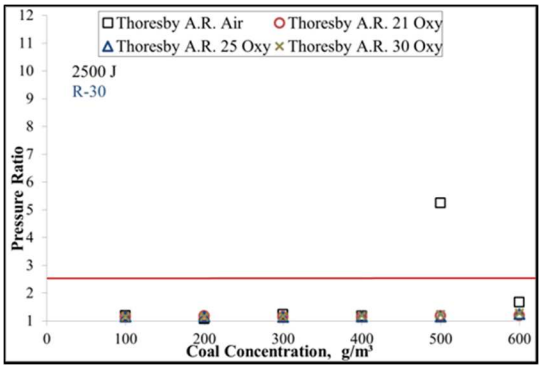

Figure 5.33. R-30 P/R vs. conc. Thoresby coal A.R. (2,500 J) for air and Oxy-combustion.

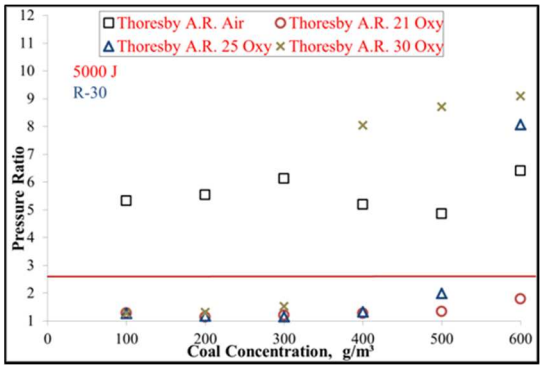

Figure 5.34. R-30 P/R vs. conc. Thoresby coal A.R. (5,000 J) for air and Oxy-combustion.

5.2.5. Coal type effect in oxy-fuel

As shown in ignition experiments on different coals in previous sections, the properties of the coal and composition of the fuel (e.g. higher volatile content) has a major impact on ignition results, as seen previously in the relevant literature discussed in Chapter 2 of this thesis [e.g. Conti and Hertzberg, (1987)]. In this section a summary of results from coal ignition tests, highlighting the fuels that are of interest for the PF milling safety case, are

shown in Table 5.1. PPC as received was more reactive than El Cerrejon G145 as received. PPC ignited nearly at all concentrations for all atmospheres tested with 2,500 J in R-20. In contrast, El Cerrejon could be handled safely in PF milling in 21 Oxy with coal concentrations ≤400 g/m^3 while in air cases it did ignite at all concentrations.

Table 5.1. Summary of results for coal ignition tests in R-20 with 2,500 J

Fuel/Conc.	100 g/m^3	200 g/m^3	300 g/m^3	400 g/m^3	500 g/m^3	600 g/m^3
PPC A.R.						
El Cerrejon G145 A.R.						

Air 21Oxy 25Oxy 30Oxy Positive Negative

Table 5.2 shows a summary of results in R-20 with 5,000J igniters for the reference coal for the OxyCAP UK project, with narrower particle size distributions compared to PCC A.R.

Table 5.2. Summary of results for coal ignition tests in R-20 with 5,000 J

Fuel/Conc.	100 g/m^3	200 g/m^3	300 g/m^3	400 g/m^3	500 g/m^3	600 g/m^3
El Cerrejon >75 µm						
El Cerrejon 75 -53 µm						
El Cerrejon <53 µm						
PPC A.R.						

Air 21Oxy 25Oxy 30Oxy Positive Negative

PPC ignited at all concentrations tested (100 g/m^3-600 g/m^3 range) in 21 Oxy and 30 Oxy except for 100 g/m^3 in 21 Oxy, which shows the high risk when milling PPC under oxy-fuel conditions. El Cerrejon yielded negative ignition at all concentrations for air, 21 Oxy, 25 Oxy and 30 Oxy when larges particle sizes were used, except for 600 g/m^3 in air and 30 Oxy. Decreasing the particle size distribution resulted in many more cases of positive ignition. It is interesting to see that for El Cerrejon 75 -53 µm size in 21 Oxy, ignition was negative for 200 g/m^3 while for the same concentration ignition was positive if testing <53 µm. This means that when milling El Cerrejon coal, it is safer operate in 21 Oxy than in air. In 21 Oxy tentatively could be safer to handle up to 200 g/m^3 concentrations of El Cerrejon without ignition and potential fire developing an explosion in the mill island.

These tentative conclusions are explored with potential implications and other relevant results from biomass experiments in Chapter 7.

6. Results and discussion from R-20/R-30 biomass ignitability experiments in air and oxy-fuel

As noted in Chapter 5 for coal dust ignition experiments, the five key parameters for biomass dust ignition tests have been considered when analysing results from experiments included in this Chapter. Some of these results on biomass ignitability have been previously published by Trabadela et al., (2014) and constitute to the author's knowledge the first oxy-biomass ignition experiments reported in a 20 litre spherical ignition chamber published for PF milling safety.

The biomasses tested were Torrefied Spruce, I2 White Wood, Miscanthus and Cereal Co-product and they have been described in Chapter 4. The ignition results in air and oxy-fuel in the R-20 and R-30 ignition chambers are reported and discussed in this Chapter 6. The OxyCAP UK project was initiated with Industry interest in development of oxy-fuel technology for use in coal power plants. Since the inception of the project in 2009, industry interest has shifted from coal as fossil fuel. Biomass has gained interest for its potential for co-firing with coal and also for the possibility of achieving net negative carbon dioxide emissions if combined with CCS. Bio-Energy with CCS (BECCS) has been mentioned in previously in this thesis and this work is intended to improve understanding of biomass dust ignition under oxy-fuel atmospheres for primary recycle (PR) and mill safety when operating PF power plants with oxy-fuel as the CCS technology.

6.1. Biomass dust ignition in air

Biomass samples were first tested in air to check ignition under standard conditions and then the results were compared with results from oxy-fuel atmospheres.

6.1.1. Biomass concentration effect in air

The concentrations of dusts tested are in the same range of 100-600 g/m^3 used for coal dust ignition experiments (Chapter 5). Torrefied Spruce (Figure 6.1) gave a quite similar ignition pattern to coal dusts for concentrations >200 g/m^3 [e.g. Figures 5.1 and 5.2], presenting a peak in P/R values around 300-400 g/m^3 with 2,500 J igniters in R-20 and then a plateau for P/R values for higher dust concentrations. Torrefied Spruce ignited at all concentrations tested with 2,500 J in R-20 except for 100 g/m^3. There is a trend of increasing P/R values at richer biomass dust concentrations until a plateau is found where

too much dust is present for the same O_2 and ignition energy available. In Figure 6.2, for I2 White Wood, a similar trend was observed with a plateau, but tests were negative not just for 100 g/m^3 but also for 500 g/m^3 with 2,500 J in R-20. P/R values were found to be lower for I2 White Wood when compared to Torrefied Spruce and this can tentatively be attributed to the characteristics of the torrefied fuel noted in Chapter 2 [Livingston, (2013)] and the higher moisture content in White Wood (9.1 % vs 3.1 % according to Tables 4.6 and 4.5 respectively).

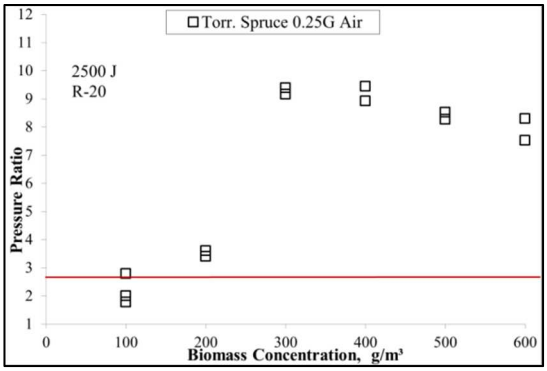

Figure 6.1. R-20 P/R vs. conc. Torrefied Spruce 0.25G (2,500 J) for air combustion.

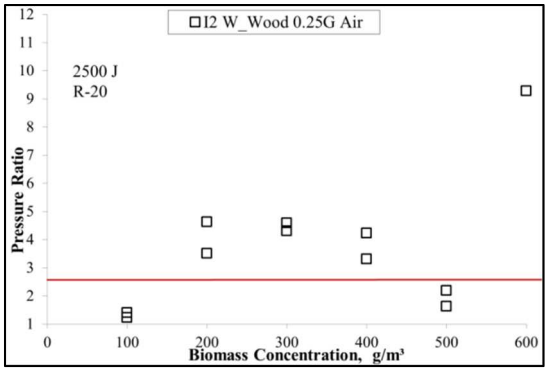

Figure 6.2. R-20 P/R vs. conc. I2 White Wood 0.25G (2,500 J) for air combustion.

In Figure 6.3, Miscanthus presented positive ignition at all concentrations tested in air with 2,500 J in R-20 except for 100 g/m^3. A clear peak in P/R values was found around 300 g/m^3 with a plateau with a negative test at 600 g/m^3 proving that the dust can self-suppress ignition if too much of it is there for the same O_2 and ignition energy available.

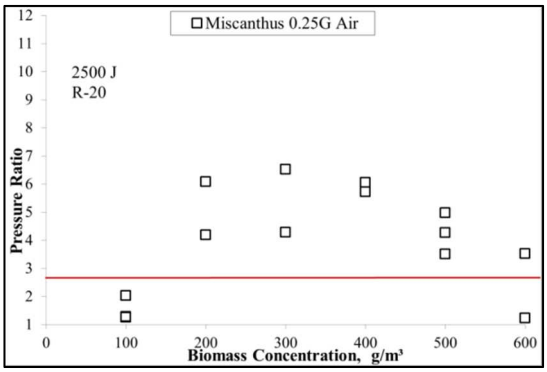

Figure 6.3. R-20 P/R vs. conc. Miscanthus 0.25G (2,500 J) for air combustion.

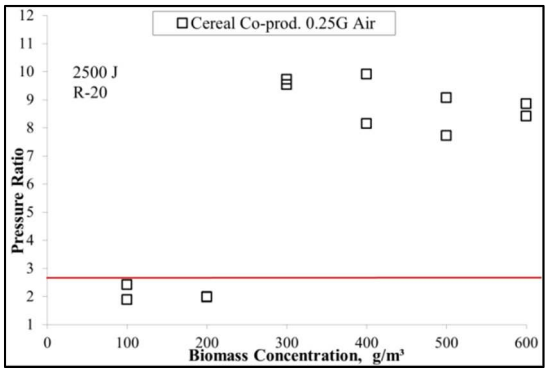

Figure 6.4. R-20 P/R vs. conc. Cereal Co-product 0.25G (2,500 J) for air combustion.

In Figure 6.4, Cereal Co-product yielded positive ignition in air for concentrations ≥300 g/m^3 with 2,500 J in R-20. A peak was detected in the region around 400 g/m^3 and then a plateau in P/R values for higher dust concentrations. However, it is important to note that P/R values are quite high, which means that Cereal Co-product was difficult to light but quite reactive once ignition had happened.

6.1.2. Biomass particle size effect in air

Evaluating biomass particle size effects is quite difficult and an adequate combination of particle size analyser and imaging techniques were not available. In this section, the same biomass, Torrefied Spruce received as pellets, has been ground with two different screens, 0.250 mm (0.25G) and 0.500 mm (0.5G) as explained in Chapter 4. The aim was to test biomass with significantly different particle size distributions. According to Table 4.9, for the Torrefied Spruce 0.25G sample the mean particle size was in 109.6-97.38 µm. Torrefied Spruce 0.5G presented a mean particle size of 203.6 µm. The different in the results for P/R values is evident, as shown in Figure 6.5.

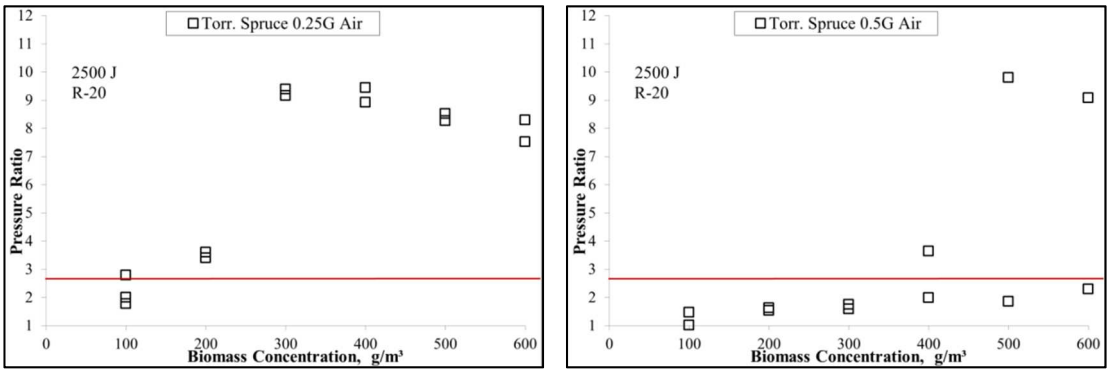

(a) **(b)**

Figure 6.5. R-20 Comparison P/R vs. conc. Torrefied Spruce 0.25G (a) and 0.5G (b) (2,500 J) for air combustion.

In Figure 6.5a, Torrefied Spruce 0.25G ignited at all concentrations ≥200 g/m^3 with 2,500 J igniters in R-20 while Torrefied Spruce 0.5G only ignited at concentrations ≥400 g/m^3, presenting a weak ignition at 400 g/m^3 (Figure 6.5b). This is tentatively attributed to larger particles present in 0.5G samples that, for the same ignition energy, cannot fully devolatilise. However, it is interesting to see that despite having much larger particles, in runs where they clearly ignite, P/R positive values obtained at 500 g/m^3 and 600 g/m^3 do not differ much from values with 0.25G samples, indicating that is devolatilisation and not

particle size that is the critical path for ignition propagation from thermal decomposition of the particles and the subsequent homogeneous combustion of generated volatiles.

For non-pelletized Cereal Co-product biomass there is no data available for 2,500 J igniters. Cereal Co-product with larger particle size needed to be tested as reference biomass in the OxyCAP UK project. Therefore, it was decided to use 5,000 J igniters and show the difference in ignition behaviour between the biomass ground (0.25G) and the biomass as received from Cranfield University, which was received sieved through a 180 µm sieve.

In Figure 6.6a, Cereal Co-product 0.25G ignited at all concentrations ≥200 g/m^3 with 5,000 J in R-20 showing a peak for 500 g/m^3. Ignition results for Cereal Co-Product <180 microns with 5,000 J in R-20 were more irregular, igniting at 300 g/m^3, 500 g/m^3 and 600 g/m^3 and yielded negative ignition of all the other concentrations (Figure 6.6b). It is important to note for this case that the P/R peak value was at 300 g/m^3 and positive values at 500 g/m^3 and 600 g/m^3 were lower than with 0.25G (Figure 6.6a). This shows that for larger biomass particle size cuts the heat-up of the particles and devolatilisation are constrained, with additional higher self-suppression ignition effect (heat sink) for the biomass dust tested.

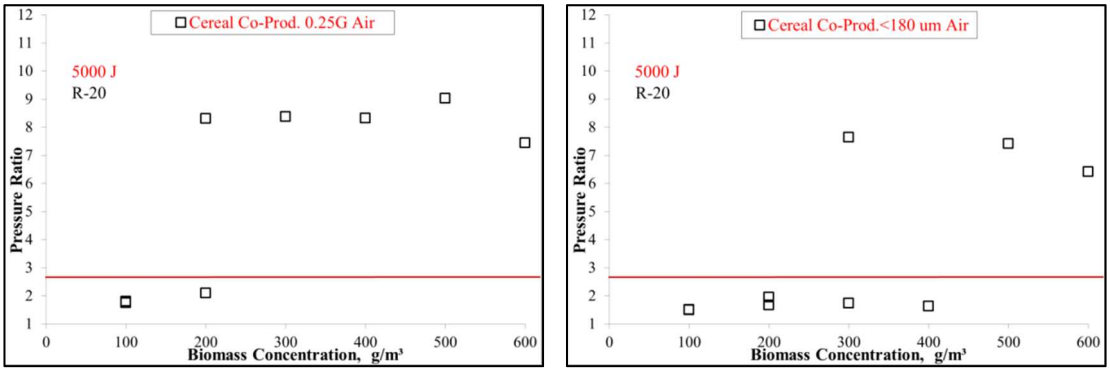

(a) **(b)**

Figure 6.6. R-20 Comparison P/R vs. conc. Cereal Co-product 0.25G (a) and sieved through 80 mesh (180 µm) (b) (5,000 J) for air combustion.

6.1.3. Ignition energy effect in biomass ignition in air

Torrefied Spruce 0.25G biomass has been tested with 2,500 J and 5,000 J in R-20 and R-30 to evaluate the ignition energy effect. The results are shown in Figures 6.7, 6.8 and 6.9. Torrefied Spruce 0.25G presented positive ignition P/R values for concentrations ≥200 g/m^3 with 2,500 J in R-20 (Figure 6.7a) while the same biomass ignited for all concentrations in

the 100-600 g/m^3 range tested with 5,000 J in R-20 (Figure 6.7b). It is significant that P/R values were quite similar for both experimental conditions except around minimum explosive concentration (MEC) for these tests, where at 200 g/m^3 concentration the use of twice the ignition energy resulted in much higher P/R values due to higher volatiles release. This particular biomass type did not ignite at 100 g/m^3 with 2,500 J (Figure 6.7a) which may suggest that this is not adequate ignition energy when testing biomass ignitability for PF milling safety.

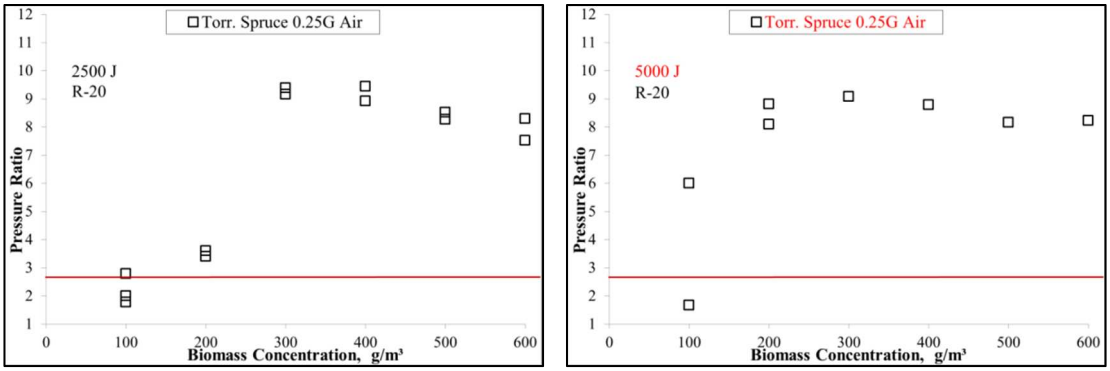

(a) **(b)**

Figure 6.7. R-20 Comparison P/R vs. conc. Torrefied Spruce 0.25G 2,500 J (a) and 0.25G 5,000 J (b) for air combustion.

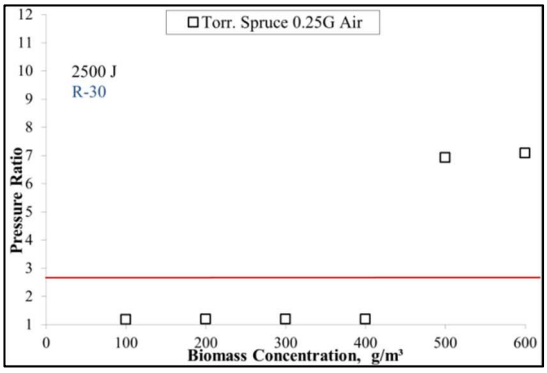

Figure 6.8. R-30 P/R vs. conc. Torrefied Spruce 0.25G (2,500 J) for air combustion.

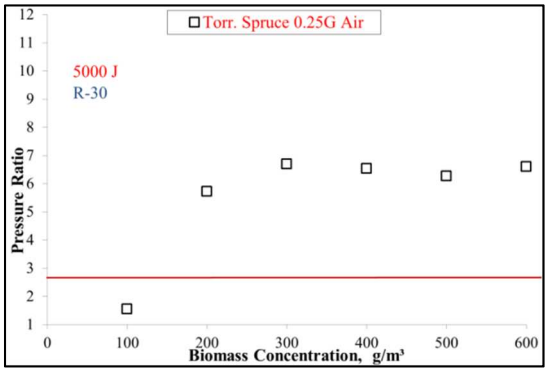

Figure 6.9. R-30 P/R vs. conc. Torrefied Spruce 0.25G (5,000 J) for air combustion.

Torrefied Spruce 0.25G ignitability has been evaluated with 2,500 J and 5,000 J in R-30 as shown in Figures 6.8 and 6.9, respectively. In Figure 6.8, Torrefied Spruce 0.25G

experiments confirmed negative for all concentrations ≤400 g/m^3 with 2,500 J. When using 5,000 J, Torrefied Spruce 0.25G yielded positive ignition for all concentrations tested except for 100 g/m^3 (Figure 6.9). There is evidence of perceived differences in ignitability depending on the strength of the ignition energy used. This reiterates questions around the adequacy of 2,500 J igniters for biomass when evaluating PF milling safety. In addition, when ignition was positive, P/R values found in R-30 were significantly lower than when testing in R-20 (Figure 6.7a and Figure 6.7b). This confirms the idea that overdriving is needed for studying PF mill safety and that using larger ignition chambers even with an increase of ignition energy can give some negative results for ignition that would be positive if using the standard volume of 20 litre ignition chambers for dusts ignition tests.

Similarly, I2 White Wood was tested in air with 2,500 J for two particle size distributions 0.25G and 0.5G in R-20 (Figure 6.10a and Figure 6.10b). In Figure 6.10b, I2 White Wood, when employing 5,000 J igniters, ignited at all concentrations tested (100 g/m^3-600 g/m^3 range) presenting a peak around 400 g/m^3 and a plateau in P/R values. Nevertheless, when using 2,500 J ignition behaviour was more erratic, and biomass samples did not ignite at 100 g/m^3 and 500 g/m^3 (Figure 6.10a). It is interesting to see that P/R values were generally much lower when 2,500 J igniters were used. This is strong evidence that 2,500 J ignition energy value is not adequate for igniting these biomass samples in R-20.

According to previous figures, when testing I2 White Wood 0.25G in R-30, with 5,000 J, biomass in air ignited at all concentrations (Figure 6.12) but presenting significantly lower P/R values when compared to those obtained under the same conditions in R-20 (Figure 6.10b). In Figure 6.11, employing 2,500 J igniters, I2 White Wood 0.25G, biomass ignition was more irregular, giving positive tests at 300 g/m^3, 400 g/m^3 and 600 g/m^3. In this case, P/R values were sustainably lower for 5,000 J (Figure 6.12) when compared to R-20 (Figure 6.10b), which tentatively confirms that the critical path for ignition here is mainly heat up of particles and devolatilisation that can be reduced due to inadequate ignition energy strength and the heat sink effect in larger volume chambers or different geometry from spherical idealisation.

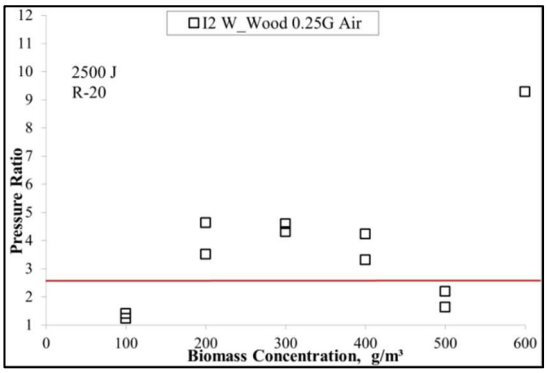

(a)

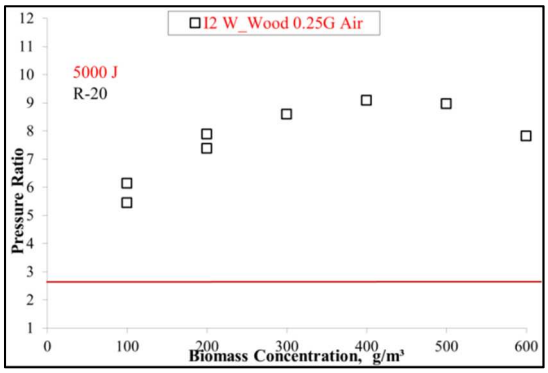

(b)

Figure 6.10. R-20 Comparison P/R vs. conc. I2 White Wood 0.25G 2,500 J (a) and 0.25G 5,000 J (b) for air combustion.

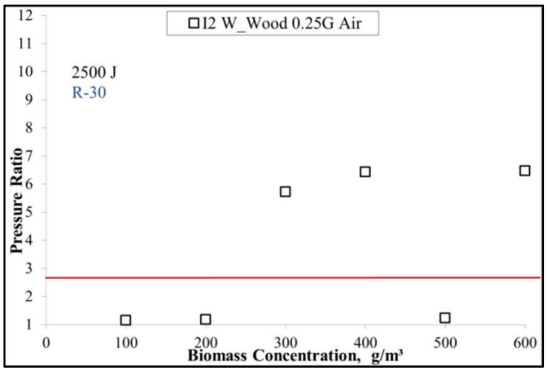

Figure 6.11. R-30 P/R vs. conc. I2 White Wood 0.25G (2,500 J) for air combustion.

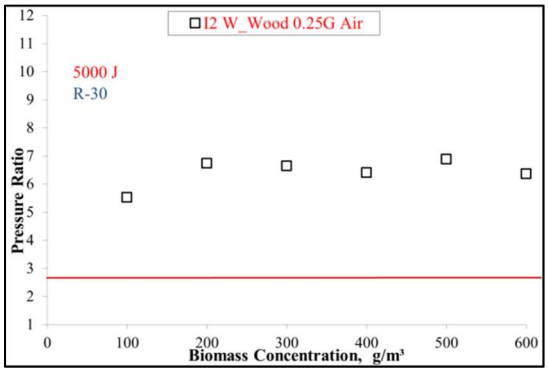

Figure 6.12. R-30 P/R vs. conc. I2 White Wood 0.25G (5,000 J) for air combustion.

In Figure 6.13, a comparison of P/R values for Miscanthus 0.25G with 2,500 J and 5,000 J igniters in R-20 is shown. Miscanthus 0.25G with 2,500 J in R-20 gave positive ignition for all concentrations tested except for 100 g/m^3 concentration (Figure 6.13a). When using 5,000 J ignition energy, Miscanthus ignited at all concentrations tested in the 100 g/m^3-600 g/m^3 range (Figure 6.13b). Both testing conditions gave peak P/R values around 300 g/m^3 but P/R values significantly decreased in the 2,500 J case, showing a lack of ignition energy for devolatilisation and homogeneous combustion of the volatiles with the same oxygen available for higher concentrations of dust.

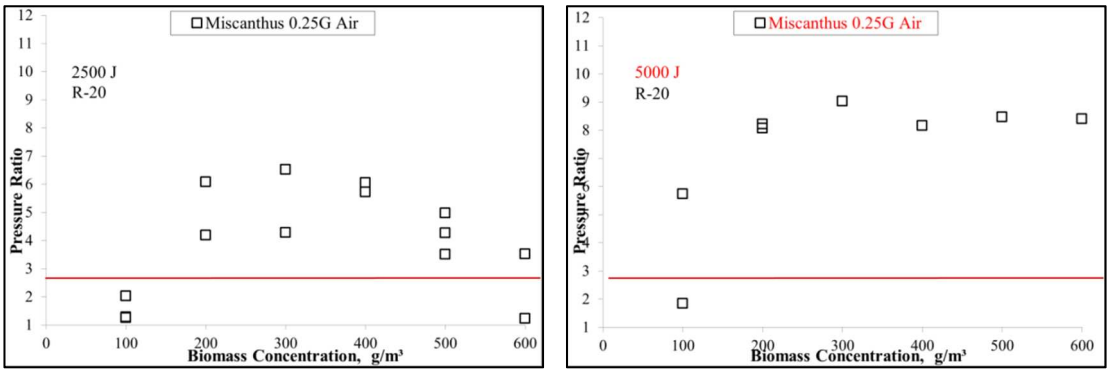

(a) **(b)**

Figure 6.13. R-20 Comparison P/R vs. conc. Miscanthus 0.25G 2,500 J (a) and 0.25G 5,000 J (b) for air combustion.

In Figure 6.14, a comparison of P/R values for Cereal Co-Product 0.25G with 2,500 J and 5,000 J igniters in R-20 is presented.

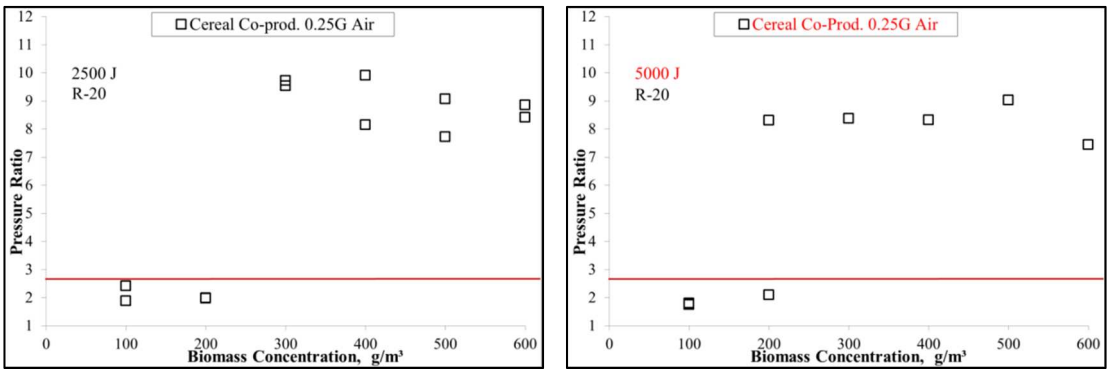

(a) **(b)**

Figure 6.14. R-20 Comparison P/R vs. conc. Cereal Co-product 0.25G 2,500 J (a) and 0.25G 5,000 J (b) for air combustion.

Cereal Co-product ground with the 0.250 mm sieve (0.25G) gave positive ignition for concentrations ≥300 g/m^3 with 2,500 J in R-20 (Figure 6.14a). When 5,000 J igniters were used, positive ignition was found for all concentrations tested except for 100 g/m^3 (Figure 6.14b). Nonetheless, it is significant that P/R values with 5,000 J igniters were slightly lower than those obtained with 2,500 J when ignition was positive. This might be a result of associated dust dispersion issues on this particular biomass. The main conclusion on identification of positive ignition is unaffected though.

6.1.4. Biomass type effect in air

The comparison of the four types of biomass tested indicates the importance of selecting the right ignition energy for devolatilisation when evaluating biomass ignitability for PF milling safety in air or oxy-fuel. When using 2,500 J ignition energy it was generally observed in this experimental programme that biomass did not ignite at 100 g/m^3 concentration for all four biomass types tested. On the other hand, it is not safe to say that biomass would not ignite in the mill because when using 5,000 J as ignition energy, P/R values for Miscanthus, I2 White Wood and Torrefied Spruce were above the 2.5 threshold for positive ignition. Thus, in air case, there is a probability that the biomass could give a "puff" or positive case of ignition that could trigger an explosion in air operation mode for PF power plants. Changing the volume and geometry of the chamber resulted in less positive ignition cases and lower P/R values. This shows that larger volume ignition chambers might be useful for K_{st} but might not be suitable to be used alone without comparison with R-20 values for PF mill safety evaluation.

6.2. Biomass dust ignition in oxy-fuel

The four biomass types have been tested in oxy-fuel conditions. Torrefied Spruce as thermally treated biomass and I2 White Wood as non-treated biomass were selected as the fuels with most experimental variation for use in oxy-fuel tests. Cereal Co-Product was also of interest as the reference biomass used by other partners for the OxyCAP UK project but it has not been that widely employed in the experimental programme due to not being that relevant for the project sponsors. A shortage of the Miscanthus sample limited the experimental variations used for this type of biomass.

6.2.1. Biomass concentration effect in oxy-fuel

The biomass concentration effects in ignition were evaluated using P/R values for a range of oxy-fuel atmospheres. K_{st} values have not been considered necessary for PF milling safety, by analogy to the air case.

Figures 6.15 and 6.16 show results for Torrefied Spruce ground with the 0.25 mm screen (0.25G) tested with 2,500 J igniters in R-20. In 21 Oxy Torrefied Spruce 0.25G clearly did not ignite at all concentrations tested in the 100 g/m^3 – 600 g/m^3 range (Figure 6.15). When under 25 Oxy, Torrefied Spruce 0.25G ignited at concentrations ≥300 g/m^3 if using 2,500 J in

R-20 ignition chamber. There was a peak for P/R values observed for 400 g/m^3 and then a plateau similarly to other fuel cases.

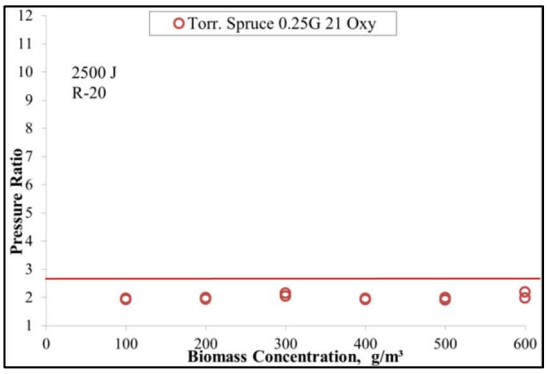

Figure 6.15. R-20 P/R vs. conc. Torrefied Spruce 0.25G (2,500 J) for 21 Oxy-combustion.

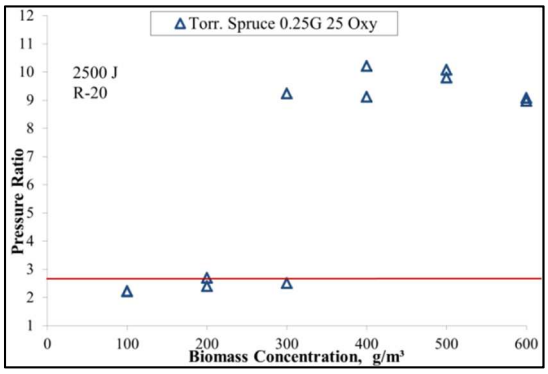

Figure 6.16. R-20 P/R vs. conc. Torrefied Spruce 0.25G (2,500 J) for 25 Oxy-combustion.

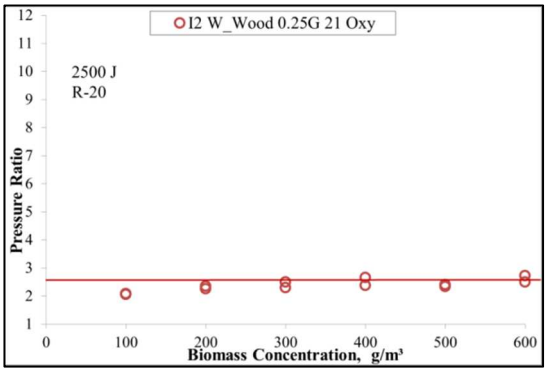

Figure 6.17. R-20 P/R vs. conc. I2 White Wood 0.25G (2,500 J) for 21 Oxy-combustion

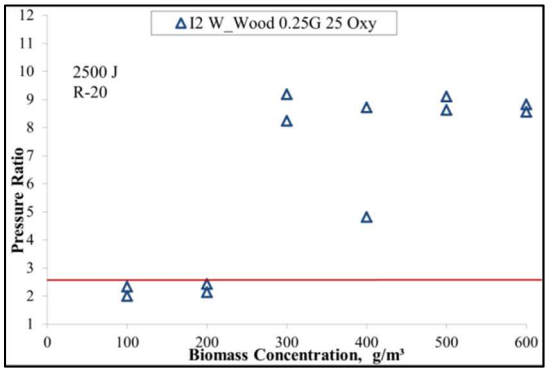

Figure 6.18. R-20 P/R vs. conc. I2 White Wood 0.25G (2,500 J) for 25 Oxy-combustion

In Figure 6.17 previously shown, I2 White wood 0.25G also gave negative ignition at all concentrations tested in the 100 g/m^3 – 600 g/m^3 range when using 2,500 J for 21 Oxy in R-20. However, when using the same ignition energy for 25 Oxy in R-20, ignition resulted positive for concentrations ≥300 g/m^3 (Figure 6.18). The P/R peak was seen on this case around 300 g/m^3 concentration.

As shown in Figure 6.19, similar results were found when Miscanthus 0.25G was tested in 21 Oxy with 2,500 J igniters in R-20. None of the concentrations tested (100 g/m^3 – 600 g/m^3 range) gave positive ignition (Figure 6.19). In contrast, when using 25 Oxy as the ignition atmosphere, then ignition was positive for concentrations ≥400 g/m^3. Dust ignition self-suppression effects were present with the characteristic plateau. Miscanthus 0.25G did not ignite at 300 g/m^3, indicating that this biomass is less reactive for the same ignition energy under 25 Oxy (Figure 6.20).

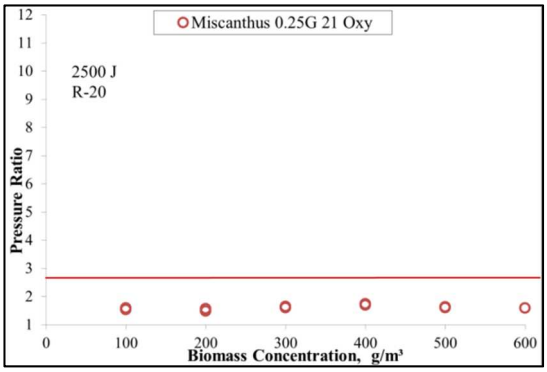

Figure 6.19. R-20 P/R vs. conc., Miscanthus 0.25G (2,500 J) for 21 Oxy-combustion.

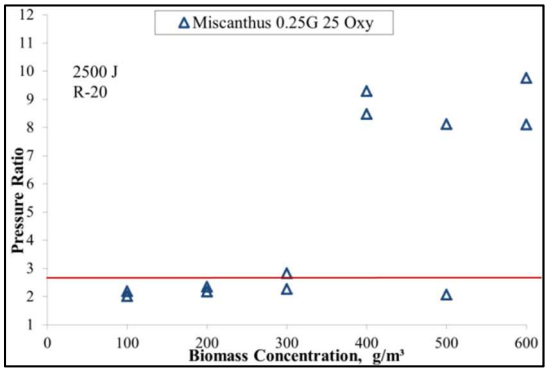

Figure 6.20. R-20 P/R vs. conc., Miscanthus 0.25G (2,500 J) for 25 Oxy-combustion.

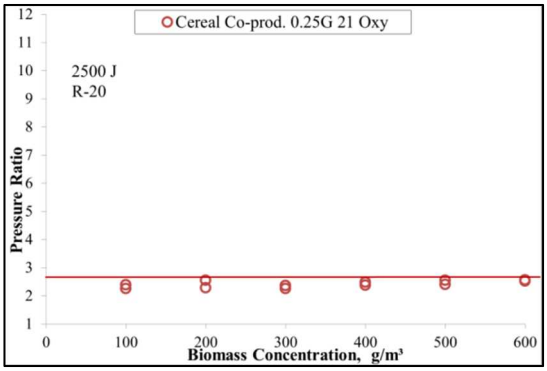

Figure 6.21. R-20 P/R vs. conc., Cereal Co-product 0.25G (2,500 J) for 21 Oxy-combustion.

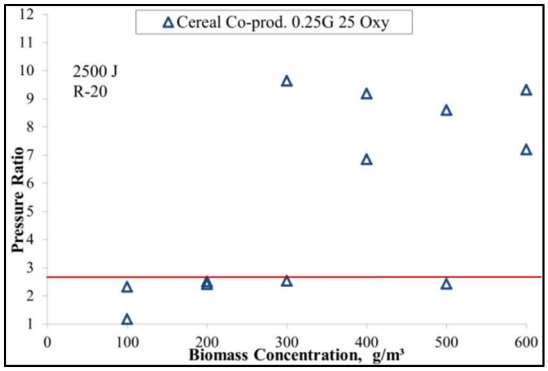

Figure 6.22. R-20 P/R vs. conc. Cereal Co-product 0.25G (2,500 J) for 25 Oxy-combustion.

In Figure 6.21, Cereal Co-product ground with the 0.25 mm screen (0.25G) did not ignite at all concentrations in the 100 g/m^3 – 600 g/m^3 range for 21 Oxy with 2,500 J in R-20. In 25 Oxy, Cereal Co-product gave P/R values above the 2.5 threshold for positive ignition for concentrations ≥300 g/m^3 when using 2,500 J in R-20 (Figure 6.22). Ignitability is similar in this case to Torrefied Spruce and I2 White Wood presented above with all showing similar plateau in P/R values for higher dust concentrations. Hence, it can be concluded that too high loading for same ignition energy-oxygen mixture tentatively can yield reduced P/R values as for coal [e.g. Cashdollar, (2000)] despite yielding positive ignition tests.

6.2.2. Biomass particle size effect in oxy-fuel

When testing biomass particle size effect under oxy-fuel conditions the approach of grinding pellets with two different aperture screens has been used, as explained in Chapter 4.

In Figure 6.23, Torrefied Spruce ground with the 0.25 mm screen (0.25G) was tested for 21-23-25-30 Oxy atmospheres with 2,500 J igniters in R-20. Torrefied Spruce 0.25G did not ignite at all in 21 Oxy. Torrefied Spruce 0.25G gave positive ignition for concentrations ≥300 g/m^3 for 23-25-30 Oxy, although in the 23 Oxy case ignition was very weak as corresponding P/R values indicate. The highest P/R values were found for the 25 Oxy series although this biomass tested positive for 200 g/m^3 in the lean loading range when in 30 Oxy case (Figure 6.23).

As shown in Figure 6.24, when evaluating the ignitability of Torrefied Spruce 0.5G, tests were negative for all concentrations in 23 Oxy with 2,500 J in R-20. These negative results for 23 Oxy led to the conclusion that 21 Oxy tests were not needed as with lower O_2 available the same dust is less likely to ignite. Torrefied Spruce 0.5G tests with 2,500 J in R-20 were also negative for all concentrations in 30 Oxy except for a sole case at 600 g/m^3 (Figure 6.24). These negatives avoid having to test 25 Oxy and would have saved the 23 Oxy experiments if they had been done before them. The only uncertainty is around 600 g/m^3 where that positive test might indicate a possible positive for 25 Oxy at the same concentration. The difference between Torrefied Spruce 0.25G mean particle size 109.6-97.38 μm and the Torrefied Spruce 0.5G mean particle size of 203.6 μm (Table 4.9) has an important effect on ignition behaviour under oxy-fuel conditions as shown in Figures 6.23 and 6.24.

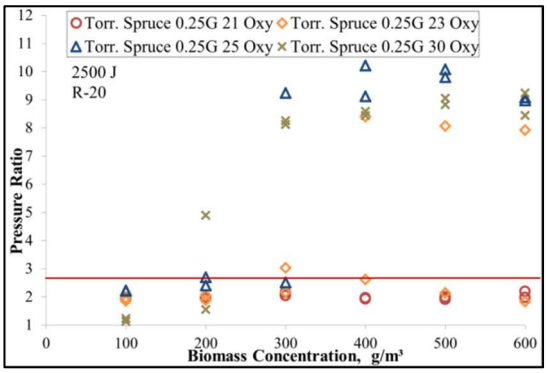

Figure 6.23. R-20 P/R vs. conc. Torrefied Spruce 0.25G (2,500 J) for 21-23-25-30 Oxy-combustion.

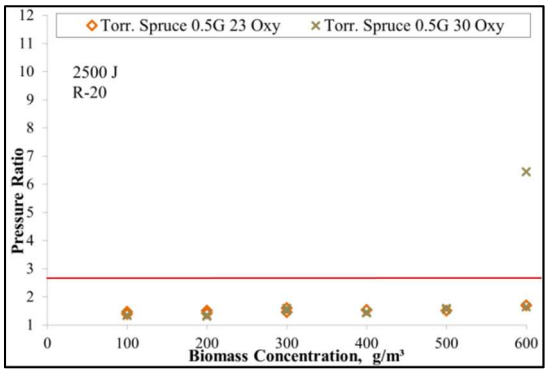

Figure 6.24. R-20 P/R vs. conc. Torrefied Spruce 0.5G (2,500 J) for 23-30 Oxy-combustion.

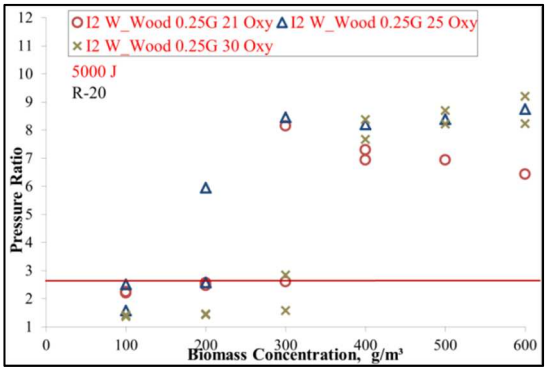

Figure 6.25. R-20 P/R vs. conc. I2 White Wood 0.25G (5,000 J) for 21-25-30 Oxy-combustion.

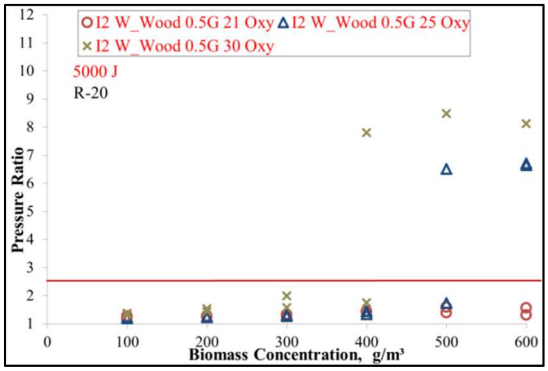

Figure 6.26. R-20 P/R vs. conc. I2 White Wood 0.5G (5,000 J) for 21-25-30 Oxy-combustion.

In Figure 6.25 shown above, I2 White Wood 0.25G was tested with 5,000 J in R-20. In 21 Oxy, ignition tests were negative for concentrations ≤300 g/m^3. When testing 25 Oxy, results were positive for concentrations ≥200 g/m^3. Surprisingly in 30 Oxy, tests were negative for 200 g/m^3 and 300 g/m^3 with positive ignition for concentrations ≥400 g/m^3 (Figure 6.25). The reason for this might be around ignition energy source effectiveness or a problem with the atmosphere inside the chamber. On this occasion, the plateau for P/R values has an ascending trend for 25 Oxy and 30 Oxy. For this study, carrying out ignition tests in 23 Oxy was not possible for these experiments but it is recommended in future work.

As Figure 6.26 shows, when larger particle size distributions were used I2 White Wood 0.5G with 5,000 J did not ignite at all concentrations for 21 Oxy. The 0.5G wood particles ignited at concentrations ≥500 g/m^3 for 25 Oxy and ≥400 g/m^3 for 30 Oxy giving more consistent results with higher O_2 availability with the same ignition energy for these set of experiments. According to Table 4.9, the difference in mean particle size, 180.7-192.9 μm for 0.25G versus 523.2 μm mean particle size for 0.5G White Wood, has a clear effect on dust ignitability (particle heat-up and devolatilisation) for the same concentration range, ignition energy (5,000 J) and ignition chamber (R-20).

Cereal Co-product, as reference biomass, was required to be tested as received (sieved through 180 μm) for the OxyCAP project. A comparison between Cereal Co-product ground pellets and sieved biomass (as received through 180 μm) is shown to evaluate the particle size effect on ignition under oxy-fuel conditions. In Figure 6.27, Cereal Co-Product ground with the 0.25 mm screen with 5,000 J igniters in R-20 gave positive ignition for concentrations ≥400 g/m^3 for 21 Oxy, ≥300 g/m^3 for 25 Oxy and 30 Oxy and even a weak positive for 100 g/m^3 in the case of 25 Oxy., When comparing with sieved Cereal Co-product particle size <180 μm, as shown in Figure 6.28, then all tests were negative for all concentrations and all atmospheres 21-25-30 Oxy with the sole exception of a test with 600 g/m^3 and 25 Oxy, which is difficult to explain (Figure 6.28). Difference in particle size distribution for 0.25G (273.6 μm mean size) versus as received (A.R.) or <180 μm (591.8 μm mean size), as shown in Table 4.9, give a clear particle size effect. The smaller the biomass particles are the easier it is to ignite them with the same ignition energy and ignition chamber volume. It is important to note here that sieving is not adequate for particle size selection in biomass due to the particle aspect ratio that allows particles that can be larger in length than diameter to pass through sieves. It is therefore acknowledged that there are limitations in the biomass particle size selection and characterisation methods used in this study.

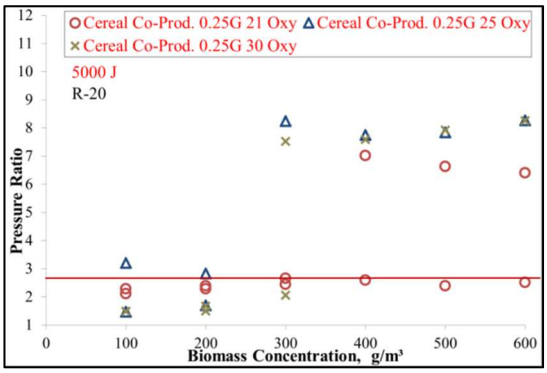

Figure 6.27. R-20 P/R vs. conc. Cereal Co-product 0.25G (5,000 J) for 21-25-30 Oxy-combustion.

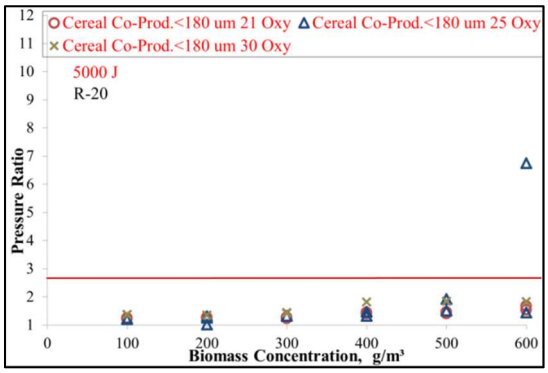

Figure 6.28. R-20 P/R vs. conc. Cereal Co-product sieved through 80 mesh (180 µm) (5,000 J) for 21-25-30 Oxy-combustion.

6.2.3. Ignition energy effect in biomass ignition in oxy-fuel

The ignition energy effect has been tested in biomass with 2,500 J and 5,000 J igniters in R-20 and in some specific cases with 10,000 J igniters in R-30 and results are reported in this section. For the same particle size, 0.25G, Torrefied Spruce was tested with 2,500 J and 5,000 J igniters in R-20. With 2,500 J, ignition was found negative for all concentrations tested in 21 Oxy (Figure 6.29) while if using 5,000 J, Torrefied Spruce 0.25G gave positive ignition P/R values for concentrations ≥400 g/m^3 (Figure 6.30). With 2,500 J, positive ignition was found for concentrations ≥300 g/m^3 in 25 Oxy while the LFL went down to 200 g/m^3 if using 5,000 J in 25 Oxy (Figure 6.30). In the 30 Oxy case, positive ignition was observed at concentrations ≥200 g/m^3 for both 2,500 J and 5,000 J igniters, although P/R values were significantly different.

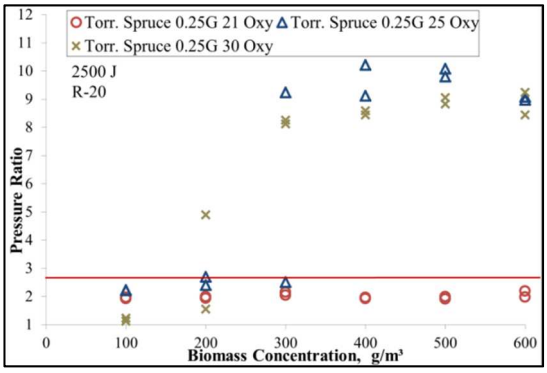

Figure 6.29. R-20 P/R vs. conc. Torrefied Spruce 0.25G (2,500 J) for 21-25-30 Oxy-combustion.

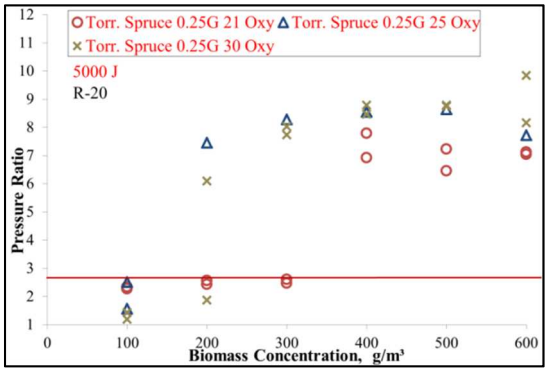

Figure 6.30. R-20 P/R vs. conc. Torrefied Spruce 0.25G (5,000 J) for 21-25-30 Oxy-combustion.

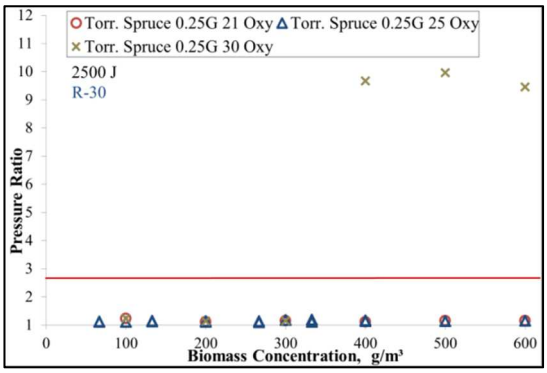

Figure 6.31. R-30 P/R vs. conc. Torrefied Spruce 0.25G (2,500 J) for 21-25-30 Oxy-combustion.

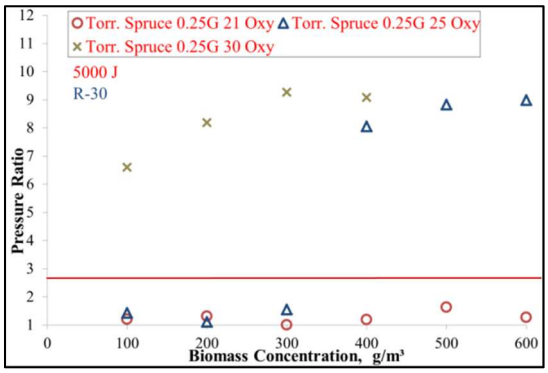

Figure 6.32. R-30 P/R vs. conc. Torrefied Spruce 0.25G (5,000 J) for 21-25-30 Oxy-combustion.

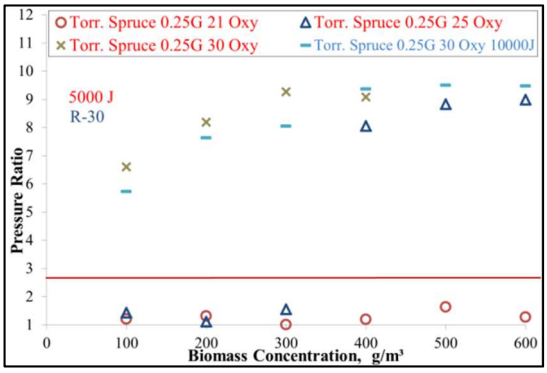

Figure 6.33. R-30 P/R vs. conc. Torrefied Spruce 0.25G (5,000 J) for 21-25-30 Oxy-combustion and (10,000 J) for 30 Oxy-combustion.

When testing Torrefied Spruce 0.25G in R-30 (Figures 6.31, 6.32 and 6.33 previously shown) there was also a significant difference in results depending on the ignition energy used. Torrefied Spruce 0.25G in R-30 with 2,500 J gave negative ignition tests at all concentrations for 21 Oxy and 25 Oxy (Figure 6.31). However, if using 5,000 J, ignition was positive for concentrations ≥400 g/m^3 in 25 Oxy (Figure 6.32). For the 30 Oxy case, with 2,500 J ignition was positive for concentrations ≥400 g/m^3 while using 5,000 J igniters gave positive ignition for all concentrations tested. It is important to note that 500 g/m^3 and 600 g/m^3 test were not undertaken intentionally due to limited biomass availability (Figure 6.32). However, despite not having experimental data it is expected that positive ignition would have been obtained for these concentrations with 5,000 J in R-30.

In addition, 10,000 J igniters were only tested for 30 Oxy in R-30 with Torrefied Spruce 0.25G (Figure 6.33) and all tests were positive for all the concentration range (100 g/m^3-600 g/m^3) showing a clear ascending trend with a final plateau in P/R values. Having tested 10,000 J for 30 Oxy and getting positive ignition shows there is interest in carrying out tests for other loadings, but the lack of time and biomass samples availability prevented this work in the present study. In any case, it is clear from the results shown than the higher the ignition energy used the more likely are positive ignition P/R values for the same fuel concentration and ignition chamber geometry and volume. However, P/R values will be higher or lower depending on ignition energy or the volume/geometry of the chamber, with R-20 tentatively selected as the benchmark chamber for the PF milling safety case.

The same experimental plan has been carried out for I2 White Wood 0.25G. As shown in Figure 6.34, I2 White Wood 0.25G with 2,500 J in R-20 gave negative ignition for 21 Oxy at all concentrations and ignited at ≥300 g/m^3 concentrations for 25 Oxy and ≥400 g/m^3 for 30 Oxy (Figure 6.34a). When using 5,000 J igniters, the MEC from tests stayed the same for 30 Oxy while for 25 Oxy ignition was positive for concentrations ≥200 g/m^3. 21 Oxy gave positive ignition with 5,000 J in R-20 for concentrations ≥400 g/m^3 (Figure 6.34b). I2 White Wood ignition tests were also carried out in R-30; with 2,500 J ignition was negative for all concentrations in the 100 g/m^3-600 g/m^3 range in 21 and 30 Oxy except for 500 g/m^3 that coincidentally gave positive ignition for 21 Oxy and 30 Oxy (Figure 6.35). If 25 Oxy tests with 2500 J in R-30 had been carried out, it is tentatively suggested that the only case within the concentrations range likely to result in a positive test would have been 500 g/m^3 in 25 Oxy, according to results displayed in Figure 6.35. When using 5,000 J, ignition was positive for I2 White Wood 0.25G for all concentrations with 21 Oxy and 30 Oxy except for 100 g/m^3 in 21 Oxy (Figure 6.36). An atmosphere of 25 Oxy is expected to give positive ignition under the same conditions with the only uncertainty being for the 100 g/m^3 value.

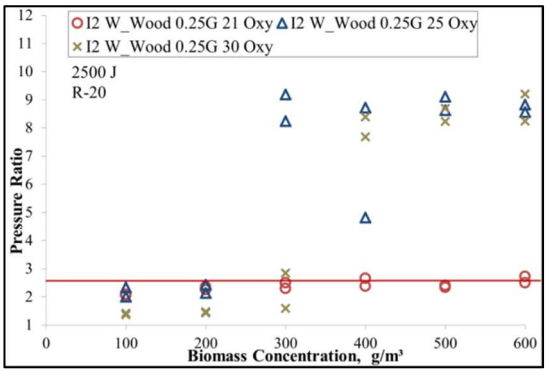

(a)

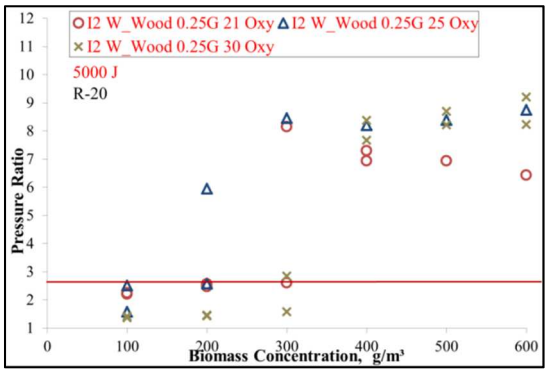

(b)

Figure 6.34. R-20 Comparison P/R vs. conc. I2 White Wood 0.25G 2,500 J (a) and 0.25G 5,000 J (b) for 21-25-30 Oxy-combustion.

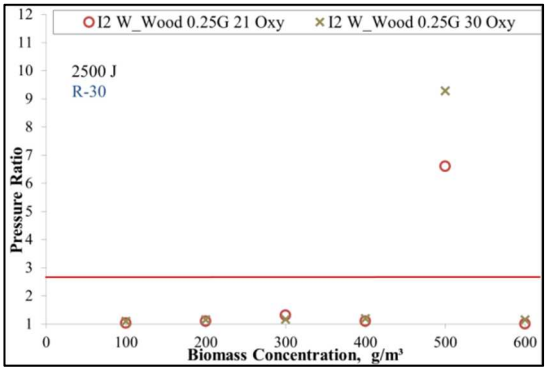

Figure 6.35. R-30 P/R vs. conc. I2 White Wood 0.25G (2,500 J) for 21-30 Oxy-combustion.

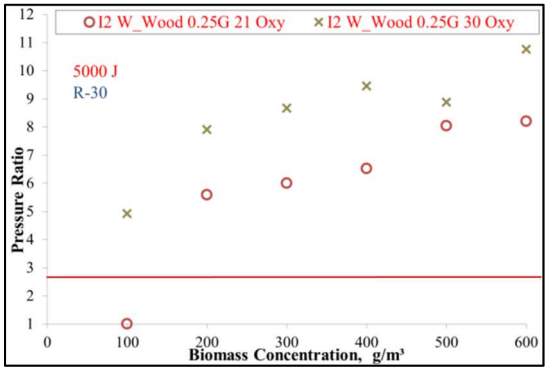

Figure 6.36. R-30 P/R vs. conc. I2 White Wood 0.25G (5,000 J) for 21-30 Oxy-combustion.

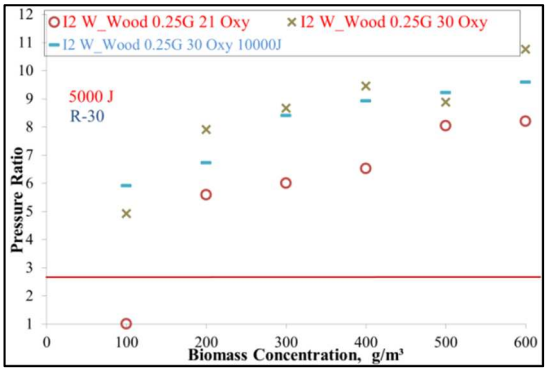

Figure 6.37. R-30 P/R vs. conc. I2 White Wood 0.25G (5,000 J) for 21-30 Oxy-combustion and (10,000 J) for 30 Oxy-combustion.

As shown previously in Figure 6.37, the use of 10,000 J igniters for 30 Oxy resulted in positive ignition of I2 White Wood 0.25G in R-30 for the entire range of concentrations tested (Figure 6.37) but with a more pronounced plateau when compared to the 5,000 J case and 30 Oxy. Tentatively, there is a volume/geometry effect in P/R values from ignition experiments depending on the ignition chamber used.

Miscanthus ground with the 0.25 mm sieve (0.25G) and tested with 2,500 J igniters in R-20 gave negative ignition for all concentrations in 21 Oxy (Figure 6.38). For the same biomass, if using 5,000 J igniters in R-20 then ignition was positive for concentrations ≥ 300 g/m^3 in 21 Oxy (Figure 6.39). In 25 Oxy, ignition was positive for all concentrations except for 100 g/m^3 with 5,000 J igniters while the MEC went up to approximately 400 g/m^3 when using 2,500 J igniters in R-20. Hence, there is a strong dependency on ignition energy strength for biomass tests and a need of overdriving using 5,000 J igniters in R-20 for PF milling safety assessments in oxy-fuel.

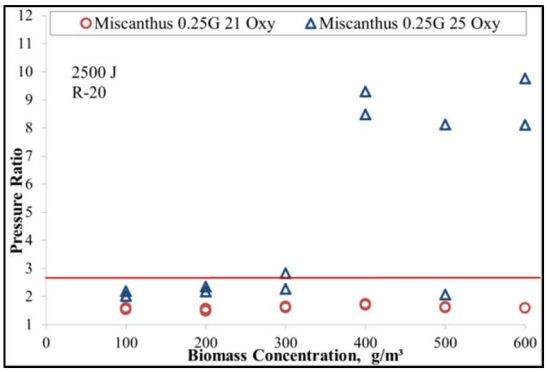

Figure 6.38. R-20 P/R vs. conc. Miscanthus 0.25G (2,500 J) for 21-25 Oxy-combustion.

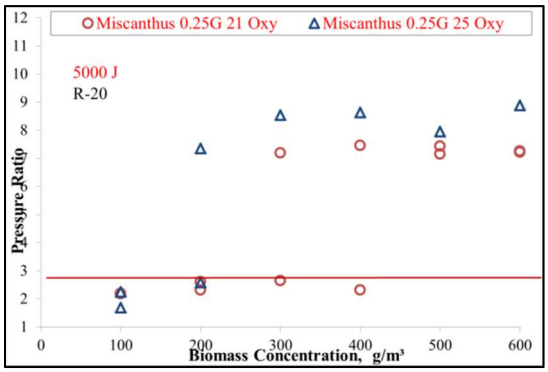

Figure 6.39. R-20 P/R vs. conc. Miscanthus 0.25G (5,000 J) for 21-25 Oxy-combustion.

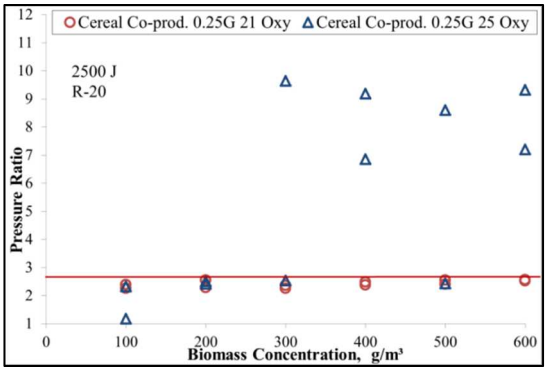

Figure 6.40. R-20 P/R vs. conc. Cereal Co-product 0.25G (2,500 J) for 21-25 Oxy-combustion.

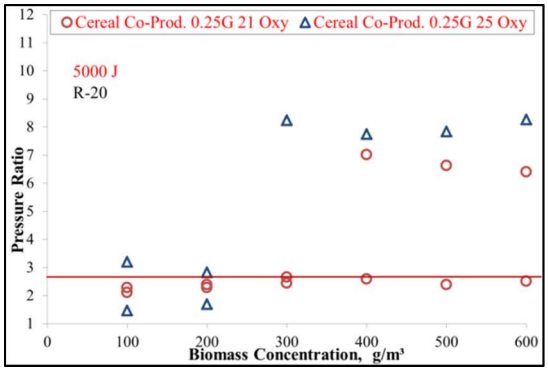

Figure 6.41. R-20 P/R vs. conc. Cereal Co-product 0.25G (5,000 J) for 21-25 Oxy-combustion.

As shown in previous Figure 6.40, Cereal Co-product 0.25G with 2,500 J in R-20 also gave negative ignition for all concentrations in 21 Oxy. However, ignition was positive for concentrations ≥300 g/m^3 in 25 Oxy (Figure 6.40). When 5,000 J igniters were used in R-20 then ignition was positive for concentrations ≥400 g/m^3 in 21 Oxy (Figure 6.41). In the same figure, for 25 Oxy, it can be seen that ignition was positive for all concentrations except for 200 g/m^3, with 5,000 J igniters giving a weak positive in 100 g/m^3 (probably scatter).

6.2.4. Atmosphere effect (O_2/CO_2 v/v %) in biomass ignition in air and oxy-fuel

The atmosphere in which the biomass dust sample is ignited has an important effect on ignition propagation. In the next series of figures, a comparison is made with air as a benchmark when looking at ignition behaviour in oxy-fuel atmospheres. It is clear that the presence of higher levels of O_2 will enhance ignition. However, it is also the presence of CO_2 that suppresses ignition when compared to inert N_2 in air added to the other effects such as particle size and ignition energy that together will determine the level of ignition propagation into a more sustained combustion process.

Torrefied Spruce as 0.25G was ignited with 2,500 J and 5,000 J in air-21-25-30 Oxy atmospheres in R-20 and results compared. In Figure 6.42, for 0.25G it seems that the highest P/R levels are reached with 25 Oxy despite the MEC as tested being 200 g/m^3 for 30 Oxy, a step lower than the 300 g/m^3 value for 25 Oxy. It is therefore not entirely clear which oxy-fuel atmosphere gives the closer pattern to air ignition case despite 30 Oxy igniting at 200 g/m^3 as in the air case. When looking at Figure 6.43, showing data for 0.25G with 5,000 J igniters in R-20, 25 Oxy and 30 Oxy test ignited at all concentrations except 100 g/m^3 while in air, Torrefied Spruce ignited at all concentrations. Regarding P/R values, in most cases 25 Oxy is closer to air behaviour.

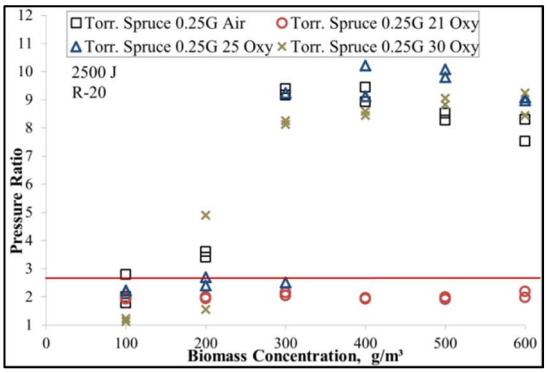

Figure 6.42. R-20 P/R vs. conc. Torrefied Spruce 0.25G (2,500 J) for air and 21-25-30 Oxy-combustion.

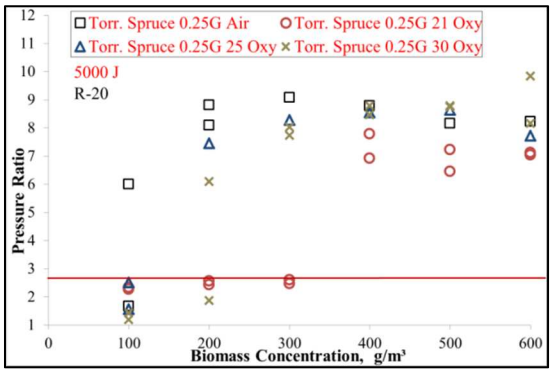

Figure 6.43. R-20 P/R vs. conc. Torrefied Spruce 0.25G (5,000 J) for air and 21-25-30 Oxy-combustion.

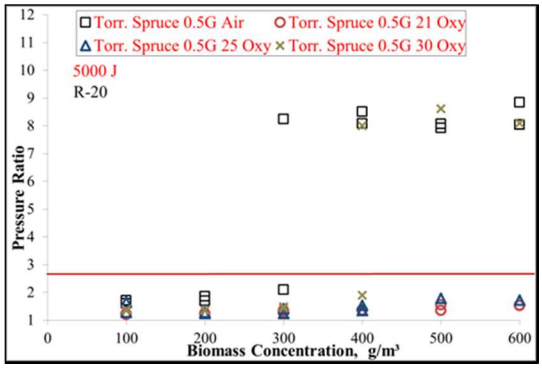

Figure 6.44. R-20 P/R vs. conc. Torrefied Spruce 0.5G (5,000 J) for air and 21-25-30 Oxy-combustion.

In Figure 6.44 shown above, with a larger biomass particle size distribution for the 0.5G sample, it now seems that air and 30 Oxy get closer in their ignition patterns but not exactly so with 30 Oxy giving negative ignition for 300 g/m^3 while the corresponding test is positive in the air case.

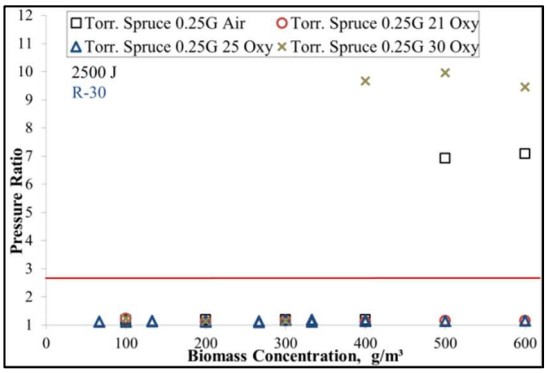

Figure 6.45. R-30 P/R vs. conc. Torrefied Spruce 0.25G (2,500 J) for air and 21-25-30 Oxy-combustion.

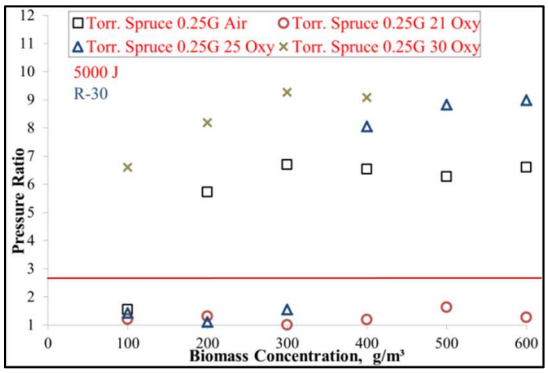

Figure 6.46. R-30 P/R vs. conc. Torrefied Spruce 0.25G (5,000 J) for air and 21-25-30 Oxy-combustion.

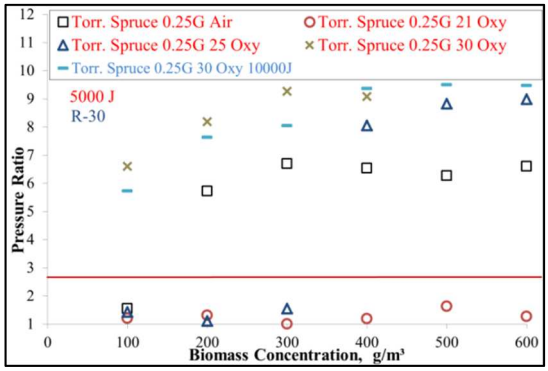

Figure 6.47. R-30 P/R vs. conc. Torrefied Spruce 0.25G (5,000 J) for air-21-25-30 Oxy-combustion and (10,000 J) for 30 Oxy-combustion.

In Figures 6.45, 6.46 and 6.47 previously shown, Torrefied Spruce 0.25G was also tested with different ignition energies in air-21-25-30 Oxy in R-30. When using 2,500 J igniters, ignition was only positive for 500 g/m^3 and 600 g/m^3 in air while in 30 Oxy tests gave positive ignition P/R values for concentrations ≥400 g/m^3. All the other test conditions with 2,500 J in R-30 gave very clear negative ignition tests (Figure 6.45). In Figure 6.46, despite not carrying out the higher concentration tests for 30 Oxy, in order to show trends it can be said that with 5,000 J in R-30, it is expected that Torrefied Spruce would ignite at all concentrations in the range in 30 Oxy, while in air it would ignite at all concentrations except for 100 g/m^3 and for 25 Oxy it would ignite only at concentrations ≥400 g/m^3. Here the divergence between air and 25 Oxy is much greater, but it is also different to the 30 Oxy case (Figure 6.46). Results in Figure 6.47 show that, if using 10,000 J igniters for the same dust in R-30, positive ignition can be confirmed for all concentrations tested (100 g/m^3-600 g/m^3).

A conclusion from this series of experiments is that it is clear that if tests are not overdriving the ignition chamber then many potential positive tests for the safety case would give negative results. When overdriving, R-20 with 5,000 J igniters (e.g. Figure 6.43) then employing 30 Oxy instead of 25 Oxy does not have major impact in determining positive ignition when compared with air. Consequently, it can be said that the finer are Torrefied Spruce particles in ignition chamber, with the presence of an adequate ignition energy strength, the lower will be the O_2 requirements in Oxy atmosphere for positive ignition. Biomass ignitability increases monotonically with an increase in O_2 in CO_2 atmospheres. Tentatively, for biomass samples 25 Oxy would give similar results to the air ignition case without having to increase O_2 to 30 % v/v in CO_2 as in coal case [Chapter 5;

Man and Gibbins, (2011)]. As biomass particle size increases, 30 Oxy would be closer to air ignition pattern due to the greater amount of O_2 available but this would not be enough to compensate for the larger particle size effect and consequent lower volatiles release from fuel. If using larger volume ignition chambers and not overdriving (i.e. 2,500 J in R-30), then MEC is expected to increase for all atmospheres. Hence, if there is a fuel that is difficult to ignite, it is safer to operate in 21 Oxy than in air for PF milling safety. When the fuel does ignite more readily the behaviour is much more erratic than in the air case with 25 Oxy and 30 Oxy giving similar patterns in the overdriven standard volume ignition chamber (R-20). Furthermore, the results arising from this experimental programme tentatively show a problem with the geometry of larger ignition chambers if not spherical. As shown in Figures 6.48 and 6.49, I2 White Wood 0.25G ignitability was evaluated with 2,500 J and 5,000 J in R-20. With 2,500 J the air ignition pattern was erratic with low P/R values although positive ignition was observed for all dust concentrations ≥200 g/m^3 except for 500 g/m^3. In 25 Oxy, White Wood 0.25G gave positive ignition ≥300 g/m^3 and 30 Oxy positive ignition ≥400 g/m^3 (Figure 6.48). Hence, there is no similarity in ignition pattern between air and Oxy if R-20 is not overdriven. In Figure 6.49, when employing 5,000 J igniters in R-20 for I2 White Wood 0.25G ignition, air gave positive ignition for all concentrations, 25 Oxy for concentrations ≥200 g/m^3 and 30 Oxy positive for concentrations ≥400 g/m^3 (Figure 6.49). When ignition was positive, the 5 % v/v O_2 increase in oxygen from 25 Oxy to 30 Oxy did not have a major impact on P/R values.

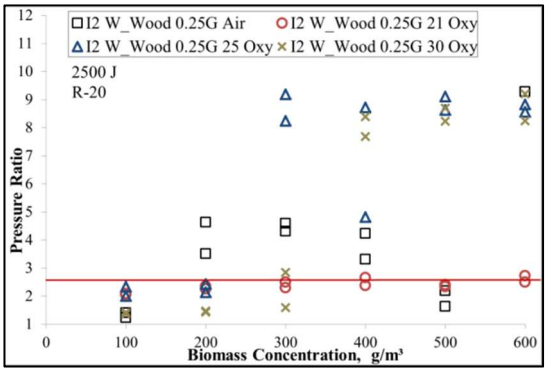

Figure 6.48. R-20 P/R vs. conc. I2 White Wood 0.25G (2,500 J) for air and 21-25-30 Oxy-combustion.

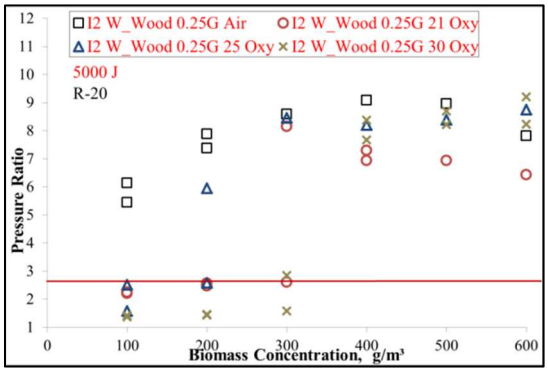

Figure 6.49. R-20 P/R vs. conc. I2 White Wood 0.25G (5,000 J) for air and 21-25-30 Oxy-combustion.

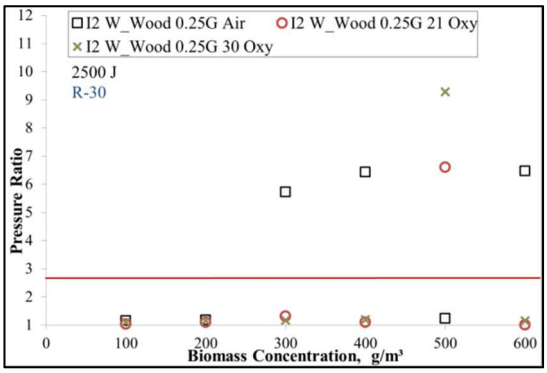

Figure 6.50. R-30 P/R vs. conc. I2 White Wood 0.25G (2,500 J) for air and 21-30 Oxy-combustion.

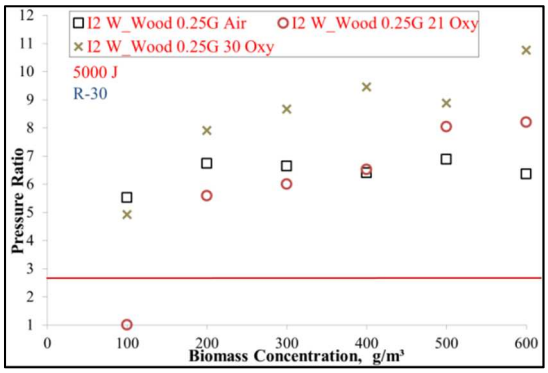

Figure 6.51. R-30 P/R vs. conc. I2 White Wood 0.25G (5,000 J) for air and 21-30 Oxy-combustion.

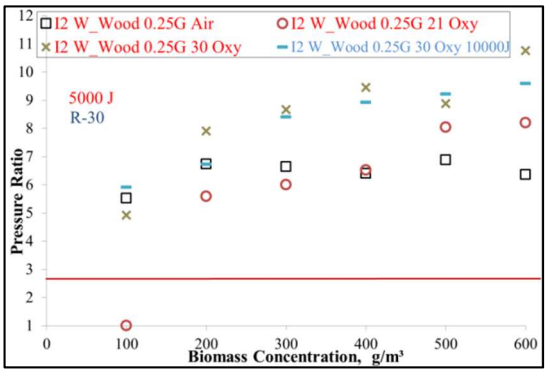

Figure 6.52. R-30 P/R vs. conc. I2 White Wood 0.25G (5,000 J) for air and 21-30 Oxy-combustion.

In Figure 6.50, when testing I2 White Wood 0.25G with 2,500 J in R-30, ignition was only positive for 500 g/m^3 in 21 Oxy and 30 Oxy, leaving that concentration as a possible test point for 25 Oxy since the others are not needed due to negative results with 30 Oxy. Air ignition gave positive ignition for 300 g/m^3, 400 g/m^3 and 600 g/m^3 but yielded a negative for 500 g/m^3 concentration (Figure 6.50). In any case, there was not similar ignition patterns for air and any of the Oxy atmospheres tested. As shown in Figure 6.51, for the same fuel dust with 5,000 J in R-30 ignition was now positive for all concentrations tested (100 g/m^3-600 g/m^3 range) for air, 21 Oxy and 30 Oxy except for 100 g/m^3 in the 21 Oxy atmosphere. There is a discrepancy for positive ignition in 21 Oxy at 200 g/m^3 in R-30 while negative in R-20 for same ignition energy and atmosphere. Also, there are positive values for 30 Oxy in 100 g/m^3-300 g/m^3 concentrations when in R-30 and negative in R-20.Looking at air ignition P/R values (Figures 6.49 and 6.51) in R-30, they were different to values in R-20 for the

same fuel dust (I2 White Wood 0.25G) and ignition energy (5,000 J) (Figure 6.49). Thus, there is not just geometry effect but igniter location, dust dispersion effectiveness and Oxy mixture distribution variations inside the larger chamber that tentatively have an influence in heat and O_2 availability plus CO_2 suppression of ignition propagation. Regarding the fuel, there will clearly be an effect of torrefaction [Chapter 2], changing fuel particles properties and eliminating moisture content of the biomass when comparing to results from standard white wood. Also grinding torrefied pellets with the same sieve size seems to yield finer particles when compared to I2 White Wood according to Table 4.9. For this biomass type it is recommended for safety cases to use R-20 and 5,000 J in the dust ignition experiments. It would be interesting to see in future work if placing the igniter exactly at the centre of R-30 would result in a different ignition pattern. In Figure 6.52 shown previously, when testing 10,000 J igniters in R-30 for I2 White Wood 0.25G, positive ignition for all concentrations tested (100 g/m^3 -600 g/m^3) in 30 Oxy is confirmed.

As shown in Figure 6.53, Miscanthus 0.25G when tested with 2,500 J igniters in R-20 gave negative ignition in 21 Oxy atmospheres at all concentrations tested and positive ignition for concentrations ≥400 g/m^3 in air dust samples ignited at all concentrations except for 100 g/m^3. P/R values for positive ignition cases in air are much lower than when using 25 Oxy where tests exhibited positive ignition (Figure 6.53). In Figure 6.54, when testing the same dust in R-20 with 5,000 J igniters, then the 25 Oxy ignition pattern was closer to the air case. Adding 5 % v/v O_2 when testing 30 Oxy did not give a similar ignition pattern to the air case and in fact some of the positives for 25 Oxy were negative in 30 Oxy (Figure 6.54). This was probably related to dust particles distribution inside R-20 but further exploration is required in future work.

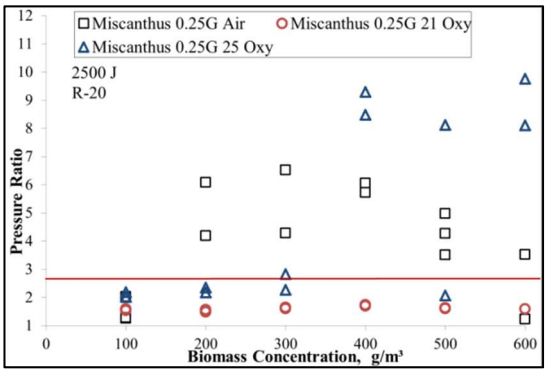

Figure 6.53. R-20 P/R vs. conc. Miscanthus 0.25G (2,500 J) for air and 21-25 Oxy-combustion.

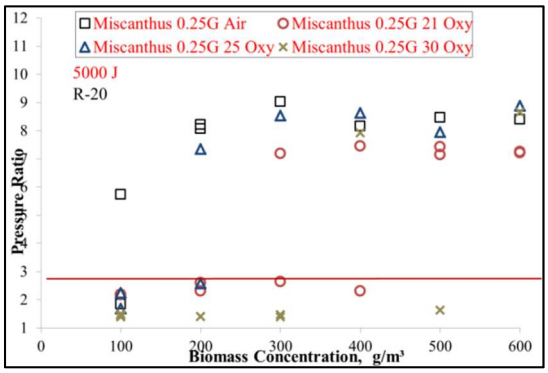

Figure 6.54. R-20 P/R vs. conc. Miscanthus 0.25G (5,000 J) for air and 21-25-30 Oxy-combustion.

Figure 6.55 shows how Cereal Co-product 0.25G tested with 2,500 J in R-20 gave positive ignition for the air case and also in 25 Oxy for dust concentrations ≥300 g/m^3. Ignition was negative for all concentrations in 21 Oxy (Figure 6.55) but when the ignition energy was increased to 5,000 J then concentrations ≥400 g/m^3 yielded positive ignition values for 21 Oxy (Figure 6.56). Adding O_2 to Oxy mixture from 25 Oxy to 30 Oxy did not have a major impact on the number of positive P/R values for 5,000 J in R-20. The weak positive ignition found for 25 Oxy in 100 g/m^3 was surprising, probably scatter due to an experimental issue in that particular ignition test. Additional work with this dust is recommended before reaching further conclusions.

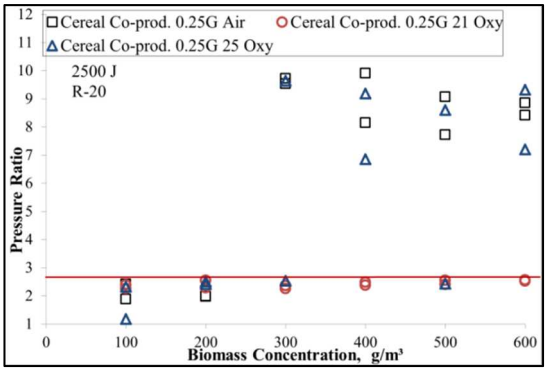

Figure 6.55. R-20 P/R vs. conc. Cereal Co-product 0.25G (2,500 J) for air and 21-25 Oxy-combustion.

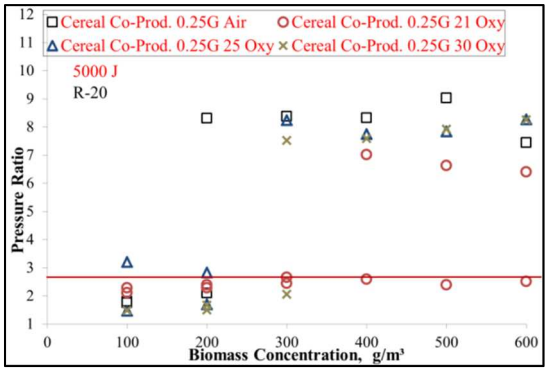

Figure 6.56. R-20 P/R vs. conc. Cereal Co-product 0.25G (5,000 J) for air and 21-25-30 Oxy-combustion.

6.2.5. Biomass type effect in oxy-fuel

The impact of biomass volatiles content has on ignition has been shown in results included in previous sections. Testing in R-20 with 2,500 J igniters all four biomasses samples in the 0.25G size range behaved similarly in 21 Oxy, giving negative ignition for all concentrations tested versus positive ignition for air case. From this work it might be concluded that 2,500 Joules ignition energy strength might not be adequate to overdrive R-20 chamber. For the same moderate ignition energy (2,500 J), then the four biomasses tested did not ignite in 21 Oxy but in air. However, when overdriving in R-20 with 5,000 J, for the higher requirements on safety, then the behaviour is substantially different and the safety case requires a more particular to fuel approach.

All four biomass types at 0.25G size with 2,500 J igniters yielded negative ignition for all concentrations when in 21 Oxy (Table 6.1). This is tentatively taken as an indication that operating mills with biomass in 21 Oxy would be safer than in air where ignition is positive for many cases. However, it is important to realise that overdriving of R-20 is not achieved by using 2,500 J. For the PF mill safety case, it is recommended to overdrive R-20 with 5,000 Joules (Table 6.2). When using 5,000 J as ignition energy, all four biomasses gave negative ignition at concentrations ≤200 g/m^3 in 21 Oxy while in air at the same concentration the four did ignite. The presence of CO_2 in the balance has a clear impact in preventing ignition propagation from fires in the mill island. Particle size seems to have a relevant impact on ignition according to previous results but further investigation is required. Implications arising from this work are discussed in Chapter 7.

Key results from this experimental campaign are summarised in Tables 6.1 and 6.2.

Table 6.1. Summary of results for biomass ignition tests in R-20 with 2,500 J

Fuel/Conc.	100 g/m^3	200 g/m^3	300 g/m^3	400 g/m^3	500 g/m^3	600 g/m^3
Torrefied Spruce 0.25G	− ⊖ △ ✕	+ ⊖ △ ✕	+ ⊖ + +	+ ⊖ + +	+ ⊖ + +	+ ⊖ + +
I2 White Wood 0.25G	− ⊖ △ ✕	+ ⊖ △ ✕	+ ⊖ + +	+ ⊖ + +	− ⊖ + +	+ ⊖ + +
Miscanthus 0.25G	− ⊖ −	+ ⊖ −	+ ⊖ −	+ ⊖ +	+ ⊖ +	+ ⊖ +
Cereal Co-Product 0.25G	− ⊖ −	− ⊖ −	+ ⊖ +	+ ⊖ +	+ ⊖ +	+ ⊖ +

Air ○ 21 Oxy △ 25 Oxy ✕ 30 Oxy + Positive − Negative

Table 6.2. Summary of results for biomass ignition tests in R-20 with 5,000 J						
Fuel/Conc.	**100 g/m^3**	**200 g/m^3**	**300 g/m^3**	**400 g/m^3**	**500 g/m^3**	**600 g/m^3**
Torrefied Spruce 0.25G						
I2 White Wood 0.25G						
Miscanthus 0.25G						
Cereal Co-Product 0.25G						
						

7. Implications arising from this thesis and recommendations for future work

7.1. Implications

Experimental work in R-20 and R-30 has shown that P/R values are sufficient to determine positive or negative ignition of coal and biomass. Practical determination of ignitability for PF mill safety is an important factor in the development of PF combustion under oxy-fuel conditions. Major implications arising from this thesis are:

1) Combustion atmosphere (O_2 content). Increasing the O_2 content up to 21 % v/v O_2 balance CO_2 in the PR for coals and biomass tested has been shown experimentally to generally be safer than operating in air combustion mode. This is an improvement of the inherent safety of the PF combustion process and a potential advantage for oxy-fuel. In the White Rose project, Alstom is designing the process with specific features, including O_2 injection from the ASU into the PR as shown in Figure 7.1

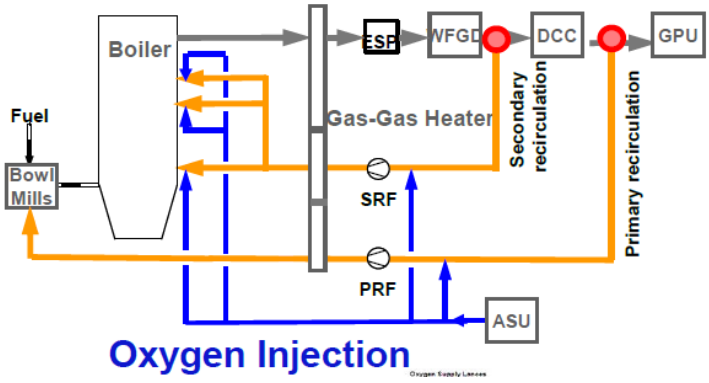

Figure 7.1. Alstom Oxy-boiler design with O_2 injection options, including O_2 injection in the PR [Levasseur et al., (2014)]

The difference in O_2 content from exhaust recirculated flue gas composition recycled up to the value of 21 % v/v O_2 provides additional flexibility for O_2 injection strategies and PF milling management to improve PF combustion in oxy-fuel, that can be particularly relevant when changing loading in the plant or using O_2 as a form of energy storage to maximise efficient ASU operation and overall plant efficiency as well as operating margins when selling electricity in the market.

When attempting to match oxy-fuel ignition behaviour to air case, for coal, this work has confirmed the conclusion of employing 30 % v/v O_2 in CO_2 to yield similar ignition pattern to the air case as reflected in the relevant literature [e.g. Man and Gibbins, (2011)]. This work as a continuation of the publication mentioned, has found and that for the four biomass types tested, 25 % v/v O_2 in CO_2 balance generally matches air ignition patterns.

2) Fuel type (volatile content). At the right ignition energy strength, volatile matter content of the fuel is the key parameter affecting ignition propagation, since devolatilisation and homogenous combustion of volatiles released is the critical path for ignition propagation. Fuels with greater volatile matter content, i.e. the four biomasses tested, have shown final pressures after constant volume combustion (P/R values) when compared to the four coals.

3) Ignition energy strength. It can be difficult to justify whether 2,500 J or 5,000 J igniters give adequate ignition energies in R-20 and R-30 for milling safety tests without the opportunity of contrasting the experimental data with results from larger ignition chambers or large scale ignitability tests in mills. However, it is clear that more ignition energy is required for the worst case scenario in PF milling safety evaluation. In R-20, 2,500 J igniters have been inadequate for testing ignition of biomasses dusts. At the same ignition energy, biomass, due to its higher volatile content shows an ease ignitability trend than for coals tested. Most importantly, in the presence of moderate ignition energy (2,500 J) these biomasses tested did not ignite in 21 Oxy and for some low loadings in 25 Oxy while did ignite for most of air ignition cases in R-20. Hence, for PF milling, it is tentatively safer to operate oxy-biomass PR in 21 Oxy than biomass in air. Further work is required to determine the right ignition energy for PF milling safety case as a fire in the mill can supply significantly high energy as potential ignition source.

4) Particle size. Coal experiments have shown that finer particle size of the fuel enhances ignitability. From experimental results for the El Cerrejon G145 particles size distributions prepared, it can be concluded that not just the ultrafine (<53 µm) but the intermediate fines (75 µm - 53 µm) play a decisive role in the ignition process, since the amount of volatiles that can be released from the ultrafine particles is limited. A certain combination of ultrafine and intermediate fines would be expected to yield higher P/R values than the fines or the entire coal sample alone despite the MEC being defined by the ultrafine content. In biomass, lessons from particle size studies are limited but it can certainly be said that the finer biomass particles enhanced ignitability. Improved dust dispersion of finer

biomass (particularly thermally treated biomass) and composition of the volatiles released played in favour of the combustion process for biomasses than in many coal tests. The lesson implied here is that biomasses tested are more difficult to light but yield higher P/R values than the coals evaluated.

5) Fuel (dust) concentration. Fuel concentration is a second order parameter as a broader range of concentrations than reported in this thesis will be found during the PF mill operation. Concentrations >200 g/m^3 are considered the worst case scenario for developing positive ignition for most fuels tested. At higher fuel loadings, i.e. in the plateau, P/R values will level off for the same O_2/ignition energy mixture available. Further work at lean loadings for accurate determination of MEC for each fuel is required. In Figure 7.2, major factors affecting ignition are summarised:

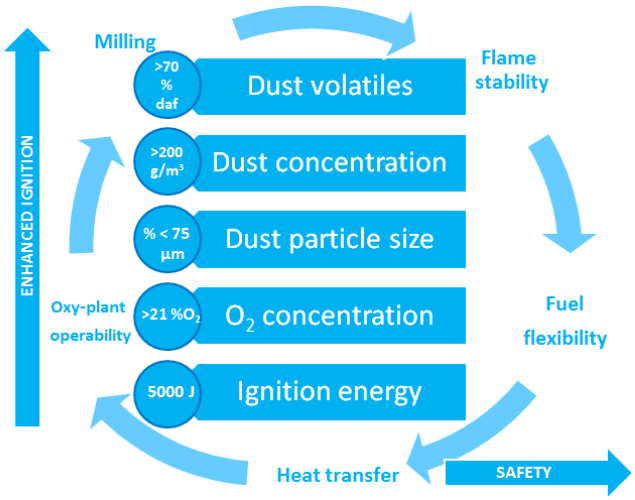

Figure 7.2. Summary of implications from PF ignition experimental programme

7.2. Recommendations for future work

The limited time available during this Ph. D. thesis after successful R-20 and R-30 design, construction and commissioning meant that not all the potential experimental work has been undertaken. Future experimental options that are recommended by the author are the following:

1) Weight loss determination and TGA work. Flower et al., (2010); Man and Gibbins, (2011), among others, have complemented ignition experiments in a 20 litre chamber with weight loss determination and TGA work for gaining a better understanding of fuel devolatilisation

process. Lack of equipment available has prevented including any related work in this thesis but future consideration of this work to enhance understanding of ignition results is desirable. It may also contribute to forensic studies to help in evaluating ignition in any future PF mill accidents.

2) Chamber volume and geometry. A comprehensive evaluation of effect of a larger volume of ignition chamber in coal and biomass ignition under oxy-fuel atmospheres by comparison with other vessels available is recommended. From this thesis, it is tentatively concluded that increasing chamber volume without overdriving can underestimate P/R values, taking into account that overdriving and effective dust dispersion in large volumes can be challenging. Experimental results from larger chambers, e.g. 1 m^3, would be useful to confirm empirically the different P/R value trends observed in R-30 when compared to R-20.

3) Operation of ignition chamber at higher initial temperature. Tests presented in this thesis are carried out at initial atmospheric pressure and ambient temperature. However, in the real PF milling operation, temperatures are expected higher than ambient. Due to the direct impact of initial temperatures on LFL values [Hertzberg and Cashdollar, (1987)], it is recommended that tests with more elevated temperatures (e.g. 50-100 °C) at the start of the experiment are carried out.

4) Real plant operation. The use of ignition chambers to the PF power plant as part of routine fuel testing is strongly recommended, particularly to evaluate ignitability when receiving a new fuel in the power plant or changing mill operating parameters.

5) Ignition experiments at constant pressure. An open ended ignition chamber or other relevant apparatus should be used in the future to evaluate coal and biomass dust ignition behaviour at constant pressure. This might provide a useful insight into ignition propagation mechanisms when not limited by constant volume.

6) Modelling work. Advances in CFD and other modelling work, with increasing literature available particularly under oxy-fuel conditions, make it very important to combine experimental data that can be recorded from these dust ignition tests with modelling work to gain a better understanding of the ignition propagation within the chamber(s). This would facilitate translation of the results into the real PF mill operation.

7) Oxy-fuel community and dusts explosion science collaboration. The author encourages a close interaction and further collaboration between the oxy-fuel community and dust explosion experts to enhance impact of common work that can lead to safer processes for low carbon power generation or negative CO_2 emissions if BECCS is implemented.

Finally, the main conclusions from this thesis are included in the following Chapter 8.

8. Conclusions

Carbon Capture and Storage (CCS) and Bio-Energy with CCS (BECCS) with sustainable biomass feedstock have to be deployed to achieve zero or potential negative CO_2 emissions available respectively, while significantly reducing the costs of Climate Change mitigation to meet 2DS targets beyond the 2020s in the post-Paris 2015 agreement. Oxy-fuel combustion is one of the key technology options being developed for implementing CCS in the power generation sector. Pulverised fuel (PF) oxy-combustion milling safety has been evaluated with attention to fuel ignitability depending on the different experimental parameters: fuel concentration, fuel particle size, ignition energy, O_2 concentration and fuel type (volatile content).

Novel ignition chambers, spherical of 20 litres (R-20) and non-spherical of 30 litres (R-30) have been designed and built at the University of Edinburgh for PF ignitability studies for evaluating PF milling safety in oxy-fuel. To the author's knowledge this was a first of a kind design of a spherical 20 litres ignition chamber that could be extended to a 30 litres volume to study ignition chamber volume and geometry impact on dust ignition behaviour. Dust explosions science methods have been applied for evaluating coal and biomass dust ignitability in R-20 and R-30 with 2,500 J, 5,000 J and 10,000 J chemical igniters activated in air, 21 % v/v O_2 in CO_2, 25 % v/v O_2 in CO_2 and 30 % v/v O_2 in CO_2 atmospheres. Fuel concentrations were in the 100 g/m^3-600 g/m^3 range. Pressure data from dust ignition at constant volume were recorded and final/initial pressure ratio (P/R) values were considered sufficient to determine if an ignition test was positive, defined when the P/R value was above a 2.5 threshold.

Pittsburgh Pulverised Coal (PPC), El Cerrejon, Kellingley and Thoresby coals were tested in this experimental programme. PPC ignited at all concentrations tested (100 g/m^3-600 g/m^3 range) in 21 Oxy and 30 Oxy except for 100 g/m^3 in 21 Oxy in R-20, which shows the high risk when milling PPC under oxy-fuel conditions. El Cerrejon yielded negative ignition at all concentrations for air, 21 Oxy, 25 Oxy and 30 Oxy in R-20 when larger particle sizes (>75 µm were tested), except for 600 g/m^3 in air and 30 Oxy. Decreasing the mean particle size of the distribution resulted in many more cases of positive ignition. For example, El Cerrejon 75 -53 µm size in 21 Oxy yielded negative for 200 g/m^3 while for the same concentration ignition was positive if testing <53 µm. However, the 75-53 µm size distribution was found

to be critical in the devolatilisation process controlling the subsequent ignition propagation due to greater abundance of volatiles. PF milling in 21 Oxy has been proven experimentally to be safer to handle for the four coals tested than in air. Tentatively, 30 Oxy gave a similar ignition pattern to air for coals, confirming previous experience available in the literature.

The biomasses tested were Torrefied Spruce, I2 White Wood, Miscanthus and Cereal Co-product. Biomasses were ground with 0.25 mm ring sieve (0.25G) and 0.5 mm ring sieve (0.5G) size distributions except for Cereal Co-product where 0.25G and <180 µm were employed. In R-20 with 2,500 J igniters, all the four biomasses samples in the 0.25G size range behaved similarly in 21 Oxy, giving negative ignition for all concentrations tested versus positive ignition for the air case. For the four biomasses tested, 2,500 Joules ignition energy strength might not be adequate to overdrive the R-20 chamber. However, when overdriving in R-20 with 5,000 J, for PF milling safety assessment, then more positive ignition cases were found. Although biomass ignited in air and 21 Oxy it appears that a wider range of ignition sources could cause problems in air. For the PF mill safety case, it is recommended to overdrive R-20 with 5,000 Joules. For 5,000 J as ignition energy all the four biomasses gave negative ignition at concentrations ≤200 g/m^3 in 21 Oxy while in air at the same concentration the four did ignite. The presence of CO_2 in the balance has a clear impact in preventing the initial ignition from fires getting established a sustained flame from volatiles combustion in the mill. Ignitability increases monotonically with finer particle size for all fuels. Tentatively, 25 Oxy matched air ignition behaviour for the biomasses tested. In addition, the irregular particle size translated into biomasses fuels being more difficult to light but yielding higher P/R values when positive ignition was found when compared to the coals tested.

Implications are that 21 Oxy is safer to operate in the PF mill than in the air case for the fuels tested. Oxygen injection in the PR up to 21 % v/v balance CO_2 could be considered for new oxy-fuel plants. Fuels with higher VM content would yield more positive ignition cases and should be dealt with extra caution in the PF mill. The use of adequate ignition energy, 5,000 J in R-20, is needed for PF mill safety evaluation. Ignitability of fuels increases monotonically with finer particle size and higher O_2 content with intermediate loadings tested yielding maximum P/R values before a plateau at higher loadings for most fuels tested. An ignition chamber volume and geometry effect was found using R-30 tests and further work is required to explore this. This work could be complemented with TGA,

forensic studies, real plant operational conditions and modelling studies to gain a better understanding of PF ignitability for evaluating PF milling safety in oxy-fuel for developing CCS and BECCS.

References

Abrahamsen, A.R., (1987), The U.K. Approach to Dust Explosibility Assessment and Its Relevance to Explosion Prevention and Protection, Industrial Dust Explosions, ASTM STP 958, Kenneth L. Cashdollar and Martin Hertzberg, Eds., American Society for Testing and Materials, Philadelphia, 1987, pp. 60-73.

Ahn, J., Okerlund, R., Fry, A. and Eddings, E.G. (2011), Sulfur trioxide formation during oxy-coal combustion International Journal of Greenhouse Gas Control, Volume 5, Supplement 1, July 2011, Pages S127-S135, ISSN 1750-5836, http://dx.doi.org/10.1016/j.ijggc.2011.05.009.

(http://www.sciencedirect.com/science/article/pii/S1750583611000697.

Allam, R.J., (2009), Improved oxygen production technologies, Energy Procedia, Volume 1, Issue 1, February 2009, Pages 461-470, ISSN 1876-6102, http://dx.doi.org/10.1016/j.egypro.2009.01.062.

(http://www.sciencedirect.com/science/article/pii/S1876610209000630)

Amyotte, P.R., Basu, A., Khan, F.I., (2003), Reduction of Dust Explosion Hazard by Fuel Substitution in Power Plants, Process Safety and Environmental Protection, Volume 81, Issue 6, November 2003, Pages 457-462, ISSN 0957-5820, http://dx.doi.org/10.1205/095758203770866629.

(http://www.sciencedirect.com/science/article/pii/S0957582003711239)

Amyotte, P.R., Pegg, M.J., Khan, F.I., (2009), Application of inherent safety principles to dust explosion prevention and mitigation, Process Safety and Environmental Protection, Volume 87, Issue 1, January 2009, Pages 35-39, ISSN 0957-5820, http://dx.doi.org/10.1016/j.psep.2008.06.007.

(http://www.sciencedirect.com/science/article/pii/S0957582008000839)

Anheden, M., Burchhardt, U., Ecke, H., Faber, R., Jidinger, O., Giering, R., Kass, H., Lysk, S., Ramström, E., Yan, J., (2011), Overview of operational experience and results from test activities in Vattenfall's 30 MWth oxyfuel pilot plant in Schwarze Pumpe, Energy Procedia, Volume 4, 2011, Pages 941-950, ISSN 1876-6102, http://dx.doi.org/10.1016/j.egypro.2011.01.140.

(http://www.sciencedirect.com/science/article/pii/S1876610211001421)

Arasto, A., Onarheim, K., Tsupari, E., Kärki, J., (2014), Bio-CCS: Feasibility comparison of large scale carbon-negative solutions, Energy Procedia, Volume 63, 2014, Pages 6756-6769, ISSN 1876-6102, http://dx.doi.org/10.1016/j.egypro.2014.11.711.

(http://www.sciencedirect.com/science/article/pii/S1876610214025260)

Babcock and Wilcox (B&W), (2005), Steam, its generation and its use, 41st Edition. ISBN-13: 978-0963457004, ASIN: B00741C6EG.

Balusamy S, Schmidt A, Hochgreb S., (2013), Flow field measurements of pulverized coal combustion using optical diagnostic techniques. Exp.Fluids. 2013; 54, 1534.

Bejarano, P.A. and Levendis, Y.A., (2008), Single-coal-particle combustion in O_2/N_2 and O_2/CO_2 environments, Combustion and Flame, Volume 153, Issues 1–2, April 2008, Pages 270-287, ISSN 0010-2180, http://dx.doi.org/10.1016/j.combustflame.2007.10.022.

(http://www.sciencedirect.com/science/article/pii/S0010218007003276)

Black, S., Szuhánszki, J., Pranzitelli, A., Ma, L., Stanger, P.J., Ingham, D.B., Pourkashanian, M., (2013), Effects of firing coal and biomass under oxy-fuel conditions in a power plant boiler using CFD modelling, (2013), Fuel, Volume 113, November 2013, Pages 780-786, ISSN 0016-2361, http://dx.doi.org/10.1016/j.fuel.2013.03.075.

(http://www.sciencedirect.com/science/article/pii/S0016236113002792)

Bloomberg New Energy Finance, (2014), Fossil fuel divestment a $5 trillion challenge, White paper 25 August 2014. Available on:

http://about.bnef.com/content/uploads/sites/4/2014/08/BNEF_DOC_2014-08-25-Fossil-Fuel-Divestment.pdf [Last Accessed 29/03/2015]

British Coal Utilisation Research Association (BCURA), (2002), Coal Bank -Coals proximate/ultimate analysis.

BCURA Coal Bank, Available on:

http://www.bcura.org/coalbank.html [Last Accessed on 29/03/2015]

British Geological Survey, (2012), Macroseismic Surveys. Available on: http://www.earthquakes.bgs.ac.uk/macroseismics/macroseismic_surveys.htm [Last Accessed on 23/02/2011].

British Standards, BS EN 14034-1 (2004), Determination of explosion characteristics of dust clouds – Part 1

British Standards, BS EN 14034-2 (2006), Determination of explosion characteristics of dust clouds – Part 2

British Standards, BS EN 14034-3 (2006), Determination of explosion characteristics of dust clouds – Part 3

British Standards, BS EN 14034-4 (2004), Determination of explosion characteristics of dust clouds – Part 4

British Standards, PD5500 (2009), Unfired Pressure Vessels.

British Standards BS ISO 3601-1:2008, (2008), Fluid power systems —O-rings —Part 1: Inside diameters, cross-sections, tolerances and designation codes.

Brown, A., (2012), El Cerrejon IC Grade 100 and Grade 145 production process, Durrans, [Personal communication].

Brown, A., (2012), El Cerrejon IC Grade 100 and Grade 145 analysis, Durrans, [Personal communication].

Bruce, A.R.W., Harrison, G.P., Gibbins, J., Chalmers, H., (2014), Assessing Operating Regimes of CCS Power Plants in High Wind and Energy Storage Scenarios, Energy Procedia, Volume 63, 2014, Pages 7529-7540, ISSN 1876-6102, http://dx.doi.org/10.1016/j.egypro.2014.11.789.

(http://www.sciencedirect.com/science/article/pii/S1876610214026046)

Brüls, H.K., Lefebvre, M.H., Berghmans, J., (1994), On deviations from ideal Chapman-Jouguet detonation velocity, Symposium (International) on Combustion, Volume 25, Issue 1, 1994, Pages 37-44, ISSN 0082-0784.

http://dx.doi.org/10.1016/S0082-0784(06)80625-9.

(http://www.sciencedirect.com/science/article/pii/S0082078406806259)

Burns C., (2012) Pictures of R-20 ignition chamber manufacturing process for the University of Edinburgh, Lazer Engineering, [Personal Communication].

Burns C., (2013) Pictures of R-30 ignition chamber manufacturing process for the University of Edinburgh, Lazer Engineering, [Personal Communication].

Capture Power Limited, (2013), Appearance and location of the White Rose Carbon Capture and Storage Project, July 2013. Available on:

http://www.whiteroseccs.co.uk/wp-content/uploads/2012/02/Appearance-and-location-of-the-White-Rose-Carbon-Capture7.pdf [Last Accessed 29/03/2015]

Capture Power Limited, (2015), White Rose CCS Project, Alstom, Drax and BOC. Available on:

http://www.whiteroseccs.co.uk/ [Last Accessed 29/03/2015]

Carini, R.C. and Hules, K.R., (1987), Coal Pulverizer Explosions, Industrial Dust Explosions, ASTM STP 958, Kenneth L. Cashdollar and Martin Hertzberg, Eds., American Society for Testing and Materials, Philadelphia, 1987, pp. 202-216.

Cashdollar K.L., (1996), Coal dust explosibility. J Loss Prevent Process Industries; Volume 9, Issue 1, 1996, Pages 65-76, ISSN 0950-4230, http://dx.doi.org/10.1016/09504230(95)00050-X.(http://www.sciencedirect.com/science/article/pii/095042309500050X)

Cashdollar, K.L., (2000), Overview of dust explosibility characteristics, Journal of Loss Prevention in the Process Industries; Volume, Issues 3-5, May 200, Pages 183-199, ISSN 0950-4230, http://dx.doi.org/10.1016/S0950-4230(99)00039-X.

(http://www.sciencedirect.com/science/article/pii/S095042309900039X)

Cashdollar, K.L., Hertzberg, M., (1983), Infrared temperatures of coal dust explosions, Combustion and Flame, Volume 51, 1983, Pages 23-35, ISSN 0010-2180, http://dx.doi.org/10.1016/0010-2180(83)90080-9.

(http://www.sciencedirect.com/science/article/pii/0010218083900809)

Cashdollar K. L. and Hertzberg, M., (1985), Explosibility test chamber for dusts and gases, American Institute of Physics, Rev. Sci. Instrum. 56, 596.

Cashdollar, K.L., Hertzberg, M., Zlochower, I.A., (1989), Effect of volatility on dust flammability limits for coals, gilsonite, and polyethylene, Symposium (International) on Combustion, Volume 22, Issue 1, 1989, Pages 1757-1765, ISSN 0082-0784, http://dx.doi.org/10.1016/S0082-0784(89)80189-4.

(http://www.sciencedirect.com/science/article/pii/S0082078489801894)

Cashdollar, K., Liebman, I. and Conti, R (1981) Three Bureau of Mines Optical Dust Probes, Bureau of Mines Report of Investigations RI 8542, Reprints from the Collection of the University of Michigan Library.

Cashdollar, K.L., Sapko, M.J., Weiss, E.S., Harris, M.L., Man, C., Harteis, S.P., Green, G.M., (2010), Recommendations for a New Rock Dusting Standard to Prevent Coal Dust Explosions in Intake Airways, NIOSH Publication No. 2010-151. Available on http://www.cdc.gov/niosh/mining/UserFiles/works/pdfs/2010-151.pdf

[Last Accessed on 29/03/2015]

Castillo, R., (2011), Thermodynamic analysis of a hard coal oxyfuel power plant with high temperature three-end membrane for air separation, Applied Energy, Volume 88, Issue 5, May 2011, Pages 1480-1493, ISSN 0306-2619, http://dx.doi.org/10.1016/j.apenergy.2010.10.044.

(http://www.sciencedirect.com/science/article/pii/S0306261910004599)

Chalmers H., (2010), Flexible operation of coal-fired power plants with post-combustion capture of carbon dioxide. Thesis for the Degree of Doctor of Philosophy in Environmental Strategy, University of Surrey, Guildford, UK

Chalmers, H., Al-Jeboori, M., Anthony, B., Balusamy, S., Black, S., Cavallo Marincola, F., Clements, A., Darabkhani, H., Dennis, J., Farrow, T., Fennell, P., Franchetti, B., Gao, L., Gibbins, J., Hochgreb, S., Hossain, M., Jurado, N., Kempf, A., Liu, H., Lu, G., Ma, L., Navarro-Martinez, L., Nimmo, W., Oakey, J., Pranzitelli, A., Scott, S., Snape, C., Sun, C.-G. , Sun, D., Szuhánszki, J., Trabadela, I., Wigley, F., Yan, Y., Pourkashanian, M., (2014), OxyCAP UK: Oxyfuel Combustion - academic Programme for the UK, Energy Procedia, Volume 63, 2014, Pages 504-510, ISSN 1876-6102, http://dx.doi.org/10.1016/j.egypro.2014.11.055.

(http://www.sciencedirect.com/science/article/pii/S1876610214018700)

Chalmers, H., Leach, M., Gibbins, J., (2011), Built-in flexibility at retrofitted power plants: What is it worth and can we afford to ignore it?, Energy Procedia, Volume 4, 2011, Pages 2596-2603, ISSN 1876-6102, http://dx.doi.org/10.1016/j.egypro.2011.02.158.

(http://www.sciencedirect.com/science/article/pii/S1876610211003559)

Chen, L., Yong, S.Z., Ghoniem, A.F., (2012), Oxy-fuel combustion of pulverized coal: Characterization, fundamentals, stabilization and CFD modeling, Progress in Energy and Combustion Science, Volume 38, Issue 2, April 2012, Pages 156-214, ISSN 0360-1285, http://dx.doi.org/10.1016/j.pecs.2011.09.003.

(http://www.sciencedirect.com/science/article/pii/S0360128511000529)

Clark, V.R. and Herzog, H. J., (2014), Can “stranded” Fossil Fuel Reserves Drive CCS Deployment?, Energy Procedia, Volume 63, 2014, Pages 7261-7271, ISSN 1876-6102, http://dx.doi.org/10.1016/j.egypro.2014.11.762.

(http://www.sciencedirect.com/science/article/pii/S1876610214025776)

Clements, A.G., Black, S., Szuhánszki, J., Stęchły, K., Pranzitelli, A., Nimmo, W., Pourkashanian, M., (2015), LES and RANS of air and oxy-coal combustion in a pilot-scale facility: Predictions of radiative heat transfer, (2015), Fuel, Available online 7 February 2015, ISSN 0016-2361, http://dx.doi.org/10.1016/j.fuel.2015.01.089.

(http://www.sciencedirect.com/science/article/pii/S001623611500109X)

Clements, B., Pomalis, R., Zheng, L., Herage, T, (2011), High pressure oxy-fuel (HiPrOx) combustion systems, In Woodhead Publishing Series in Energy, edited by Ligang Zheng, Woodhead Publishing, 2011, Pages 273-293, Oxy-Fuel Combustion for Power Generation and Carbon Dioxide (CO_2) Capture, ISBN 9781845696719, http://dx.doi.org/10.1533/9780857090980.3.273.

(http://www.sciencedirect.com/science/article/pii/B9781845696719500132)

Cloney, C.T., Ripley, R.C., Amyotte, P.R., Khan,F.I., (2013), Quantifying the effect of strong ignition sources on particle preconditioning and distribution in the 20-L chamber, Journal of Loss Prevention in the Process Industries, Volume 26, Issue 6, November 2013, Pages 1574-1582, ISSN 0950-4230, http://dx.doi.org/10.1016/j.jlp.2013.08.010.

(http://www.sciencedirect.com/science/article/pii/S0950423013001654)

Conti, R.S and Hertzberg, M ., (1987), Thermal autoignition temperatures from the 1.2-L Furnace and Their Use in Evaluating the Explosion Potential of Dusts, Industrial Dust Explosions, ASTM STP 958, Kenneth L. Cashdollar and Martin Hertzberg, Eds., American Society for Testing and Materials, Philadelphia, 1987, pp. 45-59.

Dastidar, A. G., Amyotte, P.R., Pegg, M.J., (1997), Factors influencing the suppression of coal dust explosions, Fuel, Volume 76, Issue 7, May 1997, Pages 663-670, ISSN 0016-2361, http://dx.doi.org/10.1016/S0016-2361(97)00039-2.

(http://www.sciencedirect.com/science/article/pii/S0016236197000392)

Dastidar, A. and Amyotte, P., (2002), Determination of Minimum Inerting Concentrations for Combustible Dusts in a Laboratory-Scale Chamber, Process Safety and Environmental Protection, Volume 80, Issue 6, November 2002, Pages 287-297, ISSN 0957-5820, http://dx.doi.org/10.1205/095758202321154916.

(http://www.sciencedirect.com/science/article/pii/S0957582002710525)

Department of Energy and Climate Change (DECC), (2012) UK Bioenergy Strategy April 2012. Available on:

https://www.gov.uk/government/uploads/system/uploads/attachment_data/file/48337/5142-bioenergy-strategy-.pdf [Last Accessed on 29/03/2015]

Department of Energy and Climate Change (DECC), (2013a), UK CCS Commercialisation Competition, London, UK. Available on:

https://www.gov.uk/uk-carbon-capture-and-storage-government-funding-and-support#ccs-commercialisation-competition [Last Accessed 29/03/2015]

Department of Energy and Climate Change (DECC), (2013b), CCS Cost Reduction Taskforce, London, UK. Available on:

https://www.gov.uk/government/uploads/system/uploads/attachment_data/file/201021/CCS_Cost_Reduction_Taskforce_-_Final_Report_-_May_2013.pdf [Last Accessed 29/03/2015]

Department of Energy and Climate Change (DECC), (2013c), The Energy Act, Collection of documents related (The Energy Act received Royal Assent on 18 December 2013). Available on:

https://www.gov.uk/government/collections/energy-act#documents

[Last Accessed 29/03/2015]

Department of Energy and Climate Change (DECC), (2014a), Finalised policy positions for implementation of EMR, London, UK. Available on:

https://www.gov.uk/government/uploads/system/uploads/attachment_data/file/324176/Implementing_Electricity_Market_Reform.pdf [Last Accessed 29/03/2015]

Department of Energy and Climate Change (DECC), (2014b), Next Steps in CCS: Policy Scoping Document, London, UK. Available on:

https://www.gov.uk/government/uploads/system/uploads/attachment_data/file/341995/Final_Version_Policy_Scoping_Document_PSD.pdf [Last Accessed 29/03/2015]

Department of Energy and Climate Change (DECC), (2014c), Energy Trends: December 2014, special feature article - Global coal trade. Available on: https://www.gov.uk/government/uploads/system/uploads/attachment_data/file/386895/Global_coal_trade.pdf [Last Accessed on 29/03/2015]

Department of Energy and Climate Change (DECC), (2014d) Digest of United Kingdom energy statistics (DUKES) 2014 Chapter 5 Electricity. Available on:

https://www.gov.uk/government/uploads/system/uploads/attachment_data/file/337649/chapter_5.pdf [Last Accessed 29/03/2015]

Department of Energy and Climate Change (DECC), (2014e), UK Energy Statistics, 27 March 2014. Available on:

https://www.gov.uk/government/uploads/system/uploads/attachment_data/file/296183/pn_march_14.pdf [Last Accessed on 29/03/2015]

Despommier, D., (2010), The Vertical Farm: Feeding the World in the 21st Century, Majora Carter, Reprinted by Picador; ISBN-10: 0312610696, ISBN-13: 978-0312610692.

Despommier, D., (2013), Farming up the city: the rise of urban vertical farms, Trends in Biotechnology, Volume 31, Issue 7, July 2013, Pages 388-389, ISSN 0167-7799, http://dx.doi.org/10.1016/j.tibtech.2013.03.008.

(http://www.sciencedirect.com/science/article/pii/S016777991300070X)

Dillon, D.J., White V., Allam, R.J., Wall, R.A., Gibbins, J., (2005a), Oxy combustion processes for CO_2 capture from power plant, IEA GHG report 2005/9.

Dillon, D.J., Panesar, R.S., Wall, R.A., Allam, R.J. , White, V., Gibbins, J., and Haines, M.R., (2005b), Oxy-combustion processes for CO_2 capture from advanced supercritical PF and NGCC power plant, In Greenhouse Gas Control Technologies 7, edited by E.S. Rubin D.W. Keith C.F. GilboyM. Wilson and T. Morris J. GaleK. Thambimuthu, Elsevier Science Ltd, Oxford, 2005, Pages 211-220, ISBN 9780080447049, http://dx.doi.org/10.1016/B978-008044704-9/50022-7.

(http://www.sciencedirect.com/science/article/pii/B9780080447049500227)

DTI, (2005) Pressure Equipment. Guidance Notes on the UK Regulations, April 2005, URN 05/1074. Applied by Zurich Insurance Group Ltd..

Explosive dust, picture available on:

http://www.explosivedust.com/dusttest.htm# [Last Accessed 29/03/2015]

Eckhoff, R.K., (2003), Chapter 1 - Dust Explosions—Origin, Propagation, Prevention, and Mitigation: An Overview, In Dust Explosions in the Process Industries, (Third Edition), edited by Rolf K. Eckhoff, Gulf Professional Publishing, Burlington, 2003, Pages 1-156, ISBN 9780750676021, http://dx.doi.org/10.1016/B978-075067602-1/50002-0.

EPSRC-E.ON Strategic Partnership, Carbon Capture and Storage, (2009), Oxyfuel Combustion Academic Programme for the UK (OxyCAP UK Project).

Environment Agency (EA), (2013), Best Available Techniques for Pulverised Combustion of Wood Pellets in Power Plant, September 2013. Available on:

https://www.gov.uk/government/uploads/system/uploads/attachment_data/file/296543/LIT_8880_148985.pdf

[Last Accessed on 29/03/2015]

Essenhigh, R.H., Misra, M. K., Shaw, D.W., (1989), Ignition of coal particles: A review, Combustion and Flame, Volume 77, Issue 1, July 1989, Pages 3-30, ISSN 0010-2180, http://dx.doi.org/10.1016/0010-2180(89)90101-6.

(http://www.sciencedirect.com/science/article/pii/0010218089901016)

European Commission, Directorate General for Climate Action, (2014a), Consultation on CCS Directive Evaluation. Available on:

http://www.ccs-directive-evaluation.eu/ [Last Accessed 29/03/2015]

European Commission, Directorate General for Energy and Climate Action, (2014b), Consultation on revision of the EU Emission Trading System (EU ETS) Directive, (19 December 2014 to 16 March 2015). Available on:

http://ec.europa.eu/clima/consultations/articles/0024_en.htm [Last Accessed 29/03/2015]

Faber, R., Yan, J., Stark, F., Priesnitz, S., (2011), Flue gas desulphurization for hot recycle Oxyfuel combustion: Experiences from the 30MW_{th} Oxyfuel pilot plant in Schwarze Pumpe, International Journal of Greenhouse Gas Control, Volume 5, Supplement 1, July 2011, Pages S210-S223, ISSN 1750-5836, http://dx.doi.org/10.1016/j.ijggc.2011.05.027.

(http://www.sciencedirect.com/science/article/pii/S1750583611000879)

Farrow T.S., Sun C.-G. and Snape C., (2013), Impact of biomass char on coal char burn-out under air and oxy-fuel conditions. Fuel, Volume 114, December 2013, Pages 128-134, ISSN 0016-2361, http://dx.doi.org/10.1016/j.fuel.2012.07.073.

(http://www.sciencedirect.com/science/article/pii/S0016236112006345)

Flower, M. and Gibbins, J., (2009), A radiant heating wire mesh single-particle biomass combustion apparatus, Fuel, Volume 88, Issue 12, December 2009, Pages 2418-2427, ISSN 0016-2361, http://dx.doi.org/10.1016/j.fuel.2009.02.036.

(http://www.sciencedirect.com/science/article/pii/S0016236109000829)

Flower, M., Man, C., Gibbins, J., McGlashan, N., (2010), A comparison between ignition behaviours of 7 different UK and World-Traded coals in air, and in a mixture of oxygen and carbon dioxide gases representative of oxy-combustion conditions, Internal Report, Imperial College London, 2010, London, UK.

Franchetti B.M., Cavallo Marincola F., Navarro-Martinez S., Kempf A.M., (2013), Large Eddy Simulation of a Pulverised Coal Jet Flame, Proceedings of the Combustion Institute, Volume 34, Issue 2, 2013, Pages 2419-2426, ISSN 1540-7489, http://dx.doi.org/10.1016/j.proci.2012.07.056.

(http://www.sciencedirect.com/science/article/pii/S1540748912003483)

Fry, A., Adams, B., Paschedag, A., Kazalski, P., Carney, C., Oryshchyn, D., Woodside, R., Gerdemann, S., Ochs, T., (2011), Principles for retrofitting coal burners for oxy-combustion, International Journal of Greenhouse Gas Control, Volume 5, Supplement 1, July 2011, Pages S151-S158, ISSN 1750-5836, http://dx.doi.org/10.1016/j.ijggc.2011.05.004.

(http://www.sciencedirect.com/science/article/pii/S1750583611000648)

Fuertes, A.B., Hampartsoumian, E., Williams, A., (1993), Direct measurement of ignition temperatures of pulverized coal particles, Fuel, Volume 72, Issue 9, September 1993, Pages 1287-1291, ISSN 0016-2361, http://dx.doi.org/10.1016/0016-2361(93)90127-N.

(http://www.sciencedirect.com/science/article/pii/001623619390127N)

Fujimori T. and Yamada T., (2013), Realization of oxyfuel combustion for near zero emission power generation, Proceedings of the Combustion Institute, Volume 34, Issue 2, 2013, Pages 2111-2130, ISSN 1540-7489, http://dx.doi.org/10.1016/j.proci.2012.10.004.

(http://www.sciencedirect.com/science/article/pii/S1540748912004002)

FutureGen Alliance, (2015), The FutureGen 2.0 Project. Available on:

http://futuregenalliance.org/futuregen-2-0-project/ [Last Accessed 29/03/2015]

Gale, J., (2013), CO_2 utilisation, International Journal of Greenhouse Gas Control, Volume 19, November 2013, Pages 1-2, ISSN 1750-5836, http://dx.doi.org/10.1016/j.ijggc.2013.08.006.

(http://www.sciencedirect.com/science/article/pii/S1750583613003058)

Gharebaghi, M., Hughes, K.J., Porter, R.T.J., Pourkashanian, M., Williams, A., (2011), Mercury speciation in air-coal and oxy-coal combustion: A modelling approach, Proceedings of the Combustion Institute, Volume 33, Issue 2, 2011, Pages 1779-1786, ISSN 1540-7489, http://dx.doi.org/10.1016/j.proci.2010.07.068.

(http://www.sciencedirect.com/science/article/pii/S1540748910003408)

Gibbins, J. and Chalmers, H., (2008), Preparing for global rollout: A 'developed country first' demonstration programme for rapid CCS deployment, Energy Policy, Volume 36, Issue 2, February 2008, Pages 501-507, ISSN 0301-4215, http://dx.doi.org/10.1016/j.enpol.2007.10.021.

(http://www.sciencedirect.com/science/article/pii/S0301421507004740)

Gibbins J and Chalmers, H., (2011), Is all CCS equal? Classifying CCS applications by their potential climate benefit, Energy Procedia, Volume 4, 2011, Pages 5715-5720, ISSN 1876-6102, http://dx.doi.org/10.1016/j.egypro.2011.02.566.

(http://www.sciencedirect.com/science/article/pii/S1876610211008459)

Gibbins, J., Chalmers, H., Lucquiaud, M., MacGlashan, N., Li, J., Liang, X. for IEAGHG, (2011), Retrofitting CO_2 capture to existing power plants, Report 2011/2 International Energy Agency Greenhouse Gas Control Programme, Cheltenham, UK. Available on:

http://ieaghg.org/docs/General_Docs/Reports/2011-02.pdf

[Last Accessed 29/03/2015]

Gibbins, J, Lucquiaud, M., Irons, R., Sekkappan, G., Panesar, R. for IEAGHG, (2007), CO_2 capture ready plants, IEA Greenhouse Gas R&D Programme (IEA GHG), 2007/4, May 2007. Available on:

https://www.iea.org/publications/freepublications/publication/CO2_Capture_Ready_Plants.pdf [Last Accessed 29/03/2015]

Gibbins, J. and Man, C., (2005), Effect of Coal Type and Oxy-fuel combustion parameters on pulverised coal ignition, BCURA Project, Imperial College London, London, UK.

Global CCS Institute (GCCSI), (2009), Strategic Analysis of the Global Status of Carbon Capture and Storage, Final Report 2009 Global CCS Institute, Canberra, Australia. Available on:

http://decarboni.se/sites/default/files/publications/5751/report-1-status-carbon-capture-and-storage-projects-globally.pdf [Last Accessed 29/03/2015]

Global CCS Institute (GCCSI), (2015), FutuGen 2.0 project. Available on:

http://www.globalccsinstitute.com/project/futuregen-20-project [Last Accessed 29/03/2015]

Global CCS Institute (GCCSI), (2014), The Global Status of CCS: 2014, Melbourne, Australia. Available on:

http://decarboni.se/sites/default/files/publications/180923/global-status-ccs-2014.pdf

[Last Accessed 29/03/2015]

Going, J.E., Chatrathi, K., Cashdollar, K.L., (2000), Flammability limit measurements for dusts in 20-L and 1-m^3 vessels, Journal of Loss Prevention in the Process Industries, Volume 13, Issues 3–5, May 2000, Pages 209-219, ISSN 0950-4230, http://dx.doi.org/10.1016/S0950-4230(99)00043-1.

(http://www.sciencedirect.com/science/article/pii/S0950423099000431)

Hackett, L. A., (2014), The White Rose CCS Project, European Parliament, Brussels 19th March 2014, (Personal Communication).

Henderson, C., (2015), Cofiring of biomass in coal-fired power plants – European experience, IEA Clean Coal Centre, FCO/IEA CCC Workshop, Hebei and Shandong, China, 8-9 and 13-14 January 2015. Available on:

http://www.iea-coal.org.uk/documents/83524/9188/Henderson---Cofiring-of-biomass-in-coal-fired-power-plants-%E2%80%93-European-experience

[Last Accessed 29/03/2015]

Hertzberg, M., (1991), Autoignition temperatures for coal particles dispersed in air, Fuel, Volume 70, Issue 10, October 1991, Pages 1115-1123, ISSN 0016-2361, http://dx.doi.org/10.1016/0016-2361(91)90231-X.

(http://www.sciencedirect.com/science/article/pii/001623619190231X)

Hertzberg, M., Cashdollar, K.L., Lazzara, C.P., (1981), The limits of flammability of pulverized coals and other dusts, Symposium (International) on Combustion, Volume 18, Issue 1, 1981, Pages 717-729, ISSN 0082-0784, http://dx.doi.org/10.1016/S0082-0784(81)80076-8.

(http://www.sciencedirect.com/science/article/pii/S0082078481800768)

Hertzberg, M. and Cashdollar, K.L., (1987), Introduction to Dust Explosions, Industrial Dust Explosions, ASTM STP 958, Kenneth L. Cashdollar and Martin Hertzberg, Eds., American Society for Testing and Materials, Philadelphia, 1987, pp. 5-32.

Hertzberg, M., Cashdollar, K.L., Ng, D.L., Conti, R.S., (1982), Domains of flammability and thermal ignitability for pulverized coals and other dusts: Particle size dependences and microscopic residue analyses, Symposium (International) on Combustion, Volume 19, Issue

1, 1982, Pages 1169-1180, ISSN 0082-0784, http://dx.doi.org/10.1016/S0082-0784(82)80293-2.

(http://www.sciencedirect.com/science/article/pii/S0082078482802932)

Hertzberg, M., Cashdollar, K. L., Zlochower, I.A., (1988), Flammability limit measurements for dusts and gases: Ignition energy requirements and pressure dependences, Symposium (International) on Combustion, Volume 21, Issue 1, 1988, Pages 303-313, ISSN 0082-0784, http://dx.doi.org/10.1016/S0082-0784(88)80258-3.

(http://www.sciencedirect.com/science/article/pii/S0082078488802583)

Hertzberg, M., Zlochower, I.A., Devolatilization rates and intraparticle wave structures during the combustion of pulverized coals and polymethylmethacrylate, Symposium (International) on Combustion, Volume 23, Issue 1, 1991, Pages 1247-1255, ISSN 0082-0784, http://dx.doi.org/10.1016/S0082-0784(06)80387-5.

(http://www.sciencedirect.com/science/article/pii/S0082078406803875)

Herzog, H. J., (2014), Scaling up carbon dioxide capture and storage: From megatons to gigatons, Energy Economics, Volume 33, Issue 4, July 2011, Pages 597-604, ISSN 0140-9883, http://dx.doi.org/10.1016/j.eneco.2010.11.004.

(http://www.sciencedirect.com/science/article/pii/S0140988310001921)

Higginbotham, P., White, V., Fogash, K., Guvelioglu, G., (2011a), Oxygen supply for oxyfuel CO_2 capture, International Journal of Greenhouse Gas Control 5S (2011) S194–S203.

Higginbotham, P., White, V., Fogash, K., Guvelioglu, G., (2011b), Oxygen supply for oxycoal CO_2 capture, Energy Procedia, Volume 4, 2011, Pages 884-891, ISSN 1876-6102, http://dx.doi.org/10.1016/j.egypro.2011.01.133.

(http://www.sciencedirect.com/science/article/pii/S1876610211001354)

Hochgreb, S. (2015), El Cerrejon ultimate analysis, Cambridge University, OxyCAP UK Project, [Personal communication].

Hong, J., Field, R., Gazzino, M., Ghoniem, A.F., (2010), Operating pressure dependence of the pressurized oxy-fuel combustion power cycle, Energy, Volume 35, Issue 12, December 2010, Pages 5391-5399, ISSN 0360-544.,

http://dx.doi.org/10.1016/j.energy.2010.07.016.

http://www.sciencedirect.com/science/article/pii/S0360544210003804)

Hossain MM, Lu G, Sun D and Yan Y. Three-dimensional reconstruction of flame temperature and emissivity distribution using optical tomographic and two-colour pyrometric techniques. Measurement Science and Technology 2013; 24 (7) 074010.

Holtmeyer, M.L., Kumfer, B.M., Axelbaum, R.L., (2012), Effects of biomass particle size during cofiring under air-fired and oxyfuel conditions, Applied Energy, Volume 93, May 2012, Pages 606-613, ISSN 0306-2619, http://dx.doi.org/10.1016/j.apenergy.2011.11.042.

(http://www.sciencedirect.com/science/article/pii/S0306261911007392)

Huéscar-Medina, C., Phylaktou, H.N., Sattar, H., Andrews, G.E. , Gibbs, B.M., (2013), The development of an experimental method for the determination of the minimum explosible concentration of biomass powders, Biomass and Bioenergy, Volume 53, June 2013, Pages 95-104, ISSN 0961-9534, http://dx.doi.org/10.1016/j.biombioe.2013.03.008.

(http://www.sciencedirect.com/science/article/pii/S0961953413001402)

International Energy Agency (IEA), (2012), Technology Roadmap: Bioenergy for Heat and Power OECD/IEA, Paris, France. Available on:

http://www.iea.org/publications/freepublications/publication/2012_Bioenergy_Roadmap_2nd_Edition_WEB.pdf [Last Accessed 29/03/2015]

International Energy Agency (IEA), (2013), CCS Technology Roadmap, Paris, France. Available on:

http://www.iea.org/publications/freepublications/publication/TechnologyRoadmapCarbonCaptureandStorage.pdf [Last Accessed 29/03/2015]

International Energy Agency (IEA), (2014), Energy Technology Perspectives 2014, IEA, Paris, France. Available on:
DOI: http://dx.doi.org/10.1787/energy_tech-2014-en [Last Accessed 29/03/2015]

International Energy Agency (IEA), (2014), Press release, IEA hails historic launch of carbon capture and storage project, 1st October 2014, Paris, France. Available on:

http://www.iea.org/newsroomandevents/pressreleases/2014/october/iea-hails-historic-launch-of-carbon-capture-and-storage-project.html

International Energy Agency (IEA), (2014), World Energy Outlook, Paris, France. ISBN: 978-92-64-20805-6.

International Energy Agency Greenhouse Programme (IEAGHG), (2011), Potential for biomass and carbon dioxide capture and storage, Report 2011/6. Available on:

http://www.eenews.net/assets/2011/08/04/document_cw_01.pdf

[Last Accessed 29/03/2015]

International Monetary Fund (IMF), (2014), Gross domestic product for Germany based on purchasing-power-parity (PPP) valuation of country GDP, Current international dollar Billions, gross domestic product, current prices (National currency): 3,621.357. Available on:

http://www.imf.org/external/pubs/ft/weo/2014/02/weodata/weorept.aspx?pr.x=30&pr.y=6&sy=2014&ey=2014&scsm=1&ssd=1&sort=country&ds=.&br=1&c=134&s=NGDPD%2CNGDPDPC%2CPPPGDP%2CPPPPC&grp=0&a [Last Accessed 29/03/2015]

Intergovernmental Panel on Climate Change (IPCC), (2005), IPCC Special Report on Carbon Dioxide Capture and Storage. Working Group III of the Intergovernmental Panel on Climate Change Cambridge University Press, Cambridge, UK and New York, NY, USA.

Intergovernmental Panel on Climate Change (IPCC), (2013), Assessment Report 5 (AR 5) The Physical Science Basis, Working Group I - 2013. Available on:

http://www.ipcc.ch/report/ar5/wg1/ [Last Accessed 29/03/2015]

Intergovernmental Panel on Climate Change (IPCC), (2014a), Fifth Assessment Report (AR 5) Impacts, Adaptation, and Vulnerability, Working Group II - 2014 Available on:

http://www.ipcc.ch/report/ar5/wg2/ [Last Accessed 29/03/2015]

Intergovernmental Panel on Climate Change (IPCC), (2014b) Fifth Assessment Report (AR 5) Mitigation of Climate Change, Assessing Transformation Pathways, Working Group III - 2014. Available on:

https://www.ipcc.ch/report/ar5/wg3/ [Last Accessed 29/03/2015]

Intergovernmental Panel on Climate Change (IPCC), (2014c), Fifth Assessment Report (AR 5) Summary for Policymakers and Synthesis Report, 2014. Available on:

http://www.ipcc.ch/report/ar5/syr/ [Last Accessed 29/03/2015]

International Renewable Energy Agency (IRENA), (2014), Global Bioenergy, SUPPLY AND DEMAND PROJECTIONS A working paper for REmap 2030, September 2014 Available on:

http://www.irena.org/remap/IRENA_REmap_2030_Biomass_paper_2014.pdf [Last Accessed 29/03/2015]

Jang, H.A., Kim, J.H., Jung, S.J., Back, S.K., Sung, J.H., Kim, S.H., Seo, Y.C., Keel, S.I., Liu, X., (2014), Mercury emission characteristics from coal combustion by supplying oxygen and carbon dioxide with limestone injection, Fuel Processing Technology, Volume 125, September 2014, Pages 217-222, ISSN 0378-3820, http://dx.doi.org/10.1016/j.fuproc.2014.04.003.

Johnsson, F., Reiner, D., Itaoka, K., Herzog, H., (2010), Stakeholder attitudes on Carbon Capture and Storage—An international comparison, International Journal of Greenhouse Gas Control, Volume 4, Issue 2, March 2010, Pages 410-418, ISSN 1750-5836, http://dx.doi.org/10.1016/j.ijggc.2009.09.006.

(http://www.sciencedirect.com/science/article/pii/S1750583609000942)

Jurado N., Gohari Darabkhani H., Anthony E.J., Oakey J.E., (2013), Co-firing Performance of a Retrofitted Oxy-Combustor burning Coal/Biomass Blends: Experimental and Simulation Study, 3rd Oxy-fuel Combustion Conference (OCC3), International Energy Agency Greenhouse Gases Programme (IEAGHG), Ponferrada/CIUDEN (Spain), September 2013.

Kalejaiye, O., Amyotte, P.R., Pegg, M.J., Cashdollar, K.L., (2010), Effectiveness of dust dispersion in the 20-L Siwek chamber, Journal of Loss Prevention in the Process Industries, Volume 23, Issue 1, January 2010, Pages 46-59, ISSN 0950-4230, http://dx.doi.org/10.1016/j.jlp.2009.05.008.

(http://www.sciencedirect.com/science/article/pii/S0950423009000801)

Kemp, A.G. and Kasim, S., (2013), The economics of CO_2-EOR cluster developments in the UK Central North Sea, Energy Policy, Volume 62, November 2013, Pages 1344-1355, ISSN 0301-4215, http://dx.doi.org/10.1016/j.enpol.2013.07.047.

(http://www.sciencedirect.com/science/article/pii/S0301421513006903)

Kirk, F. (2012), Technical specification for M48 Hexagon head socket cap screws DIN 912, Francis Kirk, [Personal communication].

Komaki, A., Gotou, T., Uchida, T., Yamada, T., Kiga, T., Spero, C., (2014) Operation Experiences of Oxyfuel Power Plant in Callide Oxyfuel Project, Energy Procedia, Volume 63, 2014, Pages 490-496, ISSN 1876-6102, http://dx.doi.org/10.1016/j.egypro.2014.11.053.

(http://www.sciencedirect.com/science/article/pii/S1876610214018682)

Kranzmann, A., Neddemeyer, T., Ruhl, A.S., Huenert, D., Bettge, D., Oder, G., Saliwan Neumann, R., (2011), The challenge in understanding the corrosion mechanisms under oxyfuel combustion conditions, International Journal of Greenhouse Gas Control, Volume 5, Supplement 1, July 2011, Pages S168-S178, ISSN 1750-5836, http://dx.doi.org/10.1016/j.ijggc.2011.05.029.

(http://www.sciencedirect.com/science/article/pii/S1750583611000892)

Kuai, N., Huang, W., Du, B., Yuan, J., Li, Z., Gan, Y., Tan, J., (2013), Experiment-based investigations on the effect of ignition energy on dust explosion behaviors, Journal of Loss Prevention in the Process Industries, Volume 26, Issue 4, July 2013, Pages 869-877, ISSN 0950-4230, http://dx.doi.org/10.1016/j.jlp.2013.03.005.

(http://www.sciencedirect.com/science/article/pii/S0950423013000806)

Kuczynski, K.J., Fitzgerald, F.D. , Adams, D., Glover, F.H.M., White, V., Chalmers, H., Errey, O., Stephenson, P., (2011), Dynamic modelling of oxyfuel power plant, Energy Procedia, Volume 4, 2011, Pages 2541-2547, ISSN 1876-6102, http://dx.doi.org/10.1016/j.egypro.2011.02.151.

(http://www.sciencedirect.com/science/article/pii/S1876610211003481)

Lackner, K., (2013), The thermodynamics of direct air capture of carbon dioxide, Energy, Volume 50, 1 February 2013, Pages 38-46, ISSN 0360-5442, http://dx.doi.org/10.1016/j.energy.2012.09.012.

(http://www.sciencedirect.com/science/article/pii/S0360544212006901

Laude, A. and Jonen, C., (2013), Biomass and CCS: The influence of technical change, Energy Policy, Volume 60, September 2013, Pages 916-924, ISSN 0301-4215, http://dx.doi.org/10.1016/j.enpol.2013.05.044.

(http://www.sciencedirect.com/science/article/pii/S0301421513003807)

Levasseur, A., Liljedahl G., Wilhelm, B., Lou, X., Chapman, P., (2014), Design, Development and Large-scale Demonstration of an Oxy-combustion Boiler, Alstom Power, Windsor CT, 13th Annual Conference on Carbon Capture, Utilization and Storage, April 28-May 1 2014, Pittsburgh, USA.

Lewis, B and von Elbe, G., (1961), Combustion, Flames and Explosion of Gases, Academic Press, New York, 1961, pp. 367-381.

Liang, X., Reiner, D., Li, J., (2011), Perceptions of opinion leaders towards CCS demonstration projects in China, Applied Energy, Volume 88, Issue 5, May 2011, Pages 1873-1885, ISSN 0306-2619.

http://dx.doi.org/10.1016/j.apenergy.2010.10.034.

(http://www.sciencedirect.com/science/article/pii/S0306261910004368)

Liu, Y., Wall, T., Khare, S., Gupta, R, (2011) 9 - Oxy-fuel heat transfer characteristics and impacts on boiler design, In Woodhead Publishing Series in Energy, edited by Ligang Zheng, Woodhead Publishing, 2011, Pages 166-194, Oxy-Fuel Combustion for Power Generation and Carbon Dioxide (CO_2) Capture, ISBN 9781845696719, http://dx.doi.org/10.1533/9780857090980.2.166.

(http://www.sciencedirect.com/science/article/pii/B9781845696719500090)

Livingston, W.R., (2013), The firing and co-firing of biomass in large pulverised coal boilers, Doosan Power Systems, IEA Exco Workshop Jeju, November 2013. Available on:

http://www.ieabioenergy.com/wp-content/uploads/2013/11/P07-The-firing-and-co-firing-of-biomass-in-large-pulverised-coal-boilers-Livingston.pdf

[Last Accessed 29/03/2015]

Lobera, M.P., Serra, J.M., Foghmoes, S.P., Søgaard, M., Kaiser, A., (2011), On the use of supported ceria membranes for oxyfuel process/syngas production, Journal of Membrane Science, Volumes 385–386, 1 December 2011, Pages 154-161, ISSN 0376-7388, http://dx.doi.org/10.1016/j.memsci.2011.09.031.

(http://www.sciencedirect.com/science/article/pii/S0376738811007022)

Lockwood, F., Granados, L., Leclerc, M., Lesort, A-L., Beasse, G., Delgado, M.A., Spero, C., (2014), Oxy-combustion CPU – From Pilots Towards Industrial-scale Demonstration, Energy Procedia, Volume 63, 2014, Pages 342-351, ISSN 1876-6102, http://dx.doi.org/10.1016/j.egypro.2014.11.037.

(http://www.sciencedirect.com/science/article/pii/S1876610214018529)

Lopez-Anton, M.A., Rumayor, M., Díaz-Somoano, M., Martínez-Tarazona, M.R., (2015), Influence of a CO_2-enriched flue gas on mercury capture by activated carbons, Chemical Engineering Journal, Volume 262, 15 February 2015, Pages 1237-1243, ISSN 1385-8947, http://dx.doi.org/10.1016/j.cej.2014.10.088.

(http://www.sciencedirect.com/science/article/pii/S138589471401420X)

Lucquiaud, M., (2013), 10 - CO_2 capture-ready ultra-supercritical coal power plants, In Woodhead Publishing Series in Energy, edited by Dongke Zhang, Woodhead Publishing, 2013, Pages 244-271, Ultra-Supercritical Coal Power Plants, ISBN 9780857091161, http://dx.doi.org/10.1533/9780857097514.2.244.

(http://www.sciencedirect.com/science/article/pii/B9780857091161500106)

Man, C.K. and Gibbins, J.R., (2011), Factors affecting coal particle ignition under oxyfuel combustion atmospheres, Fuel, Volume 90, Issue 1, January 2011, Pages 294-304, ISSN 0016-2361.

http://dx.doi.org/10.1016/j.fuel.2010.09.006.

(http://www.sciencedirect.com/science/article/pii/S0016236110004771)

Menimm A. (2014), Dusts particle size analysis, School of Geosciences, University of Edinburgh, [Personal communication].

Mitsui, Y., Imada, N., Kikkawa, H., Katagawa, A., (2011), Study of Hg and SO_3 behavior in flue gas of oxy-fuel combustion system, International Journal of Greenhouse Gas Control, Volume 5, Supplement 1, July 2011, Pages S143-S150, ISSN 1750-5836, http://dx.doi.org/10.1016/j.ijggc.2011.05.017.

(http://www.sciencedirect.com/science/article/pii/S1750583611000776

Morley, C., (2005), Gaseq version 0.79 Chemical Equilibrium Program. Available on:

http://www.gaseq.co.uk/ [Last Accessed 29/03/2015]

Morgan Stanley (MS), (2014), Carbon Capture and Storgae – A Realistic Solution? [Private Communication; Note: MS does not endorse any conclusions or recommendations from data shown in this document].

National Academy of Sciences (NAS), (2015), Climate Intervention: Carbon Dioxide Removal and Reliable Sequestration, National Research Council of the National Academies, The National Academies Press, Washington D.C., USA.

Normann, F., Arndersson, K., Johnsson, F. and Leckner, B., (2011), NO_x reburning in oxy-fuel combustion: a comparison between solid and gaseous fuels, International Journal of Greenhouse Gas Control 5S (2011) S120-S126

Parker, (2007), O-Ring Handbook. Handbook available on:

http://www.parker.com/literature/O-Ring%20Division%20Literature/ORD%205700.pdf

[Last Accessed 29/03/2015]

Perrin, N., Dubettier, R., Lockwood, F., Tranier, J.P., Bourhy-Weber, C., Terrien, P., (2015), Oxycombustion for coal power plants: Advantages, solutions and projects, Applied Thermal Engineering 74 75-82.

Pickard, S., Daood, S.S., Nimmo, W., Lord, R., Pourkashanian, M., (2013), Bio-CCS: Co-firing of Established Greenfield and Novel, Brownfield Biomass Resources under Air, Oxygen-enriched Air and Oxy-fuel Conditions, Energy Procedia, Volume 37, 2013, Pages 6062-6069, ISSN 1876-6102.

http://dx.doi.org/10.1016/j.egypro.2013.06.535.

(http://www.sciencedirect.com/science/article/pii/S1876610213007789)

Pickard, S., Daood, S.S., Pourkashanian, M., Nimmo, W., (2014a), Reactivity during bench-scale combustion of biomass fuels for carbon capture and storage applications, Fuel, Volume 134, 15 October 2014, Pages 171-179, ISSN 0016-2361, http://dx.doi.org/10.1016/j.fuel.2014.05.050.

(http://www.sciencedirect.com/science/article/pii/S0016236114005031)

Pickard, S.C., Daood, S.S., Pourkashanian, M., Nimmo, W., (2014b), Co-firing coal with biomass in oxygen- and carbon dioxide-enriched atmospheres for CCS applications, Fuel, Volume 137, 1 December 2014, Pages 185-192, ISSN 0016-2361, http://dx.doi.org/10.1016/j.fuel.2014.07.078.

(http://www.sciencedirect.com/science/article/pii/S0016236114007297)

Pöyry, (2013), Outlook for new coal-fired power stations in Germany, The Netherlands and Spain" A Report to DECC, April 2013, Pöyry Management Consulting (UK) Ltd. Available on:

https://www.gov.uk/government/uploads/system/uploads/attachment_data/file/194335/Poyry_Report_-_Coal_fired_power_generation_in_Germany.pdf
[Last Accessed 29/03/2015]

National Institute for Occupational Safety and Health (NIOSH), (2012) PPC Coal proximate/ultimate analysis, [Personal communication].

Reuters Agency, (2015), China's National People's Congress annual session. Available on:

http://www.reuters.com/article/2015/03/05/us-china-parliament-idUSKBN0M103M20150305 [Last Accessed 12/03/2015]

Roeder, V., Hasenbein, C., Kather, A., Evaluation and Comparison of the Part Load Behaviour of the CO_2 Capture Technologies Oxyfuel and Post-Combustion, Energy Procedia, Volume 37, 2013, Pages 2420-2431, ISSN 1876-6102, http://dx.doi.org/10.1016/j.egypro.2013.06.123.

(http://www.sciencedirect.com/science/article/pii/S1876610213003664)

Rotterdam Capture and Storage Demonstration Project (ROAD), (2015), ROAD CCS project, E.ON Benelux and GDF SUEZ Energie Nederland. Available on:

http://road2020.nl/en/ [Last Accessed 29/03/2015]

Roussanaly, S. and Grimstad, A.-A., (2014), The Economic Value of CO_2 for EOR Applications, Energy Procedia, Volume 63, 2014, Pages 7836-7843, ISSN 1876-6102, http://dx.doi.org/10.1016/j.egypro.2014.11.818.

(http://www.sciencedirect.com/science/article/pii/S1876610214026332)

Royal Dutch Shell, (2015), Peterhead CCS Project. Available on:

http://www.shell.co.uk/gbr/environment-society/environment-tpkg/peterhead-ccs-project.html [Last Access 28/02/2015]

Riaza, J., Khatami, R., Levendis, Y.A., Álvarez, L, Gil, M.V., Pevida, C., Rubiera, F., Pis, J.J., (2014), Combustion of single biomass particles in air and in oxy-fuel conditions, Biomass and Bioenergy, Volume 64, May 2014, Pages 162-174, ISSN 0961-9534, http://dx.doi.org/10.1016/j.biombioe.2014.03.018.

(http://www.sciencedirect.com/science/article/pii/S0961953414001366)

Rose J.W., Cooper J.R. and Spiers H.M., (1977), Technical data on fuel. Front Cover. Wiley, - Technology & Engineering.

Rubin, E.S., (2012), Understanding the pitfalls of CCS cost estimates, International Journal of Greenhouse Gas Control, Volume 10, September 2012, Pages 181-190, ISSN 1750-5836, http://dx.doi.org/10.1016/j.ijggc.2012.06.004.

(http://www.sciencedirect.com/science/article/pii/S1750583612001302)

Saeed, M.A., Huéscar-Medina, C., Andrews, G.E., Phylaktou, H.N., Slatter, D., Gibbs, B.M. , (2014), Agricultural waste pulverised biomass: MEC and flame speeds, Journal of Loss Prevention in the Process Industries, Available online 15 December 2014, ISSN 0950-4230, http://dx.doi.org/10.1016/j.jlp.2014.12.007.

(http://www.sciencedirect.com/science/article/pii/S095042301400223X)

Sapko, M.J., Weiss, E.S., Cashdollar, K.L., Zlochower, I.A., (2000), Experimental mine and laboratory dust explosion research at NIOSH, Journal of Loss Prevention in the Process Industries, Volume 13, Issues 3–5, May 2000, Pages 229-242, ISSN 0950-4230, http://dx.doi.org/10.1016/S0950-4230(99)00038-8.

(http://www.sciencedirect.com/science/article/pii/S0950423099000388)

Saskpower, (2014) Boundary Dam Carbon Capture Project. Available on:

http://saskpowerccs.com/ccs-projects/boundary-dam-carbon-capture-project/

[Last Access 28/02/2015]

Scheffknecht, G., Al-Makhadmeh, L., Schnell, U. and Maier, J. (2011) Oxy-fuel coal combustion – A review of the current state-of-the-art, International Journal of Greenhouse Gas Control, Volume 5, Supplement 1, July 2011, Pages S16-S35, ISSN 1750-5836, http://dx.doi.org/10.1016/j.ijggc.2011.05.020.

(http://www.sciencedirect.com/science/article/pii/S1750583611000806)

Schreiber, A., Marx, J., Zapp, P., (2013), Environmental assessment of a membrane-based air separation for a coal-fired oxyfuel power plant, Journal of Membrane Science, Volume 440, 1 August 2013, Pages 122-133, ISSN 0376-7388, http://dx.doi.org/10.1016/j.memsci.2013.03.026.

(http://www.sciencedirect.com/science/article/pii/S0376738813002214)

Selosse, S., Ricci, O., Maïzi, N., (2013), Fukushima's impact on the European power sector: The key role of CCS technologies, Energy Economics, Volume 39, September 2013, Pages 305-312, ISSN 0140-9883, http://dx.doi.org/10.1016/j.eneco.2013.05.013.

(http://www.sciencedirect.com/science/article/pii/S0140988313001011)

Shaddix, C. and Molina, A., (2011), 6 - Ignition, flame stability, and char combustion in oxy-fuel combustion, In Woodhead Publishing Series in Energy, edited by Ligang Zheng, Woodhead Publishing, 2011, Pages 101-124, Oxy-Fuel Combustion for Power Generation and Carbon Dioxide (CO_2) Capture, ISBN 9781845696719, http://dx.doi.org/10.1533/9780857090980.2.101.

(http://www.sciencedirect.com/science/article/pii/B9781845696719500065)

Shogenova, A., Piessens, K., Holloway, S., Bentham, M., Martínez, R., Flornes, K.M., Poulsen, N.E., Wójcicki, A., Sliaupa, S., Kucharič, L., Dudu, A., Persoglia, S., Hladik, V., Saftic, B., Kvassnes, A., Shogenov, K., Ivask, J., Suárez, I., Sava, C., Sorin, A., Chikkatur, A., (2014), Implementation of the EU CCS Directive in Europe: Results and Development in 2013, Energy Procedia, Volume 63, 2014, Pages 6662-6670, ISSN 1876-6102, http://dx.doi.org/10.1016/j.egypro.2014.11.700.

(http://www.sciencedirect.com/science/article/pii/S1876610214025156)

Sinnott, R.K., (2008), Coulson & Richardson Chemical Engineering Design Vol.6 4th Ed McGraw-Hill.

Siwek R. (1996), Determination of technical safety indices and factors influencing hazard evaluation of dusts, Journal of Loss Prevention in the Process Industries. Vol. 9. No. 1. pp. 21-31, 1996.

Spero, C., (2013), On O_2 levels during the milling stage at Callide, (Personal Communication) at 3rd Oxyfuel Combustion Conference (OCC3), September 2013, Ponferrada, Spain.

Spörl, R., Maier, J., Belo, L., Shah, K, Stanger,R., Wall, T., Scheffknecht, G., (2014), Mercury and SO_3 Emissions in Oxy-fuel Combustion, Energy Procedia, Volume 63, 2014, Pages 386-402, ISSN 1876-6102, http://dx.doi.org/10.1016/j.egypro.2014.11.041.

(http://www.sciencedirect.com/science/article/pii/S1876610214018566)

SSE, (2015), Peterhead CCS Project. Available on:

http://sse.com/whatwedo/ourprojectsandassets/thermal/peterheadccs/

[Last Accessed 29/03/2015]

Stanger, R., Wall, T., (2011), Sulphur impacts during pulverised coal combustion in oxy-fuel technology for carbon capture and storage. Progress in Energy and Combustion Science 37, 69-88.

Stephan, C.R. (1990). Coal dust as a fuel for fires and explosions. Report No. 01-066-90, US Mine Safety and Health Administration, Pittsburgh, PA, 10 pp.

Stern N., (2007), The Economics of Climate Change, The Stern Review Report, Crown copyright, Cambridge University Press ISBN-13 978-0-521-700801 Paperback, Cambridge, UK.

Sturgeon, D.W. , Rogerson, J.W. , Hesselmann, G.J., (2013), Doosan Power Systems OxyCoal™ Burner Technology Development, Energy Procedia, Volume 37, 2013, Pages 6481-6488, ISSN 1876-6102,

http://dx.doi.org/10.1016/j.egypro.2013.06.578.

(http://www.sciencedirect.com/science/article/pii/S1876610213008217

Tanaka, A., Sakamoto, Y., Mayumi, D., Kano, Y., Higashino, H., Suzumura, M., Sagisaka, M., Nishi, Y., Nakao, S., (2014), Schematic Feasibility Study of Bio-CCS Technology, Energy

Procedia, Volume 63, 2014, Pages 8062-8068, ISSN 1876-6102, http://dx.doi.org/10.1016/j.egypro.2014.11.843.

(http://www.sciencedirect.com/science/article/pii/S1876610214026587)

The Climate Group, (2015), China Premier Li Keqiang vows to crack down on climate laws and pollution, 6 March 2015. Available on:

http://www.theclimategroup.org/what-we-do/news-and-blogs/china-premier-li-keiqiang-vows-to-crack-down-on-climate-laws-and-pollution/

[Last Accessed 29/03/2015]

The Global Commission for the Economy and Climate, (2014), The New Climate Economy Report. Available on:

http://newclimateeconomy.report/misc/downloads/ [Last Accessed 29/03/2015]

The Trades Union Congress (TUC) and Carbon Capture and Storage Association (CCSA), (2013), A UK Vision for Carbon Capture and Storage, Orion Innovations (UK) Ltd. Available on:

www.tuc.org.uk/sites/default/files/UKVisionforCCS.doc [Last Accessed 29/03/2015]

Ting, T., Stanger, R., Wall, T., (2014), Oxyfuel CO_2 compression: The gas phase reaction of elemental mercury and NOx at high pressure and absorption into nitric acid, International Journal of Greenhouse Gas Control, Volume 29, October 2014, Pages 125-134, ISSN 1750-5836, http://dx.doi.org/10.1016/j.ijggc.2014.08.007.

(http://www.sciencedirect.com/science/article/pii/S1750583614002333)

Toftegaard, M.B., Brix, J., Jensen, P.A., Glarborg, P., Jensen, A.D., (2010), Oxy-fuel combustion of solid fuels, Progress in Energy and Combustion Science, Volume 36, Issue 5, October 2010, Pages 581-625, ISSN 0360-1285, http://dx.doi.org/10.1016/j.pecs.2010.02.001.

(http://www.sciencedirect.com/science/article/pii/S0360128510000201)

Toptas, A., Yildirim, Y., Duman, G., Yanik, J., (2015), Combustion behavior of different kinds of torrefied biomass and their blends with lignite, Bioresource Technology, Volume 177, February 2015, Pages 328-336, ISSN 0960-8524, http://dx.doi.org/10.1016/j.biortech.2014.11.072.

(http://www.sciencedirect.com/science/article/pii/S0960852414016745)

Trabadela, I., (2012), An Overview of research activities on coal dust ignition at NIOSH, US October-December 2011, OxyCAP UK Meeting, 19th April 2012, University of Edinburgh, UK.

Trabadela, I., (2012), Impact of the OxyCAP UK project, Impact statement as part of the RAPID process, phase 1, UKCCSRC Early Career Researchers Meeting, 25th June 2012, University of Leeds, UK.

Trabadela, I., Chalmers, H. and Gibbins, J., (2012), Opportunities for improving oxy-fuel flexibility and operational conditions, 9th European Conference on Coal Research and its Applications (ECCRIA9), University of Nottingham (UK) 10-12 September 2012.

Trabadela I., Chalmers H. and Gibbins J., (2013) Coal dust ignition experiments for oxy-fuel safety, 3rd Oxy-fuel Combustion Conference (OCC3), International Energy Agency Greenhouse Gases Programme (IEAGHG), Ponferrada/CIUDEN (Spain) 9-13 September 2013.

Trabadela, I., Chalmers, H. and Gibbins, J., (2014), Oxy-biomass Ignition in Air and Relevant Oxy-combustion Atmospheres for Safe Primary Recycle and Oxy-burner Development, Energy Procedia, Volume 63, 2014, Pages 403-414, ISSN 1876-6102, http://dx.doi.org/10.1016/j.egypro.2014.11.042.

(http://www.sciencedirect.com/science/article/pii/S1876610214018578)

Uchida, T., Goto, T., Yamada, T., Kiga, T., Spero, C., (2013), Oxyfuel Combustion as CO_2 Capture Technology Advancing for Practical use - Callide Oxyfuel Project -, Energy Procedia, Volume 37, 2013, Pages 1471-1479, ISSN 1876-6102, http://dx.doi.org/10.1016/j.egypro.2013.06.022.

(http://www.sciencedirect.com/science/article/pii/S1876610213002658)

UK CCS Research Centre (UKCCSRC), (2015), Centre Pilot-scale Advanced Capture Technology (PACT) facilities. Available on:

http://www.pact.ac.uk [Last Accessed 29/03/2015]

United Nations Framework Convention on Climate Change (UNFCCC), (2012), Report of the Conference of the Parties on its seventeenth session, held in Durban from 28 November to 11 December 2011, Bonn, Germany. Available on:

http://unfccc.int/resource/docs/2011/cop17/eng/09a01.pdf#page=2

[Last Accessed 29/03/2015]

United Nations Framework Convention on Climate Change (UNFCCC), (2015), Negotiating text, Work of the Contact Group on item 3, ADP Second session, part eight (2.8) 8-13 February, 12 February 2015, Geneva, Switzerland. Available on:

https://unfccc.int/files/bodies/awg/application/pdf/negotiating_text_12022015@2200.pdf

[Last Accessed 29/03/2015]

University of Edinburgh, Health and Safety Department, (2010), Health and Safety Policy - Part 4 Mechanical Equipment, the University of Edinburgh. Available on:

http://www.docs.csg.ed.ac.uk/Safety/Policy/Part4.pdf [Last Accessed 29/03/2015]

US Energy Information Administration (EIA), (2015), Market Prices and Uncertainty Report, February 2015. Available on:

http://www.eia.gov/forecasts/steo/pdf/uncertainty.pdf [Last Access 28/02/2015]

Verakis, H.C. and Nagy, J., (1987), A Brief History of Dust Explosions, Industrial Dust Explosions, ASTM STP 958, Kenneth L. Cashdollar and Martin Hertzberg, Eds., American Society for Testing and Materials, Philadelphia, 1987, pp. 342-350.

Vergragt, P.J., Markusson, N., Karlsson, H., (2011), Carbon capture and storage, bio-energy with carbon capture and storage, and the escape from the fossil-fuel lock-in, Global Environmental Change, Volume 21, Issue 2, May 2011, Pages 282-292, ISSN 0959-3780, http://dx.doi.org/10.1016/j.gloenvcha.2011.01.020.

(http://www.sciencedirect.com/science/article/pii/S0959378011000215)

Visilume, (2012), Viewport specifications.

Wall, T., Liu, Y., Spero, C., Elliott, L., Khare, S., Rathnam, R., Zeenathal, F., Moghtaderi, B., Buhre, B., Sheng, C., Gupta, R., Yamada, T., Makino, K., Yu, J., (2009), An overview on oxyfuel coal combustion—State of the art research and technology development, Chemical Engineering Research and Design, Volume 87, Issue 8, August 2009, Pages 1003-1016, ISSN 0263-8762, http://dx.doi.org/10.1016/j.cherd.2009.02.005

(http://www.sciencedirect.com/science/article/pii/S0263876209000598)

Wall, T., Stanger, R. and Santos, S., (2011), Demonstrations of coal-fired oxy-fuel technology for carbon capture and storage and issues with commercial deployment, International Journal of Greenhouse Gas Control, Volume 5, Supplement 1, July 2011, Pages S5-S15, ISSN 1750-5836, http://dx.doi.org/10.1016/j.ijggc.2011.03.014.

(http://www.sciencedirect.com/science/article/pii/S1750583611000442)

Weatherstone S., (2014), Biomass analysis for OxyCAP UK project, E.ON, [Personal communication].

White, V., Wright, A., Tappe, S., Yan, J., (2013), The Air Products Vattenfall Oxyfuel CO_2 Compression and Purification Pilot Plant at Schwarze Pumpe, Energy Procedia, Volume 37, 2013, Pages 1490-1499, ISSN 1876-6102, http://dx.doi.org/10.1016/j.egypro.2013.06.024.

(http://www.sciencedirect.com/science/article/pii/S1876610213002671)

Wilén, C., Moilanen, A., Rautalin, A., Torrent, J., Conde, E., Lodel, R., Carson, D., Timmers, P., Brehm, K., (1999), Safe Handling of Renewable Fuels and Fuel Mixtures, Technical Research Centre of Finland (1999).

Yang, M., Blyth, W., Bradley, R., Bunn, D., Clarke, C., Wilson, T., (2008), Evaluating the power investment options with uncertainty in climate policy, Energy Economics, Volume 30, Issue 4, July 2008, Pages 1933-1950, ISSN 0140-9883, http://dx.doi.org/10.1016/j.eneco.2007.06.004.

(http://www.sciencedirect.com/science/article/pii/S0140988307000801)

Yi, B., Zhang, L., Huang, F., Mao, Z., Zheng, C., (2014), Effect of H_2O on the combustion characteristics of pulverized coal in O_2/CO_2 atmosphere, Applied Energy, Volume 132, 1 November 2014, Pages 349-357, ISSN 0306-2619, http://dx.doi.org/10.1016/j.apenergy.2014.07.031.

(http://www.sciencedirect.com/science/article/pii/S0306261914007120)

Yuzbasi, N.S., and Selçuk, N., (2011), Air and oxy-fuel combustion characteristics of biomass/lignite blends in TGA-FTIR, Fuel Processing Technology, Volume 92, Issue 5, May 2011, Pages 1101-1108, ISSN 0378-3820, http://dx.doi.org/10.1016/j.fuproc.2011.01.005.

(http://www.sciencedirect.com/science/article/pii/S0378382011000233)

Zakkour, P., Scowcroft, J., Heidug, W., The Role of UNFCCC Mechanisms in Demonstration and Deployment of CCS Technologies, Energy Procedia, Volume 63, 2014, Pages 6945-6958, ISSN 1876-6102, http://dx.doi.org/10.1016/j.egypro.2014.11.728.

(http://www.sciencedirect.com/science/article/pii/S1876610214025430)

Zebian, H. and Mitsos, A., (2014), Pressurized OCC (oxy-coal combustion) process ideally flexible to the thermal load, Energy, Volume 73, 14 August 2014, Pages 416-429, ISSN 0360-5442, http://dx.doi.org/10.1016/j.energy.2014.06.031.

(http://www.sciencedirect.com/science/article/pii/S0360544214007294

Zero Emissions Platform (ZEP), (2013), CO_2 Capture and Storage (CCS). Recommendations for transitional measures to drive deployment in Europe. European Technology Platform for Zero Emission Fossiel Fuel Plants. Available on:

http://www.zeroemissionsplatform.eu/ [Last Accessed 29/03/2015]

Zhang, L., Ren, B., Huang, H., Li, Y., Ren, S., Chen, G., Zhang, H., (2015), CO_2 EOR and storage in Jilin oilfield China: Monitoring program and preliminary results, Journal of Petroleum Science and Engineering, Volume 125, January 2015, Pages 1-12, ISSN 0920-4105, http://dx.doi.org/10.1016/j.petrol.2014.11.005.

(http://www.sciencedirect.com/science/article/pii/S0920410514003659)

Publications list

Trabadela, I., Chalmers, H. and Gibbins, J., (2014), Oxy-biomass Ignition in Air and Relevant Oxy-combustion Atmospheres for Safe Primary Recycle and Oxy-burner Development, Energy Procedia, Volume 63, 2014, Pages 403-414, ISSN 1876-6102, http://dx.doi.org/10.1016/j.egypro.2014.11.042.

(http://www.sciencedirect.com/science/article/pii/S1876610214018578)

Trabadela I., Chalmers H. and Gibbins J., (2014), Experimental Ignition of biomass and coal particles in oxy-fuel atmospheres for CO_2 capture, 10th European Conference on Coal Research and its Applications (ECCRIA10), University of Hull (UK) 15-17 September 2014.

Trabadela I., Chalmers H. and Gibbins J., (2014), Comparison of biomass pulverised fuel ignition behaviour in air and oxygen/carbon dioxide mixtures using a 20-L sphere apparatus, 35th Symposium on Combustion, San Francisco, USA, 2-8 August 2014.

Trabadela I., Chalmers H. and Gibbins J., (2014), Impact of oxygen and carbon dioxide levels in pulverised fuel ignition for air to oxy-combustion power plant operation, 13th CCUS, Pittsburgh, USA, 28 April – 2 May 2014.

Trabadela I., Chalmers H. and Gibbins J., (2013) Coal dust ignition experiments for oxy-fuel safety, 3rd Oxy-fuel Combustion Conference (OCC3), International Energy Agency Greenhouse Gases Programme (IEAGHG), Ponferrada/CIUDEN (Spain) 9-13 September 2013.

Trabadela, I., Chalmers, H. and Gibbins, J., (2012), Opportunities for improving oxy-fuel flexibility and operational conditions, 9th European Conference on Coal Research and its Applications (ECCRIA9), University of Nottingham (UK) 10-12 September 2012.

Appendix

A.1. R-20 Drawings

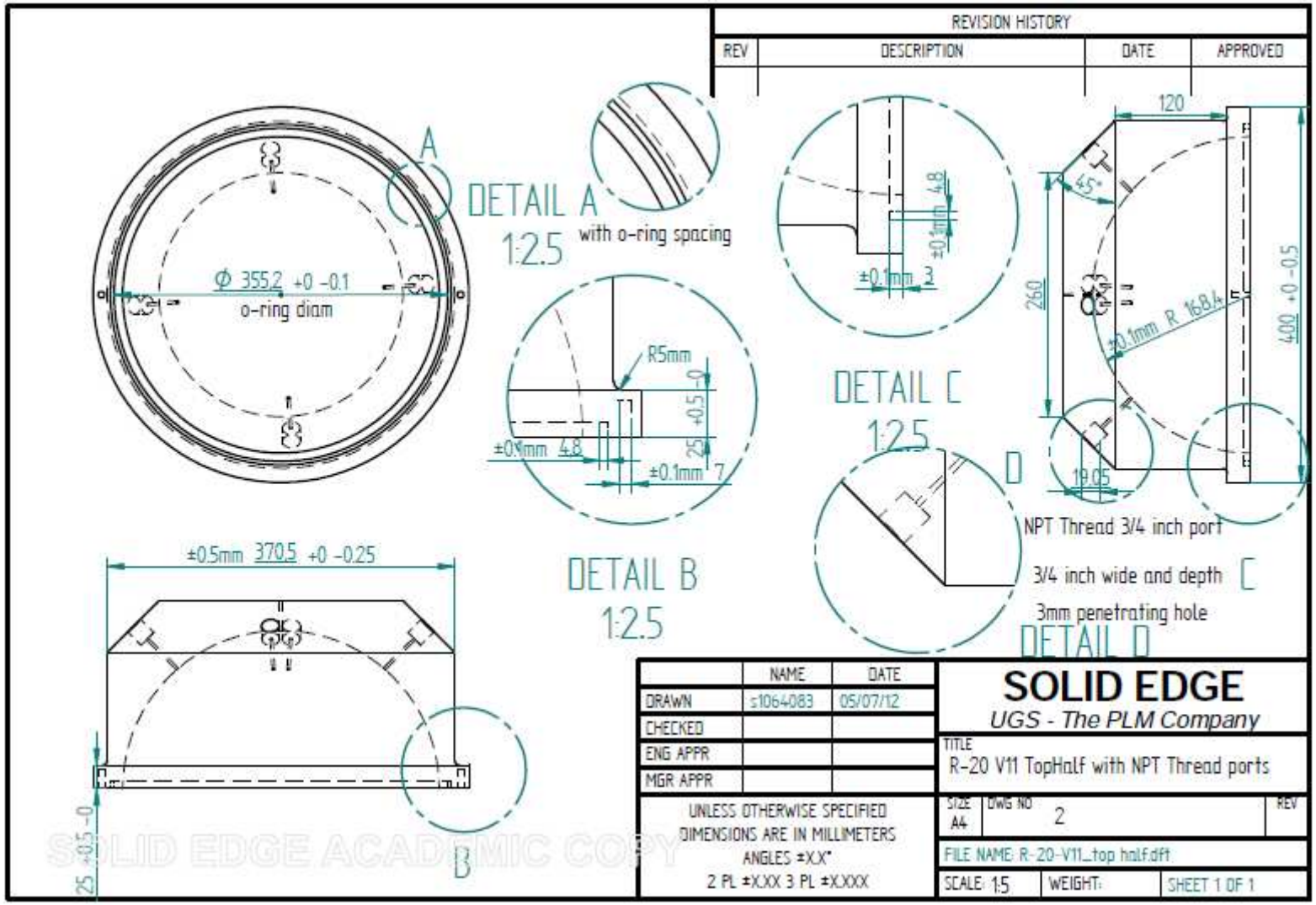

Figure A.1.1. Drawing of R-20 top half of ignition chamber with NPT thread ports

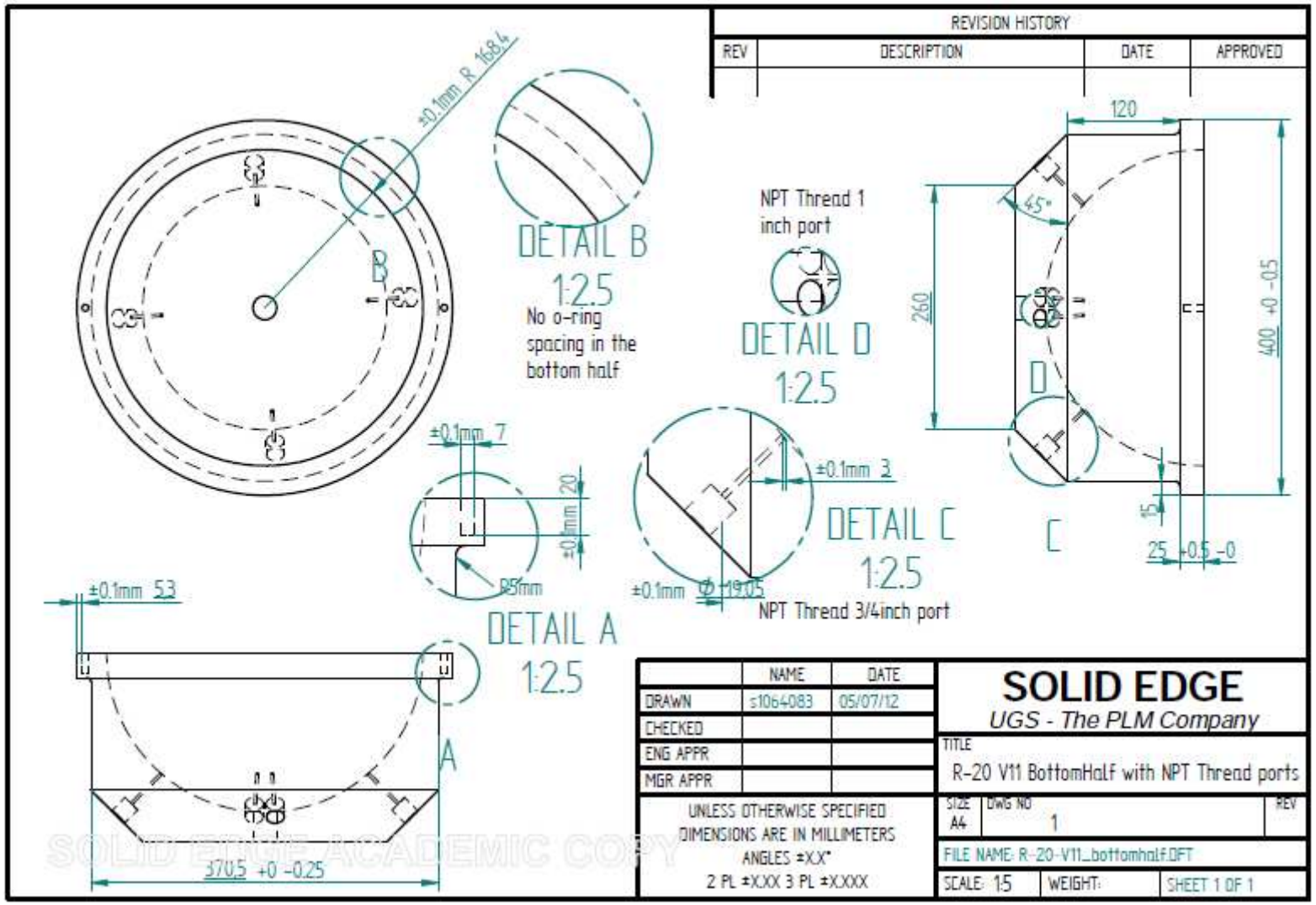

Figure A.1.2. Drawing of R-20 bottom half of ignition chamber with NPT thread ports

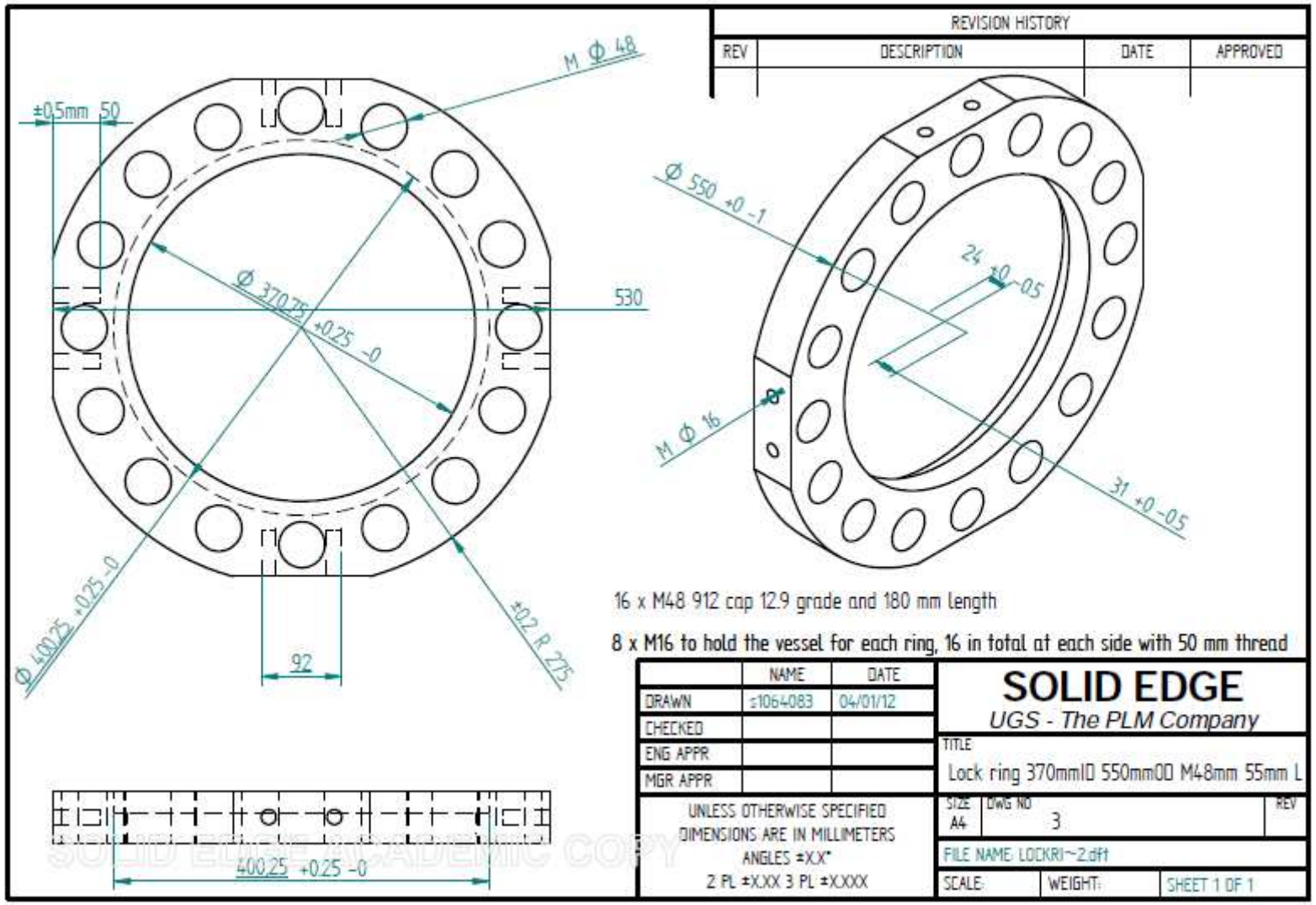

Figure A.1.3. Drawing of Lock ring 370 mm ID, 550 mm OD M48 mm 55 mm L

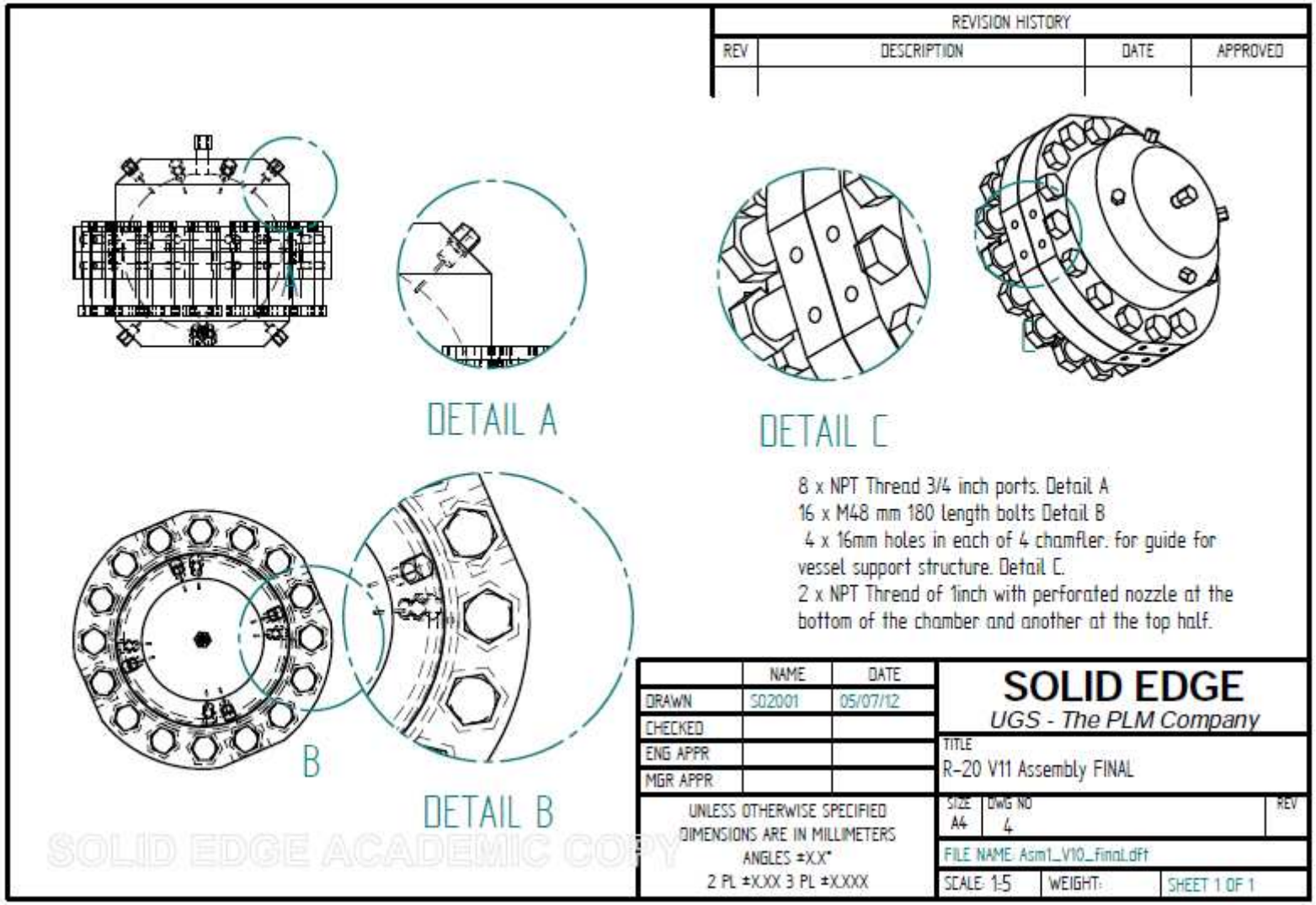

Figure A.1.4. Drawing of R-20 Assembly Final

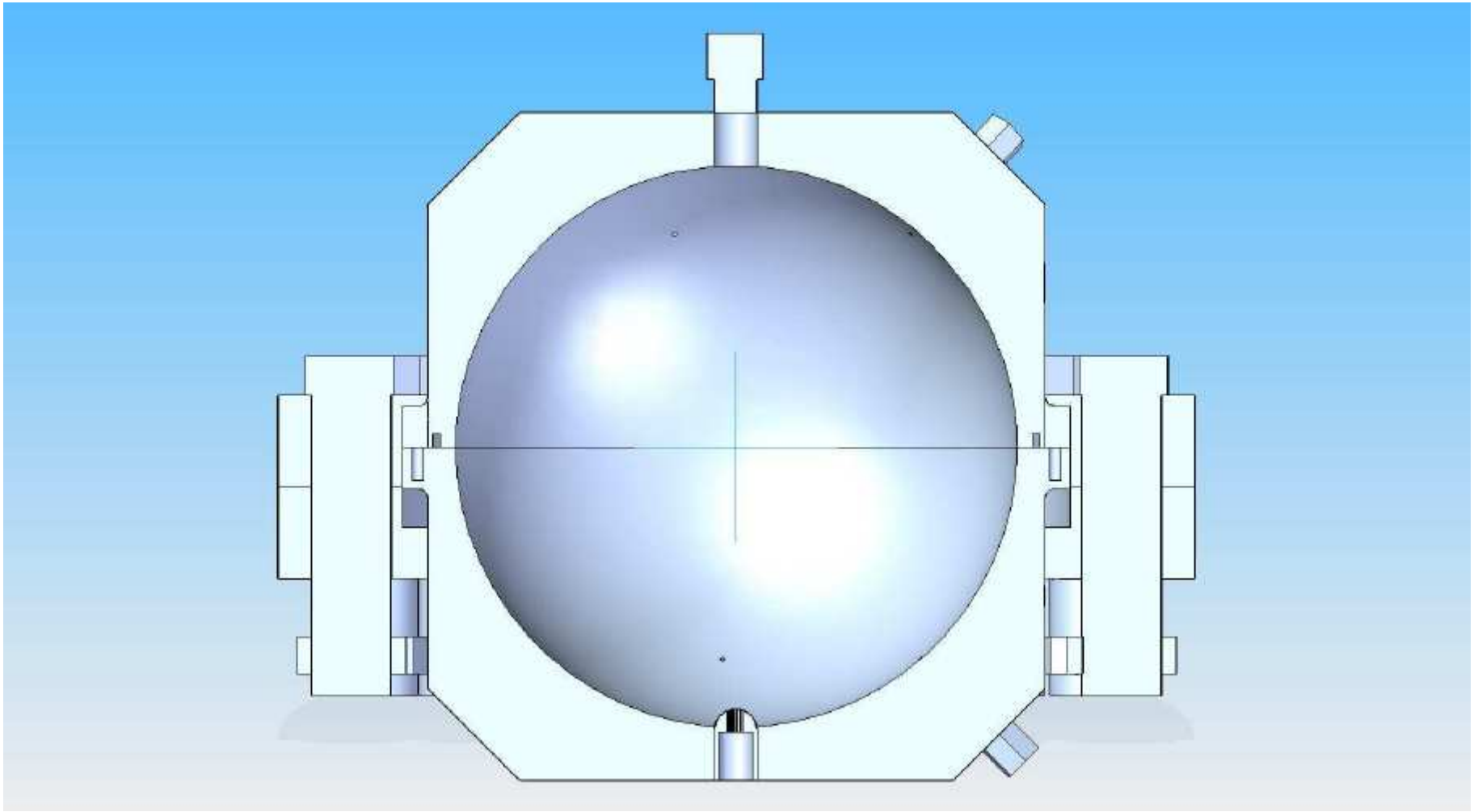

Figure A.1.5. Cross-section of R-20 ignition chamber

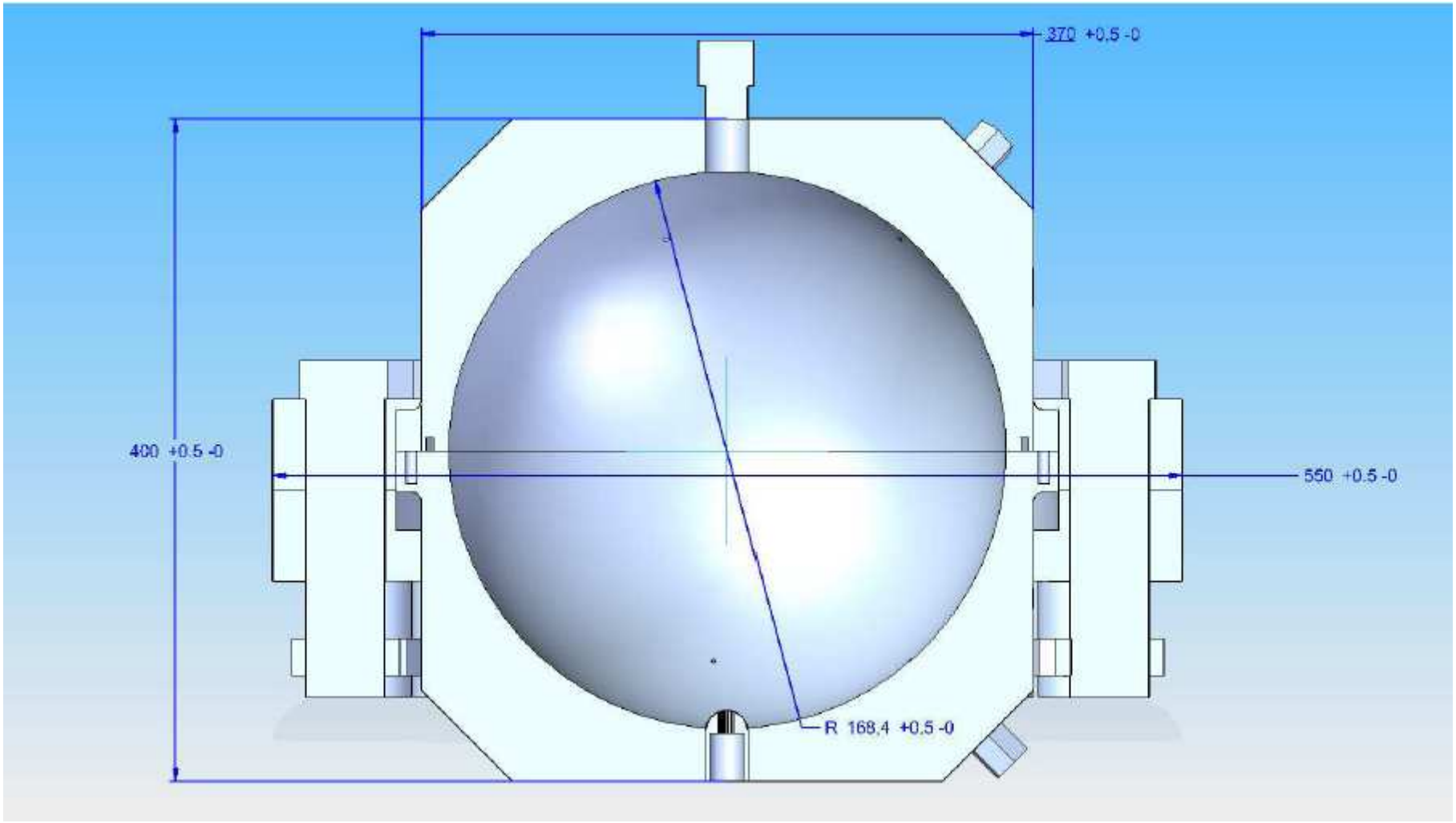

Figure A.1.6. Cross-section of R-20 ignition chamber with key dimensions

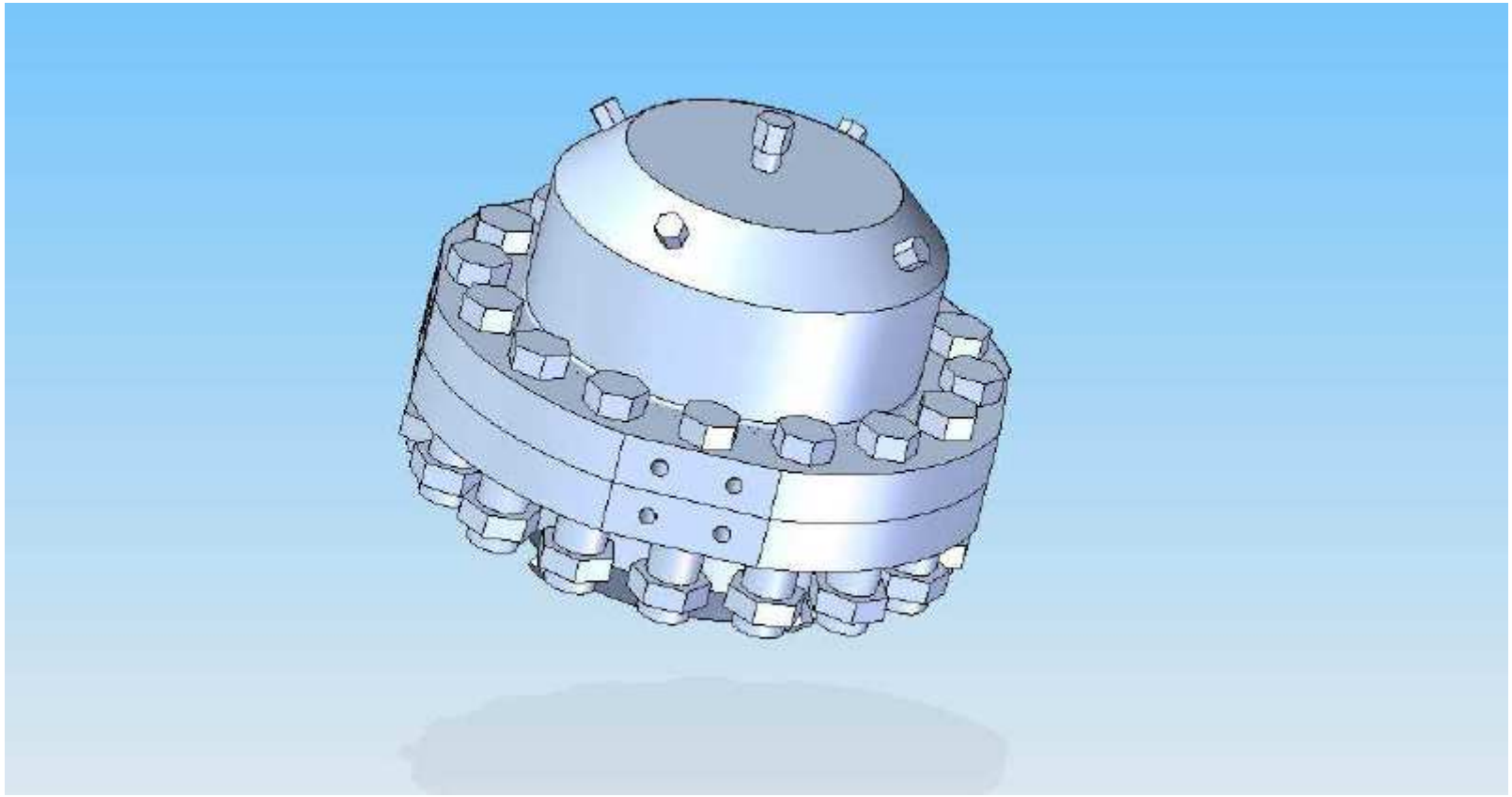

Figure A.1.7. R-20 ignition chamber isometric view

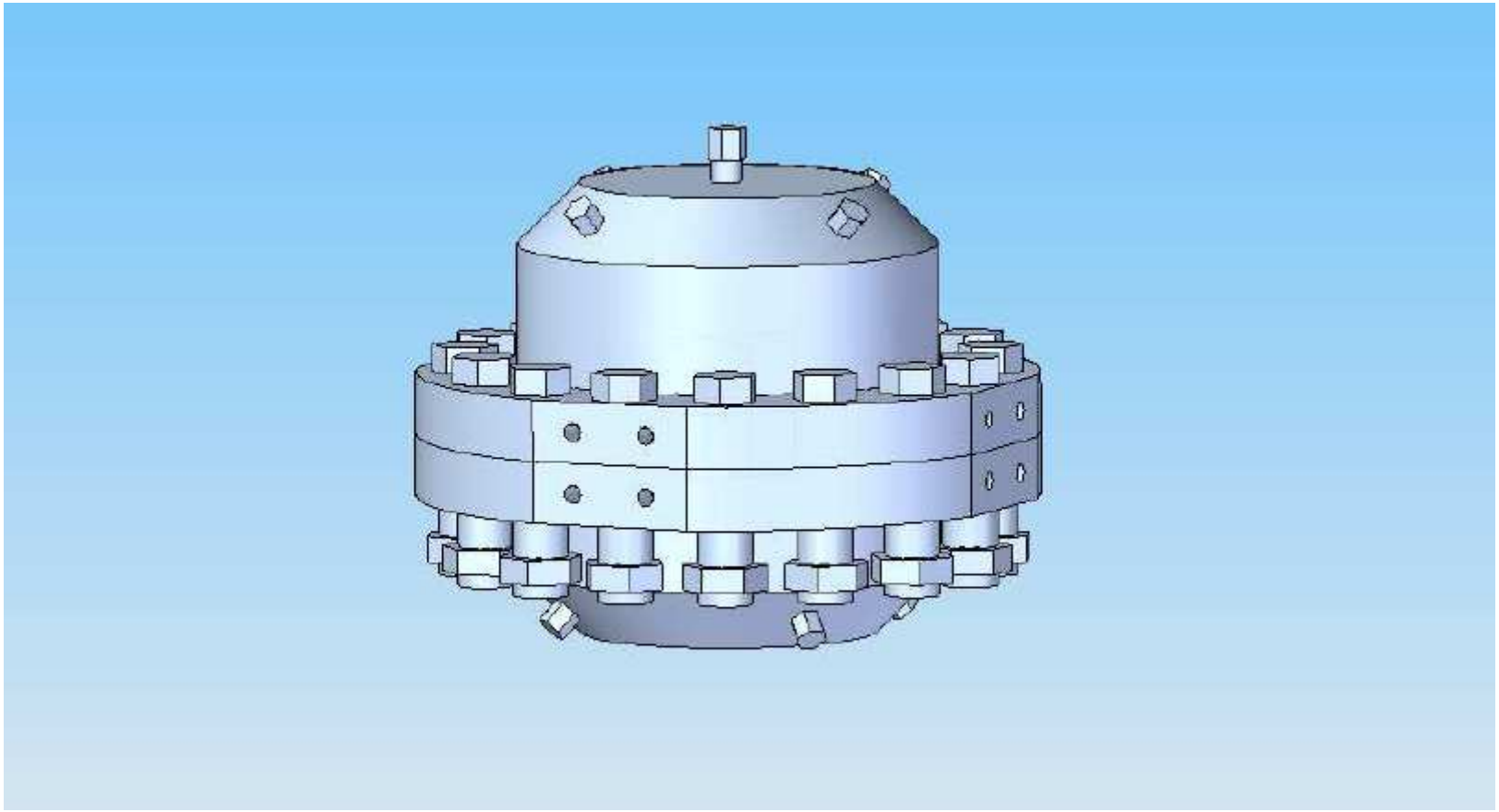

Figure A.1.8. R-20 ignition chamber front view

A.2. Drawings

(R-30)

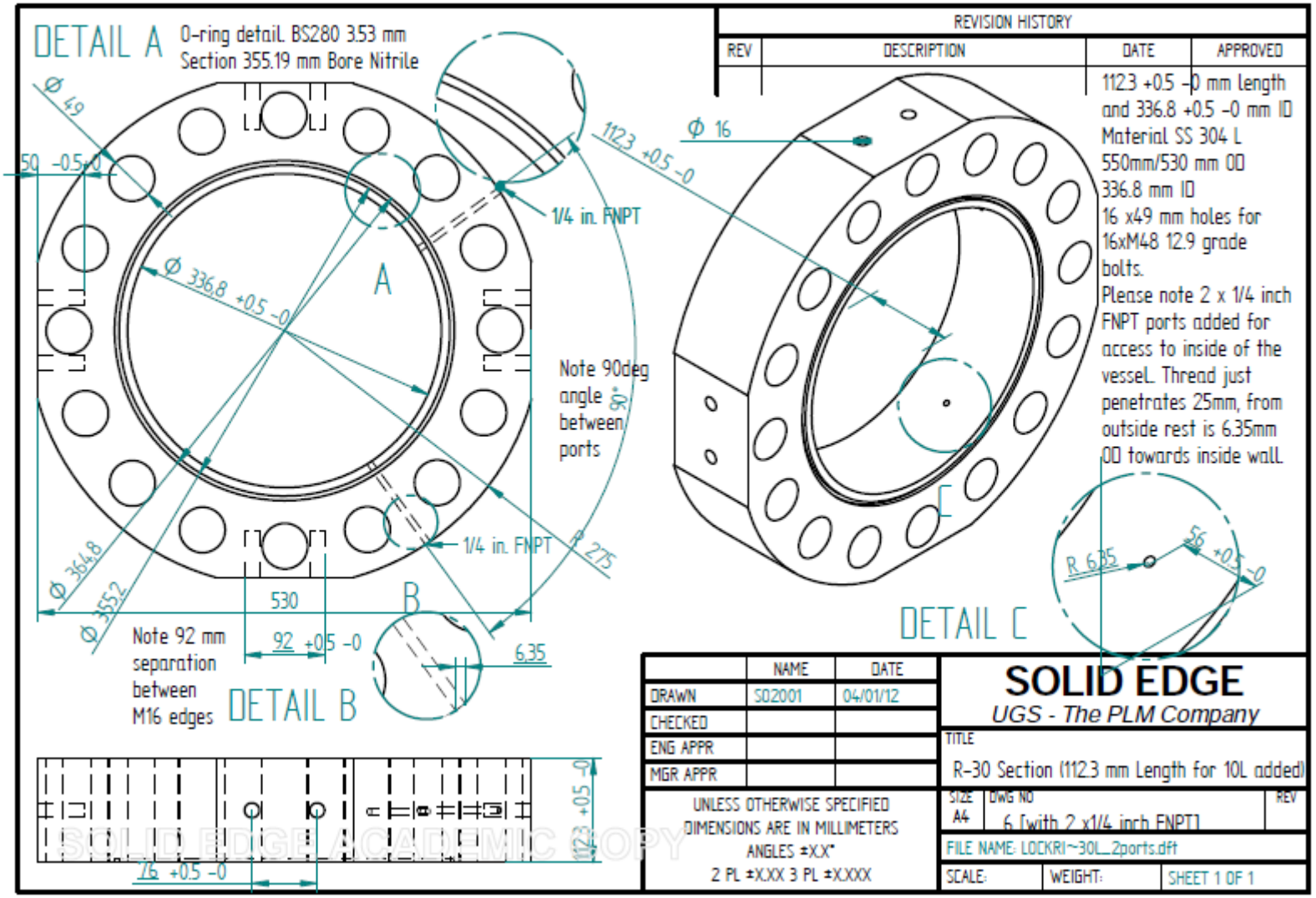

Figure A.2.1. Drawing of R-30 section (112.3 mm length for 10 L added)

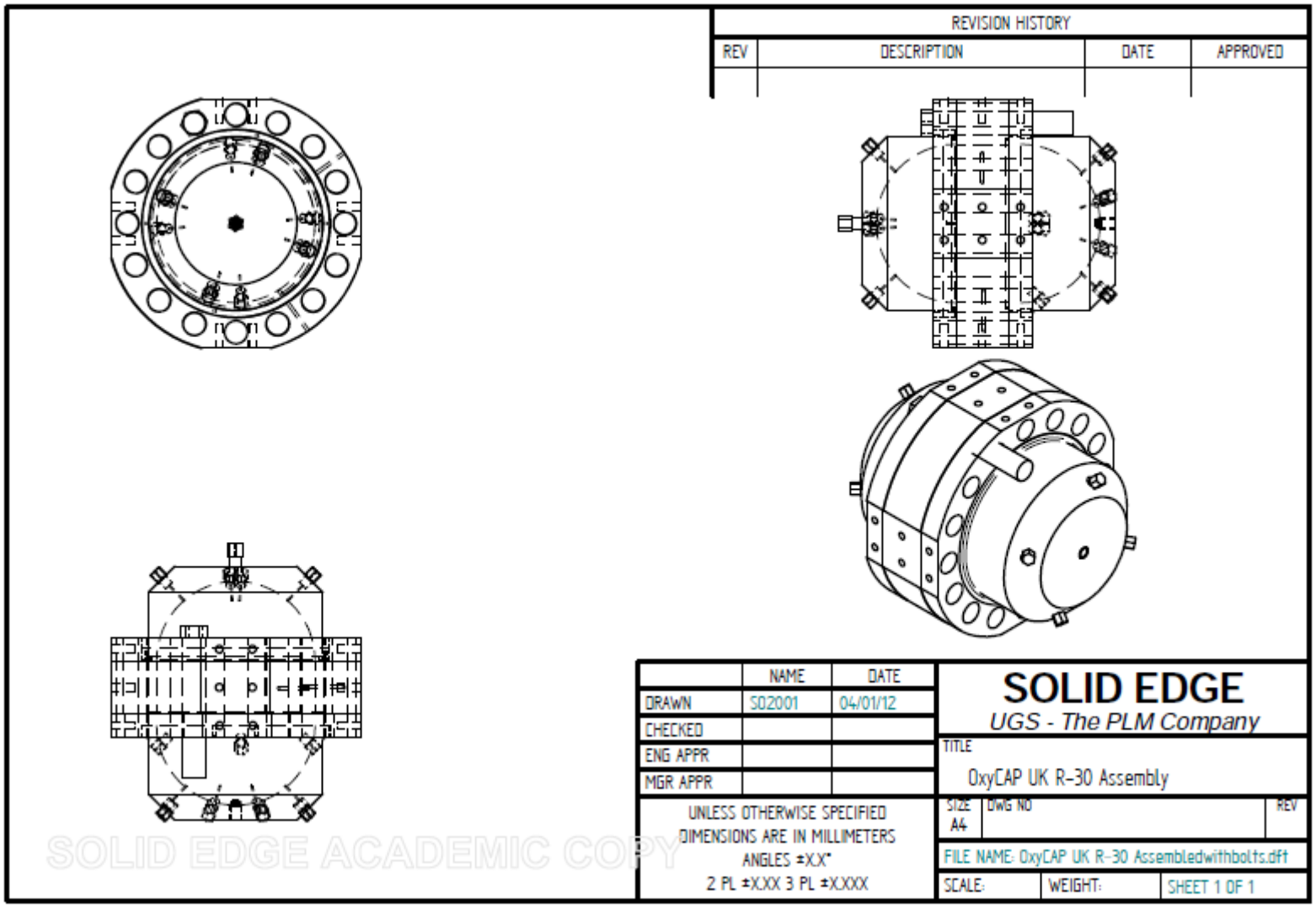

Figure A.2.2. Drawing of R-30 Assembly Final

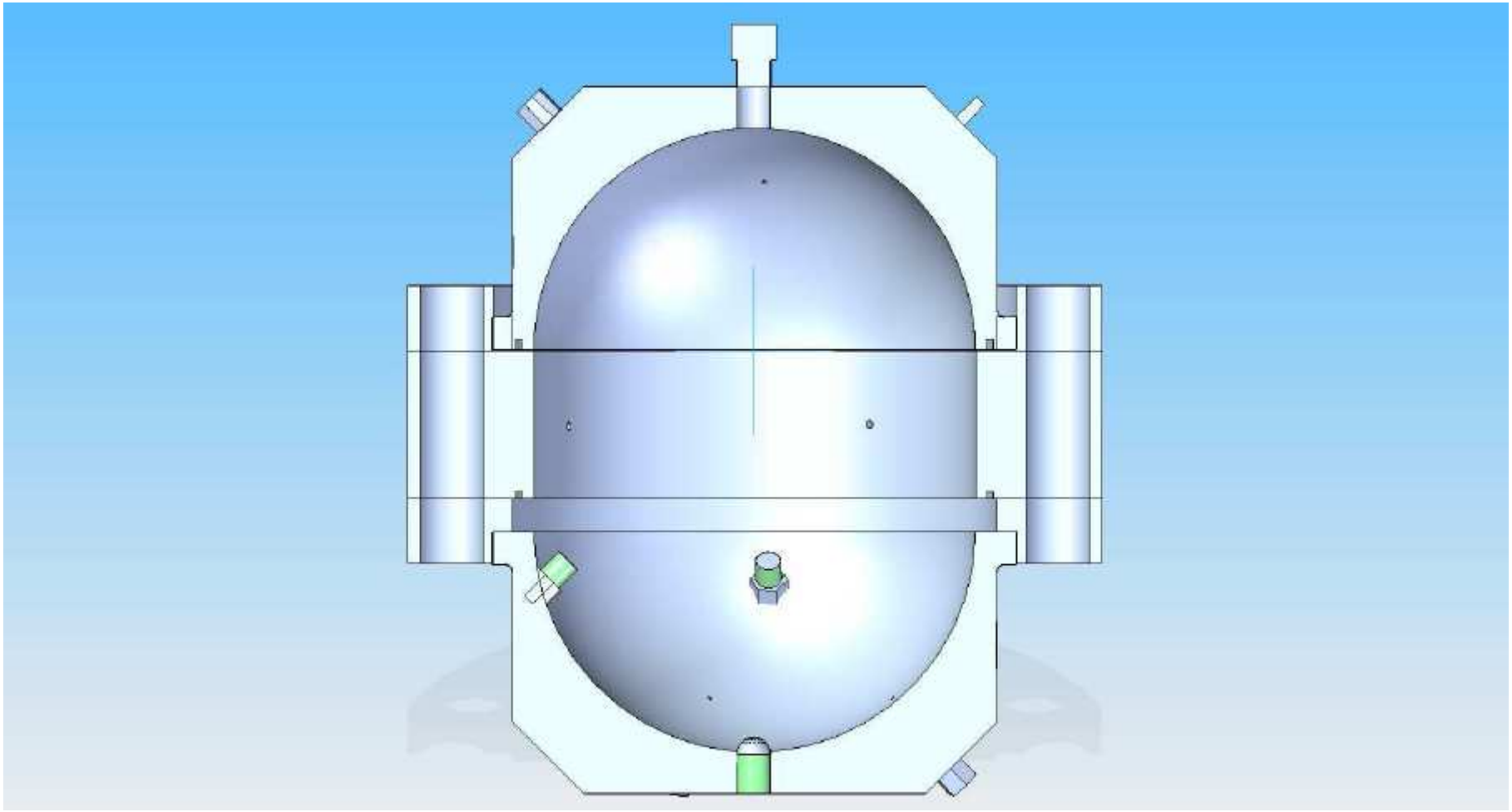

Figure A.2.3. Cross-section of R-30 ignition chamber

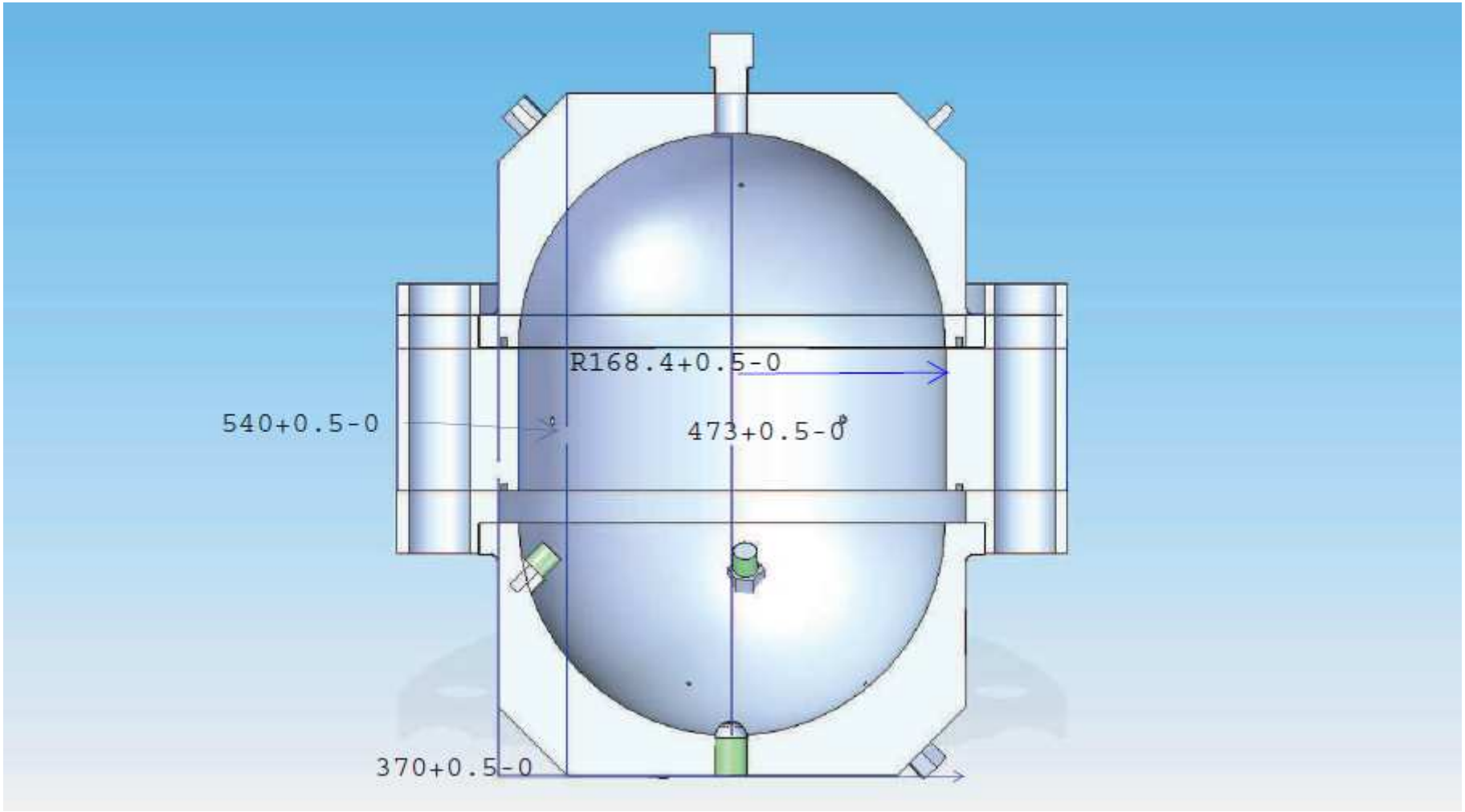

Figure A.2.4. Cross-section of R-30 ignition chamber with key dimensions

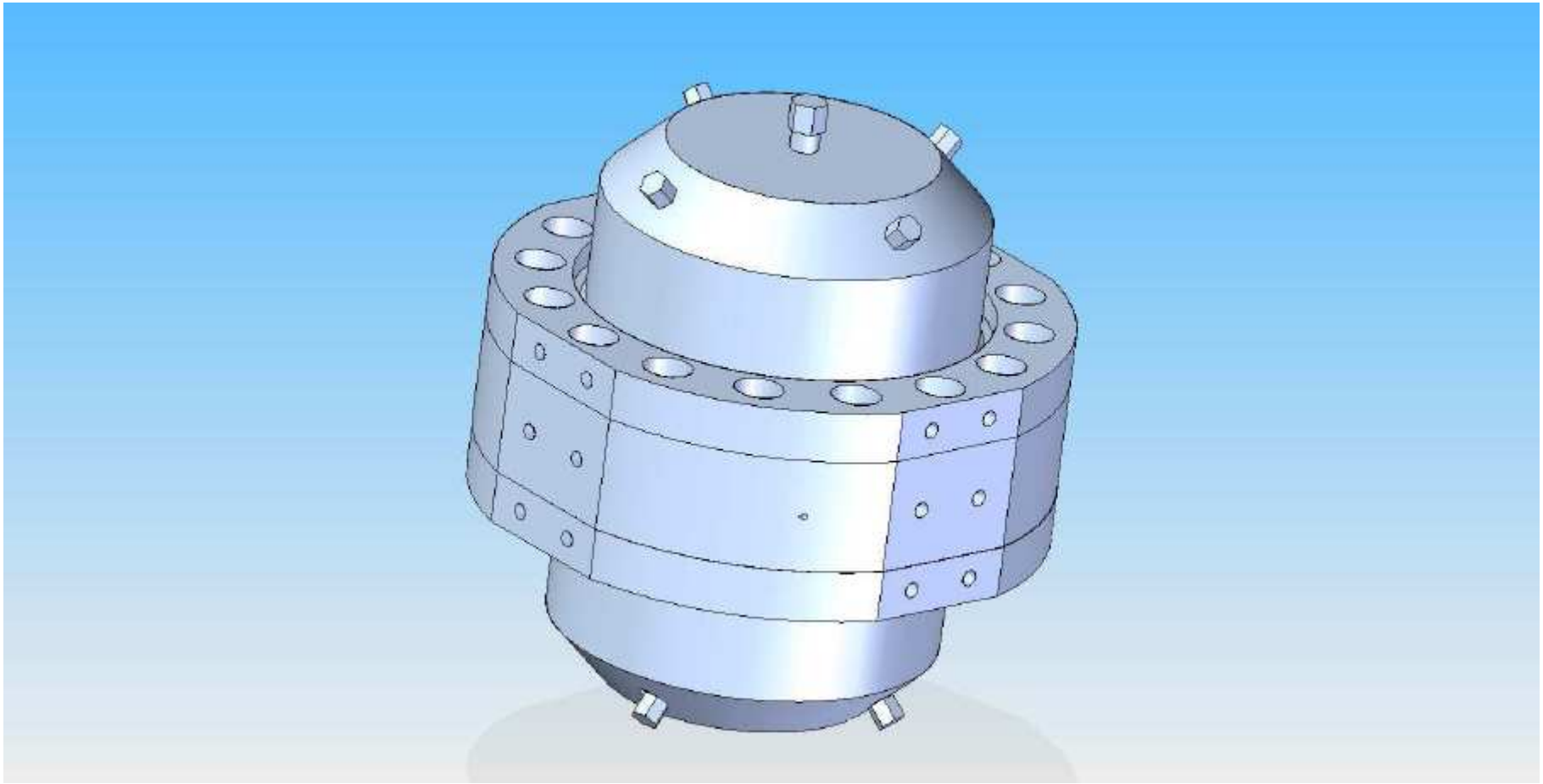

Figure A.2.5. R-30 ignition chamber isometric view

A.3. Drawings

Dispersion Nozzles

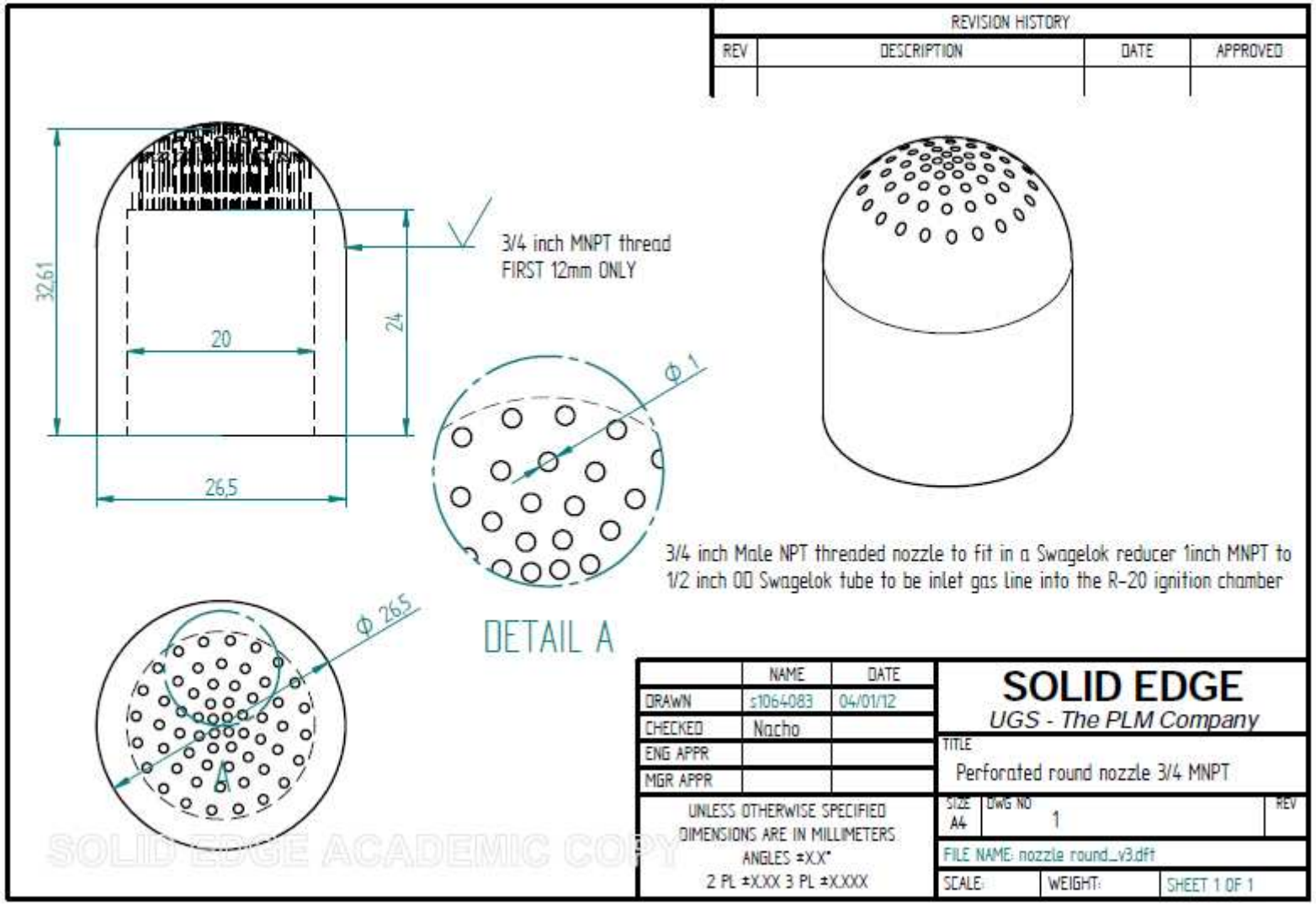

Figure A.3.1. Drawing of Perforated round nozzle ¾ inch MNPT

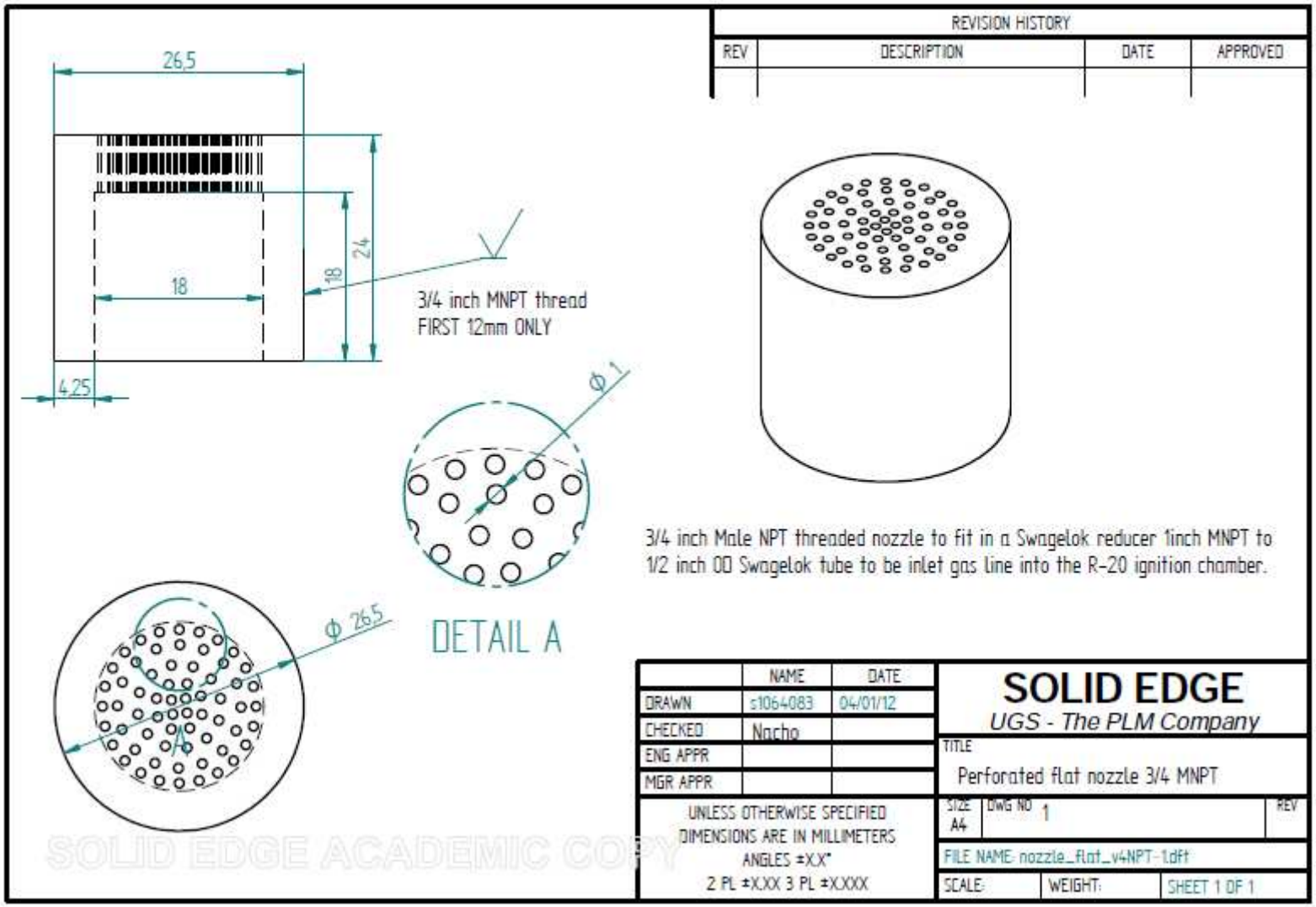

Figure A.3.2. Drawing of Perforated flat nozzle ¾ inch MNPT

A.4. Stresses analysis – ANSYS (Prof. Kamenev's group)

Directional Deformation

Subject: R-20 Author: Prof. K. Kamenev's Group Prepared For: I. Trabadela Date Tuesday, April 26, 2011

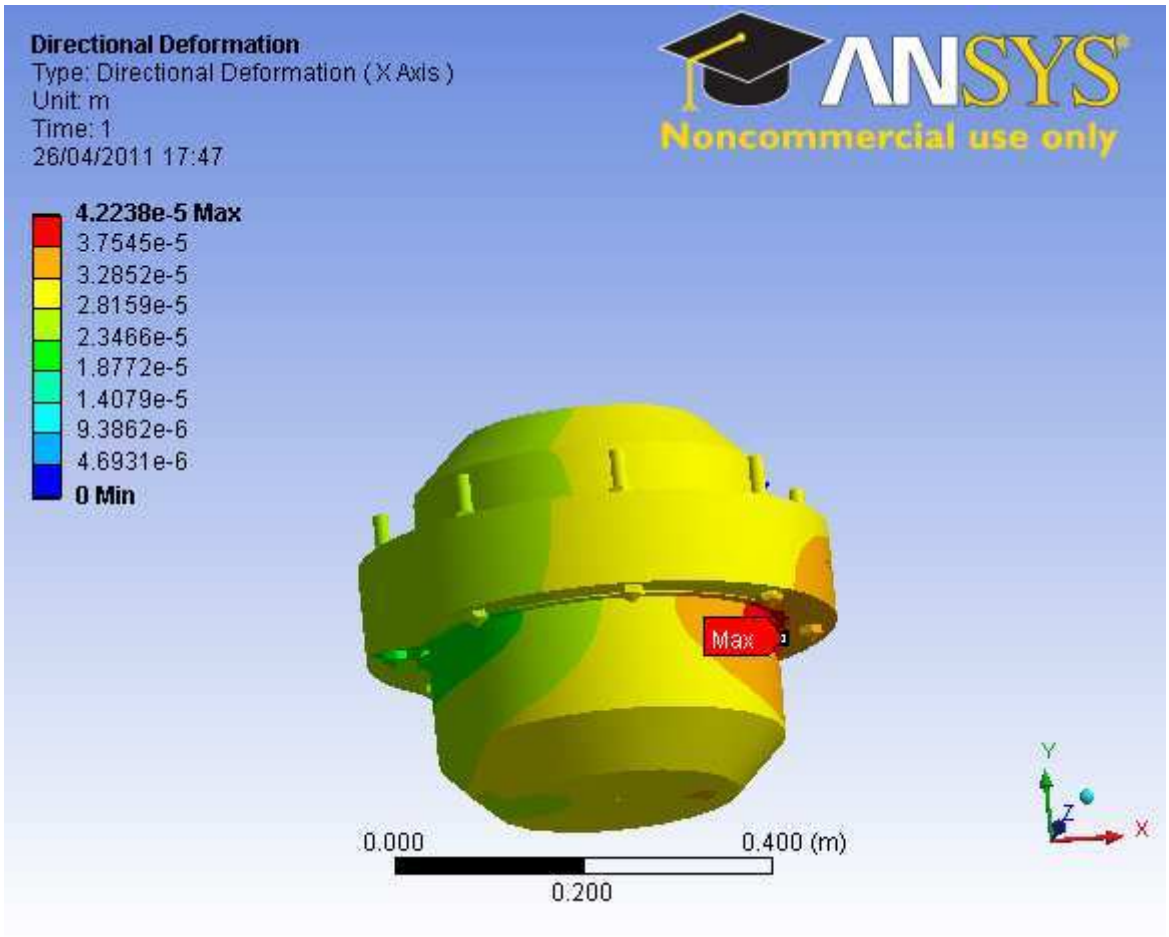

Equivalent Elastic Strain

Subject: R-20 Author: Prof. K. Kamenev's Group Prepared For: I. Trabadela Date Tuesday, April 26, 2011

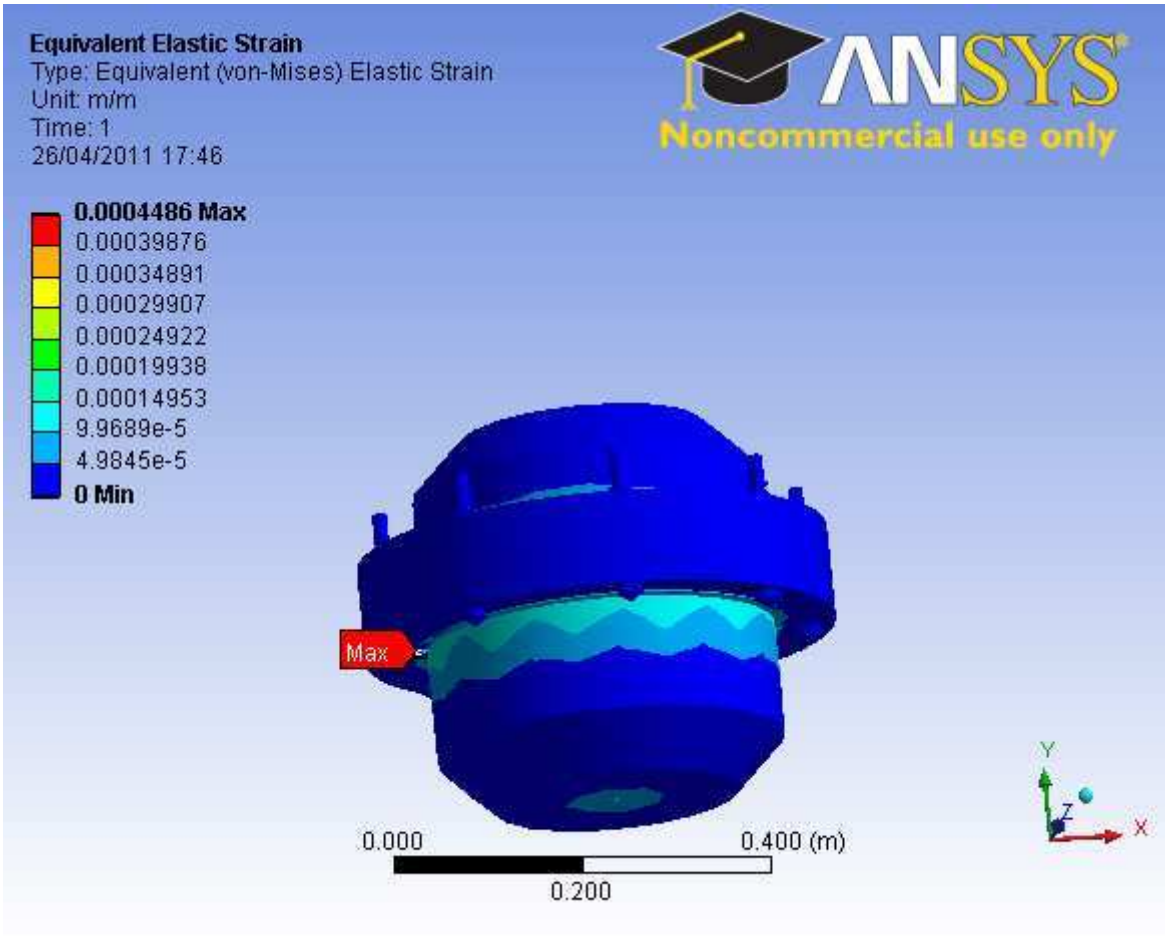

Equivalent Stress

Subject: R-20 Author: Prof. K. Kamenev's Group Prepared For: I. Trabadela Date Tuesday, April 26, 2011

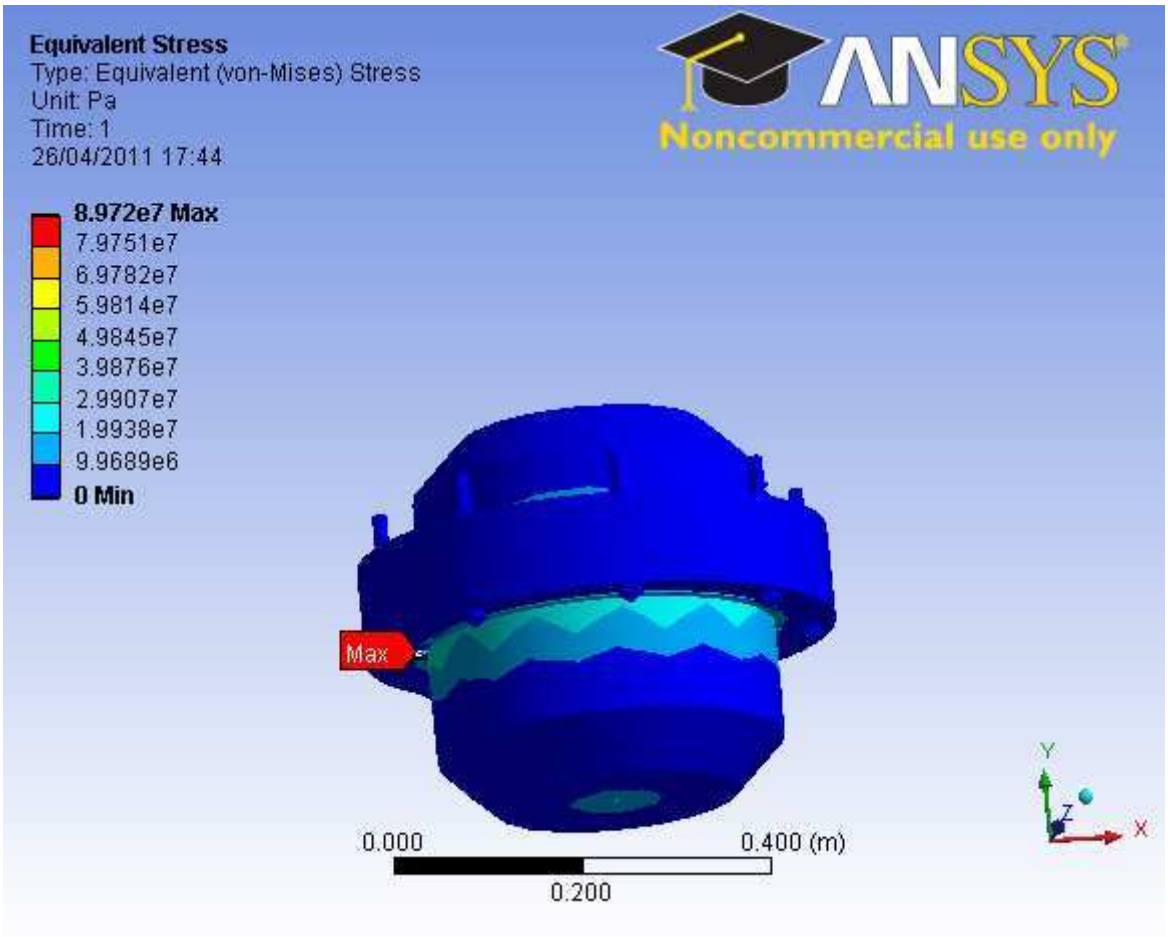

Equivalent Stress

Subject: R-20 Author: Prof. K. Kamenev's Group Prepared For: I. Trabadela Date Tuesday, April 26, 2011

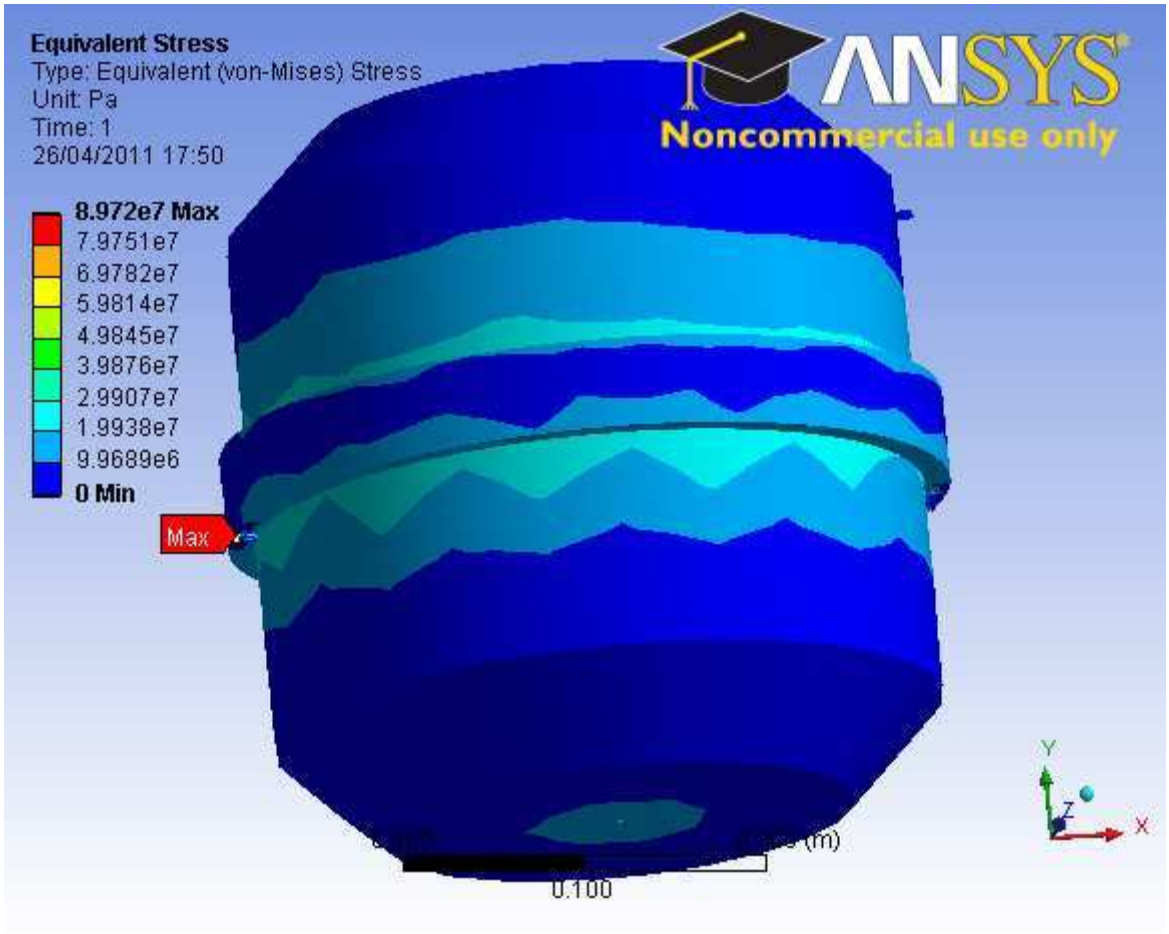

Equivalent Stress

Subject: R-20 Author: Prof. K. Kamenev's Group Prepared For: I. Trabadela Date Tuesday, April

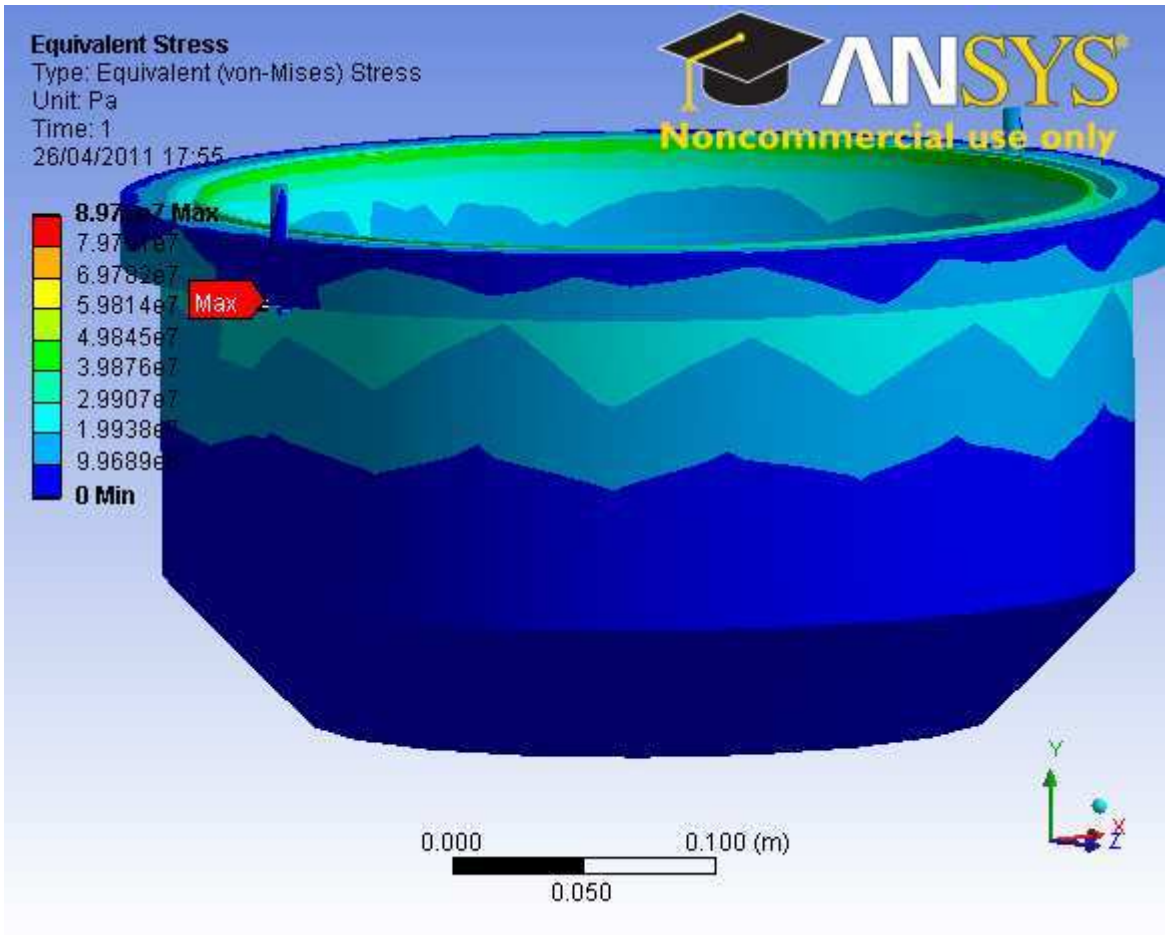

A.5. Material Specifications

Auftrag: 189881 Komm.schein: 819034 Kundenr: 11022 Ihre Ref.: 1/2115756

B. 3112900

ITALFOND
STAINLESS STEEL AND SUPERALLOYS
Tel. (+39).(030).6829811
Fax. (39).(030).6820616
Via Industriale, 1 - 25021 BAGNOLO MELLA (BS) ITALY

BESCHEINIGUNG ÜBER QUALITÄT UND WERKSTOFFPRÜFUNGEN

Certificate of quality and materials tests

ABNAHMEPRÜFZEUGNIS-Nr. AC/ 0092 **DATUM** 19/01/11
Certificate-No. DATE:

Bescheinigung über Werkstoffprüfungen nach EN 10204.3.1
Inspection certificate according to EN 10204.3.1

BESTELLER: DAMSTAHL GmbH - LANGENGELD (GERMANY)
Customer

BESTELL-Nr. : 330.166 **AUFTRAGBESTÄTIGUNG:** 100586
Order-No.: Order confirmation:

Schmelze-Nr. Heat-No.	Stücke Pieces	MATERIAL-BEZEICHNUNG Material description	WERKSTOFF-Nr. Material grade
48469	1	FORGED ROUND PEELED BAR 400 DIA Geschmiedeter und geschälter Stab dia 400	Wr. Nr. 1.4301/4307 304/304L DIN EN 10088-3 DIN EN 10272 DIN EN 10222-5 ASTM A276 ASTM A479 ASME Sec.II Part ASA479 Ed.04 NACE MR 01.75 / ISO 15156 PED 97/23 AD2000/W0

0005316949

Wärmebehandlungszustand: **Lösungsgeglüht 1050°C in Wasser abgeschreckt**
Condition of heat treatment: Solution annealed 1050° C + water quenched

Schmelzanalyse / Heat analysis

C	Mn	Si	P	S	Cr	Ni	Mo	Cu	Sn
0,022	1,83	0,35	0,030	0,0244	18,17	8,32			
Ca	**Al**	**V**	**Ti**	**W**	**Ta**	**As**	**Co**	**Nb**	**Pb**
B	**N**	**Zr**	**Sb**	**Fe**	**PRE**	Ferrit / Ferrite (%)		Korngröße ASTM E112	
	0,090								

PRÜFERGEBNISSE - TEST RESULTS ON ACTUAL BAR PROLUNGATION (per info)

Test nr.	Direction Norm	Rp0.2 [MPa]	Rp1 [MPa]	Rm [MPa]	A [%]	Z [%]	KV (10 X 10 mm) [J]	HB
1	EN/T	236	246	539	58,6	61,0	145-143-139	153
1	ASTM/T	235		542	55,0	57,9		HRc <0

Erschmelzung E.A.F. + A.O.D. / Steelmaking process E.A.F. + A.O.D. refining
Material ohne Schweißen / No welding performed on material
Material ohne Quecksilberverunreinigungen / Material free from Mercury contamination
Material durch Gammaspektrometer überprüft und ohne radioactive Verunreinigung über die nach EU-Radiation Protection 122-part 1 festgestellten Grenzwerte, wenn zugehörig / Material inspected with a gamma spectrometer and with no radioactive contamination beyond the limits provided for by the EU-Radiation Protection 122-part 1, when relevant
Mechanische Prüfungen gem./Mechanical tests performed acc.to UNI EN10002 (Probe/tensile Ø10mmx50mm) + ASTM A370 (tensile 0,5 x 2" gage specimen) + UNI EN10003/1. Bei Raumtemperatur/ At room temperature.
Besichtigung und Maßnachprüfung ohne Beanstandung /Visual inspection and dimensional control without objection
Verwechslungsprüfung durchgeführt / PMI performed
Werkstoffnach DIN EN ISO 3651 and ASTM A262 interkristallinische Korrosion bestanding/Material resistant to intercrystalline corrosion acc.to DIN EN ISO 3651 and ASTM A262 (Temp.700+/-10°Cx2h)
Chemical analysis and mechanical properties according to ASTM A182 and ASME SA182 F321

DER SACHVERSTÄNDIGE Surveyors	DER KUNDENSACHVERSTÄNDIGE Customer inspector	ITALFOND S.p.A. Der Qualitätsleiter
		ITALFOND S.p.A.

CERTIFIED TRUE
SIGNED FOR AND ON BEHALF OF RICHARD AUSTIN ALLOYS (SCOTLAND) LTD
AUTHORISED SIGNATURE
COPY OF ORIGINAL CERTIFICATE

VERIFIED TRUE COPY OF ORIGINAL TEST CERTIFICATE

304

SG2336

ACRONI

697261/7

TEHNIČNA KONTROLA
Telefon: +386 4 584 10 43
Telefax: +386 4 584 10 68
http://www.acroni.si
E-mail: anton.papler@acroni.si

B357969

Potrdilo o prevzemu 3.1/ Abnahmeprufzeugnis 3.1/ Inspection certificate 3.1

Stran/Seite/Page 1 / 2 — EN 10 204 3.1

St. / Nr. / No.	Datum / Datum / Date
310043542-1	22.05.2012

Narocilo / Bestellung Nr. / Order No.	Dobavni list / Lieferschein / Despatch note
18612 disp.34128	310043542 z/vom/from 21.05.2012

Izdelek / Erzeugnis / Product	Vrsta peci / Erschmelzunsart / Melting furnace	Znak izvedenca TK / Zeichen des sachverstandigen / Inspectors' stamp	Znak proizvajalca / Zeichen des Herstellewerks / Mark of the Manufacturer
BLECH	E+VOD	KK 4	

Specifikacije / Vorschriften / Specifications	Tip / W.nr. / Type	Pov./ Flache / Finish	Koroz. test / Int.krist.korr. / Corrosion test
ASTM A240/A 240 M/ED.11	304L/304	No.:1	ASTM A262 PRACTICE E:OK
ASME SA 240/SA240M Sect. II Part A Ed.2011	304L/304	No.:1	
PED/97/23/EC			
	X5CrNi18/10/	C2-IIa, 1D	
EN 10028-7/ED.2008,EN 10088-2/ED.05	X2CrNi18/9		EN ISO 3651-2: OK
	W.Nr.1.4301/1.4307		
			NACE MR 0175-2003
			NACE MR 0103-2007

Obseg dobave / Umfang der Lieferung / Extent of material delivery

Poz. / Pos. / Item	St. sarze / Schmelzen Nr. / Heat No.	St. plosce / Waltztafel / Plate No.	Teza neto / Gewicht / Weight kg	Dimenzije / Abmessungen / Dimensions mm	St. kom. / Stuckzahl / Quantity	St. vzorca / Probe Nr. / Sample No.
67	280341	11108	3072	32.00 / 2000 / 6000	1	11108 T
82	280219	98946	5280	55.00 / 2000 / 6000	1	98946 T

Mehanske lastnosti / Mechanische Eigenschaften / Mechanical properties

St.vzorca / Probe Nr. / Sample No.	Smer vzorca / Proben lage / Position	Nap.tecenja / Dehn grenze / Yield 0,2% MPa	Nap.tecenja / Dehn grenze / Yield 1% MPa	Nat.trdnost / Zugfestigkeit / Tensile str. MPa	Raztezek / Bruchdehnung / Elongation A5 %	A50 %	A80 %	Kontrakc. / Einschnurung / Red. of area %	Trdota / Harte / Hardness HB	Zilavost / Kerbschlag / Impact pri /smer bei /lage J	at/posit. °C
Zahteve / Anforderung. / Requirem.	MIN	210	250	520	45					60	20
	MAX			650					201		
98946 T	P	320	380	601	53.4	55.7			170	363 369 367	20
11108 T	P	262	334	590	56.2	58.6			170	352 369 364	20

G - Glava / Kopf / Top N - Noga / Fuss / Bottom V - Vzdolzno / Langs / Longitudinal P - Precno / Quer / Transverse Upogib / Biege / Bend : 0.5a

CERTIFIED TRUE
SIGNED FOR AND ON BEHALF OF
RICHARD AUSTIN ALLOYS (SCOTLAND) LTD
AUTHORISED SIGNATURE

ORIGINAL CERTIFICATE

Acroni 19/72
Zig in podpis
Firmenstempel und Unterschrift
Cesta Stamp and signature 4270 Jesenice
Clan skupine SIJ
Member of Slovenian Steel Group

ACRONI

TEHNIČNA KONTROLA
Telefon: +386 4 584 10 43
Telefax: +386 4 584 10 68
http://www.acroni.si
E-mail: anton.papler@acroni.si

69726/7

Potrdilo o prevzemu 3.1/ Abnahmeprufzeugnis 3.1/ Inspection certificate 3.1

St./Nr./No. **310043542-1**

Kemicna analiza / Chemische Zusammensetzung / Chemical Composition

Sarza/Schmelzen Nr./ Heat No.	%C	%Si	%Mn	%P	%S	%Cr	%Ni	%N	%B	%Co	Ferrite
280219	0.023	0.32	1.81	0.038	0.002	18.09	8.03	0.0900	<0.0005	0.12	
280341	0.024	0.33	1.91	0.037	0.002	18.35	8.12	0.0886	<0.0005	0.11	

8J51969

Opombe / Bemerkungen / Remarks

PRODUCT ANALYSIS:

C%	Si%	Mn%	P%	S%	Cr%	Ni%	N%	B%	Co%	Heat No.
0.024	0.34	1.92	0.038	0.002	18.43	8.20	0.0909	0,0005	0,113	28 0341
0,023	0,34	1,81	0,038	0,001	18,13	8,10	0,0922	0,0005	0,016	28 0219

WARMBEHANDLUNG : LOSUNGSGLUGEN BEI 1050°C,WASSER ABGESCHRECKT !
- OBERFLACHEN UND MASSPRUFUNG : OHNE BEANSTANDUNG NACH EN 10029 DICKE CLASS C
- PRUFUNG AUF WERKSTOFFVERWECHSLUNG : OHNE BEANSTANDUNG
- PRUFUNG AUF BESTANDIGKEIT GEGEN INTERKRISTALLINE KORROSION
  NACH EN ISO 3651-2 : OHNE BANSTANDUNG

HEAT TREATMENT : SOLUTION ANNEALED AT 1050°C, WATER QUENCHED
- VISUAL AND DIMENSIONAL CHECK : OK
- SPECTROMETER SORTING TEST : OK
- INTERGRANULAR CORROSION TEST ACCORDING TO
  ASTM A 262 PRACTICE E : OK!

Certified acc. Pressure Equipment Directive (97/23/EC)
by TÜV-CERT-Certification body for pressure equipment of the
TÜV Industrie Service G.m.b.H TÜV Süd Gruppe.

THE MATERIAL COMPLIES WITH THE REQUIREMENTS OF THE ORDER.
NO WELD REPAIR
Es wird bestätigt, daß die Lieferung den Bestellanforderungen entspricht.
We confirm herewith that the delivered material complies with the terms of the order.

CERTIFIED TRUE COPY OF ORIGINAL CERTIFICATE
SIGNED FOR AND ON BEHALF OF RICHARD AUSTIN ALLOYS (SCOTLAND) LTD
AUTHORISED SIGNATURE

Podpis in žig
Unterschrift und Stempel
Signature and stamp

19/72

Cesta Borisa Kidriča 44, 4270 Jesenice
Član skupine SIJ
Member of Slovenian Steel Group

A.6. Safety Certificates

(Zurich Engineering)

ZURICH

Ignacio Trabadela
University of Edinburgh
Institute for Materials and Processes, School of Engineering
Sanderson Building
King´s Buildings
Edinburgh
EH9 3JL

Your reference EE23428
Our reference PS13-0138
Date 13/05/2013

Examination of OxyCAP R-20 Vessel

Dear Ignacio

Zurich Engineering
126 Hagley Road
Edgbaston
Birmingham
B16 9PF

Telephone 0121 456 1311
Fax 0121 453 6527
www.zurich.co.uk/engineering

Direct phone 0121 697 9225
Direct fax 0121 697 9136
Email
daniel.perry@uk.zurich.com

We have pleasure in enclosing the following.

PS13-0138 / 001

Please note that all data relevant to the examination made by this company will be retained in our records for a period of 10 years.

We trust that this certificate fulfils your requirements.

Yours Sincerely

Daniel Perry
Project Engineer

ZURICH

Certificate of Pressure Test

Form PE3

PROJECT REFERENCE: PS13-0138 / 001

CLIENT NAME	University of Edinburgh
ADDRESS	Institute for Materials and Processes, School of Engineering, Sanderson Building, King´s Buildings, Edinburgh, EH9 3JL
CLIENT REFERENCE	EE23428

EQUIPMENT DESCRIPTION	OxyCAP R-20 Vessel
PLANT OR SERIAL NUMBER	R-20
MANUFACTURER	University of Edinburgh
DRAWING NUMBER(S)	1 sheet 1, 2 sheet 1, 3 sheet 1 & 4 sheet 1
DESIGN PRESSURE / TEMP	50 Bar

TEST INFORMATION	
COMPONENT TESTED	Shell
DATE OF TEST	19/11/2012
TEST FLUID	Water
TEST PRESSURE	75 Bar
RESULT	Satisfactory

This is to certify that the equipment identified above was subjected to a pressure test and during the test there was no evidence of leakage or weakness.

Other Observations
Zurich also reviewed material certificates, carried out material identification checks, checked main dimensions on completion and carried out final visual examination of completed vessel. This vessel has not been CE marked.

Zurich Engineering
Authorised Signatory

Daniel Perry

ZURICH
SAFed / CEOC MEMBER COMPANY
ZURICH ENGINEERING
126 Hagley Road, Edgbaston
Birmingham B16 9PF
Tel: 0121 456 1311

Date 13/05/2013

Title: Project Engineer

Zurich Engineering, 126 Hagley Road, Edgbaston, Birmingham B16 9PF. Telephone: 0121 456 1311 Fax: 0121 697 9136 Email: engineering@uk.zurich.com
Zurich Management Services Limited. Registered in England and Wales No. 2741053. Registered Office: The Zurich Centre, 3000 Parkway, Whiteley, Fareham, Hampshire, PO15 7JZ.

ZURICH

Ignacio Trabadela
University of Edinburgh
Institute for Materials and Processes, School of Engineering
Sanderson Building
King´s Buildings
Edinburgh
EH9 3JL

Your reference Ignacio Trabadela
Our reference PS13-0673
Date 08/01/2014

Modification to an OxyCAP R-20 Vessel (Extension of 20L ignition chamber (R-20) to 30L (R-30) with a thick section between two existing hemispheres)

Dear Ignacio

Zurich Engineering
126 Hagley Road
Edgbaston
Birmingham
B16 9PF

Telephone 0121 456 1311
Fax 0121 453 6527
www.zurich.co.uk/engineering

Direct phone 0121 697 9225
Direct fax 0121 697 9136
Email
daniel.perry@uk.zurich.com

We have pleasure in enclosing the following.

PS13-0673 / 001

Please note that all data relevant to the examination made by this company will be retained in our records for a period of 10 years.

We trust that this certificate fulfils your requirements.

Yours Sincerely

Daniel Perry
Project Engineer

ZURICH

Pressure Equipment Certificate
(for existing equipment)
Form PE2

PROJECT REFERENCE: PS13-0673 / 001

CLIENT NAME	University of Edinburgh
ADDRESS	Institute for Materials and Processes School of Engineering Sanderson Building King´s Buildings Edinburgh EH9 3JL
CLIENT REFERENCE	Ignacio Trabadela

EQUIPMENT DESCRIPTION	OxyCAP R-30 Vessel
WORK CARRIED OUT	Extension of 20L ignition chamber (R-20) to 30L (R-30) with the fitting of a thick section between two existing hemispheres
PLANT OR SERIAL NUMBER	R-30
FABRICATOR	University of Edinburgh
DRAWING NUMBER(S)	N/A
DESIGN PRESSURE / TEMP	50 Bar

EXAMINATION AND TESTS	Review material against material certificates Visual examination on completion of work Witness hydraulic test at 75 Bar for 15 minutes on 12/12/2013
RESULTS	Satisfactory

This is to certify that the equipment identified above was subjected to the specified examinations and tests.

NOTES

Zurich Engineering
Authorised Signatory

ZURICH
SAFed / CEOC MEMBER COMPANY
ZURICH ENGINEERING
126 Hagley Road, Edgbaston
Birmingham B16 9PF
Tel: 0121 456 1311

Date 08/01/2014

Daniel Perry

Title: Project Engineer

Zurich Engineering, 126 Hagley Road, Edgbaston, Birmingham B16 9PF. Telephone: 0121 456 1311 Fax: 0121 697 9136 Email: engineering@uk.zurich.com
Zurich Management Services Limited. Registered in England and Wales No. 2741053. Registered Office: The Zurich Centre, 3000 Parkway, Whiteley, Fareham, Hampshire, PO15 7JZ.